The roles of Ack1 in growth factor signalling and trafficking

By

SYLWIA KRAWCZYK

A thesis submitted to

The University of Birmingham

For the degree of

DOCTOR OF PHILOSOPHY

College of Life and Environmental Sciences

School of Biosciences

University of Birmingham

September 2013

Abstract

Growth factor signalling controls multiple cellular functions, such as cell growth, proliferation, migration and cell survival, and misregulation of growth factor signalling has been shown to promote cancer development and progression. The study presented within this thesis focuses on the functions of a non-receptor tyrosine kinase Ack1 (Activated Cdc42-associated kinase 1, TNK2) in epidermal growth factor (EGF) receptor (EGFR) trafficking. This study reveals that Ack1 subcellular localization greatly depends on EGF availability. Furthermore, this work also identifies a potential role for Ack1 in a non-canonical degradative pathway through its associations with several autophagosomal proteins. Analyses of a panel of the Ack1 deletion mutants further reveal key mechanistic aspects of these associations and identify the Ack1 domains which are required for these to occur. Finally, a mass spectrometric approach has been applied which identifies novel post-translational modification sites within Ack1, and in combination with stable isotope labelling of amino acids in cell culture (SILAC), has allowed for characterisation of novel Ack1 interactors.

I dedicate this thesis to my
unforgettable grandmother
Wiktoria.

Acknowledgements

The project completed has been sponsored by Cancer Research UK and I am grateful to them for this opportunity to carry out the research on a cancer-related topic.

I want to express my gratitude to my supervisors, John Heath and Joshua Rappoport, for the effort they put into my progress, their encouragement and guidance, without which I would not have been able to succeed as a scientist.

I am extremely grateful to my colleague, Debbie Cunningham, for her invaluable advice, her time and patience when discussing scientific topics, and for all the non-scientific conversations.

I thank Andy Creese for his help with mass spectrometric analysis, and Faraz Mardakheh, who, despite the distance, was always there to provide advice. I also appreciate the support I received from Farhat Khanim, and the reagents, constructs and advice I was given by Sue Brewer.

I am thankful to all my colleagues from the fifth floor, for their support and good times we had together, and for making my time at the University so pleasurable.

Finally, I would never be who I am without my parents, who gave me an example through their countless sacrifices of how to achieve my goals. And I thank Andrew, who has made all my efforts worth it.

Table of Contents

Overview 1
1 Introduction 2
1.1 Growth factors and growth factor receptors 2
1.2 Epidermal growth factor receptor 4
1.2.1 Structure 6
1.2.2 EGFR activation 6
1.2.3 EGFR ligands 10
1.2.4 EGF signalling pathway 11
1.2.5 Negative regulation of EGF signalling 16
1.2.6 EGF signalling in development 19
1.2.7 EGF signalling in cancer 21
1.3 Endocytosis and endocytic trafficking 23
1.3.1 Endocytic trafficking of growth factor receptors 29
1.3.2 Phosphorylation in endocytic sorting 32
1.3.3 Ubiquitylation in endocytic sorting 35
1.3.4 The Rab family of small GTPases in endocytic trafficking 37
1.3.5 An intersection between trafficking and signalling 42
1.4 Autophagy 48
1.4.1 Autophagy-related proteins 53
1.4.2 Sequestosome 1 59
1.4.3 Neighbour of BRCA 1 62
1.5 Activated Cdc42-associated kinase 1 (Ack1/TNK2) 63
1.5.1 Structure 63
1.5.2 Function 68
1.5.3 Ack1 in EGFR trafficking and degradation 69
1.5.4 Ack1 in cancer 71
1.5.5 Rationale for investigation of Ack1 73
1.6 Confocal Laser Scanning Microscopy 74
1.7 Mass spectrometry 76
2 Thesis Aims 78
3 Materials and Methods 79
3.1 Materials 79
3.1.1 Buffers and solutions 79
3.1.2 Antibodies and Reagents 83
3.1.3 Plasmid constructs 85

3.2 Methods 86
3.2.1 Molecular cloning 86
3.2.2 Cell culture, transfection, treatment, stimulation and lysis 87
3.2.3 Immunofluorescence and confocal microscopy 89
3.2.4 Protein analysis 91
3.2.5 Real time quantitative polymerase chain reaction 93
3.2.6 SILAC sample preparation 96
3.2.7 Mass spectometry 98
4 Ack1 functions in EGFR, but not FGFR, trafficking 102
4.1 Introduction 102
4.2 Optimising experimental conditions 103
4.2.1 Time courses of EGF and FGF stimulation in HeLa and 293T cells 103
4.2.2 Optimising conditions of Ack1 expression 107
4.2.3 Optimising conditions of EGF stimulation in LNCaP cells 109
4.3 Ack1 interacts with EGFR, but not FGFR2 114
4.4 Ack1 colocalizes with EGFR, but not FGFR2 114
4.5 Ack1 does not interact with FGFR1 117
4.6 Ack1 C-terminal truncation mutants 120
4.7 Mig6 and CBD both contribute to the colocalization with EGFR 123
4.8 Endogenous Ack1 colocalizes with endogenous EGFR upon EGF stimulation 125
4.9 Ack1 knockdown does not influence EGFR degradation 125
4.10 Ack1 knockdown results in accelerated lysosomal localization of EGFR 128
4.11 Conclusions 130
5 Ack1 endo-lysosomal localization 133
5.1 Introduction 133
5.2 Cytoplasmic localization of Ack1 134
5.3 Ack1 partially colocalizes with transferrin 138
5.4 Ack1 partially localizes to early endosomes upon EGF stimulation 140
5.5 Ack1 partially colocalizes with Rab5 upon EGF stimulation 140
5.6 Ack1 does not localize to late endosomes or recycling endosome 148
5.7 Conclusions 151
6 Ack1 autophagosomal localization 153
6.1 Introduction 153
6.2 Ack1 localizes to ubiquitin-rich compartments 154
6.3 Ack1 associates with Eps15 and Hrs 161
6.4 Ack1 interacts and colocalizes with p62/SQSTM1 and NBR1 163
6.5 p62/SQSTM1 promotes colocalization between Ack1 and NBR1 167

6.6 The UBA domain regulates association with p62/SQSTM1, but not NBR1 173
6.7 EGFR partially colocalizes with Ack1 and p62/SQSTM1 post-EGF treatment 176
6.8 Ack1 partially localizes to early phagophores upon EGF stimulation 176
6.9 Ack1 colocalizes with LC3 182
6.10 Conclusions 185
7 Identification of novel PTMs and Ack1 interactors *via* mass spectrometry 188
7.1 Introduction 188
7.2 Novel phosphorylation sites 189
7.3 Novel ubiquitylation site 197
7.4 Ack1 binding partners identified by SILAC 202
7.5 Conclusions 218
8 Discussion and future plans 220
References 229

List of Figures

Figure 1.1. Receptor tyrosine kinases 3
Figure 1.2. Structure of EGFR 7
Figure 1.3. EGF signalling pathway 12
Figure 1.4. Types of endocytosis 25
Figure 1.5. Classical endocytic route of EGFR 30
Figure 1.6. Rab-GTPases circuity 38
Figure 1.7. Examples of Rab-GTPases function in membrane trafficking 40
Figure 1.8. The process of autophagy 49
Figure 1.9. Phagophore membrane composition 52
Figure 1.10. Hierarchy of the Atg proteins in autophagosome formation 57
Figure 1.11. Domain structures of p62/SQSTM1 and NBR1 61
Figure 1.12. Domain structure of human Ack1 (isoform 1) 65
Figure 1.13. Ack1 orthologues and isoforms of human and mouse Ack1 67
Figure 1.14. Schematic of Confocal Microscope 75
Figure 3.1. Thermal cycler conditions for cDNA synthesis and RT-qPCR 95
Figure 3.2. Simplified diagram of SILAC experiment 97
Figure 4.1. Time courses of EGF and FGF stimulation for HeLa and 293T cells 105
Figure 4.2. Optimising Ack1 transfections in HeLa cells 108
Figure 4.3. Identification of potentially phosphorylated Ack1 in LNCaP cells 110
Figure 4.4. EGFR degradation upon treatment with various EGF concentrations 112
Figure 4.5. EGFR trafficking upon treatment with various EGF concentrations 113
Figure 4.6.Ack1 interacts with EGFR and Cdc42, but not with FGFR2 115
Figure 4.7. Ack1 colocalizes with EGFR, but not FGFR2 116
Figure 4.8. Ack1 colocalizes with EGFR in COS7 cells 118
Figure 4.9. Ack1 does not interact with FGFR1 upon FGF2 stimulation 119
Figure 4.10. Ack1 does not co-precipitate with kinase-active FGFR1 121
Figure 4.11. Ack1 C-terminal truncation mutants 122
Figure 4.12. The Mig6 domain and CBD regulate colocalization with EGFR 124
Figure 4.13. Endogenous Ack1 colocalizes with endogenous EGFR upon EGF treatment 126
Figure 4.14. EGFR degradation in LNCaP cells following Ack1 knockdown 127
Figure 4.15. Ack1 knockdown increases EGFR lysosomal localization 129
Figure 5.1. Ack1 does not translocate the nucleus 136
Figure 5.2. *Z*-stack of cells expressing Eps15-GFP, GFP-Ack1 and GFP-tAck1 137
Figure 5.3. Ack1 partially colocalizes with transferrin 139
Figure 5.4. Ack1 partially localizes to early endosomes upon EGF stimulation 141
Figure 5.5 Ack1 partially localizes to Rab5 upon EGF stimulation (a) and (b) 143
Figure 5.6. Ack1 partially colocalizes with Rab4 and Rab11 post-EGF treatment (a) and (b) 145
Figure 5.7. Ack1 partially colocalizes with Rab7 post-EGF treatment 147
Figure 5.8. Ack1 does not localize to late endosomes post-EGF treatment 149
Figure 5.9. Ack1 does not localize to recycling endosomes post-EGF treatment 150
Figure 6.1. Ack1 localizes to ubiquitin-rich compartments 155
Figure 6.2. Ack1 binds ubiquitin 156
Figure 6.3. EGFR colocalizes with Ack1 and ubiquitin post-EGF treatment 158
Figure 6.4. Ack1 domains required for colocalization with ubiquitin (a), (b) and (c) 159
Figure 6.5. Ack1 colocalizes with Hrs and Eps15 162

Figure 6.6. Ack1 interacts and colocalizes with p62/SQSTM1 (a), (b) and (c) 165
Figure 6.7. Ack1 only partially colocalizes with NBR1 168
Figure 6.8. p62/SQSTM1 and NBR1 co-precipitate with Ack1 170
Figure 6.9. The colocalization between Ack1, p62/SQSTM1 and NBR1 (a), (b) and (c) 171
Figure 6.10. The UBA domain mediates the colocalization with p62/SQSTM1 (a) and (b) 174
Figure 6.11. The UBA domain does not mediate the colocalization with NBR1 177
Figure 6.12. EGFR partially colocalizes with Ack1 and p62/SQSTM1 post-EGF treatment 178
Figure 6.13. Ack1 partially localizes to early phagosomes upon EGF stimulation (a) and (b) 180
Figure 6.14. Ack1 colocalizes with LC3 (a) and (b) 183
Figure 7.1. Coomassie-stained gel with immunoprecipitated Ack1 191
Figure 7.2. Ack1 sequence coverage 192
Figure 7.3. Novel phosphorylation sites at Ser102 and Ser761 193
Figure 7.4. Novel phosphorylation sites at Ser936 and the SSS region 194
Figure 7.5. Known and novel phosphorylation sites within mouse Ack1 (isoform 2) 195
Figure 7.6. Novel ubiquitylation site at Lys539 200
Figure 7.7. Known and novel ubiquitylation sites within mouse Ack1 (isoform 2) 201
Figure 7.8. Antibody cross-linking reduces the amount of immunoprecipitated proteins 203
Figure 7.9. Immunoprecipitation of myc-Ack1 204
Figure 7.10.Natural logarithm of ratios from two independent experiments 206
Figure 7.11. Proteins enriched or depleted in -EGF or +EGF sample 208
Figure 7.12. Proteins enriched in -EGF sample 209
Figure 7.13. Proteins enriched in +EGF sample 210
Figure 7.14. Proteins enriched in +EGF vs. –EGF sample and –EGF vs. +EGF sample 211
Figure 7.15. Protein clustering using STRING database 215
Figure 8.1. Proposed mechanism for the role of Ack1 in EGFR trafficking 221

List of Tables

Table 1.1. Multiple functions of EGF signalling in development and physiology 20
Table 1.2. The functions of Atg and Atg-related proteins in autophagosome biogenesis..... 55
Table 3.1. Primary antibodies used in the study..... 84
Table 3.2. Secondary antibodies used in the study..... 84
Table 3.3. cDNA synthesis mix 94
Table 3.4. Reaction mix for RT-qPCR..... 94
Table 3.5. The amounts of protein, antibody and beads used for immunoprecipitation 96
Table 6.1. Summary of the studies on Ack1 colocalization with autophagic proteins 187
Table 7.1. Prediction of the kinases which phosphorylate novel sites within Ack1 198
Table 7.2. Proteins enriched in –EGF or +EGF sample..... 212
Table 7.3. The proteins identified to bind Ack1 in an EGF-dependent manner..... 213

List of Abbreviations

Ack1	Activated Cdc42 Associated Kinase 1
ADP	Adenosine Diphosphate
Akt	Protein Kinase B (PKB)
ALK	Anaplastic Lymphoma Kinase
AMP	Adenosine Monophosphate
AP2	Adaptor Protein Complex 2
AR	Androgen Receptor
Atg	Autophagy Related Gene
ATP	Adenosine Triphosphate
Cdc42	Cell Division Cycle 42 Protein Homolog
cDNA	Complementary DNA
CRIB domain	Cdc42/Rac Interactive Binding domain
DNA	Deoxyribonucleic Acid
EGF	Epidermal Growth Factor
EGFR	Eprmal Growth Factor Receptor
EMT	Epithelial-Mesenchymal Transition
ER	Endoplasmic Reticulum
ESCRT	Endosomal Sorting Complexes Required for Transport
FGF	Fibroblast Growth Factor
FGFR	Fibroblast Growth Factor Receptor
GDP	Guanosine Diphosphate
GEF	Guanine Nucleotide Exchange Factor
GFP	Green Fluorescent Protein
Grb2	Growth Factor Receptor-bound Protein 2
GSK-3	Glycogen Synthase Kinase 2
GTP	Guanosine Triphosphate
HSP90	Heat Shock Protein 90
IRS1	Insulin Receptor Substrate 1

LC3	Microtubule-associated Protein Light Chain 3
Mdm2	Mouse Double Minute 2
Mek/Erk kinase	Mitogen-activated Protein kinase/Extracellular Signal-Regulated kinase
Mig6	Mitogen-induced gene 6
mRNA	Messenger RNA
mTOR	Mammalian Target of Rapamycin
NBR1	Neighbour of BRCA1
NRTK	Non-Receptor Tyrosine Kinase
p62/SQSTM1	Sequestosome 1
PAS	Pre-autophagosomal structure
PDGFR	Platelet-derived Growth Factor Receptor
PDK1	Phosphoinositide-Dependent Kinase 1
PE	Phosphatidylethanolamine
PH domain	Plextrin Homology domain
PIP_2	Phosphatydylinositol 4,5-biphosphate
PIP_3	Phosphatydylinositol 3, 4, 5-triphosphate
PKC	Protein kinase C
PNRC	Perinuclear Recycling Compartment
PTEN	Tensin Homologue Deleted from Chromosome 10
RNA	Ribonucleic Acid
tAck1	Truncated Ack1
Tf	Transferrin
TSC1	Tuberous Sclerosis Protein 1
TSC2	Tuberous Sclerosis Protein 2
SAM	Sterile α-Motif
SEM	Standard Error of the Mean
SILAC	Stable Isotope Labelling of Amino Acids in Cell Culture
siRNA	Small Interfering RNA
SNX9	Sortin Nextin 9

Sos	Son of Sevenless
UBA	Ubiquitin Associated
WT	Wild Type
WWOX	WW domain-containing Oxidoreductase

Overview

Growth factors control processes such as cellular proliferation and directed cell migration, and deregulated signalling through growth factor receptors is associated with oncogenesis and other pathologies. The field of growth factors and growth factor receptors has been extensively studied for decades, leading to the development of drugs administered, for example, as treatments of cancer. There is still a great deal of debate on the mechanisms underlying the regulation of growth factor signalling and trafficking pathways; however, new evidence has emerged which demonstrates the interdependence of these two apparently distinct areas.

One of the proteins implicated in the regulation of growth factor signalling and trafficking is Ack1 (activated Cdc42-associated kinase 1). This non-receptor tyrosine kinase (NRTK) has been shown to regulate epidermal growth factor receptor (EGFR) degradation, leading to down regulation of EGF signalling; however, the precise roles for Ack1 in this context remain elusive. In addition to its functions in EGF signalling pathway, Ack1 contains a clathrin binding domain, which makes it a very interesting protein to study in the field of clathrin-mediated endocytosis (CME). CME is the major internalization pathway for many cell-surface receptors, including EGFR.

The overall focus of the study presented in this thesis is to investigate the functions of Ack1 in the context of growth factor receptor signalling and trafficking.

1 Introduction

1.1 Growth factors and growth factor receptors

Growth factors were first discovered in the 1950s by Stanley Cohen and Rita Levi-Montalcini. Neuronal growth factor was the first identified in 1953 (Levimontalcini *et al.*, 1954), followed by the discovery of epidermal growth factor (EGF), which was isolated and described in 1962 (Cohen, 1962). These two discoveries had a large influence on the fields of cell biology and medicine, as evidenced by the awarding of the Nobel Prize in Physiology or Medicine in 1986 to Cohen and Levi-Montalcini (Garfield, 1987). These findings also led to identification of other growth factors and their receptors, and their function within the cell, thus allowing a greater understanding of the basis of many growth factor-related pathologies (Garfield, 1987).

Since these initial discoveries, growth factors have been shown to regulate many cellular processes including cell growth, proliferation, differentiation, migration and survival (Turner and Grose, 2010; Avraham and Yarden, 2011). Growth factor signalling is crucial for correct cellular functions and misregulation of this signalling may lead to many disorders. One of the main fields in which aberrant growth factor signalling is being extensively studied is neoplastic transformation, an abnormal growth and proliferation of cells, which may lead to cancer development (Rajkumar, 2001; Turner and Grose, 2010). So far, 58 receptor tyrosine kinases (RTKs) have been identified in *Homo sapiens* alone, and are further divided into 20 subfamilies, *e.g.* the epidermal growth factor receptor (EGFR), the vascular EGFR (vEGFR) and the fibroblast growth factor receptor (FGFR) families, examples of which are shown in **Figure 1.1** (Lemmon and Schlessinger, 2010).

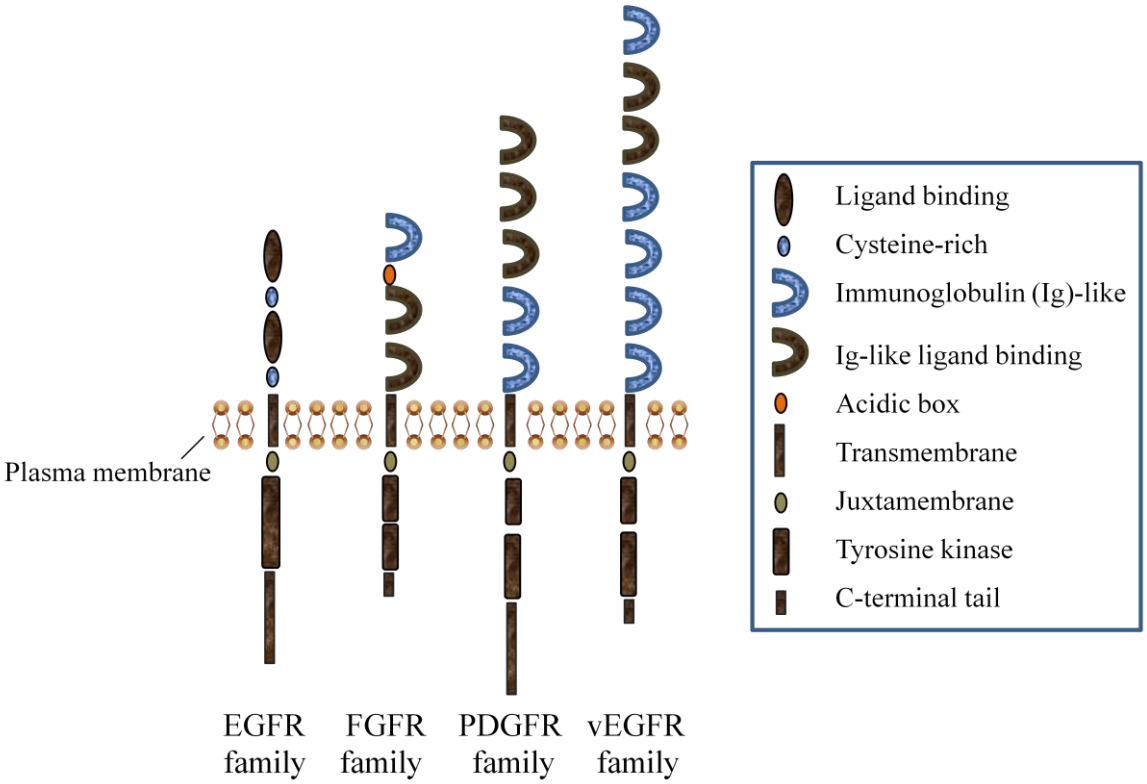

Figure 1.1. Receptor tyrosine kinases

The examples of the RTK families are presented. RTKs, which reside at the plasma membrane, comprise an extracellular portion, single transmembrane domain and an intracellular portion. Adapted from (Lemmon and Schlessinger, 2010).

RTKs can be characterized as cell-surface receptors that bind extracellular ligands, such as growth factors or hormones (Gschwind *et al.*, 2004). They all share a similar structure, which includes an extracellular ligand-binding domain, a single transmembrane helix and a cytoplasmic region, itself containing a juxtamembrane domain, a tyrosine kinase domain and a C-terminal tail (**Figure 1.1**) (Lemmon and Schlessinger, 2010). The majority of RTKs present at the plasma membrane are monomers (Schlessinger, 2000). Ligand binding stabilises dimeric or oligomeric states of RTKs, which in turn enhance intrinsic tyrosine kinase activity (Schlessinger, 1988; Gschwind *et al.*, 2004). Once a stable complex is formed, activated receptor dimers trans-phosphorylate, *i.e.* phosphorylate the opposed bound monomer. This results in autophosphorylation of key tyrosine residues within the catalytic loop of the kinase domain, which further stimulates tyrosine kinase activity (Schlessinger, 1988; Gschwind *et al.*, 2004). Phosphorylated tyrosine residues also function as docking sites for other proteins and signalling molecules, described later in **Chapter 1.2.4** (Lemmon and Schlessinger, 2010). Importantly, it has been shown that the autophosphorylation events occur in a precise order, and that the initial phosphorylation events enhance the catalytic function of the kinase domain, whereas subsequent phosphorylation events enable recruitment of signalling proteins. Typically, the recruited proteins contain the phosphotyrosine binding (PTB) domain and the Src homology-2 (SH2) domain, a conserved motif that recognizes phosphorylated tyrosine residues (Lemmon and Schlessinger, 2010).

1.2 Epidermal growth factor receptor

Epidermal growth factor receptor (EGFR), also known as ErbB1 or Her1 (human epidermal growth factor receptor 1), is perhaps the most studied among all RTKs. EGFR is a member of the EGFR/ErbB family of RTKs that also includes ErbB2/Neu/Her2, ErbB3/Her3 and ErbB4/Her4 (Hynes *et al.*, 2001). Ligand binding to ErbB receptors has been shown to be

highly controlled, and different ligands recognise particular ErbB receptors. Upon ligand binding, members of the ErbB family can homodimerise or heterodimerise with one another, thus bringing additional diversity in signalling properties. Importantly, heterodimers acquire new signalling properties rather than a sum of properties of two homodimers. For example, stimulation of NIH3T3 cells co-expressing ErbB2 and ErbB4 with neu differentiation factor, a growth factor that binds ErbB3 and ErbB4, led to activation of signal transducer and activator of transcription 5b (STAT5b); however, STAT5b was not activated in cells co-expressing ErbB1 and ErbB4, or ErbB2 and ErbB3 (Olayioye *et al.*, 1999; Schneider and Wolf, 2009). The signalling cascades activated by the members of the EGFR family play pivotal roles in embryogenesis. This came to light in 1995, when it was shown that mice lacking ErbB2 and ErbB4 die during embryonic development due to failure in development of myocardial trabeculae in the heart ventricle (Gassmann *et al.*, 1995; Chan *et al.*, 2002). Additionally, signalling through ErbB receptors also promotes angiogenesis, and aberrant ErbB signalling vastly contributes to development of various types of cancer (Casanova *et al.*, 2002; Klos *et al.*, 2006; Burgess, 2008).

Following ligand binding at the plasma membrane, EGFR has been shown to be internalized mainly through a certain type of endocytosis called clathrin-mediated endocytosis (CME) described later in **Chapter 1.3** (Rappoport and Simon, 2009). Endocytosis followed by EGFR sorting for lysosomal degradation, as well as dephosphorylation of activated EGFRs by cellular phosphatases (described in **Chapter 1.2.5**) play fundamental roles in downregulation of EGF signalling (Avraham and Yarden, 2011).

1.2.1 Structure

As a prototypical RTK, EGFR shares similar structural features with other RTKs, as it consists of an extracellular ligand-binding region, single transmembrane domain and an intracellular tyrosine kinase domain, shown in **Figure 1.2**. The high-resolution crystal structure of the ErbB receptors reveals that within the extracellular portion they all contain two large beta-helical domains (L1 (I) and L2 (III)) and two small cysteine-rich regions (S1 (II) and S2 (IV)), which contain several disulfide bounded modules. Since the domains I and III are homologous, as are domain II and IV, it has been proposed that the extracellular portion evolved by gene duplication of the region containing domains I and II (Leahy, 2004). A single-spanning α-helical transmembrane (TM) domain is followed by a juxtamembrane (JM) region, a tyrosine kinase domain and an intracellular C-terminal tail. The TM domain has been shown to stabilise receptor dimerisation (Jorissen *et al.*, 2003). Relatively little is known about the functions of the JM domain and the C-terminal region, although multiple tyrosine and lysine residues characterised within the C-terminus have been found to regulate EGFR activation (Ferguson, 2008; Goh *et al.*, 2010).

1.2.2 EGFR activation

In an inactive state, the extracellular domain II interacts with domain IV *via* a hairpin loop, also known as a ‘dimerisation arm’, thus preventing an interaction between domains I and III (Cho and Leahy, 2002; Ferguson *et al.*, 2003). Ligand binding to domain I and III brings them into close proximity resulting in disruption of the interaction between domains II and IV. As a result, the hairpin loop from domain II is free and can interact with another receptor molecule (Garrett *et al.*, 2002; Ogiso *et al.*, 2002).

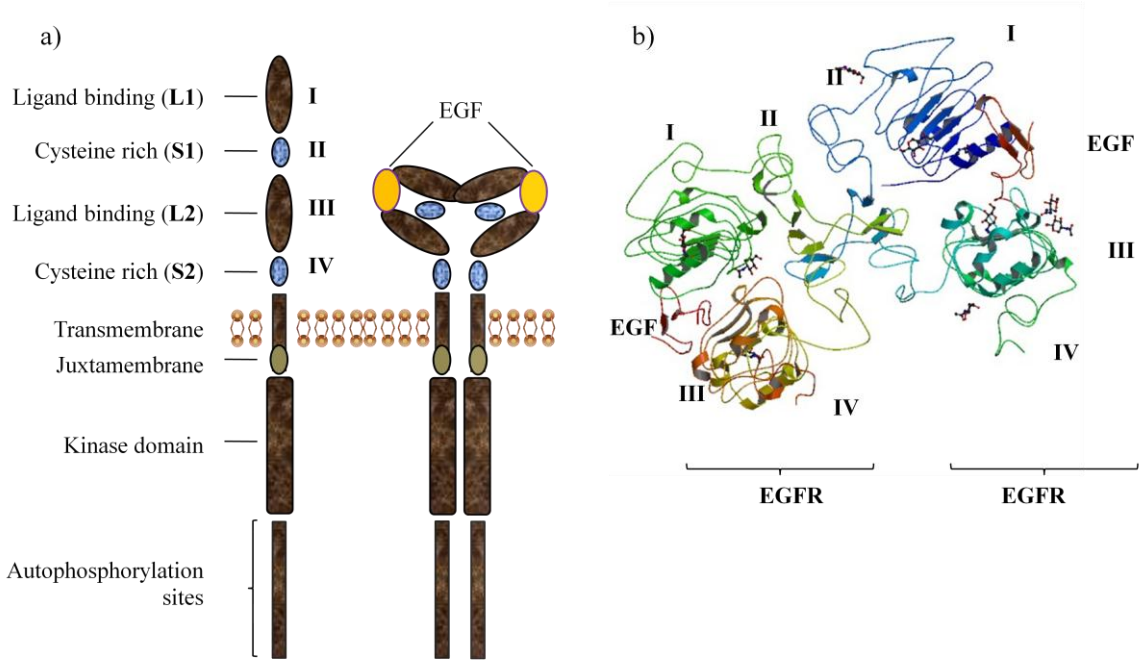

Figure 1.2. Structure of EGFR

a) Schematic structure of EGFR comprises the extracellular portion with the ligand binding and cysteine rich domains, a single transmembrane domain and adjacent juxtamembrane domain, and the cytoplasmic portion that comprises the tyrosine kinase domain and the C-terminal tail; on the right: schematic of EGFR dimer with two EGF molecules. Adapted from (Lemmon and Schlessinger, 2010); **b)** Crystal structure of the EGFR extracellular domains bound to EGF resolved by Ogiso *et al.* (Ogiso *et al.*, 2002), from the Protein Data Bank database (www.rscb.org).

This is unusual among RTKs, as typically the ligand mediates an interaction between two receptor molecules, *e.g.* in the case of FGFR, the dimer is stabilised by direct interaction between the ligand and the adjacent receptor (Plotnikov *et al.*, 1999). In the case of EGFR, however, receptor dimeriation is mediated by receptors themselves. The ligand binds simultaneously to the domain I and III of the same receptor, and the released dimerisation arm of domain II is able to interact with domain II in the partner receptor molecule. This has been proposed to be true for three members of the ErbB family: EGFR, ErbB3 and ErbB4. In the case of ErbB2, the extracellular domain of the receptor has been shown to be in an active conformation in the absence of ligand, and domains I and III have been found to be in a close proximity (Cho *et al.*, 2003; Garrett *et al.*, 2003). This may explain why ErbB2 over-expression leads to tumorigenesis, since the close proximity of domain I and III disrupts the interaction between domain II and IV, leading to ligand-independent dimerisation. Similarly, this may be the reason why no ErbB2 ligand has been described, as there may not be enough space for any ligand to bind between the interacting domains I and III (Cho *et al.*, 2003; Garrett *et al.*, 2003). Additionally, although the ErbB2 extracellular domain structure resembles that of an active EGFR dimer, the negatively charged dimerisation arm and the pocket into which it would dock prevents ErbB2 homodimerisation and promotes heterodimerisation with other ErbB receptors (Garrett *et al.*, 2003).

In the case of EGFR, the interaction between domain II and IV observed in an inactive 'tethered' state of the receptor does not seem to be sufficient to inhibit receptor activation. This was shown with mutations disrupting this interaction and thus exposing the dimerisation arm, which did not lead to receptor dimerisation or activation (Mattoon *et al.*, 2004; Walker *et al.*, 2004). Therefore other factors have been proposed to additionally stabilise an inactive state of the receptor, or to promote receptor activation. For example, the conformational

changes within the domain II following ligand binding may promote receptor dimerisation and activation (Dawson *et al.*, 2005). Also, a linkage between domains II and III has been proposed to be very rigid and stabilised by disulfide bond, thus promoting formation of an inactive conformation even when the interaction between domains II and IV is removed (Dawson *et al.*, 2007). Finally, oligosaccharides which are not entirely visualised in the crystal structure, have been proposed to sterically restrict the position of the domains involved in dimerisation, and thus ligand binding could potentially disrupt these restrictions (Dawson *et al.*, 2007).

In addition to the unusual mechanism of EGFR dimerisation, EGFR tyrosine kinase activation is also unique among other RTKs. Typically, the autoinhibitory interactions within the kinase domain are disrupted by *trans*-autophosphorylation, *e.g.* in the case of FGFR or insulin receptor; however, EGFR autophosphorylation is not required for activation. This has been shown using mutant EGFR with a tyrosine residue within the activation loop replaced by phenylalanine, which was activated to a similar level as wild type EGFR (Gotoh *et al.*, 1992; Zhang *et al.*, 2006). Additionally, it has been shown that two leucine residues within the activation loop of EGFR (Leu834 and Leu837) provide an autoinhibitory mechanism through packing against a crucial catalytical region (helix αC) within the N-lobe of the kinase domain and thus reinforcing its displaced orientation. In accordance with this, replacement of Leu834 with arginine has been found to promote EGFR activation (Zhang *et al.*, 2006). Therefore an allosteric model of EGFR activation has been proposed, which suggests that upon receptor dimerisation, an asymmetric interaction takes place between the C-lobe of one receptor tyrosine kinase ('activator') and the N-lobe (helix αC) of the other receptor ('receiver'). This leads to the activation of the kinase domain of the 'receiver', which then phosphorylates the C-terminal tail of the other receptor, and *vice-versa*, leading to receptor *trans*-

autophosphorylation (Zhang *et al.*, 2006). Additionally, the juxtamembrane (JM) domain of EGFR may also contribute to receptor dimerisation and activation, and it has been suggested that the flexibility of the JM domain may enable the kinase domains to switch positions and activate each other (Zhang *et al.*, 2006; Thiel and Carpenter, 2007; Jura *et al.*, 2009).

1.2.3 EGFR ligands

Currently there are seven EGFR ligands characterised, some of which may also activate ErbB3 and ErbB4. The EGFR ligands include EGF, transforming growth factor-α (TGF-α), heparin-binding EGF (HB-EGF), amphiregulin (AREG), betacellulin (BTC), epiregulin (EREG) amd epigen (Roepstorff *et al.*, 2009; Schneider and Wolf, 2009). Additionally, another group of ligands collectively known as neuregulin typically activate ErbB3 and ErbB4. As explained above (**Chapter 1.2.2**), no ligand has yet been described for ErbB2 (Leahy, 2004; Schneider and Wolf, 2009). The EGFR ligands all contain the EGF module, an approximately 40 amino acid-long motif with six conserved cysteine residues forming three disulfide bonds and three loops. Upon synthesis, the EGFR ligands traffic to the plasma membrane, where the extracellular EGF module undergoes enzymatic cleavage resulting in a soluble ligand being released to the intracellular matrix. The cytoplasmic tail regulates ligand targeting to the plasma membrane, and upon cleavage of the EGF module, it has been proposed to regulate gene transcription (Schneider and Wolf, 2009).

The EGFR ligands share little sequence identity (approximately 25 %) and differ in biochemical properties, such as the presence and distribution of glycosylation sites. Additionally, they may exhibit different activities, *e.g.* autocrine, paracrine or juxtacrine activity (Harris *et al.*, 2003; Schneider and Wolf, 2009). They also vary in their affinity to EGFR and in the effects they exert on EGF signalling and EGFR trafficking (Roepstorff *et*

al., 2009), which is described in more detail in **Chapter 1.3.1**. Binding of all known EGFR ligands results in EGFR endocytosis and trafficking towards early endosomes; however, each ligand differentially regulates trafficking through the lysosomal and recycling compartments. Additionally, binding of some of the ligands has been shown to be more persistent in acidic pH, *e.g.* EGFR binding of HB-EGF, BTC and AREG has been found to be more acid-resistant than that of EGF or TGF-α (Roepstorff *et al.*, 2009). Furthermore, EGFR stimulation with HB-EGF and BTC have been shown to result in complete EGFR degradation, whereas both TGF-α and EREG led to EGFR recycling to the plasma membrane. EGF, which is the only EGFR ligand used throughout the study presented in this thesis, has been shown to promote EGFR degradation; however, some recycling can also be detected (Roepstorff *et al.*, 2009).

1.2.4 EGF signalling pathway

Currently the EGF signalling and EGFR trafficking pathways are being extensively investigated and an intersection, or a mutual interplay, between EGFR trafficking (explained in **Chapter 1.3.1**) and signalling is emerging. There are several major signalling pathways activated by the EGF-EGFR complex; these include the Ras/MAPK, PI3K/Akt, PLCγ/PKC and JAK/STAT pathways (Jorissen *et al.*, 2003). Activation of these cascades promotes cell proliferation, migration and cell survival. Interestingly, activation of particular signalling pathways may predominantly lead to different phenotypes; *e.g.* activation of PI3K/Akt pathway has been predominantly linked to cell proliferation and cell survival, whereas activation of PLCγ/PKC pathway has been found to promote cell migration (Chen *et al.*, 1994; Jorissen *et al.*, 2003). The schematic representation of the EGF signalling cascades is shown in **Figure 1.3**.

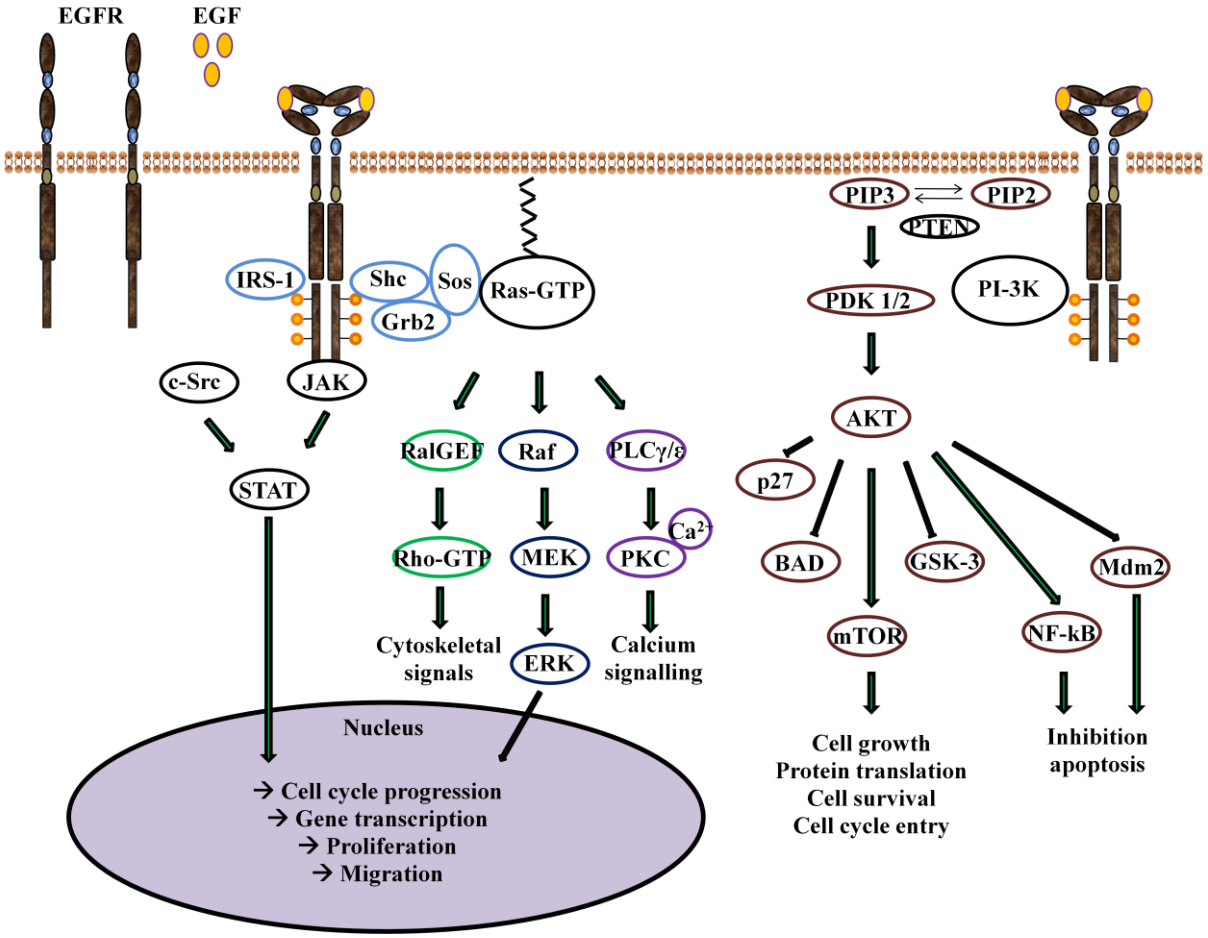

Figure 1.3. EGF signalling pathway

Upon ligand binding, EGFRs at the plasma membrane dimerise and *trans*-autophosphorylate, thus triggering series of phosphorylation and dephosphorylation events within various signalling molecules. All these changes modify gene expression, regulate cytoskeletal rearrangements, promote cell growth and survival, and inhibit apoptosis. Adapted from (Jorissen *et al.*, 2003; Reuter *et al.*, 2007).

As described in **Chapter 1.2.2**, upon ligand binding EGFRs dimerise, leading to activation of the kinase domains and *trans*-autophosphorylation of the intracellular tyrosine residues (Honegger *et al.*, 1989; Ferguson, 2008). These phosphorylation events allow for interaction with proteins containing Src homology 2 (SH2) and phospho-tyrosine binding (PTB) domains, such as adaptor proteins (the proteins that lack an enzymatic function, but contain at least two protein binding motifs, thus allowing binding of at least two signalling molecules at the same time) (Flynn, 2001). For example an adaptor protein Shc interacts with phosphorylated EGFR through its SH2 and PTB domains (Rozakisadcock *et al.*, 1992).

Following interaction with activated receptor, phosphorylated Shc associates with a complex composed of an adaptor protein growth factor receptor-bound protein 2 (Grb2) and son of sevenless (Sos), a guanine nucleotide exchange factor (GEF) (described in more detail in **Chapter 1.3.4**). In the Shc-Grb2-Sos complex, the SH2 domain of Grb2 binds phosphorylated Shc, whereas the Src homology 3 (SH3) domain interacts with proline-rich region within Sos (Rozakisadcock *et al.*, 1992; Simon and Schreiber, 1995). When recruited to the plasma membrane, Sos activates a membrane resident Ras, leading to recruitment of downstream effectors of Ras and initiation of multiple signalling cascades (Sakaguchi *et al.*, 1998; Kyriakis, 2009). Grb2 has also been shown to interact with phosphorylated EGFR directly through its SH2 domain (Rozakisadcock *et al.*, 1992). Furthermore, during early stages of receptor internalization, Grb2 has been identified as recruiting Cbl, a ubiquitin ligase, thus allowing for EGFR ubiquitylation (described in **Chapter 1.3.3**) (Jiang *et al.*, 2003).

The Ras/MAPK pathway is one of the major signalling cascades activated downstream of EGFR. When Ras is stimulated by the Shc-Grb2-Sos complex, it becomes active through conversion of guanosine diphosphate (GDP) to guanosine triphosphate (GTP) (explained in

Chapter 1.3.3) (McCubrey *et al.*, 2007). Activated Ras recruits Raf to the plasma membrane, which is followed by multiple phosphorylation and dephosphorylation events within Raf domains (McCubrey *et al.*, 2007). Activated Raf phosphorylates mitogen-activated protein kinase/extracellular signal-regulated kinases 1 and 2 (MAPK/Erk 1/2), which activate many downstream targets. MAPK/Erk 1/2 can also translocate to the nucleus and phosphorylate various transcription factors, thus modifying gene expression (McCubrey *et al.*, 2007). Ras/MAPK activation promotes entry into cell cycle and cell proliferation (Avraham and Yarden, 2011), and stimulates cell migration possibly through focal adhesion (adhesion between the cell and the extracellular matrix) disassembly (Jorissen *et al.*, 2003).

Apart from activation of Raf, there are other downstream targets of Ras. For example RalGEF interacts with activated Ras and promotes the GDP to GTP exchange within Ral, a small Ras-like GTPase. This leads to the activation of RhoGTPases, for example Cdc42, leading to cytoskeletal rearrangements and cell migration (Cantor *et al.*, 1995; Jullienflores *et al.*, 1995). In addition to Raf and RalGEFs, phospholipase C gamma and epsilon (PLCγ/ε) are other Ras effectors (Kelley *et al.*, 2001). PLCγ/ε perform hydrolysis of phosphatidylinosidol 4,5-biphosphate (PIP_2) to diacylglycerol (DAG), which activates protein kinase C (PKC), and to inositol 1,4,5-triphosphate (IP_3), which mediates intracellular calcium release (Rhee, 2001). Signalling *via* PLCγ/ε has been proposed to regulate cell migration. In particular, activated PLCγ promotes release of actin-modifying proteins from the plasma membrane, which then bind actin filaments thus regulating actin cytoskeleton reorganization (Chen *et al.*, 1996).

Another major signalling cascade downstream of EGFR is the PI3K/Akt pathway. PI3K is composed of two subunits: a regulatory subunit p85 and a catalytic subunit p110. The SH2 domain of p85 associates with phosphorylated EGFR, resulting in PI3K recruitment to the

plasma membrane. PI3K then binds and phosphorylates PIP_2 leading to formation of phosphatidylinositol 3,4,5-triphosphate (PIP_3), which is a second messenger that binds plextrin homology (PH) domains in target proteins (Kyriakis, 2009). Conversion of PIP_2 to PIP_3 is negatively regulated by phosphatase and tensin homologue deleted from chromosome 10 (PTEN), which dephosphorylates PIP_3 back to PIP_2 (Chalhoub and Baker, 2009). PIP_3 recruits phosphoinositide-dependent kinase 1 (PDK1) and Akt, a serine-threonine kinase, both of which contain PH domains. This close proximity enables PDK1 to phosphorylate Akt, which integrates and coordinates multiple signalling pathways. Activation of the PI3K/Akt pathway is perhaps the most prominent regulator of cellular functions, promoting anti-apoptotic responses, cell cycle entry and cell survival (Jorissen *et al.*, 2003).

When activated, Akt phosphorylates diverse downstream proteins, some of which are inhibited, *e.g.* BAD (a pro-apoptotic member of the Bcl-2 family) (Datta *et al.*, 1997), whilst others are activated. Through phosphorylation of κB inhibitor (IκB), which is subsequently degraded, Akt facilitates activation of NFκB (nuclear factor κ-light-chain-enhancer of activated B cells), leading to transcription of anti-apoptotic genes (Bai *et al.*, 2009). Additionally, Akt phosphorylates mouse double minute homolog 2 (Mdm2), a negative regulator of p53, thus downregulating p53-mediated apoptosis (Ogawara *et al.*, 2002). By phosphorylation of tuberous sclerosis protein 2 (TSC2), Akt inhibits GTPase activity of TSC1 and TSC2 dimer toward Rheb (RAS homologue enriched in brain), enabling Rheb to activate mammalian target of rapamycin (mTOR), leading to protein synthesis and cell survival (Courtney *et al.*, 2010). Akt also phosphorylates cell cycle inhibitor p27, leading to its degradation (Fujita *et al.*, 2002) and inhibits glycogen synthase kinase 3 (GSK-3), a protein which induces apoptosis (Pap and Cooper, 1998). Therefore, Akt promotes cell survival and activation of anti-apoptotic mechanisms.

There are other proteins which can be recruited to active EGFR, *e.g.* Janus kinase (JAK), which associates and phosphorylates signal transducers and activators of transcription (STATs) leading to STATs translocation to the nucleus (Andl *et al.*, 2004). Nevertheless, JAK-independent and likely Src-dependent STAT activation has also been reported (Rawlings *et al.*, 2004). Activated EGFR also binds and phosphorylates insulin receptor substrate 1 (IRS1), which in turn may activate several signalling pathways, for example the PI3K/Akt pathway (Knowlden *et al.*, 2008; Metz and Houghton, 2011).

The Src family of non-receptor tyrosine kinases comprises other important regulators of EGF signalling. The SH2 domain of Src has been found to bind EGFR upon EGF stimulation; however, it is unclear whether Src acts downstream of the EGF signalling cascade, or whether it is required for receptor activation (Biscardi *et al.*, 1999; Jorissen *et al.*, 2003). For example, EGFR kinase inhibitor has been shown to inhibit EGF-dependent Src activation in colon cancer cells, suggesting that Src acts downstream of EGFR (Mao *et al.*, 1997). Similarly, EGFR has also been shown to activate Src following EGF treatment in epidermoid cancer cells, and Src activation then stimulated clathrin redistribution and EGFR endocytosis (Wilde *et al.*, 1999). On the other hand, Src overexpression in breast cancer cells has been shown to result in EGFR phosphorylation, thus suggesting that EGFR activation may occur downstream of Src (Biscardi *et al.*, 1999).

1.2.5 Negative regulation of EGF signalling

Taking into consideration how many important cellular functions are regulated by EGF signalling, it is understandable that mechanisms exist which tightly control these signalling pathways and protect cells from aberrant activation. The negative feedback regulation may be roughly divided into two types of response: early, or primary, and secondary response

(Avraham and Yarden, 2011). The early loop involves the events that take place immediately upon ligand binding and therefore are mainly restricted to the cellular components already present within the cell. These include receptor endocytosis, protein modifications such as dephosphorylation and ubiquitylation (described in **Chapter 1.3.2** and **Chapter 1.3.3**), as well as degradation of a group of microRNAs which would otherwise negatively regulate gene expression. In contrast, the late loop involves the regulation of the EGF-stimulated response by newly synthesized proteins and RNAs. Activation of the late loop leads to modulation of cellular functions such as metabolism and membrane biogenesis. The secondary response also leads to an establishment of a newly acquired cellular state, *e.g.* in a process of epithelial-mesenchymal transition, in which highly organized epithelial cells lose their polarity and become motile (Avraham and Yarden, 2011).

Receptor endocytosis (described later in **Chapter 1.3**) is perhaps the most prominent signal attenuator. It is also the first step for the activated receptor towards lysosomal degradation, thus allowing for desensitization from continuous ligand stimulation (Beguinot *et al.*, 1984; Roepstorff *et al.*, 2009). Endocytosis removes growth factor receptors from the plasma membrane; however, signalling is not simply abrogated upon receptor internalization, but rather continues from within endosomes (Vieira *et al.*, 1996) (described in more detail in **Chapter 1.3.4**). In general, acidic pH of the endosomes leads to the dissociation of the ligand-receptor complexes. As described in **Chapter 1.2.3**, different ligands vary in their affinity for EGFR, and some dissociate from EGFR earlier than others, thus leading to signal attenuation and receptor recycling, *e.g.* TGF-α. Other ligands, *e.g.* HB-EGF, bind EGFR more efficiently and therefore do not dissociate from the receptor until the endosomes become highly acidic (Roepstorff *et al.*, 2009).

Apart from internalization, EGFR dephosphorylation by phosphatases is another mechanism of signal attenuation. For example, receptor-type protein-tyrosine phosphatase-κ (RPTP-κ) has been shown to dephosphorylate EGFR in human keratinocytes, and RPTP-κ knockdown (KD) resulted in increased EGFR and Erk phosphorylation both at the basal levels, and following EGF stimulation (Xu *et al.*, 2005). Therefore, EGFR dephosphorylation leads to inhibition of EGF signalling. In addition to dephosphorylation, ubiquitylation (described in more detail in **Chapter 1.3.3**) also contributes to signal downregulation. Ubiquitylation, a post-translational modification that involves the attachment of ubiquitin to lysine residues on a target protein, has been proposed to be critical for lysosomal targeting and degradation of EGFR, but not for EGFR endocytosis (Staub and Rotin, 2006; Huang *et al.*, 2006a; Seshacharyulu *et al.*, 2012). This has been shown with the EGFR mutants, in which several lysine residues within the kinase domain were mutated to arginines; these mutants were poorly ubiquitylated and failed to undergo degradation when compared to the wild-type EGFR (Huang *et al.*, 2006a).

There are several proteins described to act as negative regulators of EGF signalling. For example Mig6/RALT is an adaptor protein that has been shown to interact with the tyrosine kinase domain of EGFR following ligand binding and to inhibit EGF signalling (Zhang *et al.*, 2007). *Mig6* knockout mice showed hyperactivation of EGFR and downstream signalling pathways, further supporting the suppressive effects of Mig6 on EGF signalling (Ferby *et al.*, 2006). Fibroblast growth factor receptor substrate 2β (FRS2β) has similarly been shown to act as an EGFR inhibitor. FRS2β has been found to bind EGFR independently of ligand stimulation and to inhibit EGFR autophosphorylation following EGF treatment, through interaction with Erk2 (Huang *et al.*, 2006b). Another example includes suppressors of the cytokine signalling (SOCS) and leucine-rich repeats and immunoglobulin-like domains 1

(LRIG1). Expression of both groups of proteins is enhanced following EGF stimulation, and they have been proposed to recruit the E3 ubiquitin ligases RING-box protein 1 (RBX1) and Cbl, respectively, resulting in EGFR ubiquitylation and degradation (Gur *et al.*, 2004; Kario *et al.*, 2005; Gotoh, 2009).

1.2.6 EGF signalling in development

EGF was first isolated from the salivary gland of mice, and characterized as a factor promoting eyelid opening and teeth development (Cohen, 1962). Following from this discovery, numerous approaches were undertaken to investigate the functions of EGF and EGF signalling in development. Removal of salivary glands resulted in reduced EGF levels in mice, and this led to a decrease in the thickness of the epidermis (Tsutsumi *et al.*, 1987), and in reduced size of the mammary glands (Okamoto and Oka, 1984). Further studies with dominant negative EGFR confirmed the functions of EGF signalling in development of the mammary duct (Xie *et al.*, 1997), whereas a point mutation within the EGFR kinase domain which dramatically impaired EGFR kinase activity, led to abnormalities in skin development (Luetteke *et al.*, 1994). Studies on mice with disrupted *EGFR* gene revealed that EGF signalling is critical for embryogenesis; depending on the genetic background, disruption of the *EGFR* gene led to early or late embryonic death, or post-natal death, due to multiple organ failure (Threadgill *et al.*, 1995). Similar studies emphasized the functions of EGF signalling in epithelia development, and impaired epithelial maturation in mice lacking functional *EGFR* gene has been proposed as a cause for a multiple organ failure (Miettinen *et al.*, 1995). On the other hand, mice injected with EGF showed delay in body weight gain and in neurobehavioural development (Calamandrei and Alleva, 1989). These studies established EGF signalling as a critical determinant in proper embryo development. Examples of EGF signalling functions in this context are presented in **Table 1.1**.

Skin	Differentiation and survival of keratinocytes Development of hair follicles Hair cycle progression
Lung	Maturation of type II pneumocytes Branching morphogenesis
Heart	Differentiation of valve mesenchymal cells Formation of semilunar valves
Brain	Survival of cortical astrocytes Migration of postmitotic neurons Controling migration and/or differentiation of astrocytes
Bone	Inhibition of chondrocyte and osteoblast differentiation Proliferation of osteoblasts
Liver	Proliferation of hepatocytes Liver regeneration

Table 1.1. Multiple functions of EGF signalling in development and physiology

Examples of the functions for the EGF signalling in organogenesis. Adapted from (Sibilia *et al.*, 2007).

1.2.7 EGF signalling in cancer

Due to multiple signalling pathways activated downstream of EGFR which promote cell proliferation, migration and survival, as described in **Chapter 1.2.4**, it is understandable that misregulation of EGF signalling may lead to uncontrolled cell proliferation and ultimately cancer. *EGFR* gene amplifications, aberrant EGFR expression and mutations within the *EGFR* gene have all been found in different types of cancer (Avraham and Yarden, 2011). For example, mutations within the *EGFR* gene can contribute to ligand-independent receptor activation (Normanno *et al.*, 2006; Lemmon and Schlessinger, 2010). In particular, mutant EGFRs frequently display a basal level of activation, which is sufficient to stimulate downstream signalling cascades, but insufficient to target EGFR for degradation (Avraham and Yarden, 2011).

The majority of high-grade astrocytic gliomas exhibit EGFR overexpression and this has been correlated with *EGFR* gene amplification (Libermann *et al.*, 1985; Kuan *et al.*, 2001). EGFR overexpression has been further identified as a result of both gene amplifications and increased transcription, and has been linked to early stages of tumorigenesis in several cancer types, such as oral, lung and prostate cancers (Grandis and Sok, 2004). In the case of non-small cell lung cancer (NSCLC), which represents the majority of all lung cancers (Sharma *et al.*, 2007), EGFR has been found overexpressed in over 60 % of cancers (Hirsch *et al.*, 2003), and increased EGFR levels have been associated with shorter survival (Veale *et al.*, 1993). Additionally, in a subset of NSCLCs activating mutations within the *EGFR* gene have been shown to lead to activation of downstream signalling cascades, and drugs targeting EGFR kinase activity are currently in clinical use (Hirsch *et al.*, 2003; Sharma *et al.*, 2007). Similarly, EGFR overexpression has been identified in approximately 70 % of colorectal tumors and has been associated with increased cancer cell metastasis, and monoclonal

antibodies targetting EGFR are currently in use for a subgroup of patients with this type of cancer (Radinsky *et al.*, 1995; Yarom and Jonker, 2011).

As mentioned above, mutations within the *EGFR* gene may also promote cancer development. For example, an in-frame deletion mutant of EGFR, EGFRvIII, with deletion of exons two through to seven, has been reported to be constitutively active and oncogenic. This has been suggested to be the most common in-frame deletion mutant of EGFR and to be exclusively expressed in cancers, such as brain, breast, lung and prostate cancers (Grandis and Sok, 2004; Seshacharyulu *et al.*, 2012). Additionally in gliomas, tandem duplications of the regions of the *EGFR* gene within the extracellular or intracellular portion of the receptor have been characterized (Kuan *et al.*, 2001). Several mutations within the kinase domain of EGFR have also been detected in a subgroup of patients with NSCLC, *e.g.* in-frame deletions, with overlapping deletion of four amino acids (Leu747, Arg748, Glu749, Ala750), and point mutations of Leu858Arg, Leu861Gln and Cys719Gly (Lynch *et al.*, 2004). All of these mutations have been proposed to drive tumorigenesis, and the patients carrying these mutations have been found to respond to the therapy with EGFR kinase inhibitor; however, an additional mutation within the EGFR kinase domain (Thr790Met) in these tumours has been linked with cancer relapse and acquired resistance to the EGFR inhibitor (Kobayashi *et al.*, 2005).

In addition, infections with some oncogenic viruses have been found to promote EGFR overexpression and activation. For example, the Epstein-Barr virus encodes the latent membrane protein 1, which has been shown to induce expression and activation of EGFR (Miller *et al.*, 1995), and infection with hepatitis B virus has been found to induce EGFR expression in liver cancer cells (Menzo *et al.*, 1993). Finally, EGF signalling plays critical roles in angiogenesis, *e.g.* EGF signalling *via* PI3K has been found to increase mRNA

levels of pro-angiogenic factors, such as vesicular EGF (vEGF) (Petit *et al.*, 1997; Maity *et al.*, 2000).

1.3 Endocytosis and endocytic trafficking

The first reports on the discovery of clathrin-mediated endocytosis (CME) come from the 1960s, when coated pits were seen by electron microscopy to pinch off from the plasma membrane of mosquito oocytes (Roth and Porter, 1964). The pits carrying yolk proteins were pinching off from the membrane and ultimately uncoating. Similar structures were observed following uptake of horseradish peroxidise in the epithelium of the rat vas deferens (Friend and Farquhar, 1967). These studies led to identification of a particular type of endocytosis, known as clathrin-mediated endocytosis (CME) (described below). Clathrin was first isolated and characterised by Barbara Pearse in 1976. She isolated coated vesicles from bovine and pig brains, adrenal medulla and lymphoma cell line and identified clathrin as the major component of these vesicles. She also described lattice structures of clathrin and proposed that the vesicles are coated by a hexagonal and pentagonal network of clathrin subunits (Pearse, 1976). In addition to CME, further studies revealed the co-existence of clathrin-independent endocytosis (CIE), when uptake of cholera and tetanus toxins *via* non-coated invaginations was discovered in liver cells (Montesano *et al.*, 1982).

Endocytosis (internalisation), the process by which a cell absorbs extracellular molecules, *e.g.* hormones, cytokines and growth factors, is prevalent throughout evolution and can be distinguished in plants (Samaj *et al.*, 2004) and recently in bacteria (Jermy, 2010). When a membrane invaginates, a vesicle (or a phagosome in phagocytosis; described below) pinches off from the membrane and traffics within the cell (Soldati and Schliwa, 2006). Internalised cargoes are delivered to various destinations, *e.g.* to lysosomes for degradation, or back to the

plasma membrane for recycling (Sorkin and von Zastrow, 2009). During these processes, internalised molecules provide nutrients and activate multiple signalling pathways, thus providing information for the cell, *e.g.* whether to grow, proliferate or undergo apoptosis. Therefore, endocytosis enables the cell to sense and react to external stimuli.

There are two types of endocytosis described: phagocytosis and pinocytosis. The former involves the engulfment of particles into a phagosome, whereas the latter describes the uptake of fluid, extracellular ligands and integral membrane proteins into a vesicle. In phagocytosis, membrane protrusions surround an object and engulf it with assistance of motor proteins (Soldati and Schliwa, 2006). With respect to the work presented in this thesis, phagocytosis is not investigated and therefore the term endocytosis is strictly limited to pinocytosis. The types of endocytosis are summarised in **Figure 1.4**.

There are many different types of endocytosis, some of which are understood better than the others. The most studied and the best characterised mechanism of internalisation is CME. Clathrin, a protein which regulates the formation of coated vesicles, plays a major role in transport between organelles, plasma membrane and endosomes (Ohno, 2006). Clathrin forms a triskelion composed of three heavy and three light chains, and assembles into lattice structures on the membrane in places enriched in PIP_2 (Madshus and Stang, 2009). Clathrin itself cannot bind membranes, and thus requires adaptor proteins such as adaptor protein complex 2 (AP2), which bind both clathrin and membrane lipids and proteins (Ohno, 2006). Newly formed vesicles pinch off from the plasma membrane with engagement of the GTPase dynamin (Mayor and Pagano, 2007). Upon internalisation, vesicles uncoat and clathrin recycles back to the plasma membrane (Lemmon, 2001).

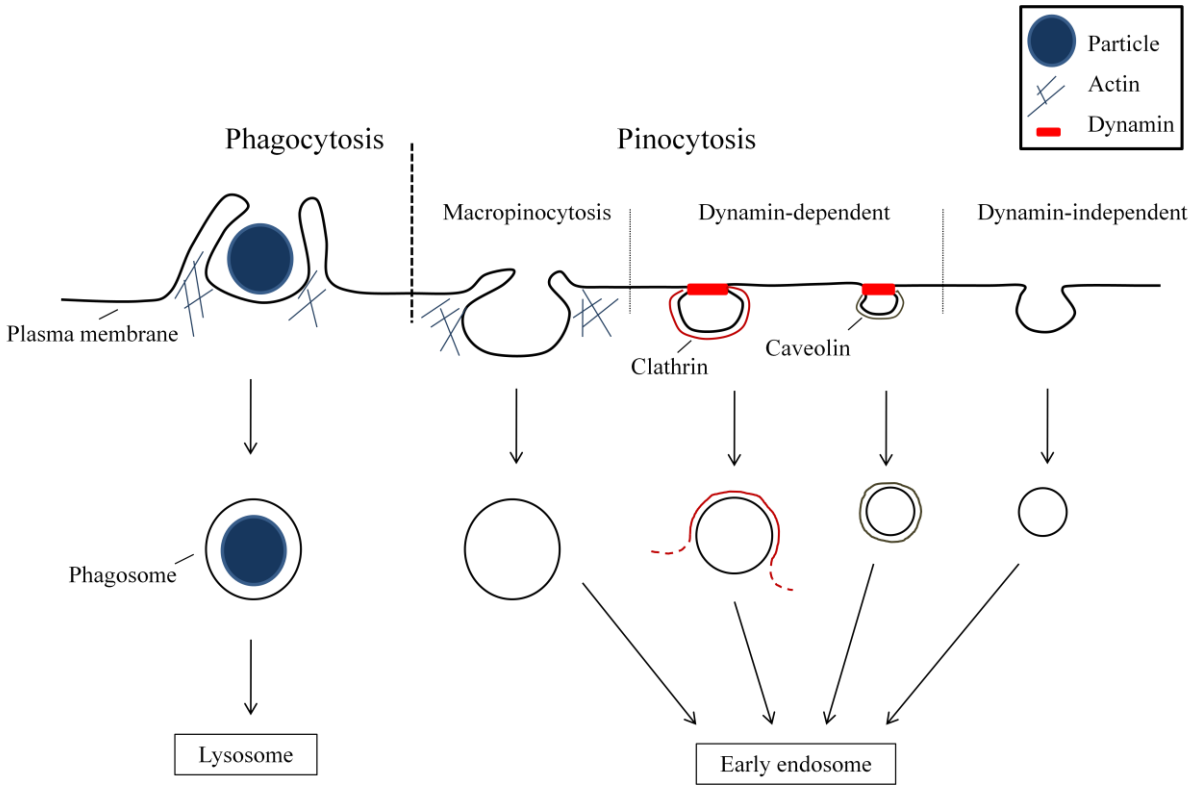

Figure 1.4. Types of endocytosis

Phagocytosis is a type of endocytosis in which a particle is engulfed by membrane protrusions known as lamellopodia. Motor proteins myosins are also involved in this process. In the process of pinocytosis, fluid is engulfed by the plasma membrane. Macropinocytosis morphologically resembles phagocytosis and involves myosins. Clathrin-mediated endocytosis is a dynamin-dependent process, in which dynamin pinches off the vesicle from the membrane. Caveolar endocytosis similarly requires dynamin. Clathrin- and caveolar-independent endocytosis does not require dynamin and is poorly characterised. Upon endocytosis, the vesicles or phagosomes traffic to subcellular destinations. Adapted from (Soldati and Schliwa, 2006; Mayor and Pagano, 2007).

Apart from CME, which is a dynamin-dependent type of internalisation, there also exist an undefined number of CIE pathways, which can be further divided into two major groups: dynamin-dependent and dynamin-independent (Mayor and Pagano, 2007). Caveolar endocytosis, which is the best characterised among CIE, is a dynamin-dependent pathway. In this internalisation route, the vesicles formed are smaller compared to clathrin-coated pits, and are marked by the presence of a protein called caveolin; they are also enriched in sphingolipids and cholesterol (Mayor and Pagano, 2007).

Apart from caveolar endocytotis, another recognised dynamin-dependent pathway is RhoA-dependent internalisation (Mayor and Pagano, 2007). It has been proposed that this pathway requires the action of a small GTPase RhoA to recruit the actin machinery. Other example of CIE dynamin-independent endocytosis is Cdc42-regulated internalization (Mayor and Pagano, 2007). In this pathway, a small GTPase Cdc42 has been proposed to recruit actin-polymerization machinery in a manner which is highly sensitive to cholesterol levels (Mayor and Pagano, 2007). Finally, macropinocytosis is the type of endyctosis considered as a bulk process, morphologically similar to phagocytosis, in which the fluid uptake takes place through large membrane invaginations with involvement of a motor protein myosin (Soldati and Schliwa, 2006).

Following internalisation the vesicle traffics towards early (sorting) endosomes. Interestingly, a novel type of endosomes has been characterised in addition to early endosomes, marked by the presence of Rab5 and Rab5 effectors DCC (deleted in colorectal cancer)-interacting proteins 13 α and β (APPL1 and APPL2), but not early endosome antigen 1 (EEA1) (described in **Chapter 1.3.4**); however, only a minority of internalised EGF has been found

within APPL-positive endosomes and the majority localizes within EEA1-positive early endosomes (Miaczynska *et al.*, 2004a; Miaczynska *et al.*, 2004b).

There are two proposed models of the progression between early and late endosomes. In the first model proposed by Griffiths and Gruenberg in 1991 (Griffiths and Gruenberg, 1991), the early and late endosomes are stable compartments and the carrier vesicles shuttle between them to provide internalised cargo. In support of this model, both early and late endosomes have been shown to have a complex structural organisation, as compared to the carrier vesicles, and to differ in polypeptide composition. Additionally, *in vitro* experiments show that early and late endosomes do not fuse with each other; however, the carrier vesicles have been found to fuse with late endosomes. Finally, the studies with polarised cells identify two sets of early endosomes (apical and basolateral). Both of these sets have been proposed to have a separate population of carrier vesicles, whose content is mixed within the late endosomal compartment, indicating that fusion takes place between carrier vesicles and late endosomes (Griffiths and Gruenberg, 1991).

In the other model proposed by Murphy in 1991 (Murphy, 1991), the endosomes are transient compartments undergoing maturation, during which their composition and properties change. This model argues that the separation of fractions of early endosomes, late endosomes and lysosomes is possible due to rate-limiting steps in the process of endosomal maturation. Furthermore, the early endosomal fraction may also contain recycling vesicles, leading to the observed differences in the composition between early and late endosomes. Further alterations in the content of the cytoplasmic proteins bound to early or late endosomal membranes may result from the pH changes during endosomal maturation, *e.g.* some proteins may dissociate from the membranes upon endosome acidification, since late endosomes are more acidic than

early endosomes (Clague, 1998). Additionally, a study by Rink *et al.* argues that the conversion between Rab GTPases, in particular Rab5 and Rab7 (described in **Chapter 1.3.4**), is a determinant for endosomal progression and that the endosomal cargo becomes progressively enriched in fewer and larger endosomes (Rink *et al.*, 2005). These data therefore also support the maturation model. Nevertheless, Murphy does not exclude the possibility that, while some processes involve endosomal maturation, others may engage carrier vesicles shuttling between compartments. In the process of phagocytosis, in which large molecules are internalised, the maturation model is more preferable, as large particles may not fit into carrier vesicles. In contrast, the stable endosomal model is proposed to be more applicable to the other types of endocytosis (Soldati and Schliwa, 2006).

From early endosomes, the internalised lipids, proteins and other molecules can be delivered back to the plasma membrane, either through fast or slow recycling; the latter involves transit through the perinuclear recycling compartment (PNRC) (Soldati and Schliwa, 2006). Alternatively, the cargo can be delivered to late endosomes and ultimately to lysosomes for degradation, or to the *trans*-Golgi network (TGN), which is the major sorting hub in thesecretory pathway. From TGN the cargo can be delivered to different cellular destinations (Gu *et al.*, 2001; Soldati and Schliwa, 2006).

The vesicles move along microtubules and this is directed by motor proteins, which associate with membrane lipids, membrane proteins or adaptor proteins within the vesicles. Following endocytosis, the vesicles traffic towards the negatively charged microtubule minus-ends. At later stages, microtubule plus-end transport also takes place, *e.g.* between early and recycling endosomes or between *trans*-Golgi network and late endosomes. This bidirectional transport has been proposed to promote scattered distribution of organelles, as well as organelle encounters and fissions (Soldati and Schliwa, 2006). The long-range transport of vesicles and

organelles, *e.g.* from the perinuclear compartments to the cell periphery, has been proposed to involve microtubules, whereas the vesicle trafficking steps during short-range transport are controlled by actin cytoskeleton (Soldati and Schliwa, 2006).

1.3.1 Endocytic trafficking of growth factor receptors

Ligand-bound RTKs activate multiple signalling pathways at the cell surface and undergo regulated endocytosis primarily through clathrin-dependent pathways (Aguilar and Wendland, 2005; Goh *et al.*, 2010; Lemmon and Schlessinger, 2010) (**Figure 1.5**). EGFR has been shown to be internalized at the pre-formed clathrin clusters (Rappoport and Simon, 2009). Nevertheless, a substantial role for clathrin-independent pathways in RTKs internalization has also been proposed, especially when cells are treated with higher ligand concentrations (Yamazaki *et al.*, 2002; Haglund *et al.*, 2003; Sigismund *et al.*, 2005).

In the case of EGFR, ligand binding results in receptor internalization and trafficking towards early endosomes, where it is sorted for recycling or degradation. Stimulation with a particular ligand determines EGFR fate, *i.e.* recycling or degradation, as described in **Chapter 1.2.3**. This has been shown to largely depend on the persistence of ligand binding in the acidic pH of the endosomes. In particular, the majority of ligands which remain bound to EGFR at a relatively low pH (pH 4.0-5.0), such as HB-EGF and BTC, promote increased EGFR ubiquitylation and degradation, whereas the ligands which dissociate from EGFR at higher pH (pH 6.0-7.0), such as TGF-α, promote EGFR recycling (Roepstorff *et al.*, 2009). Endocytosis has been proposed to play a major role in the regulation of signal attenuation, *via* removal of RTKs from the plasma membrane (Lemmon and Schlessinger, 2010).

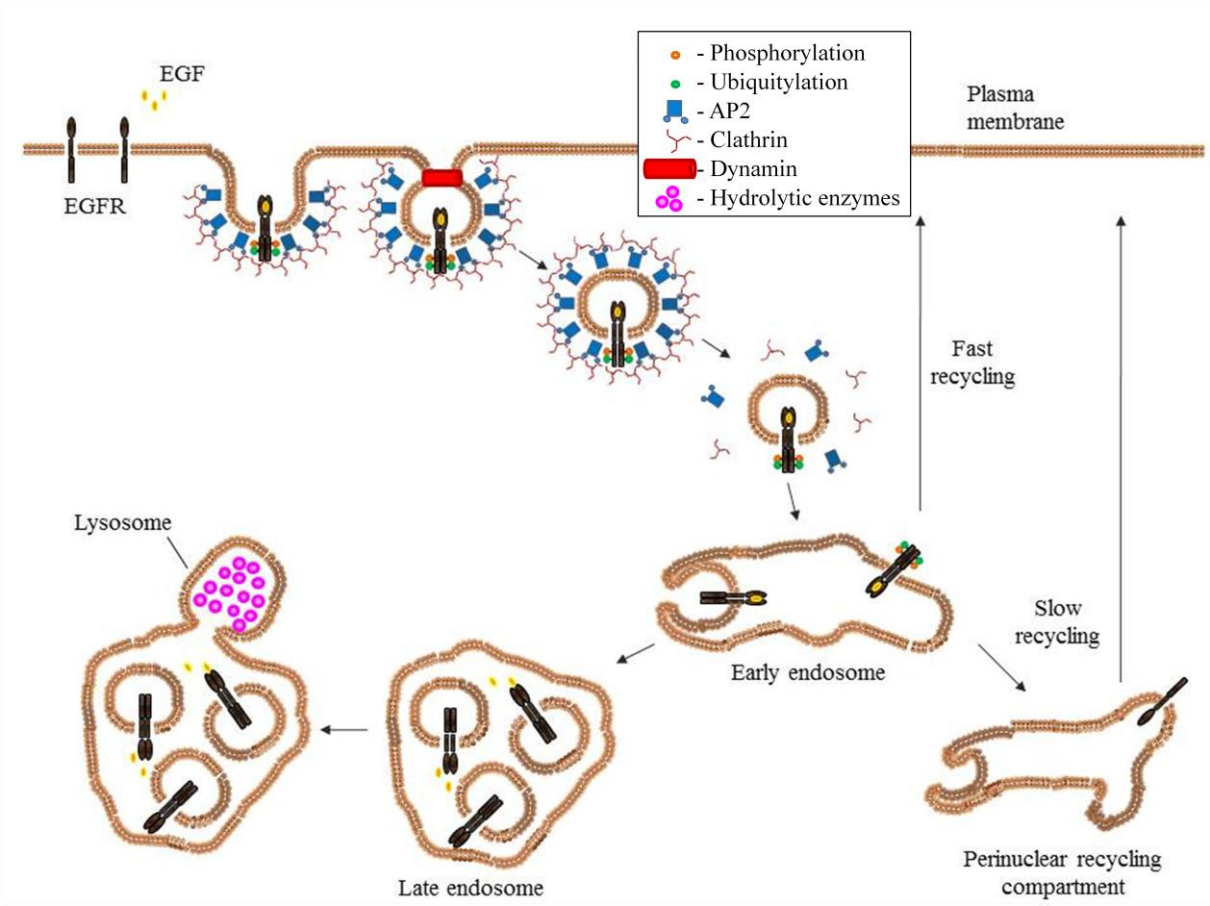

Figure 1.5. Classical endocytic route of EGFR

Upon ligand binding, EGFRs dimerise, *trans*-autophosphorylate and become ubiquitylated. Activated EGFRs undergo clathrin-mediated internalisation, with assistance of adaptor protein 2 (AP2) complex and dynamin. Internalised EGFRs traffic through the endo-lysosomal pathway for degradation. Alternatively, endocytosed EGFRs may be recycled back to the plasma membrane. Adapted from (Soldati and Schliwa, 2006).

Nevertheless, recent reports show that growth factor signalling is not abrogated by receptor internalization, rather it continues from within endosomes (Wang *et al.*, 2002; Miaczynska *et al.*, 2004b; Le Roy and Wrana, 2005; von Zastrow and Sorkin, 2007). Therefore, a strong interplay between RTK trafficking and signalling is emerging, with the suggestion that activated receptors sense signals which control intracellular trafficking, and *vice versa*, subcellular compartmentalisation regulates signalling outcomes.

As described later in **Chapter 1.3.3**, EGFR ubiquitylation has been found to promote EGFR sorting within early endosomes for degradation (Duan *et al.*, 2003) and several proteins and protein complexes have been found to regulate this step. These include Cbl, a RING-domain E3 ubiquitin ligase which mediates EGFR ubiquitylation (Levkowitz *et al.*, 1998; Lipkowitz, 2003), and endosomal sorting complex required for transport (ESCRT) complexes-0 (the hepatocyte growth factor (Hrs)-regulated tyrosine kinase substrate/signal-transducing adaptor molecule (STAM) complex), I, II and III, which regulate EGFR sorting for degradation (Urbe, 2005; Clague *et al.*, 2012). The ESCRT-0 complex recognizes and sequesters ubiquitylated cargo within early endosomes, and recruits the ESCRT-I complex. ESCRT-I and II further concentrate ubiquitylated cargo, whereas ESCRT-III is recruited by ESCRT-II and promotes membrane budding and formation of intraluminal vesicles. Importantly, ESCRT-III does not bind ubiquitin, but it engages deubiquitylating enzymes and other proteins to enable removal of ubiquitin and disassembly of the ESCRT machinery. Ultimately, the ESCRT components are released from the limiting membranes of late endosomes by the action of adenosine triphosphatase (ATPase) vacoular protein sorting 4 (Vps4) (Williams and Urbe, 2007; Roxrud *et al.*, 2010).

Two major ubiquitin-binding domains present within the proteins that recognize ubiquitylated cargo include the ubiquitin-interacting motif (UIM) and the ubiquitin-associated (UBA) domain. Hrs and STAM, two components of the ESCRT-0 complex, both contain the UIMs as well as the N-terminal VHS (Vps27 (yeast homolog of Hrs)/Hrs/STAM) domains, which provide further ubiquitin-binding sites (Clague *et al.*, 2012). These ubiquitin-binding proteins recognise ubiquitylated cargo, such as EGFR, which is designated for degradation. Many components of the ESCRT complexes are monoubiquitylated themselves, thus providing additional opportunities for interactions with ubiquitin-binding proteins (Clague *et al.*, 2012). Furthermore, deubiquitylating enzymes which remove attached ubiquitin moieteies, such as ubiquitin-specific protease Y (UBPY) and associated molecule with the SH3 domain of STAM (AMSH), have also been proposed to regulate degradation of ubiquitylated cargo (described in more detail in **Chapter 1.3.3**). Thus, the fate of ubiquitylated cargo greatly depends on the balance between ubiquitylating and deubiquitiylating activities.

1.3.2 Phosphorylation in endocytic sorting

Post-translational modifications (PTMs) of the EGFR cytoplasmic domains, in particular phosphorylation and ubiquitylation, have been shown to greatly regulate receptor trafficking and signalling (Deribe *et al.*, 2010). Phosphorylation, an attachment of a phosphate to a serine, threonine or tyrosine residue on a substrate, is the most commonly researched PTM that regulates cell signalling. It is catalysed by kinases, and mechanisms have evolved to control the specificity of substrate recognition. In particular, the features of the kinase active site and the docking sites on the substrate ensure substrate specificity. Additionally, the subcellular localization of kinases and/or their substrates may promote or prevent phosphorylation from occuring, as may the presence or absence of the scaffold proteins. Finally, the action of phosphatases results in removal of the attached phosphate groups from

the proteins (Ubersax and Ferrell, 2007). Thus, the processes of phosphorylation and dephosphorylation are tightly controlled by multiple mechanisms.

Protein kinases are the third largest family of genes, representing approximately 2 % of the human genome, and can be divided into two major groups: the serine/threonine kinases and the tyrosine kinases; however, dual specificity kinases also exist which can phosphorylate serine, threonine and tyrosine residues (Ubersax and Ferrell, 2007; Endicott *et al.*, 2012). The majority of kinases show different conformations between inactive and active states and are often activated by phosphorylation, dimerization or by scaffold proteins (Endicott *et al.*, 2012). An active conformation of helix αC within the kinase domain may be stabilised through different mechanisms, *e.g.* through dephosphorylation of Tyr527 followed by phosphorylation of Tyr416 in Src kinase (Cartwright *et al.*, 1987; Kmiecik and Shalloway, 1987), through cyclin A binding to the cylin-dependent kinase 2 (CDK2) which leads to conformational changes and CDK2 activation (Jeffrey *et al.*, 1995), or through dimerisation as in the case of EGFR (described in **Chapter 1.2.2**).

In the process of phosphorylation, a γ-phosphate from adenosine triphosphate (ATP) is transferred onto the hydroxyl group of a tyrosine, serine or threonine residue. In the case of serine/threonine kinases, local negative charges that develop during catalysis have been shown to be stabilised by a lysine residue, which is localized two residues away from the conserved catalytic aspartate, whereas in the tyrosine kinases this role has been assigned to an arginine located four residues away (Endicott *et al.*, 2012). The process of phosphorylation also requires magnesium ions, which regulate the correct orientation of the ATP substrate and additionally stabilise the negative charges during catalysis. Although both ATP and the substrate have an unlimited access to the catalytic site of the kinase, ATP is usually the first to

bind to the catalytic site due to its high concentrations within the cell. Kinetic studies also revealed that the catalytic step is fast and that the rate-limiting factor is release of adenosine diphosphate (ADP) (Adams and Taylor, 1992; Shaffer *et al.*, 2001; Waas *et al.*, 2003).

Phosphorylation events following ligand stimulation have been found to regulate receptor endocytosis, trafficking and signalling. For example, phosphorylation of EGFR pathway substrate 15 (Eps15) by EGFR has been shown to be required for EGFR endocytosis (Confalonieri *et al.*, 2000). Additionally, Src has been proposed to regulate endocytosis through phosphorylation of clathrin heavy chain which promotes clathrin redistribution (Wilde *et al.*, 1999), whereas PKC phosphorylation of EGFR at Thr654 has been found to enhance EGFR recycling and decrease degradation (Bao *et al.*, 2000). Furthermore, protein phosphorylation creates the binding sites for many proteins and lipids that recognise phosphorylated residues, leading to activation of signalling pathways which regulate cellular functions. As the binding between receptor and ligand is preserved within the endosomal membranes, the signalling from receptor dimers continues to activate other molecules (Sorkin *et al.*, 1988; Grimes *et al.*, 1996; Roepstorff *et al.*, 2009).

As mentioned above, the level of phosphorylation is opposed by the action of cellular phosphatases (Ostman and Bohmer, 2001) and the balance between the activity of kinases and phosphatases modifies signalling outcomes. Phosphatases, similarly to kinases, can be divided into two major groups: protein serine/threonine phosphatases (PSPs) and protein tyrosine phosphatases (PTPs), although dual activity phosphatases also exist. In the case of PTP, the catalysis involves the cysteinyl-phosphate intermediate, which then undergoes hydrolysis by the glutamine residue within PTP. In contrast, PSPs catalyse direct hydrolysis of the substrate, without an intermediate and in the presence of metal ions (Barford *et al.*, 1998; Tonks, 2006).

1.3.3 Ubiquitylation in endocytic sorting

Ubiquitylation is the process of a covalent attachment of ubiquitin, a 76 amino acid protein, to a lysine residue within a protein. Ubiquitin attachment has been recognized as a destructive tag and has been shown to promote protein degradation *via* lysosomal and proteasomal degradative pathways. The process of ubiquitylation involves the sequential action of an E1 ubiquitin-activating enzyme, an E2 ubiquitin-conjugating enzyme and an E3 ubiquitin ligase. In particular, ubiquitin has been shown to be activated by the E1 activating enzyme, which transfers ubiquitin moiety to the E2 conjugating enzyme; the E3 ligase has been shown to bind both the E2-ubiquitin thioester and the substrate, and to transfer the ubiqutin moiety onto the substrate. The specificity of the ubiquitylation reaction is conferred by the recognition of particular E3 ligases for particular substrates (Deshaies and Joazeiro, 2009).

Ubiquitin contains seven intrinsic lysine residues (Lys6, Lys11, Lys27, Lys29, Lys33, Lys48, Lys63) which themselves may be ubiquitylated, thus providing additional divergence to the ubiquitin-dependent signalling and trafficking (Chen and Sun, 2009; Clague *et al.*, 2012). For example, monoubiquitylation and Lys63-oligoubiquitylation (attachment of ubiquitin to a Lys63 residue within a ubiquitin moiety) have been proposed to regulate endocytosis and lysosomal degradation, whereas Lys48 polyubiquitylation promotes proteasomal degradation (Chau *et al.*, 1989; Finley *et al.*, 1994; Haglund *et al.*, 2003; Mosesson *et al.*, 2003; Urbe, 2005; Huang *et al.*, 2006a). Lys63 polyubiquitylation has been shown to regulate both proteasomal and lysosomal degradation, as well as to promote RTK endocytosis (Huang *et al.*, 2006a; Lauwers *et al.*, 2009; Saeki *et al.*, 2009; Boname *et al.*, 2010). Additionally, the linear ubiquitin chain assembly complex (LUBAC), an E3 ubiquitin ligase, has been identified to promote formation of linear ubiquitin chains, in which the C-terminal glycine residue of one ubiquitin moiety is linked to the N-terminal methionine residue of another

(Kulathu and Komander, 2012; Tokunaga and Iwai, 2012). Linear polyubiquitylation has been associated with activation of the canonical nuclear factor κB (NFκB) signalling pathway. NFκB activation, which may be triggered by pathogens or pro-inflammatory cytokines such as tumour necrosis factor α (TNFα), requires several ubiquitylation events and formation of the Lys63-linked and linear polyubiquitylated substrates. These then recruit kinase-ubiquitin-adaptor complexes, which activate inhibitor of NFκB (IκB) complex (IKK). Active IKK phosphorylates IκB, leading to its Lys48-polyubiquitylation and degradation. Upon IκB degradation, NFκB translocates to the nucleus and regulates gene expression (Tokunaga and Iwai, 2012). Therefore, ubiquitylation also regulates non-degradative signalling pathways.

In the case of EGFR, ubiquitylation of the lysine residues within the kinase domain has been described (Huang *et al.*, 2006a; Huang *et al.*, 2007; Goh *et al.*, 2010) and EGFR mono- and polyubiquitylation has been found to regulate EGFR trafficking and degradation (Huang *et al.*, 2006a; Eden *et al.*, 2012). Although ubiquitylation has been shown to be dispensable for EGFR internalization (Duan *et al.*, 2003; Huang *et al.*, 2007), it has been found to promote EGFR endocytosis. In particular, mutant EGFR with multiple lysine residues substituted to arginines was poorly internalized (Goh *et al.*, 2010). EGFR ubiquitylation has been found to be critical for EGF-stimulated formation of intraluminal vesicles of late endosomes, and thus for EGFR degradation. This was shown with the negligibly ubiquitylated EGFR mutant, whose degradation was impaired and recycling enhanced due to impaired binding of the ESCRT machinery (Eden *et al.*, 2012).

Furthermore, EGFR deubiquitylation has also been shown to influence EGFR trafficking. For example, knockdown of UBPY deubiquitylase has been found to retain EGFR in clustered endosomes and severly impaired EGFR deubiquitylation and degradation (Row *et al.*, 2006). This is proposed to be due to polyubiquitylation and proteasomal degradation of critical

components of ESCRT machinery, such as Hrs and STAM, which occurs in the absence of UBPY. In contrast, knockdown of AMSH deubiquitylase has been found to enhance EGFR degradation, and AMSH has been suggested to promote EGFR deubiquitylation and recycling (McCullough *et al.*, 2004). Interestingly, AMSH and UBPY both bind the same SH3 domain of STAM and have been suggested to compete for its binding (Kato *et al.*, 2000; Row *et al.*, 2006).

1.3.4 The Rab family of small GTPases in endocytic trafficking

As discussed above, following endocytosis the internalized cargo traffics *via* the endocytic compartments. This movement between different membrane compartments and organelles is regulated by multiple mechanisms and interactions, and the Rab family of GTPases are the most pronounced regulators of the intracellular trafficking (Zerial and McBride, 2001; Stenmark, 2009).

Rab GTPases exist in two conformational states: an active GTP-bound state and an inactive state in a GDP-bound form, as shown in **Figure 1.6**. The switch from inactive to active form is catalysed by guanine nucleotide exchange factors (GEFs) and release of GDP is immediately followed by binding of GTP due to its high concentrations within the cell. When active, Rab-GTPases activate multiple downstream effectors, *e.g.* kinases and phosphatases. The conversion to the inactive form is mediated by GTPase-activating proteins (GAPs) and by intrinsic GTPase activity of Rab proteins, which results in hydrolysis of GTP (Fukui *et al.*, 1997; Wada *et al.*, 1997; Cuif *et al.*, 1999; Chamberlain *et al.*, 2004; Yoshimura *et al.*, 2010).

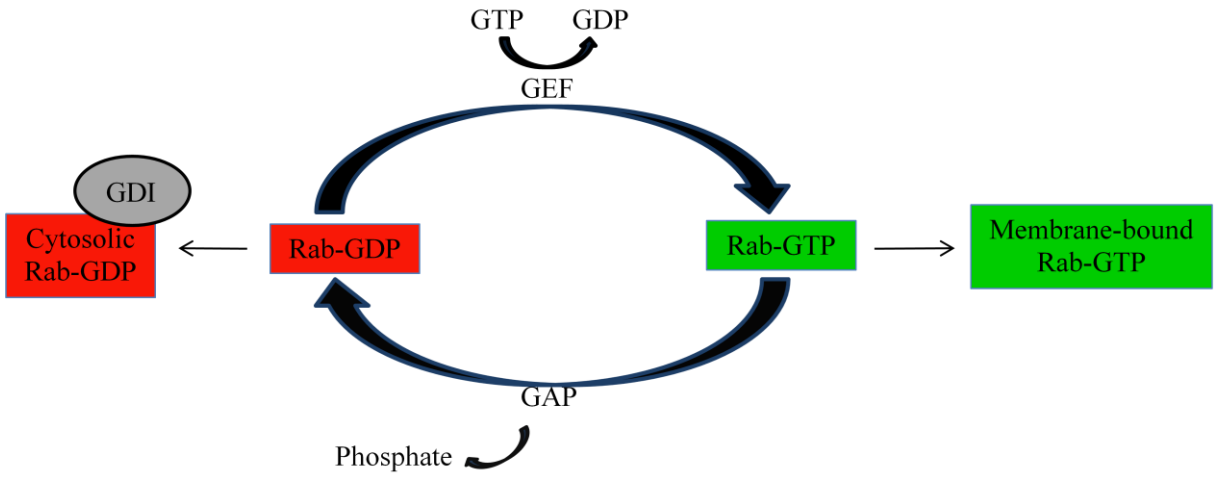

Figure 1.6. Rab-GTPases circuity

Conversion of an inactive GDP-bound form of Rab proteins to an active GTP-bound form is catalysed by guanine nucleotide exchange factors (GEFs), whereas conversion of GTP-to-GDP form is mediated by GTPase activating proteins (GAPs). GDP-dissociation inhibitor (GDI) prevents GDP release and stabilises the GDP-bound form. It also regulates Rab GTPases cycles between the cytosol and the membrane. Adapted from (Stenmark, 2009).

Upon synthesis, inactive Rab proteins are posttranslationally modified by geranylgeranyl transferase, which catalyses an attachment of one or two hydrophobic geranylgeranyl groups onto the C-terminal cysteine residues (Kinsella and Maltese, 1992). This is proposed to enable the Rab proteins to be anchored to the lipid membranes of subcellular compartments. Modified Rab proteins associate with Rab GDP dissociation inhibitors (GDIs) and are transported to their destination by GDI displacement factors (Ullrich *et al.*, 1993; Soldati *et al.*, 1994; An *et al.*, 2003). The specific subcellular localization of different Rab proteins is an important factor in organizing intracellular traffic (Zerial and McBride, 2001).

As explained above, Rab GTPases play fundamental roles at the various stages of membrane trafficking. Examples include regulation of the early endosomal membrane fusion by Rab5 (Stenmark *et al.*, 1994) or regulation of transport from endosomes to Golgi apparatus by Rab9, which promotes formation and docking of transport vesicles (Carroll *et al.*, 2001). Rab5 has also been found to facilitate vesicle uncoating following clathrin-mediated endocytosis (Semerdjieva *et al.*, 2008). Examples of the functions of chosen Rab GTPases are shown in **Figure 1.7**.

Rab proteins also coordinate vesicle motility along microtubules, *e.g.* Rab11 directly and indirectly interacts with the motor proteins myosins (Hales *et al.*, 2002; Roland *et al.*, 2007). Interestingly, plus- and minus-end transport along microtubules is regulated by different members of the Rab family. In particular, the minus-end trafficking of late endosomes has been shown to be regulated by Rab7 effector Rab-interacting lysosomal protein (RILP), which recruits a complex of motor proteins (Cantalupo *et al.*, 2001; Jordens *et al.*, 2001).

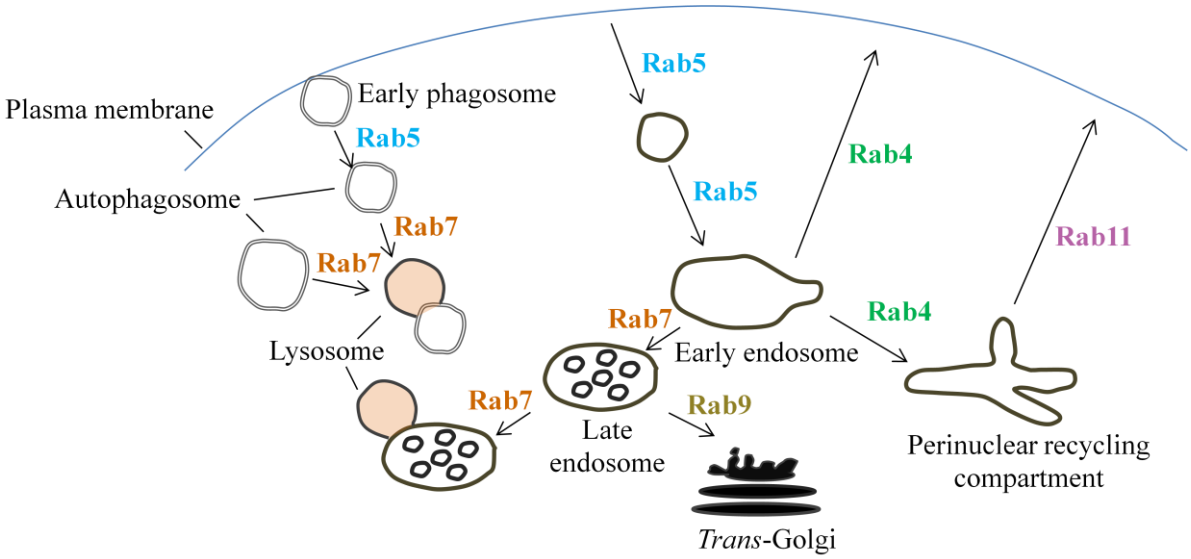

Figure 1.7. Examples of Rab-GTPases function in membrane trafficking

Rab4 regulates fast recycling and trafficking from early endosomes; Rab5 mediates trafficking from the plasma membrane towards early endosomes; Rab7 promotes fusion with lysosomes; Rab9 mediates transport from endosomes to Golgi apparatus; Rab11 regulates slow recycling. Adapted from (Stenmark, 2009).

On the other hand, the plus-end movement of early endosomes towards the plasma membrane has been found to be regulated by the motor protein kinesin and to depend on the activity of Rab5 and its effector vacuolar protein sorting 34 (Vps34) (Hoepfner *et al.*, 2005).

In addition, Rab GTPases are critical for membrane fusion events. This has been widely studied in the case of Rab5, which was shown to promote fusion between early endosomal membranes. In particular, early endosome antigen 1 (EEA1) and rabenosyn 5, two Rab5 effectors, have been proposed to regulate fusion between Rab5-positive vesicles, *via* their association with the components of fusion machinery, such as soluble NSF attachment protein receptor (SNARE) proteins (Stenmark *et al.*, 1994; Christoforidis *et al.*, 1999; Nielsen *et al.*, 2000).

The majority of the effectors are recruited by Rab GTPases from the cytosol, although in some cases the effectors are permamently located within organelles or compartments. This was shown to be the case for Rab1 effector Golgi matrix protein GM130, which is localized within the Golgi apparatus and facilitates the fusion of the vesicles with the *cis*-Golgi network (Moyer *et al.*, 2001).

An interesting feature of the Rab proteins is their specific subcellular localization. For example, the membrane of the early endosomes has been shown to be rich in Rab5, which controls vesicle fusion, and Rab4, which regulates recycling (Chavrier *et al.*, 1990; Vandersluijs *et al.*, 1991; Bucci *et al.*, 1992; Vandersluijs *et al.*, 1992; Clague, 1998). Rab5 has also been found to localize to early and late phagosomes and to regulate autophagosome maturation (Vieira *et al.*, 2003; Ravikumar *et al.*, 2008). Furthermore, recycling endosomes have been demonstrated to contain Rab4, wchich regulates trafficking from early endosomes, and Rab11, which enables delivery to the plasma membrane (Ullrich *et al.*, 1996; Ren *et al.*,

1998). Late endosomes contain Rab7, which controls trafficking to lysosomes, and Rab9 which regulates trafficking to the *trans*-Golgi network (Chavrier *et al.*, 1990; Lombardi *et al.*, 1993; Soldati *et al.*, 1994; Clague, 1998). Rab7 has also been found within autophagosomes and has been shown to regulate the fusion between autophagosomes and lysosomes (Harrison *et al.*, 2003; Vieira *et al.*, 2003). Therefore, several different Rab GTPases can localize to the same compartment, e.g. early endosomes are enriched in Rab4 and Rab5, and recycling endosomes in Rab4 and Rab11. An interesting proposal by Zerial and McBride suggests that when Rab GTPases localize to a particular membrane, they are present within distinct microdomains, which have different composition and function (Zerial and McBride, 2001). These microdomains enriched in a particular Rab GTPase and its effectors would interact with one another, but display a relatively stable composition, and the internalised cargo would traffic sequentially through these microdomains (Zerial and McBride, 2001).

From these characteristics of the Rab family emerges an extremely attractive image of the specific cellular markers which are widely used as a tool for marking distinct subcellular compartments in the fields of cell biology and membrane trafficking.

1.3.5 An intersection between trafficking and signalling

The finding that EGF bound in a highly specific manner to human fibroblasts (Carpenter *et al.*, 1975; Carpenter and Cohen, 1976) was followed by identification of EGF receptor in A-431 epidermoid cancer cells (Cohen *et al.*, 1980; Cohen *et al.*, 1982). Since then, the number of studies investigating the mechanisms and funtions of endocytosis and trafficking of growth factor receptors has blossomed. Primarily, it was thought that EGFR signalling takes place at the plasma membrane, and endocytosis along with receptor trafficking towards lysosomes were perceived solely as mechanisms for signal attenuation; this was proposed by Cohen and

Carpenter in 1979 (Carpenter and Cohen, 1979). Further studies on B-cell antigen receptor (BCR) supported this notion by showing that actin depolarisation along with inhibition of CME sufficiently blocks BCR internalisation, yet leads to prolonged phosphorylation of BCR and Erk signalling (Stoddart *et al.*, 2005). Similarly, studies on the mutant EGFR with truncated C-terminus that did not internalise revealed that EGFR activation at the plasma membrane is sufficient to induce mitogenic responses and thus internalisation and degradation serve as mechanisms for signal attenuation (Wells *et al.*, 1990). Nevertheless, since more and more research has been carried out, the view that the growth factor signalling is not abrogated following endocytosis has emerged, and currently the determination of the signalling outcomes of the receptors at the plasma membrane and within endosomes is a major topic of investigation.

The roles for RTK endocytosis and endocytic trafficking in signal transduction first came into light in 1985 when Cohen and Fava isolated internalised vesicles from A-431 cells, and found phosphorylated and enzymatically active EGFR present within these vesicles, which was able to phosphorylate its substrate (Cohen and Fava, 1985). Following this discovery, they proposed that endocytosis may act as an underlying mechanism for providing active ligand-receptor complexes into intracellular compartments, which activate substrates not available at the plasma membrane. In support of this, similar studies described EGF-bound and active EGFR present within endosomes (Lai *et al.*, 1989). These discoveries suggest that EGFR phosphorylation and activation is not abrogated upon endocytosis, and it may potentially be an important regulator of intracellular trafficking.

In order to to reveal the functions of protein kinases in endocytosis, a genome-wide screen of human kinases has been completed in HeLa cells (Pelkmans *et al.*, 2005). In the study the mRNA levels of human kinases were downregulated using RNA interference (knockdown),

and the consequences were analysed for the internalisation of two viruses: vesicular stomatitis virus (VSV) which enters through CME, and simian virus 40 (SV40) which enters through caveolar endocytosis as well as clathrin and caveolin-independent endocytosis. This screen identified approximately 200 kinases as modulating endocytosis. For example, knockdown of the members of the mTOR signalling pathway inhibited CME of VSV as well as endocytic trafficking of transferrin (Tf), an iron-binding protein that binds Tf receptor (TfR) at the cell surface and undergoes CME. Endocytosis of SV40 was inhibited following depletion of Src and focal adhesion kinase (FAK), which control integrin-mediated focal adhesion assembly, thus indicating that focal adhesion and integrin signalling regulates endocytosis of SV40. Interestingly, knockdown of a subset of kinases promoted VSV and SV40 endocytosis. For example, Ack1 knockdown has been found to promote SV40 internalisation, and it has been proposed that SV40 endocytosis is inhibited by Cdc42- and Ack1-mediated actin polymerisation. In contrast, knockdown of p21-activated kinase PAK1, which is a Cdc42 effector that promotes actin depolymerisation, increased VSV endocytosis and suppressed SV40 internalisation. Therefore, the data presented in this study reveal the complex modulation of CME and CIE *via* the potential signalling networks regulated by particular kinases (Pelkmans *et al.*, 2005).

In addition to EGFR phosphorylation, EGFR ubiquitylation and association with ubiquitin-binding proteins have been proposed as an underlying mechanism for CIE of EGFR. This came into light when the ubiquitin-binding proteins: Eps15, Eps15-related protein (Eps15R) and epsin have been shown to be required for CIE of the EGFR chimera, which was fused to ubiquitin and thus endocytosed exclusively through CIE (Sigismund *et al.*, 2005). This was shown by the triple knockdown experiments (Eps15, Eps15R and epsin knockdown), in which CIE of the EGFR chimera was blocked; however, CIE progressed normally in single

knockdowns thus indicating that these proteins play redundant roles in CIE of EGFR (Sigismund *et al.*, 2005). Furthermore, rescue experiments with Eps15, but not mutant Eps15 unable to bind ubiquitin, were able to restore EGFR endocytosis. Therefore, ubiquitylation has been proposed as a prerequisite for EGFR internalisation *via* CIE. Additionally, triple knockdown also resulted in a substantial reduction in CME, indicating that these proteins also contribute to CME of EGFR. Intrestingly, EGFR degradation, but not downstream signalling, has been shown to be enhanced in the case of CIE, thus suggesting that EGF signalling is more efficient when EGFR enters *via* CME, which is followed by EGFR recycling to the plasma membrane (Sigismund *et al.*, 2005; Sigismund *et al.*, 2008).

Interestingly, the studies on EGFR internalisation show that upon stimulation with low doses of EGF (1-2 ng/ml), EGFR is internalised almost exclusively through CME, whereas upon treatment with high doses of EGF (20-100 ng/ml) approximately half the receptors enter through CIE (Sigismund *et al.*, 2005; Sigismund *et al.*, 2008). These studies also demonstrate that the majority of the receptors entering through CME are recycled back to the plasma membrane, whereas those entering through CIE are almost exclusively degraded (Sigismund *et al.*, 2008). CME has been found to be required for sustained EGF signalling and gene expression following ligand stimulation, as knockdown of the components of CME machinery, such as clathrin or AP2, decreased EGFR recycling and dramatically shortened the longevitity of the Erk1/2 and Akt signalling. Importantly, inhibition of CME or CIE had no effect on phosphorylation of an adaptor protein Shc (Vieira *et al.*, 1996; Sousa *et al.*, 2012). Thus, even though the first phosphorylation events took place under CME inhibition, possibly at the plasma membrane, the prolonged signalling was dramatically reduced indicating that CME is critical for sustained signalling and gene expression downstream of EGFR activation (Sigismund *et al.*, 2008).

Another study supporting the notion that endocytosis is required for signal propagation employed HeLa cells conditionally expressing wild type (WT) or mutant (K44A) dynamin, which inhibits dynamin-dependent endocytosis. This study revealed that phosphorylation of EGFR, Erk1/2 and PI3K subunit p85 were reduced upon inhibition of endocytosis (Damke *et al.*, 1994; Vieira *et al.*, 1996). These results argue that the transit of EGFR through the endocytic system is required to induce complete activation of EGFR and downstream signalling cascades. Interestingly, PLCγ and Shc phosphorylation were increased in the presence of the K44A mutant, and this mutant promoted cell proliferation upon EGF treatment. Therefore, endocytosis-deficient, less phosphorylated EGFR has been found to stimulate cell proliferation, and increased PLCγ and Shc phosphorylation has been counted for enhanced proliferative potential of the endocytosis-deficient cells (Vieira *et al.*, 1996).

Additionally, subcellular distribution of late endosomes has been proposed to affect EGF signalling (Taub *et al.*, 2007). In particular, when endosomes were mislocalized to the cell periphery due to disrupted transport of the organelles toward the cell centre, the activation of EGFR downstream targets Erk, p38 (MAPK) and transcription factors following EGF treatment was enhanced, whereas EGFR degradation was delayed. In contrast, clustering of the late endosomes in the perinuclear region due to expression of a dominant-active Rab7 had different effects on signalling outputs. In this case, activation of Erk was also enhanced and EGFR degradation was reduced; however, activation of p38 (MAPK) was not affected, whereas activation of transcription factors was decreased (Taub *et al.*, 2007). Therefore, EGFR subcellular localization and trafficking *via* endocytic compartments have further been proposed to modulate signalling outputs.

In contrast to the presented reports on the regulation of cell signalling by endocytosis and endocytic trafficking, the global analysis of the function of endocytosis in RTK signalling reveals that EGFR endocytosis is dispensable for activation of several major signalling pathways. The study was performed on isotopically labelled HeLa cells in order to quantitatively characterise the changes in protein phosphorylation following administration of dynasore, which inhibits dynamin-dependent internalisation (Omerovic *et al.*, 2012). Cells were additionally treated with EGF to determine proteins activated upon EGF treatment. The data show that several signalling cascades are initiated by receptors arrested at the plasma membrane, indicating that endocytosis is dispensable for their activation. In particular, several kinases regulating MAPK signalling pathway, such as MAPK1, MAPK7 and MAPK14, have been found to be phosphorylated upon EGF stimulation independently of dynasore treatment. Other EGF-sensitive proteins phosphorylated in the presence of dynasore include Cbl, PLCy, Eps15 and Erk1. In contrast, the members of the ESCRT machinery involved in endosomal sorting have been identified as sensitive to inhibition of endocytosis, and phosphorylation of Hrs, STAM and Rab7 has been found dramatically decreased in dynasore-treated cells (Omerovic *et al.*, 2012). The requirement for EGFR endocytosis to phosphorylate Hrs has further been shown with mutant (K44A) dynamin, as well as with incubation in hyperosmotic medium, both of which have been shown to inhibit endocytosis (Heuser and Anderson, 1989; Urbe *et al.*, 2000). Therefore, endocytosis has been proposed to be dispensable for activation of several signalling pathways, but to be critical for phosphorylation and activation of the ESCRT components.

Further support of the notion that endocytosis is not a prerequisite for activation of particular signalling cascades comes from the study of mouse fibroblasts with inducible knockout of dynamin (Sousa *et al.*, 2012). In these cells ligand-induced EGFR endocytosis was inhibited,

yet EGFR phosphorylation and ubiquitylation were both increased. Interestingly, whereas activation of Erk was similar to the control, activation of Akt was enhanced in dynamin knockout cells. Together these results indicate that RTK signalling occurs predominantly at the plasma membrane and that ligand-induced endocytosis and trafficking act as the mechanisms for signal attenuation.

In summary, an intersection between signalling and trafficking pathways is unclear and data exist supporting the regulation of signalling by endocytosis and endocytic trafficking, and the modulation of trafficking by cell signalling.

1.4 Autophagy

Apart from lysosomal degradation which is the classical way of RTK degradation (described in more detail in **Chapter 1.3.1**), there exist other non-canonical degradative pathways, *e.g.* autophagy (Kraft *et al.*, 2010). In this process, ubiquitylated protein aggregates, organelles and bacteria are engulfed in double-membrane structures called autophagosomes, which fuse with lysosomes to undergo degradation (Kraft *et al.*, 2010). The schematic process of autophagy is presented in **Figure 1.8**.

Autophagy (Greek '*self-eating'*) is perceived as one of the mechanisms of programmed cell death, along with apoptosis and necrosis, which is accompanied by autophagosome formation, cell shrinkage and degradation of organelles (Ouyang *et al.*, 2012).

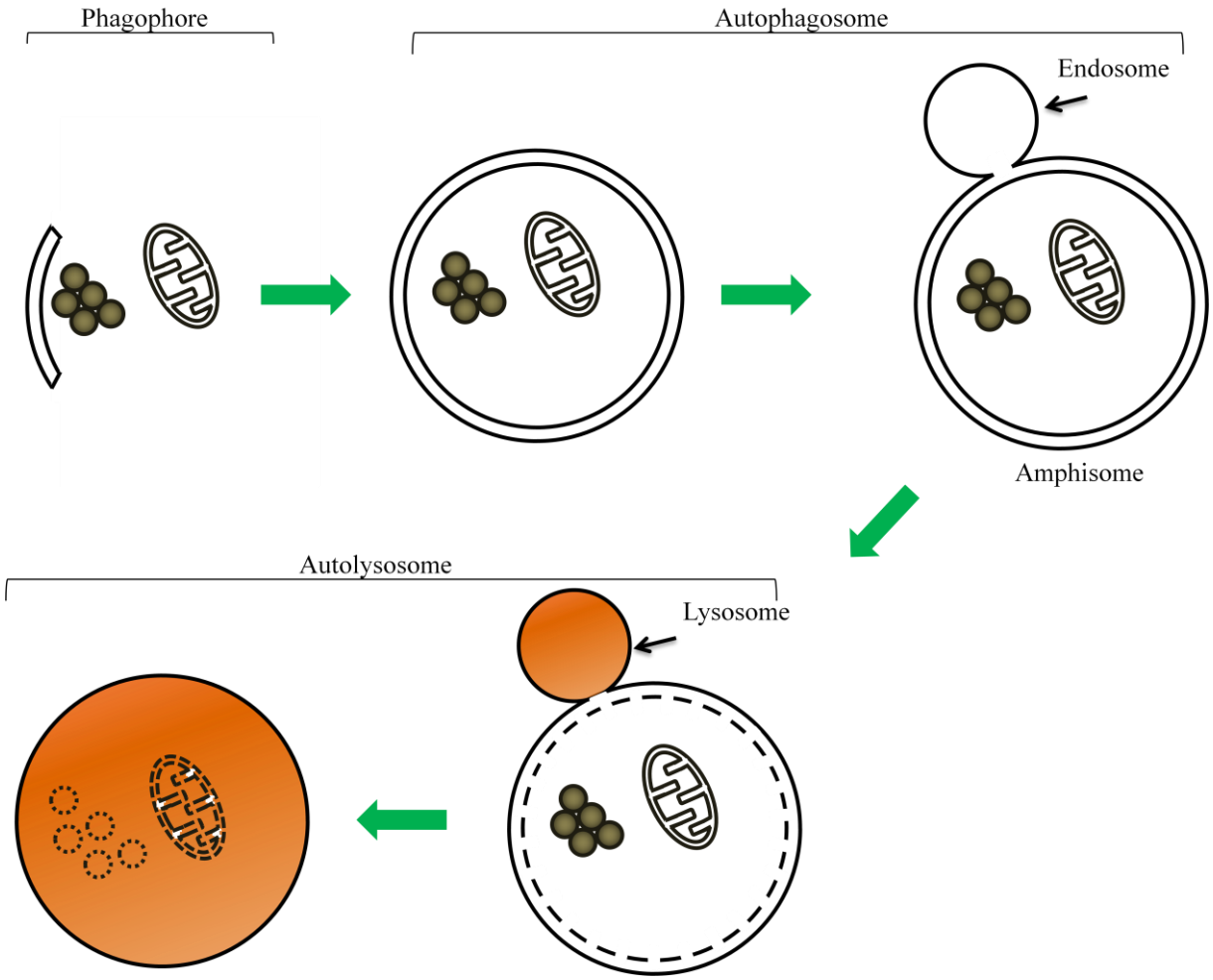

Figure 1.8. The process of autophagy

In the process of autophagy, isolation membranes, or phagophore, engulf ubiquitylated proteins, protein aggregates, organelles and bacteria. Membrane closure results in an autophagosome formation, and fusion with endosomes enables autophagosome maturation. In the final step of the process autophagosome fuses with lysosome, which acidifies the content of autophagosome, thus enabling degradation. Adapted from (Mizushima, 2007; Kraft *et al.*, 2010).

In contrast to apoptosis, the cytoskeletal degradation is delayed until the late stages, along with caspase activity and DNA fragmentation. In contrast to necrosis, autophagy does not induce tissue inflammation (Levine and Yuan, 2005). So far three types of autophagy have been distinguished in mammals. The first type, known as macroautophagy, is the most common and involves formation of double membrane autophagosomes. The second type, microautophagy, describes a direct engulfment of the ubiquitylated cargo by the lysosome. The final type, chaperone-mediated autophagy (CMA), does not require cargo ubiquitylation but rather depends on a sequence recognition by the chaperone complex (Ravikumar *et al.*, 2009). The work presented in this thesis is focused on the first type, macroautophagy, which for simplicity is referred to as autophagy.

On the other hand, autophagy is also perceived as a cell-survival mechanism, providing amino acids and fatty acids during starvation and removing damaged organelles, toxic proteins and bacteria (Levine and Yuan, 2005). Autophagy has long been perceived as a bulk process, in which double membranes randomly engulf the cytoplasm. Nevertheless, recently it has emerged that certain proteins specifically recognise ubiquitylated cargo and target it for autophagosomal degradation.

The source of a double membrane required for autophagosome formation is unclear, with plasma membrane (Ravikumar *et al.*, 2010; Ravikumar *et al.*, 2010), mitochondria (Hailey *et al.*, 2010) and endoplastic reticulum (ER) (Hayashi-Nishino *et al.*, 2009) all proposed to provide the autophagosomal membrane. Interestingly, the ER-mitochondrion interface has been proposed to be the original source of the membrane, whereas other structures to be important for membrane expansion (Lamb *et al.*, 2013). Additionally, fusion of autophagosomes with endosomes has been shown to be required for autophagosome maturation (Razi *et al.*, 2009; Tooze and Razi, 2009). Depending on the cargo engulfed by the

autophagosomal membrane, several types of autophagy can be distinguished. For example, mitophagy is the process of the autophagosomal degradation of mitochondria, aggrephagy – of protein aggregates, pexophagy – of peroxisomes, and xenophagy – of viruses and bacteria (Lamb *et al.*, 2013).

As mentioned above, the process of selective autophagy has been shown to be mediated by several groups of proteins. In particular, a family of autophagy related gene (Atg) proteins have been shown to be essential for autophagosome formation. The Atg proteins, of which there are 35, with 18 being essential during autophagosome formation and throughout the process, were first identified in yeast (Mizushima *et al.*, 2011). Numerous Atg proteins have mammalian homologues, for example microtubule-associated protein light chain 3 (LC3) is an Atg8 homologue in mammals and it associates with autophagosomal membranes. Other proteins implicated in autophagic clearance are sequestosome 1 (p62/SQSTM1) and neighbour of BRCA1 (NBR1), both of which are proposed to act as receptors targeting ubiquitylated cargo for autophagic degradation (Lamark *et al.*, 2009). **Figure 1.9** presents a schematic composition of a phagophore (pre-autophagosomal structure) during autophagosome formation.

One of the mechanisms of autophagy induction by nutrient deprivation is through the inhibition of the mTOR complex 1 (mTORC1) by the TSC1/2 complex. Upon nutrient starvation, the reduction in the ATP to AMP ratio is sensed by the 5'-AMP-activated protein kinase (AMPK).

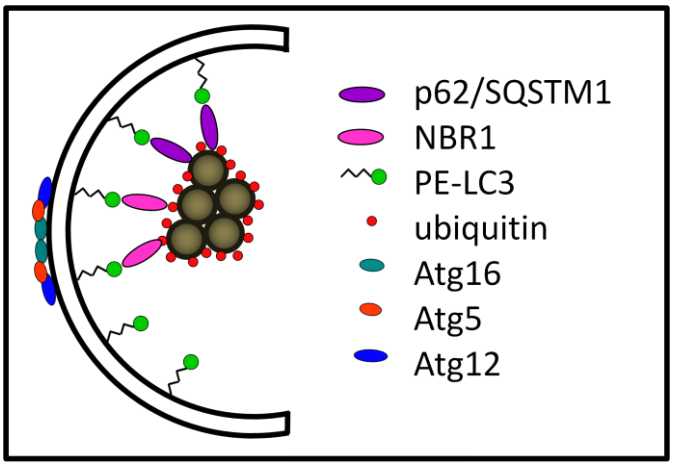

Figure 1.9. Phagophore membrane composition

Atg5-Atg12-Atg16 complex is essential for phagophore formation and it dissociates shortly before or after membrane closure, when the autophagosome is formed. The UBA domain of p62/SQSTM1 recognises ubiquitylated proteins or organelles, whereas the LC3-Interacting Region (LIR) binds LC3, which is conjugated to phosphatidylethanolamine (PE) and isolating membrane.Adapted from (Lamark *et al.*, 2009; Johansen and Lamark, 2011).

AMPK phosphorylates the TSC1/2 complex leading to the inhibition of a small GTPase Rheb, which would otherwise activate mTORC1 (Courtney *et al.*, 2010; Jung *et al.*, 2010) (as described in **Chapter 1.2.4**).

1.4.1 Autophagy-related proteins

Recently, an excellent review by Mizushima *et al.* described the complexity of the processes of autophagosome formation, maturation and degradation, which are tightly regulated by the sequential action of the autophagy-related (Atg) family of proteins (Mizushima *et al.*, 2011). The Atg proteins have emerged as essential throughout the process, from the formation of the isolation membranes (phagophores), membrane closure, autophagosome maturation through to fusion with lysosomes for degradation.

Although autophagy in mammals was first identified and named in 1960s by Christian de Duve following his discovery of lysosomes, which was awarded with the Nobel Prize in Physiology and Medicine in 1974 (Klionsky, 2008), it was not characterised in depth due to technical limitations. In particular, the visualisation of autophagy was restricted to electron microscopy, and the biochemical assays were technically complicated. Subsequent discovery of autophagy in yeast accelerated the investigations into the process, as studying budding yeast was technically less difficult, and the genetic studies were relatively simple. In 1992 Takeshige *et al.* noticed that under starvation, yeast strains deficient in vacuolar proteases accumulated autophagic bodies within the vacuoles (Takeshige *et al.*, 1992). The Atg proteins were then discovered in yeast and later mammalian homologues were also described. So far 35 *ATG* genes have been identified in yeast, and 15 of these (Atg1-10, Atg12-14; Atg16, Atg18, Atg29 and Atg31) have been identified as essential for autophagosome formation (Mizushima, 2007; Nakatogawa *et al.*, 2009; Mizushima *et al.*, 2011).

They can be divided into five complexes: the Atg1/ULK kinase and its regulators complex; the class III PI3K complex; the Atg2-Atg18 complex, Atg9 and other proteins; the Atg12 conjugation system; and the Atg8/LC3 conjugation system. This is summarised in **Table 1.2**.

Initial reports on the functions of the Atg proteins come from 1990s. The protease-deficient strain of yeast was treated with mutagenic agent and placed in starvation medium: the cells which did not accumulate autophagic bodies within the vacuoles were selected, leading to identification of the *Atg1* gene. Since the Atg1 mutants exhibited lower viability under starvation conditions, the loss of viability was further used as a screening test for isolation of other mutants, leading to identification of another 14 *Atg* genes (Atg2-10, Atg12-14, Atg16-17) (Tsukada and Ohsumi, 1993). As different groups named newly characterised genes and proteins in different ways, in 2003 Klionsky *et al.* proposed a unified nomenclature system, and the Atg name is now widely utilised (Klionsky *et al.*, 2003).

The studies in yeast with fluorescently tagged Atg proteins revealed the existence of the pre-autophagosomal structure (PAS), to which several Atg and Atg-related proteins localize (Suzuki *et al.*, 2001). These studies suggest that during starvation, enhanced activity of the Atg1 kinase complex promotes formation of PAS. The Atg12-Atg5 conjugate is also found to be required for formation of PAS and for recruitment of phosphatidylethanolamine (PE)-conjugated Atg8. Furthermore, Atg16 has been found in complex with Atg12-Atg5, and Atg16 along with class III PI3K complex have been proposed to recruit Atg5 and Atg8-PE to PAS. Atg9 has also been shown to regulate Atg8-PE localization to PAS. Additionally, Atg13 and Atg17 (a counterpart of mammalian FIP200 (Hara and Mizushima, 2009)) have been proposed to be essential for Atg1 activation in the first steps of autophagy induction (Kamada *et al.*, 2000).

Mammalian	Yeast	Function
Atg1/ULK kinase and its regulators – promotes autophagosome formation		
ULK 1/2	yeast Atg1	The complex stably associates and localizes to the forming autophagosome
Atg13	yeast Atg13	
Atg101	-	
FIP200	-	
Class III PI3K complex – produces phosphatidylinositol-3-phoosphate (PI3P)		
Vps34	yeast Vps34	The complex produces PI3P thus stimulating autophagy
Vps15	yeast Vps15	
Beclin 1	yeast Atg6 (Vps30)	
Atg14L	yeast Atg14	
AMBRA1	-	
Other proteins: Atg2-Atg18/WIPI complex, Atg9 and others		
Atg2A/B	yeast Atg2	Atg9L1/2, WIPI1-4 and VMP1 localize to the autophagosome membranes; Atg2 and Atg18/WIPI form a complex and regulate Atg9 dynamics; WIPI/Atg18 binds PI3P
Atg9L1/2	yeast Atg9	
WIPI1-4	yeast Atg18	
DECP1	-	
VMP1	-	
Atg12 conjugation system – determines and promotes Atg8/LC3 lipidation site		
Atg12	yeast Atg12	The Atg5-12-16L complex localizes to the outer membrane of the autophagosome and is required for membrane elongation and Atg8/LC3 conjugation
Atg7	yeast Atg7	
Atg10	yeast Atg10	
Atg5	yeast Atg5	
Atg16L1/2	yeast Atg16	
Atg8/LC3 conjugation system – regulates membrane tethering and fusion		
LC3A-C, GABARAP, GABARAPL1, L2 (GATE-16), L3	yeast Atg8	The Atg8/LC3 complex with phosphatidylethanolamine are essential for membrane elongation and closure, and for interaction with p62/SQSTM1, NBR1 and other receptors
Atg4A-D	yeast Atg4	
Atg7	yeast Atg7	
Atg3	yeast Atg3	

Table 1.2. The functions of Atg and Atg-related proteins in autophagosome biogenesis

The Atg proteins required for autophagosome formation in yeast and mammals. Adapted from (Hara and Mizushima, 2009; Nakatogawa *et al.*, 2009; Mizushima *et al.*, 2011).

Furthermore, systematic analysis of the yeast strains expressing fluorescently tagged Atg proteins, in which the *Atg* genes were individually disrupted, led to identification of the hierarchy of PAS organisation, shown in **Figure 1.10** (Suzuki *et al.*, 2007). In this hierarchic model Atg17 acts upstream of PAS formation, and further characterisation of Atg29 and Atg31 revealed that Atg29 and Atg31 form a complex with Atg17 (Kawamata *et al.*, 2005; Kabeya *et al.*, 2007; Kabeya *et al.*, 2009). In mammals structures similar to PAS have also been described as being rich in autophagic factors and closely associated with endoplasmic reticulum (ER) (Itakura and Mizushima, 2010).

Although the function of Atg9 is not fully understood, it is the only integral membrane protein among the Atg proteins; it has been shown to be recruited by Atg17 to PAS, self-associate and promote membrane flow at the early stages of PAS formation (Noda *et al.*, 2000; He *et al.*, 2008; Sekito *et al.*, 2009). Atg8 (mammalian LC3) and Atg12 have been described as ubiquitin-like proteins and their attachment to phosphatidylethanolamine (PE) and to Atg5, respectively, has been shown to be mediated *via* an E1 enzyme Atg7 and the E2 enzymes Atg3 and Atg10, respectively. In particular, the C-terminal glycine residue of Atg8 has been found covalently attached to an amino group of PE, and in the case of Atg12, the glycine residue has been found attached to the lysine residue within Atg5 (Mizushima *et al.*, 1998; Shintani *et al.*, 1999; Tanida *et al.*, 1999; Ichimura *et al.*, 2000). A yeast two-hybrid screen with Atg12 as a bait identified Atg16 interaction with the Atg12-Atg5 conjugate, and Atg16 has further been shown to directly interact with Atg5 and preferentially with the Atg12-Atg5 conjugate. Atg16 has further been found to homo-oligomerise, thus resulting in formation of the Atg12-Atg5-Atg16 complex (Mizushima *et al.*, 1999).

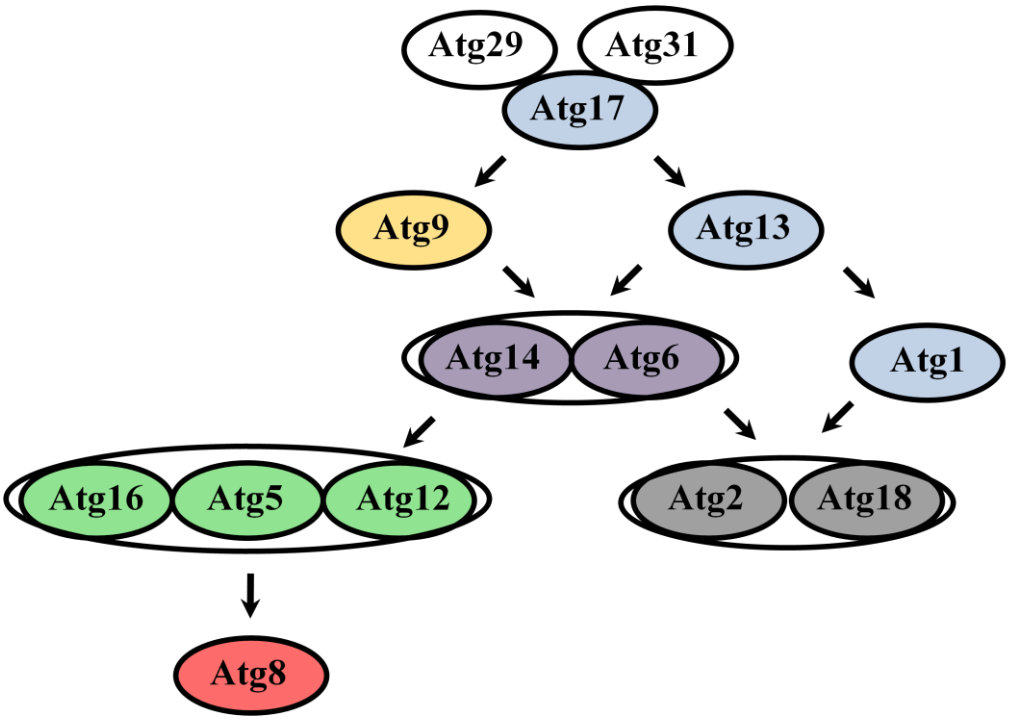

Figure 1.10. Hierarchy of the Atg proteins in autophagosome formation

The proposed hierarchy model of Atg proteins during autophagosome formation. Colours indicate members of the same complexes: Blue: Atg1/ULK complex; Orange: Atg9; Violet: PI3K complex; Grey: Atg2-Atg18/WIPI complex; Green: Atg12 conjugation system; Red: Atg8/LC3 conjugation system; Transparent: Atg29 and Atg31 which form a ternary complex with Atg17. Adapted from (Mizushima *et al.*, 2011).

Interestingly, Atg5 has been shown to localize to pre-autophagosomal structures (phagophores or isolation membranes), but not to enclosed, fully formed autophagosomes or autolysosomes, and has been proposed to dissociate shortly before or after membrane closure. Additionally, conjugation of Atg12 to Atg5 has been found required for the elongation of the isolation membranes (Mizushima *et al.*, 2001). The Atg12-Atg5 conjugate has been identified to recruit Atg8 to a forming autophagosome, and whereas the Atg12-Atg5-Atg16 complex predominantly localizes to the outer membrane of pre-autophagosomal structures, PE-conjugated Atg8 is found on both inner and outer membranes of autophagosomes (Mizushima *et al.*, 2001; Mizushima *et al.*, 2003).

LC3 was first isolated from bovine brain as binding to microtubules and identified as a subunit of the microtubule associated protein 1 (MAP1) (Kuznetsov and Gelfand, 1987). Two forms of LC3 have been since characterised: the cytosolic LC3-I and the autophagic membranes-associated LC3-II (Kabeya *et al.*, 2000). LC3 was found to be present both on the membranes and within autophagosomes. LC3-I is suggested to originate from a newly-synthesized full-length precursor protein upon the C-terminal cleavage by Atg4, which results in an exposure of the C-terminal glycine. Under starvation conditions, LC3-I is further processed into LC3-II, and the amount of LC3-II has been shown to increase along with enhanced autophagosomal activity (Kabeya *et al.*, 2000; Kirisako *et al.*, 2000). The LC3-II form has been shown to be PE-conjugated (Kabeya *et al.*, 2004), and this is critical for isolation membrane elongation, as the Atg3 knockout mice, which are deficient in formation of the PE-conjugated LC3 (LC3-II), show malfunctions in isolation membrane elongation and closure and die within one day of birth (Sou *et al.*, 2008).

Golgi-associated ATPase enhancer of 16 kDa (GATE16) and γ–aminobutyric-acid-type-A-receptor-associated protein (GABARAP), two other mammalian homologues of yeast Atg8, have similarly been found to exist in two forms: cytosolic form I and the autophagosomal membrane-bound PE-conjugated form II (Kabeya *et al.*, 2004). Like LC3, formation of PE-conjugated GABARAP and GATE-16 have been proposed to be modified by subsequent actions of Atg7 and Atg3 (Tanida *et al.*, 2003). Although all of these Atg8 homologues have been found to be essential for autophagosome formation, they act at different stages of this process. In particular, LC3 has been found to regulate membrane elongation, whereas GATE-16 and GABARAP have been shown to be required at later stages of autophagosome maturation (Weidberg *et al.*, 2010).

1.4.2 Sequestosome 1

Sequestosome 1 (p62/SQSTM1) was first identified as a 62 kDa protein that bound the lymphocyte-specific protein tyrosine kinase (LCK), a member of the Src family of kinases which regulates T-cell signalling (Park *et al.*, 1995). Later, two groups independently showed that p62/SQSTM1 binds atypical protein kinases C (aPKCs) and p62/SQSTM1 has been proposed to act as a scaffold protein bringing in close proximity aPKCs and other proteins (Puls *et al.*, 1997; Sanchez *et al.*, 1998). Further studies defined the roles for p62/SQSTM1 in activation of NFκB signalling, which regulates cellular inflammatory responses to tumor necrosis factor α (TNFα) and interleukin 1 (Sanz *et al.*, 1999; Sanz *et al.*, 2000). Since then, multiple functions of p62/SQSTM1 in cell signalling have been discovered.

In the literature, p62/SQSTM1 has a well established role as a scaffold protein and is well recognised for its function in bone remodelling. This came into light when p62/SQSTM1 knockout mice treated with an osteoclastogenic stimulus had severely reduced number of

osteoclasts. Further studies *in vitro* and *in vivo* confirmed the role for p62/SQSTM1 in induced osteoclastogenesis (Duran *et al.*, 2004). Another study with p62/SQSTM1 knockout mice revealed its role in cell metabolism through inhibition of adipogenesis, and p62/SQSTM1 has been identified as a protective factor against obesity and insulin resistance (Rodriguez *et al.*, 2006). Intensive studies into the structure and function of p62/SQSTM1 revealed that it can bind ubiquitylated proteins through its UBA domain (Vadlamudi *et al.*, 1996; Geetha and Wooten, 2002). This led to identification of the p62/SQSTM1 functions in the autophagosomal degradation of ubiquitylated cargo (Vadlamudi *et al.*, 1996; Bjorkoy *et al.*, 2005). In particular, p62/SQSTM1 has been proposed to act as an autophagic receptor that recruits autophagic machinery to the poliubiquitylated cargo and is degraded alongside in the process. Thus, p62 has a well established function in selective autophagy of the ubiquitylated cargo, both as an autophagic receptor and a substrate. Interestingly, p62/SQSTM1 has been proposed to have a protective effect against protein aggregate-induced neurodegeneration, such as Huntington's disease, as p62/SQSTM1 downregulation in cells expressing mutant huntingtin resulted in increased cell death (Bjorkoy *et al.*, 2005).

The structure of p62/SQSTM1 was further analysed and an LC3-interacting region (LIR) has been identified, which mediates direct interaction with LC3 and related Atg8 homologues (Pankiv *et al.*, 2007). Additionally, the domain structure of p62, shown in **Figure 1.11**, also includes the Phox and Bem (PB1) domain, which regulates protein oligomerisation and protein-protein interactions, ZZ-type zinc finger domain and TRAF6 binding domain (Moscat and Diaz-Meco, 2009).

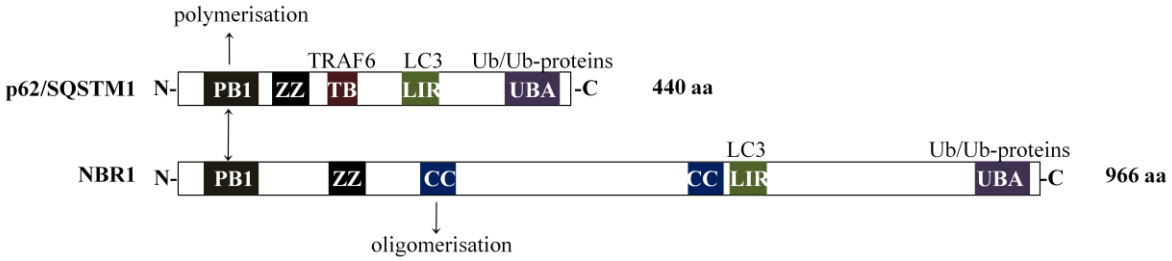

Figure 1.11. Domain structures of p62/SQSTM1 and NBR1

Despite the size differences, the domain structures of p62/SQSTM1 and NBR1 are similar, including N-terminal Phox and Bem 1 (PB1) domain which regulates protein-protein interaction and polymerisation, zinc finger domain (ZZ), LC3-interacting region (LIR) and the C-terminal ubiquitin-association domain (UBA). p62/SQSTM1 also contains TRAF6 binding domain (TB), and NBR1 has two coiled-coil (CC) domains which enable protein oligomerisation. Adapted from (Lamark *et al.*, 2009; Moscat and Diaz-Meco, 2012).

1.4.3 Neighbour of BRCA 1

Neighbour of BRCA1 (NBR1) was originally isolated in a screen with a polyclonal antiserum against ovarian carcinoma antigen, and was identified to have ZZ-type zinc finger and coiled-coil domains. The *NBR1* gene locus was found in the close proximity to the *BRCA1* gene, mutation of which is a predisposing factor for development of breast and ovarian cancer (Hall *et al.*, 1990; Campbell *et al.*, 1994; Teng *et al.*, 2008). Studies into the functions of NBR1 identified several proteins as NBR1 interactors in yeast two-hybrid screen. For example, NBR1 has been found to bind fasciculation and elongation protein zeta-1 (FIZ1), which is a PKC-ζ interacting partner, and thus NBR1 has been proposed to act in PKC-ζ signalling pathway. Another example include calcium and integrin binding protein (CIB), which binds Fnk/Snk and FIZ1 (Whitehouse *et al.*, 2002). NBR1 was further identified as a substrate for the kinase domain of the giant muscle protein titin, thus has been proposed to regulate signalling pathway which controls muscle gene expression (Lange *et al.*, 2005).

Further studies revealed that the PB1 domain present within NBR1 mediates its interaction with p62/SQSTM1, as well as enables self-association (Lamark *et al.*, 2003). Computational analysis also predicted the presence of the C-terminal UBA domain within NBR1 (Dimitrov *et al.*, 2001), which was later shown to bind ubiqutin (Kirkin *et al.*, 2009). NBR1 has been also found to bind the Atg8 homologues *via* the LIR motif and, like p62/SQSTM1, has been proposed to regulate autophagosomal degradation of ubiquitylated cargo (Kirkin *et al.*, 2009). NBR domain structure is shown in **Figure 1.11**. Interestingly, NBR1 also localizes to late endosomes, and Mardakheh *et al.* showed that NBR1 autophagosomal and late endosomal localizations are independent of each other, suggesting that the function of NBR1 in each context may be different (Mardakheh *et al.*, 2010). Additionally, they also showed that NBR1 association with Sprouty-related EVH1 domain-containing protein (Spred2) promotes ligand-

mediated RTK degradation, whereas NBR1 on its own acts as an RTK degradation inhibitor (Mardakheh *et al.*, 2009; Mardakheh *et al.*, 2010).

1.5 Activated Cdc42-associated kinase 1 (Ack1/TNK2)

To fully understand how growth factors and their receptors function within the cell, it is important to investigate binding partners and proteins that regulate RTK internalization and trafficking. One such protein is activated Cdc42-associated kinase 1 (Ack1) alternatively known as tyrosine kinase non-receptor 2 (TNK2); TNK2 being its official gene name (www.uniprot.org) (UniProt, 2012). The name TNK2 was first reported by Howlin *et al.* (Howlin *et al.*, 2008) in a study on breast cancer cells, in which Ack1 depletion reduced the number of cell-surface EGFRs, cell migration and invasion. Manser *et al.* who identified the protein first (Manser *et al.*, 1993) referred to it as Ack1 and, as this is the term that is most widely accepted, the name Ack1 will be used throughout this thesis. Ack1 is a non-RTK (NRTK) that has been implicated in signalling and trafficking of several RTKs, in particular EGFR, but the mechanisms underlying regulation of growth factor signalling and trafficking by Ack1 remain poorly understood (Shen *et al.*, 2007; Grovdal *et al.*, 2008; Lin *et al.*, 2010).

1.5.1 Structure

Ack1 was first identified as a protein specifically interacting with GTP-bound Cdc42 (cell division cycle 42), but not with other members of the same family of Rho GTPases, such as Rac or Rho (Manser *et al.*, 1993). The Ack1 messenger RNA (mRNA) was isolated from the human hippocampus (Manser *et al.*, 1993), where it has been shown to be the most abundant; other tissues with high Ack1 expression include spleen, thymus and liver, although Ack1 has been shown to be ubiquitously expressed (Galisteo *et al.*, 2006).

Ack1 is a relatively large protein with a molecular weight identified as approximately 120 kDa (Mahajan *et al.*, 2005) to 140 kDa (Shen *et al.*, 2007) and it consists of multiple domains, as shown in **Figure 1.12**. For example, Ack1 has been shown to contain a tyrosine kinase domain allowing substrate phosphorylation, and an N-terminal sterile α motif (SAM) enabling protein oligomerization (Mahajan and Mahajan, 2010; Prieto-Echaguee *et al.*, 2010). In addition, the SAM domain has been proposed to mediate membrane localization, as a mutant Ack1 comprising only the SAM and the kinase domain localizes predominantly at the plasma membrane (Prieto-Echaguee *et al.*, 2010). In contrast, full-length protein has been identified to display cytoplasmic localization; however, some reports also describe a potential nuclear translocation of Ack1 (Ahmed *et al.*, 2004; Mahajan *et al.*, 2010). Apart from the tyrosine kinase domain and SAM, Ack1 also contains an SH3 domain (Prieto-Echague and Miller, 2011), which enables binding to proline-rich regions of other proteins. Additionally, the large C-terminal proline-rich region within Ack1 has been identified to bind SH3 domains of other proteins (Prieto-Echague and Miller, 2011).

Interestingly, Ack1 has a unique domain composition among other NRTKs, with the SH3 domain being located C-terminal to the kinase domain (**Figure 1.12**). In other NRTKs, such as Src, the SH3 domain is located N-terminal to the kinase domain, and so it may interact with the C-terminal proline-rich region within the same protein. This comprises an autoinhibitory mechanism which may be abolished, for example, upon phosphorylation (Prieto-Echague and Miller, 2011). It is unclear whether Ack1 in autoinhibited by a similar mechanism. For example, the studies on the crystal structure of Ack1 showed that Ack1 is in an active conformation independently of phosphorylation (Lougheed *et al.*, 2004); however, phosphorylation would slightly increase kinase activity (Yokoyama and Miller, 2003).

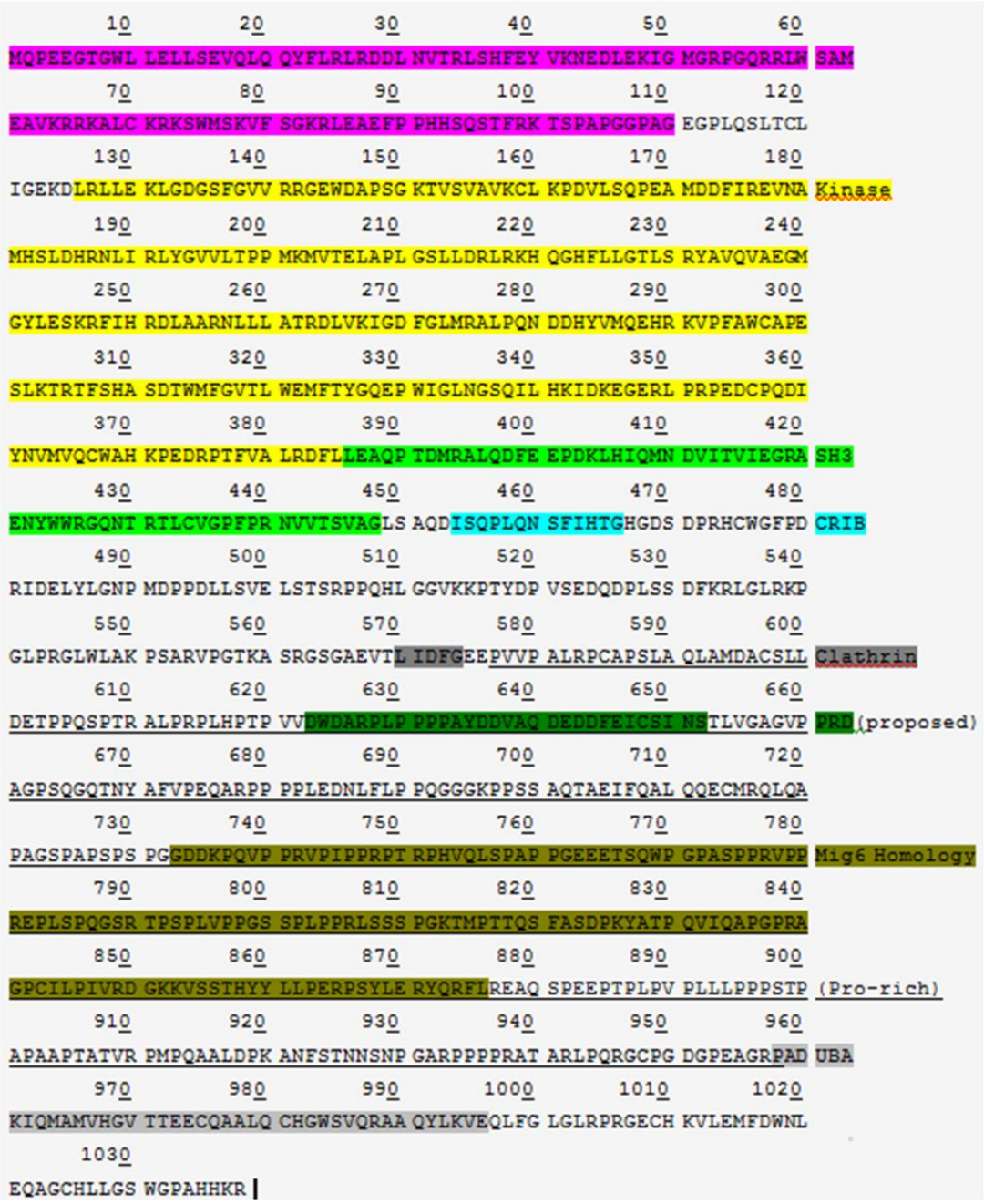

Figure 1.12. Domain structure of human Ack1 (isoform 1)

N-terminal sterile-α motif (SAM) followed by the tyrosine kinase domain, Src homology 3 (SH3) domain, clathrin box (clathrin binding domain), Mig6-homology domain (EGFR binding domain) and the C-terminal ubiquitin-associated (UBA) domain. Underlined is the proline-rich region within the C-terminal portion of Ack1. From UniProt (www.uniprot.org) (UniProt, 2012) and (Teo *et al.*, 2001).

In contrast, a recent study by Lin *et al.* suggests that the SH3 domain of Ack1 interacts with the Mig6-homology domain leading to autoinhibition of the kinase activity, and that the interaction with Grb2 or Cdc42 would release the autoinhibitory state and activate Ack1 (Lin *et al.*, 2012).

Ack1 also contains a Cdc42/Rac interacting binding (CRIB) domain and binds specifically to GTP-bound Cdc42, but not Rac or Rho (Prieto-Echague and Miller, 2011; Miller, 2011). Recently, a clathrin binding domain (CBD) has been identified in the central region of the protein, and Ack1 has been shown to bind clathrin heavy chain (Teo *et al.*, 2001). Additionally, a Mig6-homology domain (Mig6) has been identified within the C-terminal proline-rich region of Ack1, and the Mig6 domain has been shown to be important for EGFR binding (Shen *et al.*, 2007). Finally, a ubiquitin-associated (UBA) domain has been determined at the C-terminus of Ack1 (Prieto-Echague and Miller, 2011), which has been shown to be crucial for mediating interactions with ubiquitin and ubiquitylated proteins, and may potentially be important for targeting ubiquitylated proteins for degradation (Chan *et al.*, 2009).

The Ack family comprises human and murine Ack1, human Tnk1, murine Ack1 (TNK2) and Kos1 (TNK1), bovine Ack2, *Drosophila melanogaster* DACK and DPR2 and *Caenorhabditis elegans* Ark-1 (Galisteo *et al.*, 2006; Miller, 2011). These are schematically shown in **Figure 1.13 a**. There exist three isoforms of human Ack1 and three isoforms of mouse Ack1, shown in **Figure 1.13 b**, which are described at the Universal Protein Resource (UniProt) database (www.uniprot.org) (UniProt, 2012). In humans, isoforms 1 and 3 are relatively similar. In contrast, isoform 2 is much smaller as it is approximately half the size of the full-length protein.

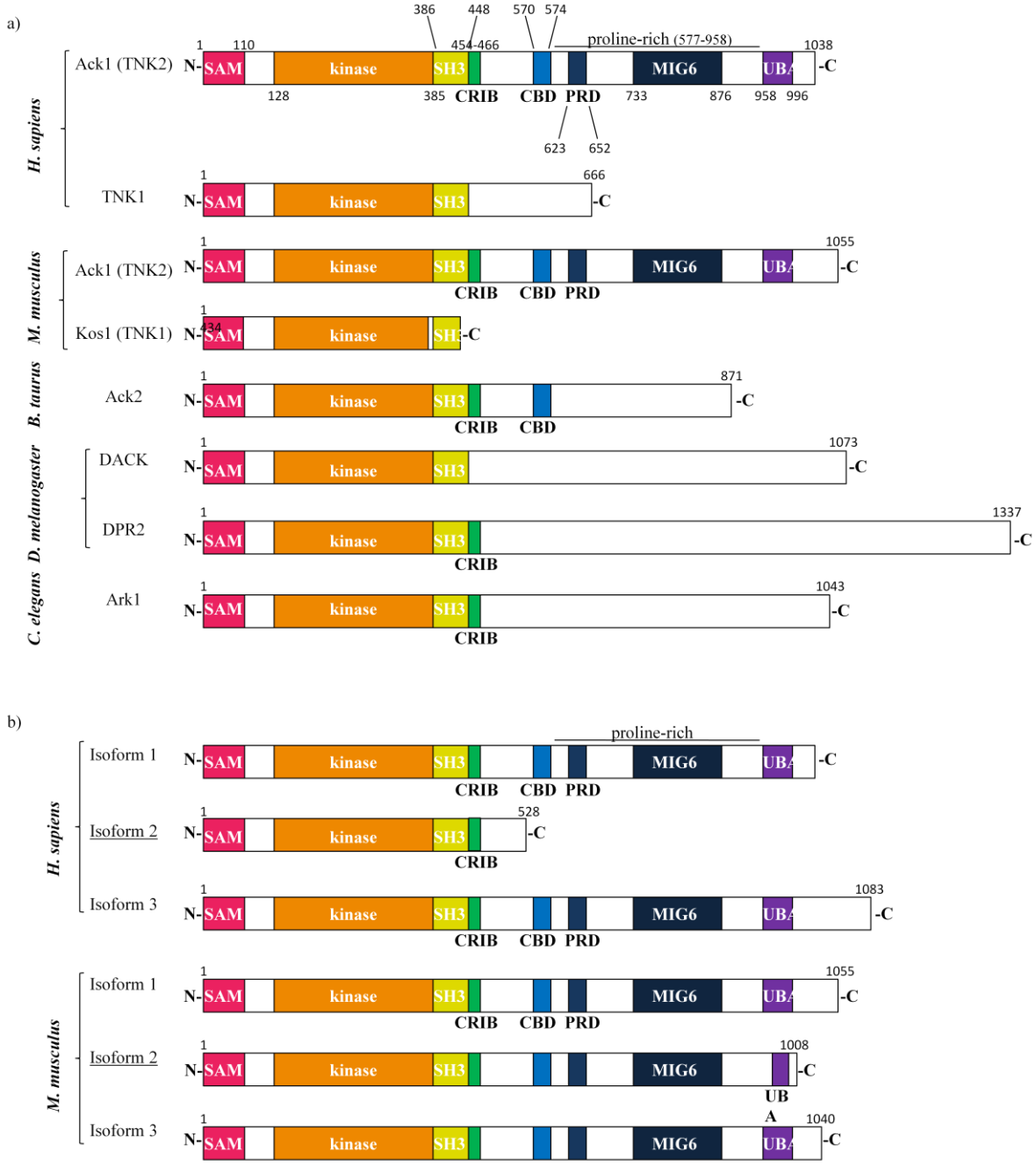

Figure 1.13. Ack1 orthologues and isoforms of human and mouse Ack1

a) Orthologues of human Ack1 (TNK2) and TNK1**; b)** isoforms of human (*Homo sapiens*) and mouse (*Mus musculus*) Ack1; human and mouse isoforms 2 (underlined) were expressed throughtout the study presented. Adapted from (Miller, 2011) and from www.uniprot.org (UniProt, 2012).

There do not exist any experimental data regarding this isoform, and it is speculated that it may be produced at very low levels due to an aberrant mRNA splicing and a premature stop codon within the open reading frame of the *Ack1* gene (www.uniprot.org) (UniProt, 2012). In mouse, all three Ack1 isoforms are relatively similar. For the purpose of the work presented in this thesis, the expression of mouse Ack1 isoform 2 was employed along with human Ack1 isoform 2 (truncated Ack1) (**Figure 1.13 b**).

1.5.2 Function

There are a number of proteins identified to interact with Ack1, some of which are involved in endocytosis and trafficking, *e.g.* clathrin (Teo *et al.*, 2001), sorting nextin 9 (SNX9) and synaptojanin (Yeow-Fong *et al.*, 2005). In addition, Ack1 has been found to interact, directly or indirectly, with several RTKs such as EGFR (Shen *et al.*, 2007), platelet-derived growth factor receptor (PDGFR) (Galisteo *et al.*, 2006) and Mer (Mahajan *et al.*, 2005). Other Ack1 interactors include transcription activators, *e.g.* androgen receptor (AR) (Mahajan *et al.*, 2005; Mahajan and Mahajan, 2010) and adaptor proteins, *e.g.* Grb2 (Pao-Chun *et al.*, 2009). Of note, Grb2 has also been shown to mediate an interaction between Ack1 and several other RTKs, such as Axl, leukocyte receptor tyrosine kinase and anaplastic lymphoma kinase (Pao-Chun *et al.*, 2009). All these interactions reveal a wide range of functions that Ack1 may potentially exert within the cell, *e.g.* during endocytosis, trafficking or signalling. Additionally, Ack1 has also been found to promote carcinogenesis, and both high expression and activation of Ack1 have been linked to cancer development (Mahajan *et al.*, 2005; Mahajan and Mahajan, 2010). Moreover, the *Ack1* gene has been identified as anti-apoptotic when profiling of human kinases, and Ack1 has been shown to promote growth of Ewing's sarcoma, a type of bone cancer (Arora *et al.*, 2010). The carcinogenic properties of Ack1 are described later in **Chapter 1.5.4**.

Looking into the role of Ack1 in more detail, upon interaction with active Cdc42, Ack1 has been shown to phosphorylate p130Cas and promote integrin-mediated cell migration (Modzelewska *et al.*, 2006). Additionally, upon activation by RTKs, Ack1 has been found to phosphorylate Akt, leading to Akt membrane translocation and activation (Mahajan *et al.*, 2010). Ack1 has also been identified to colocalize with clathrin and α-adaptin, a component of AP2 complexes (Teo *et al.*, 2001), thus indicating a potential function in endocytosis. Additionally, moderately overexpressed Ack1 and a kinase-dead Ack1 mutant have been found to stimulate uptake of transferrin (Teo *et al.*, 2001), which is internalised through CME (Le Roy and Wrana, 2005). These results indicate that Ack1 may play a pivotal role in regulating clathrin-dependent internalization *e.g. via* stimulation of clathrin assembly at the plasma membrane. In contrast, highly expressed Ack1 has been shown to inhibit transferrin uptake as a result of clathrin aggregation, thus suggesting that the level of Ack1 expression may influence transferrin internalisation (Teo *et al.*, 2001). In addition to a potential function in endocytosis, Ack1 has also been identified to bind both mono- and polyubiquitin *via* the UBA domain (Shen *et al.*, 2007), and to be ubiquitylated by Nedd4 ubiquitin ligases in response to EGF stimulation (Chan *et al.*, 2009; Lin *et al.*, 2010). These features of Ack1 have been further shown to be essential for regulation of ligand-induced EGFR degradation, as expression of the UBA domain-deletion mutant of Ack1 significantly reduced EGFR degradation when compared to WT Ack1 (Shen *et al.*, 2007).

1.5.3 Ack1 in EGFR trafficking and degradation

Ack1 has been implicated in the regulation of EGFR trafficking and degradation (Shen *et al.*, 2007; Grovdal *et al.*, 2008); however, the precise mechanism of regulation remains unclear. For example, Grøvdal *et al.* (Grovdal *et al.*, 2008) showed that Ack1 partially colocalizes with fluorescently labelled EGF on early endosomes following EGF stimulation. They also found

that high levels of Ack1 expression reduce EGFR internalisation, and this was proposed to be the result of clathrin aggregation. Interestingly, knockdown of the *Ack1* gene expression also inhibited EGFR endocytosis (Grovdal *et al.*, 2008). These data therefore suggest that the level of Ack1 expression is critical for EGFR internalisation. In addition, both overexpression and knockdown of Ack1 led to accumulation of EGF on early endosomes upon EGF stimulation, whereas in control cells the majority of EGF localized to the internal vesicles of late endosomes, thus indicating that Ack1 may play a role in lysosomal sorting of EGFR (Grovdal *et al.*, 2008). Finally, Ack1 knockdown resulted in increased EGF recycling and decreased degradation (Grovdal *et al.*, 2008). These data therefore indicate that Ack1 functions in EGFR trafficking and potentially plays important regulatory roles during EGFR endocytosis, trafficking and sorting for lysosomal degradation.

Another study by Shen *et al.* (Shen *et al.*, 2007) showed that endogenous Ack1 co-precipitates with endogenous EGFR following EGF stimulation, but not pre-EGF treatment. In particular, the interaction first occurs at 5 to 10 minutes following EGF stimulation and is still distinguishable upon three hours of EGF stimulation. In contrast, an interaction between ectopically expressed Ack1 and EGFR is observed much quicker, within one minute of EGF stimulation (Shen *et al.*, 2007). Furthermore, Shen *et al.* also found that ectopically expressed, and not endogenous, Ack1 interacts with activated EGFR at the plasma membrane (Shen *et al.*, 2007). These data therefore indicate that endogenous Ack1 may be restricted within subcellular compartments, from which it may be released following EGF stimulation. In contrast, when Ack1 is overexpressed, it may be readily available for interaction with EGFR close to the plasma membrane (Shen *et al.*, 2007). Importantly, the EGFR tyrosine kinase activity has been found to be essential for this interaction, as both the kinase-inactive mutant of EGFR failed to bind Ack1 and the EGFR tyrosine kinase inhibitor blocked this interaction

(Shen *et al.*, 2007). Additionally, an interaction between Ack1 and EGFR is preceded by EGFR association with Cbl, a ubiquitin ligase, and EGFR ubiquitylation (Shen *et al.*, 2007). This may suggest that EGFR ubiquitylation is required for interaction with Ack1; however, the EGFR mutant unable to bind Cbl has also been shown to bind Ack1, thus indicating that EGFR ubiquitylation may not play a major role and other mechanisms regulate the association between Ack1 and EGFR (Shen *et al.*, 2007). Nevertheless, as mentioned in **Chapter 1.5.2**, expression of the UBA domain-deletion mutant of Ack1 reduced EGFR degradation thus indicating that binding of ubiquitin or ubiquitylated proteins by Ack1 promotes EGFR degradation.

Another important outcome from the work by Shen *et al.* (Shen *et al.*, 2007) is an indication that the Mig6-homology domain of Ack1 is required for EGFR binding (Shen *et al.*, 2007). As described in **Chapter 1.2.5**, Mig6 is an adaptor protein which inhibits EGF signalling (Zhang *et al.*, 2007). Whether Ack1 plays a similar role to Mig6 in this context remains elusive. Further investigation revealed that Grb2 regulates the association between Ack1 and EGFR through binding to the SH3 domain of Ack1 and releasing the autoinhibited conformation (Lin *et al.*, 2012).

1.5.4 Ack1 in cancer

Apart from the important roles that Ack1 may potentially play in endocytosis, trafficking and signalling, the studies also reveal that Ack1 contributes to cancer development and cancer progression. For example, constitutively active Ack1 has been identified to induce tumorigenesis *in vivo* (Mahajan *et al.*, 2005). Additionally, Ack1 has been found to promote cancer metastasis, as Ack1 knockdown inhibited migration of breast cancer cells (Howlin *et al.*, 2008). Furthermore, Ack1 has been shown to bind and phosphorylate tumor suppressor

WW domain-containing oxidoreductase (Wwox), which then may become polyubiquitylated and degraded. This has been shown to result in downregulation of Wwox and hence Ack1 would contribute to carcinogenesis (Mahajan *et al.*, 2005). Phosphorylation of androgen receptor, a transcription factor, by Ack1 has been proposed as another mechanism contributing to cancer progression *via* activation of transcription of genes involved in cancer progression (Mahajan *et al.*, 2007).

Further reports show that Ack1 knockdown results in upregulation of E-cadherin, an indicator of the epithelial phenotype, and downregulation of N-cadherin, an indicator of mesenchymal phenotype (Chua *et al.*, 2010). Epithelial-mesenchymal transition (EMT) is a process in which cells lose their epithelial characteristics, such as polarisation or remaining within the epithelial layer, and acquire mesenchymal characteristics, such as fibroblast-like morphology and high motility. EMT is often observed during malignant transformation and is considered as a hallmark of cancer (Thiery and Sleeman, 2006). Thus, Ack1 has been proposed to contribute to tumorigenesis through promoting EMT (Chua *et al.*, 2010). Interestingly, Ack1 knockdown has been found to sensitize renal carcinoma cells, which express high levels of EGFR, to treatment with EGFR inhibitor, and led to increased cell apoptosis (Chua *et al.*, 2010). These data therefore potentially provide a novel therapeutic approach in cancers with high levels of EGFR expression, to combine the therapy against EGFR and Ack1 in tumors that are resistant for treatment with EGFR inhibitors.

Sequencing of the genome of human cancers revealed several somatic and germline mutations within the *Ack1* gene (Greenman *et al.*, 2007). In particular, somatic mutation Met409Ile has been found in gastric cancer, Arg34Leu in lung cancer, and Arg99Gln and Glu346Lys in ovarian cancer (Greenman *et al.*, 2007). The effects of these mutations on Ack1 function were

further investigated (Prieto-Echaguee *et al.*, 2010). All four mutations have been shown to promote Ack1 autophosphorylation and activation, and Arg34Leu, Met409I and Glu346Lys also resulted in increased cell migration. Additionally, the Glu346Lys mutation has been found to promote anchorage-independent cell growth. This mutation, which is located within the C-lobe of the kinase domain, has been proposed to disrupt the inhibitory interaction between the kinase domain and the Mig6-homology domain, leading to Ack1 activation (Prieto-Echaguee *et al.*, 2010). Another somatic mutation within the UBA domain, the Ser985Asn substitution, has been found to promote cell migration, proliferation and mitogenic signalling. The Ser985Asn mutant was unable to bind ubiquitin and has been shown defective in EGFR downregulation due to reduced EGFR ubiquitylation (Chua *et al.*, 2010).

Interestingly, although *Ack1* knockout mice are not currently available (www.mousephenotype.org), knockout of the *TNK1* gene in mice has been shown to result in formation of spontaneous tumours (Hoare *et al.*, 2008). Therefore, surprisingly, TNK1 has been proposed to function as a tumour suppressor through inhibition of Ras signalling.

1.5.5 Rationale for investigation of Ack1

Previous work by Cunningham *et al.* identified proteins that are phosphorylated downstream of FGFR activation in a Src family kinase (SFK)-dependent manner (Cunningham *et al.*, 2010). Specifically, cells isotopically labelled using stable isotope labelling of amino acids in cell culture (SILAC) technique (described in more detail in **Chapter 7**) were treated with FGF in the presence or absence of the SFK inhibitor. The proteins phosphorylated in FGF-treated cells whose phosphorylation decreased in the presence of the inhibitor were recognised as those implicated in FGF signalling pathway which require SFKs for activation.

Prior to these SILAC experiments, preliminary non-quantitative experiments were performed in which phosphorylated peptides were enriched from FGF-treated cells (D. L. Cunningham, S. M. M. Sweet and J. K. Heath, unpublished work). Ack1 was identified and selected as an interesting molecule to research in the context of FGF due to its known role in EGF signalling pathway (Shen *et al.*, 2007; Grovdal *et al.*, 2008); however, further quantitative studies by Dr. D. L. Cunningham did not confirm Ack1 functions downstream of FGFR activation, neither did the work presented within this thesis (**Chapter 4**).

1.6 Confocal Laser Scanning Microscopy

Current cell biology uses multiple imaging techniques to study the localization, function and dynamics of molecules and compartments of interest. There are a vast number of microscopy techniques which enable understanding of the processes which take place both at the cell membrane and within the cell, *e.g.* total internal reflection fluorescent (TIRF) microscopy, epi-fluorescence microscopy, confocal microscopy, two-photon microscopy and super resolution microscopy. Each of these techniques has its advantages and disadvantages and may be used for a specific purpose, *e.g.* TIRF microscopy allows visualisation of events taking place at the adherent plasma membrane. Throughout this project confocal fluorescent microscope has been used to study subcellular dynamics, a schematic of which is shown in **Figure 1.14**.

The term ‘confocal’ arises from the conjugation of the focal point (‘confocal’) of the lens within an objective with a pinhole, which largely improves image quality by blocking out of focus light. The first confocal microscope was invented by Marvin Minsky in the 1950s (Semwogerere and Weeks, 2005). As a light source he used a zirconium arc lamp, which delivered an intensely bright white light.

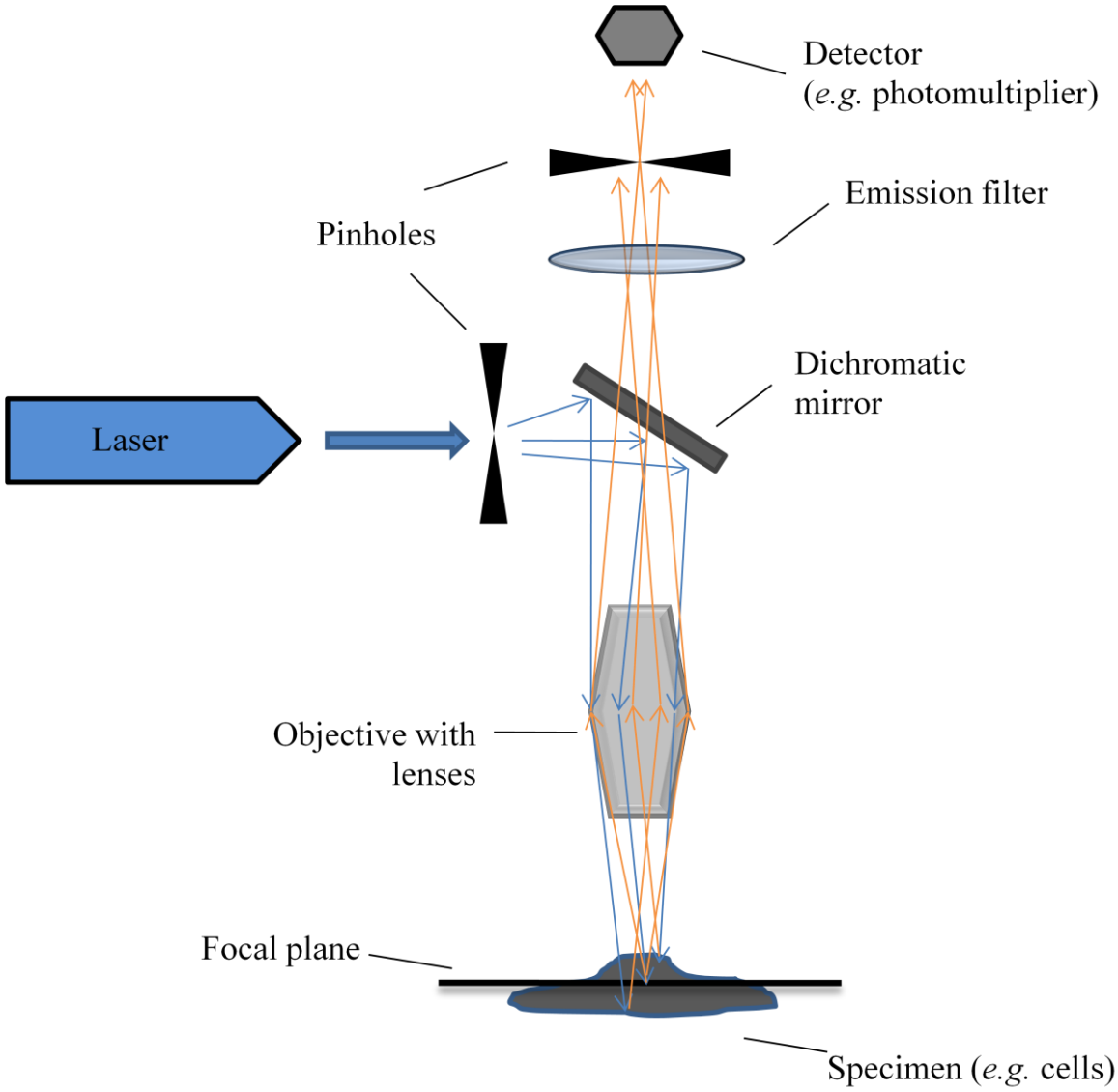

Figure 1.14. Schematic of Confocal Microscope

A laser beam passes through the pinhole and reflects from the dichromatic mirror, and follows through the system of lenses within an objective. The beam excites fluorophores within the specimen, both within the focal plane and outside. The fluorescent light passes through the dichromatic mirror and an emission filter, which selects the emission wavelength and eliminates the excitation light. Adapted from (Semwogerere and Weeks, 2005).

Minsky incorporated two pinholes into his microscope: first after the light source to eliminate scattered light, and the second before the detector to eliminate out-of-focus light. Further elimination of scattered light was obtained by point-by-point illumination of a specimen, due to moving the stage with the specimen. From then, confocal microscopes have developed while retaining the pinhole system and the point-by-point illumination of the specimen, which is typically obtained by the horizontal and vertical scanning mirrors that regulate the light source, a laser beam. Currently the confocal microscopes work either by reflecting the light from the specimen or by promoting fluorescence from the fluorophores present within the specimen. The main drawback is the limitation of the resolution of the confocal microscope images, typically around 200 nm, due to the diffraction of light (Semwogerere and Weeks, 2005).

1.7 Mass spectrometry

Mass spectrometry is an analytical technique that enables ion separation depending on mass-to-charge (*m/z*) ratio. The positively or negatively charged ions are formed during ionisation and are separated by electrical or magnetic field according to their *m/z* ratio. In the mass spectrum, the *m/z* ratio is presented on the *x* axis, and the abundance of an ion on the *y* axis (El-Aneed *et al.*, 2009). There are many different isonisation techniques used in mass spectrometry, ranging from electron impact (EI), chemical ionization (CI), plasma desorption (PD), fast atom bombardment (FAB), liquid secondary ion mass spectrometry (LSIMS), matrix-assisted laser-desorption isonisation (MALDI) and electrospray ionization (ESI). Ions formed through these techniques are analysed according to their *m/z* ratio by a mass analyser (El-Aneed *et al.*, 2009). Additional analysis is achieved by the use of tandem mass spectrometry (MS/MS) techniques, in which a specific ion is selected and undergoes fragmentation. The most common MS/MS techniques used for proteomic analysis include

collision-induced dissociation (CID) and electron transfer dissociation (ETD) (Jones and Cooper, 2011).

CID technique excites ions to collide with the neutral gases, such as helium or nitrogen. This collision results in an increase in an internal vibrational energy leading to the cleavage of the weakest bond within the ion. In peptides and proteins, CID typically results in amide bond cleavage ($N\text{-}C_O$) leading to formation *b* and *y* ions. In CID, labile PTMs, such as phosphorylation , ubiquitylation or nitrosylation (attachment of the nitric oxide group), are cleaved thus limiting localization of the site of modification (Jones and Cooper, 2011).

Unlike in CID, in ETD the cleavage is radical, not thermal, resulting in the preservation of labile PTMs. A trapped gas-phase ion collides with a radical anion (*e.g.* anthracene) resulting in the transfer of a low energy electron. Typically the backbone bond N-Cα is cleaved leading to the formation of *c* and *z* ions, or disulfide bonds. Since its development, ETD (and the similar electron capture dissociation (ECD)) has been widely used for the successful identification of labile PTMs (Jones and Cooper, 2011). In the work presented in this thesis, ESI has been used for ionization, and CID and ETD tandem MS/MS techniques were employed.

2 Thesis Aims

The aim of this thesis is to understand the molecular mechanisms by which Ack1 regulates EGFR trafficking and degradation. As described above, due to extensive actions that EGF signalling exerts within the cell, signal attenuation through endocytosis and degradation of EGF receptor is fundamental for proper cellular function. When these controlling measures are not efficient, this could potentially create a perfect envioronment for neoplastic transformation. In this context, Ack1 implication into EGFR trafficking and degradation have been described previously; nevertheless, the more precise mechanisms of the action remains elusive and incomplete.

Specifically, this work aims to investigate the following:

- Ack1 association with EGFR, whether it is a specific feature of the kinase, or whether it can interact also with other RTKs, such as FGFR (**Chapter 4**)
- Ack1 subcellular localization in steady-state cells, upon serum-starvation and stimulation with EGF (**Chapter 5**)
- Ack1 association with autophagic proteins and its potential involvement in the process of selective autophagy (**Chapter 6**)
- Identification of novel post-translational modifications and Ack1 binding partners through mass spectrometry (**Chapter 7**).

3 Materials and Methods

3.1 Materials

3.1.1 Buffers and solutions

Bacterial culturing:

- Lysogeny broth (LB): 20 % LB broth (Sigma-Aldrich) (w/v)
- Ampicilin plates: LB, 15 g/l bactoagar (BD) 100 mg/l ampicilin (Sigma-Aldrich)
- Kanamycin plates: LB, 15 g/l bactoagar (BD). 50 mg/l kanamycin (Sigma-Aldrich)

DNA manipulation:

- DNA loading buffer (6X) (Invitrogen)
- Tris, borate, ethylenediaminetetraacetic acid (EDTA) (TBE) buffer (5X): 54 g/l Tris (Thermo Fisher Scientific), 27.5 g boric acid (Thermo Fisher Scientific), 0.01 M EDTA pH 8.0 (Sigma-Aldrich)

Protein manipulation:

- Triton X-100 cell lysis buffer: 0.05 M tris (Thermo Fisher Scientific)-hydrochloric acid (HCl) (Thermo Fisher Scientific), 0.15 M sodium chloride (NaCl) (Thermo Fisher Scientific), 1 % triton X-100 (Sigma-Aldrich) (v/v), 0.001 M sodium orthovanadate (Na_3VO_4) (Sigma-Aldrich), 0.05 M sodium fluoride (NaF) (Sigma-Aldrich), 0.025 M β-glycerophosphate (Sigma-Aldrich), complete protease inhibitor cocktail tablets (Roche Applied Science): 1 tablet per 10 ml (contains EDTA; final concentration 0.001 M)
- SDS Sample buffer (2X): 0.125 M tris (Thermo Fisher Scientific)-HCl (Thermo Fisher Scientific) pH 6.8, 20 % glycerol (Thermo Fisher Scientific) (v/v), 4 % SDS (Thermo Fisher Scientific) (w/v), 0.1 % bromophenol blue (Sigma-Aldrich) (w/v), 10 % β-mercaptoethanol (Sigma-Aldrich) (v/v)

- LDS sample buffer (4X) (Invitrogen)
- Reducing agent (10X) (Invitrogen)
- MOPS/SDS running buffer (20X) (Invitrogen)
- Tris-glycine transfer buffer: 0.025 M tris (Thermo Fisher Scientific), 0.2 M glycine (Thermo Fisher Scientific), 10 % methanol (Thermo Fisher Scientific) (v/v)
- Phosphate buffered saline (PBS): PBS pH 7.2 tablets (Oxoid) made up according to manufacturer's instructions
- PBST washing buffer: PBS (Oxoid), 0.1 % tween 20 (Sigma-Aldrich) (v/v)
- PVDF stripping buffer (Li-Cor)
- Immunoblotting blocking buffer: PBS (Oxoid), 50 % odyssey blocking buffer (Licor) (v/v), 0.1 % tween 20 (Sigma-Aldrich) (v/v)

Immunoprecipitation:

for Protein G-Sepharose Fast Flow beads (Sigma-Aldrich)

- Stock solution (2X): 0.1 M tris (Thermo Fisher Scientific)-HCl (Thermo Fisher Scientific) pH 7.4, 0.1 % triton X-100 (Sigma-Aldrich) (v/v), 0.3 M NaCl (Thermo Fisher Scientific)

for Dynabeads Protein G (Invitrogen)

- Wash buffer: PBS (Oxoid), 0.02 % tween 20 (Sigma-Aldrich) (v/v)

for GFP-Trap (Chromotek)

- Dilution buffer: 0.01 M tris (Thermo Fisher Scientific)-HCl (Thermo Fisher Scientific) pH 7.5, 0.15 M NaCl (Thermo Fisher Scientific), 0.0005 M EDTA (Sigma-Aldrich), complete protease inhibitor cocktail tablets (Roche Applied Science): 1 tablet per 10 ml (contains EDTA; final concentration 0.001 M)
- Wash buffer: 0.001 M tris (Thermo Fisher Scientific)-HCl (Thermo Fisher Scientific) pH 7.5, 0.5 M NaCl (Thermo Fisher Scientific), 0.0005 M EDTA (Sigma-Aldrich), complete

protease inhibitor cocktail tablets (Roche Applied Science): 1 tablet per 10 ml (contains EDTA; final concentration 0.001 M)

Antibody cross-linking:

- Wash buffer: 0.2 M triethanolamine (TEA) (Sigma-Aldrich) pH 8.2
- Cross-linking buffer: 0.02 M dimethyl pimelidate dihydrochloride (Sigma-Aldrich), 0.2 M TEA (Sigma-Aldrich) pH 8,2
- Quenching buffer: 0.05 M tris (Thermo Fisher Scientific)-HCl (Thermo Fisher Scientific) pH 7.5
- Elution buffer: 1 M glycine (Thermo Fisher Scientific) pH 3.0

Immunofluorescence:

- Fixation solution: PBS (Oxoid), 4 % paraformaldehyde (Electron Microscopy Sciences) (v/v)
- Alternative fixation solution: methanol (Thermo Fisher Scientific) (-20 °C)
- Wash buffer: PBS (Oxoid)
- Permeabilisation buffer: PBS (Oxoid), 0.1 % triton X-100 (Sigma-Aldrich) (v/v)
- Alternative permeabilisation buffer: PBS (Oxoid), 0.2 % triton X-100 (Sigma-Aldrich) (v/v)
- Blocking buffer: PBS (Oxoid), 10 % goat serum (Invitrogen) (v/v), 5 % bovine serum albumin (BSA) (Sigma-Aldrich) (w/v)
- Antibody solution: PBS (Oxoid), 1 % goat serum (Sigma-Aldrich) (v/v)

Live-cell imaging:

- Cell imaging medium: 10 mM HEPES (Sigma-Aldrich)-Hank’s balanced salt solution (HBSS) (Sigma-Aldrich) pH 7.4

In-gel digestion:

- Gel fixation solution: 55 % methanol (Thermo Fisher Scientific) (v,v), 11 % acetic acid (Thermo Fisher Scientific) (v,v)
- Gel staining with Coomassie: 0.1 % brilliant blue R (Sigma-Aldrich) in gel fixation solution
- Gel destain solution: 7.5 % acetic acid (Thermo Fisher Scientific) (v,v), 5 % methanol (Thermo Fisher Scientific) (v,v)
- Destaining solution: 30 % acetonitrile (JT Baker) (v/v)
- Dehydration and washing buffer: 50 % acetonitrile (JT Baker) (v/v), 25 mM ammonium bicarbonate (Fluka)
- Rehydration and washing buffer: 0.025 M ammonium bicarbonate (Fluka)
- Reduction buffer: 0.01 M dithiothreitol (DTT) (Sigma-Aldrich), 0.025 M ammonium bicarbonate (Fluka)
- Alkylation buffer: 0.055 M iodoacetamide (Sigma-Aldrich), 0.025 M ammonium bicarbonate (Fluka)
- Trypsin resuspension solution: 0.05 M acetic acid (Thermo Fisher Scientific)
- Trypsin digestion solution: 12.5 mg/l trypsin (Promega), 0.025 M ammonium bicarbonate (Fluka)
- Peptide extraction solutions: 50 % and 100 % acetonitrile (JT Baker) (v/v)

TiO_2 enrichment:

- Conditioning solution: 0.4 % trifluoroacetic acid (TFA) (Thermo Fisher Scientific) (v/v), 80 % acetonitrile (JT Baker) (v/v)
- Equilibration solution: 25 % solution B (lactic acid) (Hichram) (v/v), 75 % conditioning solution (v/v)

Desalting:

- Wetting solution: 100 % acetonitrile (JT Baker)
- Equilibration and washing solution: 0.1 % TFA (v/v) (Thermo Fisher Scientific)
- Elution buffer: 0.1 % formic acid (Fisons, Ipswich, UK) (v/v), 50 % acetonitrile (JT Baker) (v/v)

Cell culture:

- Poly-D lysine coating solution: 0.1 g/l poly-D-lysine (Sigma-Aldrich)

3.1.2 Antibodies and Reagents

Table 3.1 and **Table 3.2** present primary and secondary antibodies used in this study, respectively. Additionally, anti-phospho-EGF receptor (Y1045) antibody raised in rabbit was provided by Dr. Elena Odintsova (University of Birmingham, Birmingham, UK) and normal mouse IgG was purchased from Santa Cruz Biotechnology. Alexa Fluor 488- and 568-transferrin conjugates and Lysotracker Red DND-99 were purchased from Invitrogen. The FGF2 was made in-house (work by Miss S. Brewer). Briefly, the protein (155 amino acids; 18 kDa) was expressed in *E.coli* from the bacterial expression vector pFC80 (provided by Dr Antonella Isacchi, Pharmacia & Upjohn, Milan, Italy) and purified by heparin-column chromatography. EGF, heparin sodium salt, albumin from bovine serum (BSA), glycerol-2-phosphate and leptomycin B were from Sigma-Aldrich. FGFR inhibitor SU5402 and EGFR inhibitor BIBX 1382 were from Calbiochem. Fetal bovine serum (FBS) was from Biosera, donor bovine serum (DBS), goat serum (GS) were from Invitrogen. Bafilomycin A1 was purchased from Merck Millipore. Small interfering RNA (siRNA) against TNK2 and non-targeting iRNA control were from Dharmacon. Human cancer cell line blot was purchased from G. Biosciences.

Primary Antibody	Species	Manufacturer	Dilution
GFP (D5.1)	RM	Cell Signalling Technology	1:1000 (WB)
Phospho FGF Receptor (Tyr 653/654)	MM	Cell Signalling Technology	1:1000 (WB)
HA-Tag (C29F4)	MM	Cell Signalling Technology	1:1000 (WB)
EGFR	RP	Cell Signalling Technology	1:1000 (WB)
EEA1	RP	Cell Signalling Technology	1:100 (IF)
Ack1 (A-11)	MM	Santa Cruz Biotechnology	1:25 (IF) - 1:250 (WB)
PLCγ1	RP	Santa Cruz Biotechnology	1:1000 (WB)
Bek (C-17)	RP	Santa Cruz Biotechnology	1:1000 (WB)
Ack1 (C20)	RP	Santa Cruz Biotechnology	1:25 (IF) - 1:1000 (WB)
Flg (C-15)	RP	Santa Cruz Biotechnology	1:1000 (WB)
EGFR (R-1)	MM	Santa Cruz Biotechnology	1:50 (IF)
SQSTM1	RP	Santa Cruz Biotechnology	1:50 (IF) - 1:1000 (WB)
SQSTM1 (clone 2C11)	MM	Abnova	1:50 (IF) - 1:1000 (WB)
Ack1 (phospho Y284)	RP	Abcam	1:1000 (WB)
LBPA	MM	Echelon Biosciences	1:500 (IF)
Rab11	RP	Invitrogen	1:12.5 (IF)
Atg16L	RP	MBL International	1:500 (IF)
Phosphotyrosine 4G10	MM	Millipore	1:2000 (WB)
Phosphotyrosine PY20	MM	MP Biomedicals	1:2000 (WB)
Myc (clone 9E10)	MM	Roche Applied Science	1:2000 (WB)
α-tubulin	MM	Sigma-Aldrich	1:10,000 (WB)

Table 3.1. Primary antibodies used in the study

Table presents primary antibodies used in the study. MM-mouse monoclonal, RP-rabbit polyclonal, RM-rabbit monoclonal. IF-immunofluorescence, WB-Western blotting.

Secondary Antibody	Species	Manufacturer	Dilution
Alexa Fluor 488 Conjugated	Goat anti-mouse	Invitrogen	1:200 (IF)
Alexa Fluor 488 Conjugated	Goat anti-rabbit	Invitrogen	1:200 (IF)
Alexa Fluor 568 Conjugated	Goat anti-mouse	Invitrogen	1:200 (IF)
Alexa Fluor 568 Conjugated	Goat anti-rabbit	Invitrogen	1:200 (IF)
Alexa Fluor 633 Conjugated	Goat anti-mouse	Invitrogen	1:200 (IF)
Alexa Fluor 633 Conjugated	Goat anti-rabbit	Invitrogen	1:200 (IF)
HRP-conjugated IgG (FC)	Goat anti-human	Pierce	1:10,000 (WB)
Odyssey 680	Goat anti-mouse	Li-Cor	1:10,000 (WB)
Odyssey 680	Goat anti-rabbit	Li-Cor	1:10,000 (WB)
Odyssey 800CW	Goat anti-mouse	Li-Cor	1:10,000 (WB)
Odyssey 800CW	Goat anti-rabbit	Li-Cor	1:10,000 (WB)

Table 3.2. Secondary antibodies used in the study

Table presents secondary antibodies used in the study. IF: immunofluorescence, WB: Western blotting.

3.1.3 Plasmid constructs

The murine Ack1 isoform 2 (1008 a.a.) amino terminal myc-tagged in pcDNA3 vector and GFP-tagged in pEGFP-C1 vector were provided by Dr. Wannian Yang (Geisinger, Danville, PA, USA). For mCherry-Ack1, Open Reading Frame (ORF) was subcloned into pmCherry-C1 vector (Clontech). ORF of human Ack1 isoform 2 (528 aa; truncated Ack1) (UniProt Identifier: Q07912-2) in a Gateway (Invitrogen) pDONR vector (Open Biosciences) was subcloned into GFP-pcDNA3 and myc-PRK5 vectors. Human FGFR2-pEGFR-N2 was provided by Prof. John Ladbury (University of Texas M. D. Anderson Cancer Center, Houston, TX). hFGFR1-pcDNA3.1 was provided by Associate Prof. Pamela Maher (Scripps Research Institute, CA, USA), human IgG1 Fc-fused FGFR1 constructs (kinase active, kinase dead, transmembrane and VT-) in pEF-BOS-ires-Topaz vectors were described previously (Burgar *et al.*, 2002). EGFR-pEGFP-N1 was provided by Prof. Alexander Sorkin (University of Pittsburgh, Pittsburgh, PA, USA), pcDNA-3 L61-Cdc42-GFP encoding GFP-tagged constitutively active Cdc42 (caCdc42) was provided by Dr. Neil Hotchin (University of Birmingham, Birmingham, UK). pEGFP-C3-Rab4a and pEGFP-C2-Rab11a were gifts from Prof. Marino Zerial (Max Planck Institute of Molecular Cell Biology and Genetics, Dresden, Germany), vector encoding GFP-tagged Rab7 was provided by Dr. Simon Johnston (University of Birmingham, Birmingham, UK). Rab5-EGFP and Eps15-pEGFP-C2 were provided by Dr. Alexandre Benmerah (Cochin Institute, Paris, France). Ubiquitin/HA fusion in pMT123 vector was provided by Prof. Ronald Hay, University of St. Andrews, North Haugh, St. Andrews, Fife, UK). Flag-p62/SQSTM1 in pcDNA3.1 vector was provided by Prof. Robert Layfield (University of Nottingham, Nottingham, UK). Rat pEGFP-LC3 was kindly provided by Prof. Tamotsu Yoshimori (Osaka University, Osaka, Japan).

3.2 Methods

3.2.1 Molecular cloning

Transformation of competent cells:

1 µl of plasmid cDNA (pcDNA) was added to 50 µl of *Escherichia coli* strain DH5α and bacteria were incubated for 30 minutes on ice, following by a heat-shock for 45 sec at 42 °C and 2 minutes incubation on ice. 600 µl of LB was added and bacteria were incubated for 1 hour at 37 °C, with agitation, to allow for expression of an antibotic-resistance gene. 100 to 250 µl of the cells were then plated onto ampicilin or kanamycin plate and incubated overnight at 37 °C, allowing for growth of the antibiotic-resistant clones.

Miniprep and Maxiprep:

A bacterial colony was chosen from an agar plate and cultured for additional ~8 hours for Mini-prep or overnight for Maxiprep in LB with relevant antibiotic at the same concentrations. Bacteria were harvested by centrifuging for 15 minutes at 6,000 g at 4 °C. Plasmid cDNA was purified with Plasmid Maxiprep or Miniprep kits from Qiagen. Briefly, bacteria were resuspended and lysed, plasmid cDNA was loaded onto the column, then washed and eluted. Plasmid cDNA was precipitated with isopropanol, washed with 70 % ethanol and resuspended in distilled H_2O. pcDNA concentration was determined by measuring absorbance at 260 nm using M501 UV/Visible Spectrophotometer (Camspec), and the purity of pcDNA was determined by 260 nm/ 280 nm absorbance ratio.

Ack1 C-terminal truncation mutants (work performed by Miss S. Brewer):

C-terminal truncations of murine Ack1 isoform 2 were generated *via* PCR from a full-length construct using forward and reverse primers with EcoR1 and BamH1 digestion sites, respectively. The linear products were digested with EcoR1 and BamH1 restriction enzymes

(New England Biolabs, Ipswich, MA, USA) and ligated with pmCherry-C1 vector using T4 ligase (New England Biolabs). The following primers were used: forward primer for all mutants: TGAGTCCGTAGAATTCGATGCAGCCGGAGGAGGGA and reverse primers for ΔUBA mutant (1-910 a.a.) TAGCCTAAGTGGATCCTCATCTGACGGTGGCAGT, ΔMIG6 mutant (1-680 a.a.) TAGCCTAAGTGGATCCTCAGGGCATCTGCGCCTG, ΔPRD mutant (1-610 a.a.) TAGCCTAAGTGGATCCTCACCGTGTGGGGCTCTG.

3.2.2 Cell culture, transfection, treatment, stimulation and lysis

Cell culture:

Human Embryonic Kidney epithelial 293T (293T) and human cervival adenocarcinoma (HeLa) cells were cultured in Dulbeco's Modified Eagle Medium (DMEM) supplemented with 10% FBS (v/v) with 100 I.U./ml penicillin and 0.1 mg/ml streptomycin (Sigma-Aldrich), with addition of 2 mM L-glutamine (Sigma-Aldrich), at 37 °C with 5% CO_2. Cells were generally split every three to four days using 0.05 % Trypsin-EDTA (Invitrogen). Androgen-sensitive human prostate adenocarcinoma (LNCaP) cells were cultured in Roswell Park Memorial Institute (RPMI) medium supplemented with 10% FBS (v/v) with 100 I.U./ml penicillin and 0.1 mg/ml streptomycin (Sigma-Aldrich), with addition of 2 mM L-glutamine (Sigma-Aldrich), at 37 °C with 5% CO_2. Cells were generally split once a week. Since cells were weakly adherent, no trypsinisation was required prior to splitting, and flasks could be knocked gently by hand to detach the cells.

Transfection:

293T and HeLa cells transfection using GeneJuice

Cells were transfected with GeneJuice Transfection Reagent (Novagen), according to the manufacturer's instructions. Briefly, the cells were plated in 35 mm dish at $3x10^{5}$ cells/ml

concentration in the case of HeLa cells and at $4x10^5$ cells/ml concentration in the case of 293T cells. The next day, 3 µg cDNA, 6 µl GeneJuice and 100 µl antibiotic- and serum-free medium was added drop-wise to the cells. Incubation was continued for further 48 hours to allow for protein expression.

LNCaP cells transfection using Lipofectamine 2000

Cells were transfected with Lipofectamine according to manufacturer's instructions. Briefly, cells were plated at $5x10^5$ cells/ml concentration in 35 mm dish. The next day, 3-4 µg cDNA and/or 100 pmol RNAi, 10 µl Lipofectamine 2000 and 500 µl antibiotic- and serum-free medium was added drop-wise to the cells. Incubation was continued for further 48 hours to allow for protein expression and/or siRNA knockdown.

Treatment:

Bafilomycin A (inhibitor of lysosomal acidification): cells were incubated with 400 nM bafilomycin A1 for four hours prior to EGF stimulation.

BIBX 1382 (EGFR kinase inhibitor): cells were serum-starved for four hours, the final hour in the presence of BIBX 1382 (10 µM unless otherwise stated).

Leptomycin B (inhibitor of nuclear export): cells were serum-starved for four hours following EGF stimulation in the presence of leptomycin B (10 ng/ml).

Stimulation:

Cells were serum-starved for 4 hours, unless otherwise stated. Following serum-starvation, cells were stimulated with FGF2 to the final concentration of 20 ng/ml and heparin to the final concentration 10 µg/ml, for 20 minutes. In the case of EGF, cells were stimulated for different times (as indicated), and the final concentration of EGF was 100 ng/ml in HeLa and 293T cells, and 20 ng/ml in LNCaP cells.

Cell lysis:

Cells were washed with PBS and lysed with triton X-100 lysis buffer for 30 minutes on ice. Lysed cells were cleared by centrifugation at 14,000 g for 25 minutes at 4 °C, and the pellets were discarded. Total protein concentration of the cleared lysate was determined by Coomassie (*Bradford*) Protein *Assay* Kit (Pierce) according to the manufacturer's instructions, with E max spectrophotometer (Molecular Devices). Cell lysates were adjusted to the same protein concentration per experiment.

3.2.3 Immunofluorescence and confocal microscopy

Immunofluorescence:

Cells were plated onto coverslips 24 hours prior to immunostaining. In the case of LNCaP cells, coverslips were coated with poly-D-lysine to enable the cells to attach to coverslips. Cells were washed twice with ice-cold PBS and fixed in 4 % paraformaldehyde (PFA; Electron Microscopy Sciences). Fixed cells were permeabilised with 0.1 % triton X-100 (Sigma-Aldrich) in ice-cold PBS for 5 minutes at room temperature (RT) or with 0.2 % triton X-100 (Sigma-Aldrich) in ice-cold PBS for 3 minutes at RT. The cells were subsequently incubated with blocking buffer for one hour at RT, following by overnight incubation with primary antibodies at 4 °C, and one hour incubation with secondary antibodies at RT. Coverslips with cells were mounted using either HydroMount (National Diagnostics), ProLong Gold (Invitrogen) or Vectashield Mounting Medium with DAPI (Vector Laboratories). All images were acquired through Nikon A1R Confocal/TIRF Microscope (Nikon) with the *NIS-Elements* Software (version 3.1 and 4.0) (Nikon). For transferrin-488 or transferrin-568 data, cells were serum starved for 10 minutes and incubated with transferrin at the final concentration of 10 µg/ml for indicated times prior to fixation. For lysotracker data, HeLa cells were incubated for two hours with lysotracker at the final concentration of 100 nM

prior to fixation, whereas LNCaP cells were incubated 30 minutes with lysotracker prior to live-cell imaging.

Confocal Microscopy:

Single section images were acquired by Nikon A1R confocal microscope using 60X objective lens, with pinhole size 1 µm. All images were analysed with *NIS Elements* software. Two methods of quantification were employed: quantification using the Pearson's Correlation Coefficient (PCC) and as a percentage (described below). The PCC method was particularly useful when the fluorescent signal from one or both channels was diffused and thus would be difficult to quantify using the other method (described below). Quantification as a percentage was employed when the fluorescent signal from both channels was clear to distinguish. Additionally, as the PCC method turned out to be much quicker, it was additionally employed throughout the study presented within this thesis. In both cases, minimum three cells were quantified per experiment, from minimum three experiments.

Quantification using Pearson's Correlation Coefficient:

A line was drawn around a cell, and the value of PCC (the correlation between two channels) was taken (Zinchuk *et al.*, 2007; Adler and Parmryd, 2010). In the case of pixel movement, one channel was shifted one pixel at time relatively to the other channel, up to ten pixels. Gradual decrease in the value of PCC was perceived as a genuine colocalization between two channels, whereas no change in this value was assument as no colocalization between channels.

Quantification as a percentage:

The puncta within one channel representing a particular protein within the cell were circled, and the colocalization with another channel was quantified. As a control, the circles were

moved into the areas absent in the particular protein, and the random colocalization with another channel was quantified.

Statistical analysis:

All the data were analysed in Microsoft Excell using two-tailed Student t-Test, from minimum three experiments, with at least three cells being counted per experiment.

3.2.4 Protein analysis

Immunoprecipitation:

For Protein G-Sepharose beads (Sigma-Aldrich), cell lysates were incubated for 1 hour with an antibody followed by one hour incubation with the beads. In the case of IgG-conjugated FGFR1, cell lysates were incubated for one hour with Protein G-Sepharose beads only. Beads were subsequently separated by short centrifugation, washed five times with stock solution (2X) and resuspended in SDS sample buffer (2X). For GFP-trap, cell lysates were incubated one hour with GFP-conjugated beads, followed by separation by short centrifugation (agarose beads) or magnetic separation (magnetic beads). Beads were washed succesively with dilution and wash buffer and resuspended in SDS sample buffer (2X) or in NP LDS sample buffer (4X) (Invitrogen) with sample reducing buffer (10X) (Invitrogen). For Dynabeads (Invitrogen), magnetic beads were incubated with primary antibody in wash buffer for 10 minutes at RT and subsequently with cell lysates for 30 minutes at 4 °C. Beads were separated on magnet and washed three times with ice-cold PBS and resuspended in NP LDS sample buffer (4X) with sample reducing buffer (10X). All samples in sample buffer were boiled for 10 minutes at 95 °C.

SDS PAGE and Western blotting:

For analysis of whole cell lysate, SDS sample buffer (2X) or LDS sample buffer (4X) with sample reducing agent (10X) was added to lysates and the samples were boiled for 5 minutes at 95 °C. Otherwise, the samples were used after performing immunoprecipitation. For SDS PAGE analysis, samples were resolved on NuPAGE 4-12 % pre-cast Bis-Tris Gels (Invitrogen) using MOPS/SDS running buffer. For immunoblotting (western blotting), proteins were transferred to Immobilon-FL PVDF membranes (Milipore) at 4 °C using Tris-Glycine transfer buffer at 100 V for 1:15 hours. The membranes were then incubated with methanol for two minutes and air-dried. Dried membranes were incubated overnight with primary antibody diluted in immunoblotting blocking buffer, washed three times for 5 minutes with PBST, followed by incubation with secondary antibody in the same buffer. Membranes were washes again three times for 5 minutes with PBST, placed in PBS and imaged *via Odyssey* Application Software *version 3.0* with Odyssey Imaging System (Li-Cor). In the case of Fc-conjugated FGFR1, the proteins were transferred onto nitrocellulose membranes (Li-Cor), which were then blocked for one hour in 5 % dried milk powder in PBST. The membranes were incubated with HRP-conjugated secondary goat anti-human antibody diluted in 5 % dried milk powder in PBST. The membranes were washed with PBST and following by a final wash with PBS. The membranes were then incubated with ECL Western blotting substrate (Pierce) according to manufacturer's instructions. Finally, the proteins were visualised on Hyperfilm (Amersham Biosciences Inc.).

Antibody cross-linking:

Dynabeads were incubated with antibody for 10 minutes at RT. The beads were then washed with 0.02 % tween 20 in PBS, followed by two additional washes in wash buffer. The beads were then resuspended in cross-linking buffer and incubated for 30 minutes at RT. This was followed by washing for 15 minutes with quenching buffer and 5 minutes with elution buffer.

The beads were then washed three times with 0.02 % tween 20 in PBS and resuspended in this buffer. This was followed by incubation with cell lysates and further stages of immunoprecipitation with Dynabeads (described earlier).

3.2.5 Real time quantitative polymerase chain reaction

LNCaP cells were transfected with short interfering RNA (siRNA) targeting Ack1 mRNA (Dharmacon), or non-targeting RNAi (control) (Dharmacon). 48 hours post-transfection cells were trypsinised, centrifuged and total RNA was purified using RNeasy Mini kit (Qiagen), according to the manufacturer's instructions. RNA concentration was determined by measuring absorbance at 260 nm and 280 nm using a NanoDrop. The ratio of absorbance at 260 nm to 280 nm determined the purity of RNA. cDNA was synthesized with Veriti Thermal Cycler (Applied Biosystems) using High Capacity cDNA Reverse Transcription kit (Invitrogen), as shown in **Table 3.3** The thermal cycler conditions are shown in **Figure 3.1 a**.

Upon synthesis, cDNA was diluted with distilled H_2O to the final concentration 25 ng/µl. The reaction mix was prepared as shown in **Table 3.4** and the real-time quantitative polymerase chain reaction (RT-qPCR) was performed with TNK2 primers (Applied Biosystems) and TaqMan Universal Master Mix (Applied Biosystems) using ABI Prism 7000 Sequence Detection System (Applied Biosystems). Ribosomal 18S (r18S) (Applied Biosystems) was used as a control. The thermal cycler conditions are shown in **Figure 3.1 b**. The data were analysed using ABI Prism 7000 SDS Software. To analyse the level of Ack1 knockdown, statistical analysis was performed in Microsoft Excell using two-tailed Student t-Test from three experiments.

cDNA synthesis mix	**Supplier**	**Volume per sample**
RT buffer (10X)	Invitrogen	2 µl
25X deoxiribonucleotide triphosphates	Invitrogen	0.8 µl
10X random primers	Invitrogen	2 µl
MultiScribe Reverse Transcriptase (50 U/µl)	Invitrogen	1 µl
RNase-free H_2O	Qiagen	4.2 µl
RNA (0.2 µg/µl)	-	10 µl

Table 3.3. cDNA synthesis mix

The table shows the components of the cDNA synthesis mix as volume per sample.

Reaction mix	**Supplier**	**Volume per sample**
2X TaqMan Universal Master Mix	Applied Biosystems	10 µl
20X primers (TNK2 or r18S)	Applied Biosystems	1 µl
RNase-free H_2O	Qiagen	9 µl
cDNA (25 ng/µl)	-	1 µl

Table 3.4. Reaction mix for RT-qPCR

The table presents the components of the reaction mix for RT-qPCR as volume per sample.

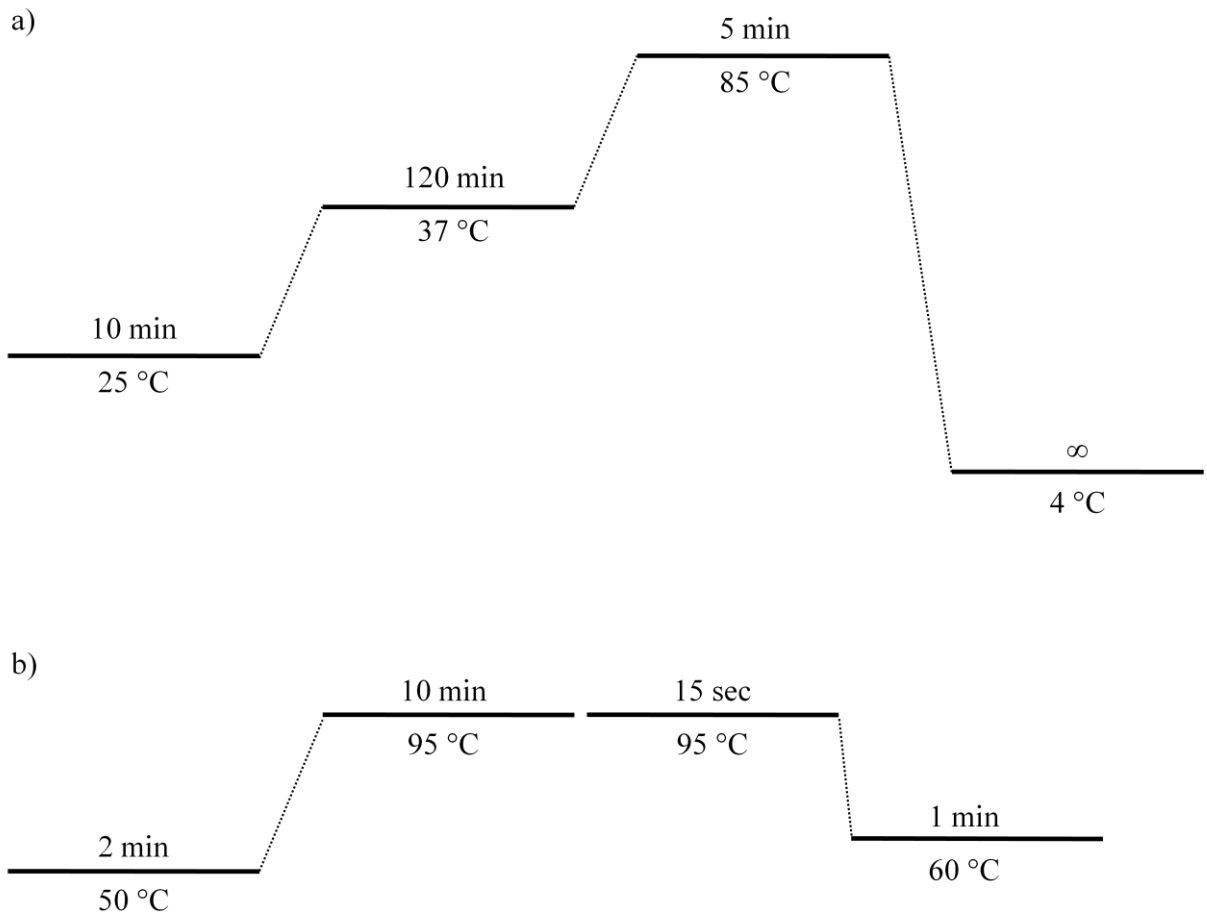

Figure 3.1. Thermal cycler conditions for cDNA synthesis and RT-qPCR

The schematic presents the thermal cycler conditions used for cDNA synthesis **(a)** and when performing RT-qPCR **(b)**.

3.2.6 SILAC sample preparation

Stable isotope labelling of amino acids in cell culture (SILAC) labeling:

For SILAC labeling, 293T cells were cultured in amino acid deficient SILAC DMEM (Thermo Fisher Scientific) supplementd with 0.1 mg/ml isotopically normal L-arginine and L-lysine (R0K0) (Sigma-Aldrich) ("light"), with $^{13}C_6$ L-arginine and 4,4,5,5-D4 L-lysine (R6K4) (Goss Scientific) ("medium"), or with $^{13}C_6$ $^{15}N_4$ L-arginine and $^{13}C_6$ $^{15}N_2$ L-lysine (R10K8) (Goss Scientific) ("heavy"), 0.1 mg/ml streptomycin and 100 I.U./ml penicillin, and 0.5 mg/ml proline (Sigma-Aldrich) and 10 % dialyzed FBS (Labtech International). The cells were cultured in SILAC medium for at least five doubling times to allow for incorporation of labeled amino acids (Cunningham *et al.*, 2010).

Cell transfection, cell treatment and immunoprecipitation:

Labeled 293T cells in "light" medium were untransfected, whereas cells in "medium" and "heavy" media were transfected with myc-Ack1, shown in **Figure 3.2**. The cells were serum-starved for four hours and "heavy" cells were stimulated with EGF for 15 minutes. The cells were lysed and cell lysates were incubated with α-myc antibody, or with α-myc antibody previously cross-linked to the beads. Immunoprecipitates were mixed and subjected to trypsin digestion (**Chapter 3.2.7**). Two independent experiments were performed, each with and without antibody cross-linking, as summarized in **Table 3.5**.

Experiment	Amount of proteins	α-myc antibody	Dynabeads	Cross-linking
1	10 mg	20 µg/10 µl beads	160 µl	Yes
	10 mg	20 µg/10 µl beads	160 µl	No
2	10 mg	20 µg/10 µl beads	160 µl	Yes
	10 mg	20 µg/10 µl beads	160 µl	No

Table 3.5. The amounts of protein, antibody and beads used for immunoprecipitation

The table shows the approximate amounts of proteins, the antibody and Dynabeads used for immunoprecipitation of isotopically labelled 293T cells.

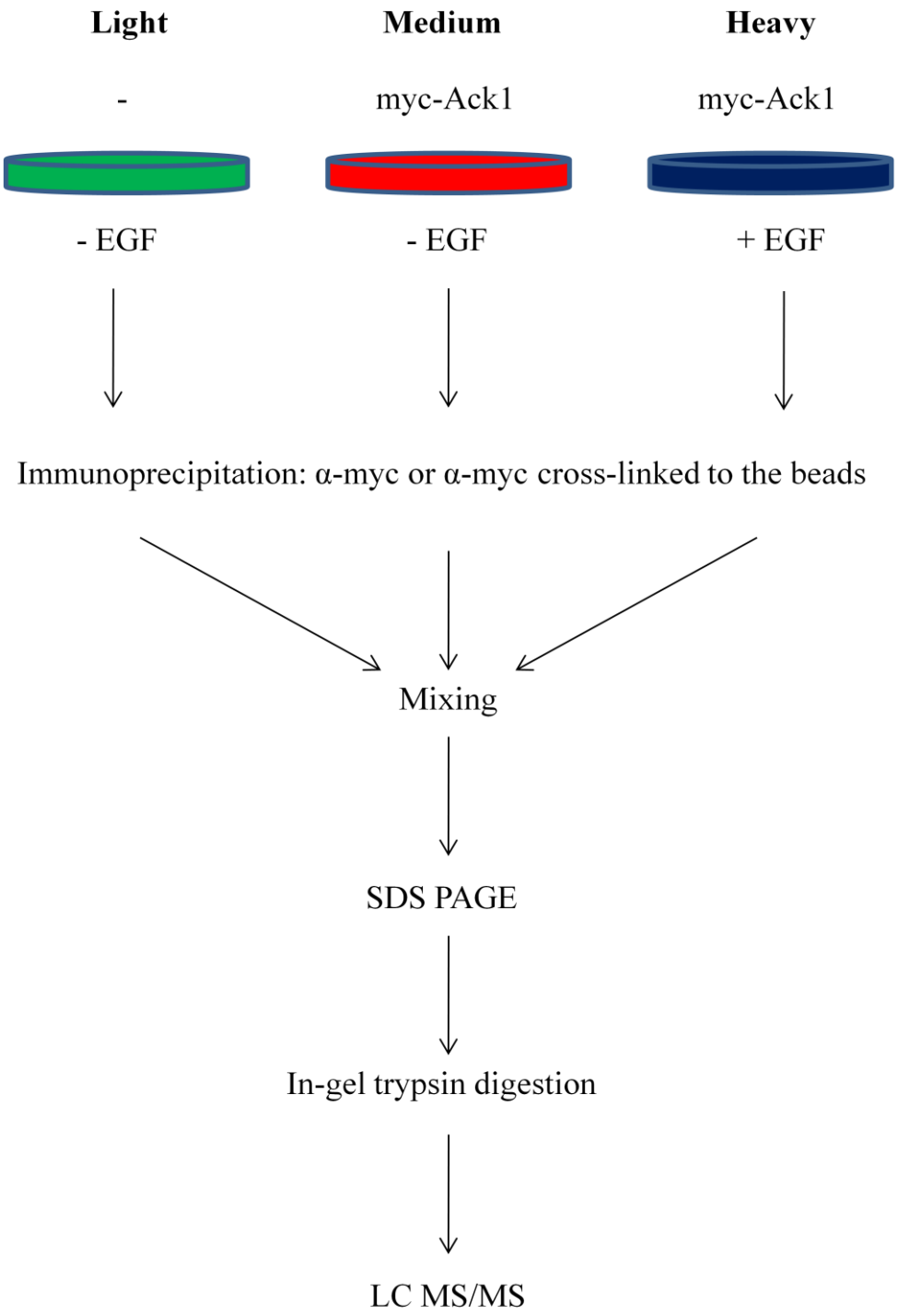

Figure 3.2. Simplified diagram of SILAC experiment

293T cells were cultured in "light", "medium" or "heavy" SILAC media. "Medium" and "heavy" cells were transfected with myc-Ack1. Subsequently, the cells were serum-starved for four hours and "heavy" cells were stimulated with EGF for 15 minutes. The cells were lysed and cell lysates were incubated with α-myc antibody (alone or cross-linked to the beads). Immunoprecipitates were washed, mixed, washed again and subjected to SDS PAGE (**Chapter 3.2.4**) followed by Coomassie staining, in-gel trypsin digestion, desalting and LC-MS/MS (described in **Chapter 3.2.7**).

3.2.7 Mass spectometry

In-gel trypsin digestion:

Immunoprecipitates were separate on the NuPAGE 4-12 % pre-cast Bis-Tris gels. The gels were fixed for 10 minutes in gel fixation solution followed by staining in Coomassie gel staining solution to enable visualization of proteins. The gels were next destained with gel destain solution for several hours at RT. The gels were divided into multiple pieces and destained with destaining solution for 15 minutes with agitation. Gel pieces were washed with dehydration and washing buffer until no staining remained followed by vacuum centrifugation for 5 minutes. Gel pieces were rehydrated in reduction buffer and subsequently resuspended in Alkylation buffer for 45 minutes protected from light. This allowed for alkylation of reduced cysteine side chains. Gel pieces were washed for 5 minutes with rehydration and washing buffer, and twice for 5 minutes with dehydration and washing buffer, and subsequently dried by vacuum centrifugation for 5 minutes. Trypsin digestion solution was added to the gel pieces and allowed to rehydrate for 10 minutes on ice. Excess of trypsin was removed and gels were covered with rehydration and washing buffer, and left overnight at 37 °C. The next day, formic acid was added to the final concentration of 0.5 % and the supernatant was transferred into a new tube. Further extraction was done with Peptide extraction solutions. The supernatants were dried with vacuum centrifuge, and the remaining peptides were resuspended in 0.1 % formic acid. The samples were stored at -20 °C.

TiO_2 enrichment:

For phosphopeptide enrichement, titanium dioxide columns were conditioned with conditioning solution and equilibrated with equilibration solution. Samples were loaded onto the column with equilibration solution and centrifuged. The flow-through was loaded back on to the column and centrifuged again to maximize the binding of the peptides. The column

was washed with equilibration and conditioning solution and centrifuged. Peptides were eluted with 1.75 % ammonia solution upon centrifugation. The flow-through was re-loaded on the column to maximize elution of the peptides, and centrifuged. The samples were dried in vacuum centrifuge and phosphor-enriched peptides were resuspended in 0.1 % formic acid.

Desalting using Zip-Tips:

Zip-tip was wetted in wetting solution and equilibrated in equilibration and washing solution. Peptides in 0.1 % formic acid were loaded onto the tip, aspirated and dispensed several times to allow for maximum binding. The tip was washed with equilibration and washing solution, and the peptides were eluted with elution buffer. The sample was then dried in a vacuum centrifuge and the peptides were resuspended in 0.1 % formic acid.

Liquid chromatography (work performed by Dr. A. J. Creese):

Peptides were loaded onto a 150 mm Acclaim PepMap100 C_{18} column (LC Packings, Sunnyvale, CA, USA) in mobile phase A (water and 0.1 % formic acid) (JT Baker and Sigma-Aldrich). Peptides were separated over a linear gradient from 3.2 % to 44 % mobile phase B (acetonitrile and 0.1 % formic acid) (JT Baker and Sigma-Aldrich) with a flow rate of 350 nl/min. The column was then washed with 90 % mobile phase B before re-equilibrating at 3.2 % mobile phase B. The column oven was heated to 35 ^{o}C. The LC system was coupled to an Advion Triversa Nanomate, which infused the peptides with a spray voltage of 1.7 kV. Peptides were infused directly into the LTQ-Orbitrap Velos ETD (Thermo Fisher Scientific).

Tandem mass spectrometry MS/MS (work performed by Dr. A. J. Creese):

The mass spectrometer performed a full FT-MS scan (*m/z* 380-1600) and subsequent collision induced dissociation (CID) MS/MS scans of the seven most abundant ions above a threshold of 1,000. Survey scans were acquired in the Orbitrap with a resolution of 60,000 at *m/z* 400.

Precursor ions were subjected to CID in the linear ion trap. Width of the precursor isolation window was *m/z* 2 and only multiply charged precursor ions were subjected to CID. CID was performed with helium gas at normalized collision energy of 35 % (target 5 x 10^4, maximum fill time 100 ms). CID activation was performed for 10 ms. Dynamic exclusion repeat count was set to 1 with duration of 60 s. Data acquisition was controlled by Xcalibur 2.1 (Thermo Fisher Scientific).

Identificatication of PTMs (work performed by Dr. A. J. Creese):

The database search was performed in Proteome Discoverer (V1.2.0.208). The search engine was Mascot (version 2.2.4) and the database used was the mouse International Protein Index (IPI) database (version 3.84). The parameters for the searches were as follows: precursor mass tolerance 10 ppm, fragment mass tolerance 0.5 Da, a maximum of 2 missed cleavages, the enzyme was specified as trypsin. The cleavage was restricted when adjacent to proline. Carbamidomethylation (Cys) was set as a static modification. The variable modifications were phosphorylation (Ser, Thr, Tyr), oxidation (Met), deamidation (Asn, Gln) and ubiquitylation (Lys). The data were filtered with 0.01 (1 %) false discovery rate (FDR) using a reversed database.

Analysing SILAC data (work performed by Dr. A. J. Creese):

Mass spectra were processed using the MaxQuant software (version 1.3.0.5). Data were searched using the Andromeda search engine against a human Swiss Prot database (downloaded 9th Jan 2013) containing forward and reverse sequences, supplemented with common contaminants (including keratin, trypsin, BSA). The human database contained 174,900 protein entries (87,450 of which were reversed-sequence versions). The search parameters were: minimum peptide length 7, precursor ion mass tolerance 7 ppm, fragment ion mass tolerance 0.5 Da, cleavage enzyme trypsin/P, and a total of 2 missed cleavages were

allowed. Carbamidomethylation (Cys) was set as a fixed modification and oxidation (Met), acetylation (peptide N-terminus) were set as variable modifications. The appropriate SILAC labels were selected and the maximum labelled amino acids was set to 3. The peptide and protein false-discovery rate (FDR) was set to 0.01 (1%).

Further analysis of SILAC data:

Further analysis of SILAC data was performed in Perseus (version 1.4.0.8). Normalised ratios were filtered for reverse peptide sequence and contaminants, and log-transformed. Only proteins identified in a minimum of two out of four experiments (two independent experiments, each with and without antibody cross-linking to the beads) were considered as potential binding partners for Ack1. Significance A was applied with Benjamini-Hochberg FDR multiple testing correction-adjusted p-values calculated from Mann-Whitney-Wilcoxon tests.

4 Ack1 functions in EGFR, but not FGFR, trafficking

4.1 Introduction

Understanding the mechanisms underlying growth factor signalling and receptor tyrosine kinase (RTK) trafficking could potentially greatly improve the methods of treatment of patients with growth factor signalling-related diseases, such as cancer. Much research has been carried out in order to specify the pathways of RTK trafficking and the outcomes of RTK activation; however, due to the number and diversity of growth factor and growth factor receptors, and the complexity of the signalling networks downstream of RTK activation, there are still many unanswered questions and areas that require more in-depth investigation.

Ack1 belongs to the Ack family of non-receptor protein kinases. Other similar families include Src family, focal adhesion kinase (FAK) and Abl family, and a total of ten families of non-receptor tyroskine kinases have been identified to date (Blume-Jensen and Hunter, 2001). Ack1 is activated following stimulation with EGF, PDGF and insulin (Galisteo *et al.*, 2006). Ack2, an alternatively spliced isoform of Ack1, has been found to bind SNX9, which regulates receptor trafficking and degradation (Lin *et al.*, 2002). Furthermore, Ack1 binds clathrin and thus it may regulate CME (Teo *et al.*, 2001). The Mig6-homology domain within the C-terminal portion of Ack1 has been proposed to regulate an interaction between Ack1 and active EGFR (Shen *et al.*, 2007). It has been shown that Mig6 binds directly ligand-bound EGFR and inhibits EGFR activation (Zhang *et al.*, 2007). However, a recent study has shown that in the case of Ack1, the interaction with EGFR involves Grb2 (Lin *et al.*, 2012). In particular, it has been proposed that Ack1 is autoinhibited by an interaction between the SH3 domain and Mig6 domain, and that EGFR activation promotes Grb2 binding to Mig6 domain

of Ack1 and disrupts Ack1 autoinhibition. An indirect interaction between Ack1 and other RTKs, such as Axl, LTK and ALK, has also been reported and similarly has been shown to be mediated by Grb2 (Pao-Chun *et al.*, 2009). Thus, Ack1 has been identified as an important player in subcellular trafficking.

In this chapter the nature of the association between Ack1 and EGFR is further investigated. Both endogenous and ectopically expressed Ack1 colocalizes with EGFR following EGF stimulation. Similarly, Ack1 colocalizes with constitutively active Cdc42, a known Ack1 interactor. In contrast, no colocalization or interaction is found in the case of FGFR. The Ack1 domains regulating the colocalization with EGFR have been determined. Surprisingly and in contrast to other studies, Ack1 knockdown (KD) does not dramatically influence the level of EGFR degradation; however, Ack1 KD accelerates EGFR localization to lysosomes, thus indicating that Ack1 regulates EGFR trafficking.

4.2 Optimising experimental conditions

4.2.1 Time courses of EGF and FGF stimulation in HeLa and 293T cells

The activation of RTKs and downstream signalling molecules is both time and concentration sensitive. Following stimulation with a particular ligand, various proteins are being modified depending on the time, concentration and the cellular context. For example, in human epithelial type 2 cells, EGFR ligands have been shown to differentially influence EGFR trafficking depending on ligand concentration and the duration of stimulation (Roepstorff *et al.*, 2009). In particular, at low EGF concentrations (0.01 nM) very little EGFR internalisation may be observed, whereas at higher concentrations (10 nM and above) approximately half of the cell surface EGFRs are internalised. Additionally, stimulation with a particular ligand differently influences EGFR ubiquitylation, *e.g.* BTC treatment promotes much stronger

EGFR ubiquitylation than EGF or TGF-α (Roepstorff *et al.*, 2009). In the case of Hrs, it has been shown in B16-F1 cells that the strongest Hrs phosphorylation takes places shortly after HGF stimulation (2.5-15 min), and almost disappears after 1 hour of stimulation (Komada and Kitamura, 1995). In HeLa cells, stimulation with EGF at low concentrations (0.125 ng/ml) results in the most pronounced Erk phosphorylation at 10-15 minutes of stimulation, and at 30-60 minutes the phosphorylation almost disappears. In contrast, at higher concentrations (50 ng/ml) strong Erk phosphorylation can be observed between 3 and 30 minutes (Schoeberl *et al.*, 2002). Therefore, determination of the cell responses to the particular ligand in every cell line is extremely important.

In the study presented in this thesis, the experiments were predominantly performed on HeLa, 293T and LNCaP cells, and EGF and FGF2 were the only ligands used. In the case of HeLa and 293T cells, previously described ligand concentrations have been employed (Row *et al.*, 2006; Row *et al.*, 2007; Mardakheh *et al.*, 2009; Mardakheh *et al.*, 2010). These include the final concentration of 100 ng/ml in the case of EGF and 20 ng/ml in the case of FGF2, with addition of 10 µg/ml of heparine. For LNCaP cells, the determination of the optimal conditions for EGF stimulation is described in **Chapter 4.2.3**.

In order to determine the best timing conditions for EGF and FGF2 stimulation, the cells were incubated with ligand for various times, lysed and the samples were analysed *via* Western blotting. In addition, similar experiments were performed on the cells ectopically expressing EGFR and FGFR2, as these conditions have also been employed throughout the study presented in this thesis. The data are collected and shown in **Figure 4.1**.

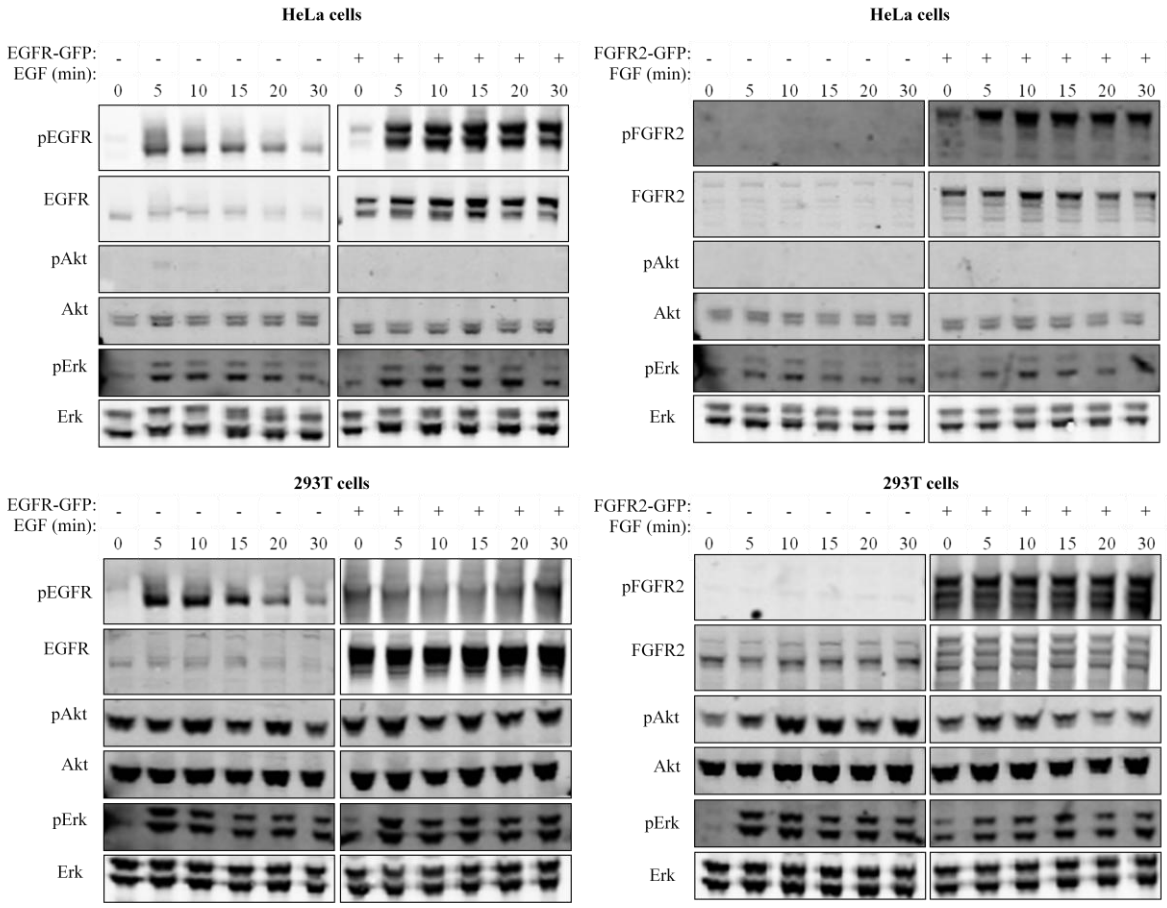

Figure 4.1. Time courses of EGF and FGF stimulation for HeLa and 293T cells

HeLa and 293T cells transfected with EGFR-GFP or FGFR2-GFP or untransfected, were serum-starved for four hours and stimulated with EGF (100 ng/ml) or FGF2 (20 ng/ml) and heparin (10 µg/ml) for indicated times. The cells were lysed and the cell lysates were subjected to SDS PAGE and Western blotting with α-phospho EGFR, α-EGFR, α-phospho Akt, α-Akt, α-phospho Erk and α-Erk antibodies.

EGFR phosphorylation in both HeLa and 293T cells can be distinguished in every condition (**Figure 4.1**). Strong EGFR phosphorylation following EGF treatment is observed in HeLa cells expressing EGFR at the endogenous level, as well as in cells with ectopically expressed EGFR. In 293T cells, strong EGFR activation post-EGF treatment is seen at the endogenous level, whereas ectopically expressed EGFR exhibits strong phosphorylation independently of ligand stimulation. In the case of Erk activation, strong Erk phosphorylation is observed in both cell lines in every condition following EGF stimulation. Surprisingly, no changes in Akt phosphorylation are seen in any conditions.

HeLa cells have been found to express only a minor level of endogenous FGFRs and therefore the FGF response is expected to be minimal (Francavilla *et al.*, 2009). Consistently, no detectable levels of FGFR2 can be found in HeLa cells, and only minimal Erk phosphorylation is noted (**Figure 4.1**). In contrast, FGF treatment of HeLa cells ectopically expressing FGFR2 has been found to promote phosphorylation and activation of downstream signalling cascades (Auciello *et al.*, 2013). Accordingly, in the case of ectopically expressed FGFR2, strong FGFR2 phosphorylation is observed and Erk activation can be distinguished following EGF treatment. In 293T cells, relatively strong expression of endogenous FGFR2 has been reported (Mardakheh *et al.*, 2010). Indeed, endogenous FGFR2 can be detected in 293T cells. Although its phosphorylation upon FGF stimulation is minimal, strong Erk activation can be observed following FGF treatment. In the case of ectopically expressed FGFR2 in 293T cells, strong FGFR2 phosphorylation is observed independently of ligand stimulation, and Erk activation is detected following FGF stimulation. A subtle increase in Akt phosphorylation following FGF stimulation can be distinguished in 293T cells expressing endogenous FGFR2 and the cells with ectopically expressed FGFR2.

Considering the results presented in **Figure 4.1**, the optimal timing of stimulation with EGF and FGF2 would be between 5 and 20 minutes of ligand stimulation in both cell lines, as the most pronounced phosphorylation of RTKs and Erk can be observed between these time points; however, at the early stages of ligand stimulation RTKs are likely to be present in a close proximity to the plasma membrane and therefore unable to interact with proteins that are present within intracellular compartments, *e.g.* late endosomes. Therefore, in the case of HeLa and 293T cells ectopically expressing FGFR2, the cells were stimuilated with FGF2 for 20 minutes, at which stage FGFR1 and Erk phosphorylation are still strong. In the case of EGF, the most common time point used is 30 minutes in both cell lines. At this time point phosphorylation of EGFR and Erk are still distinguishable, and a portion of EGFR should be present within intracellular compartments and thus be able to associate with other intracellular molecules (Roepstorff *et al.*, 2009); however, some signal may be lost due to possible EGFR recycling. Therefore, in many instances, several time points have been employed to enable for the most precise determination of the localization, interactions or modifications of particular proteins.

4.2.2 Optimising conditions of Ack1 expression

Further optimisation was applied to determine the most efficient transfection with Ack1. For this purpose, HeLa cells were transfected with mCherry-Ack1 and cultured for further 24, 48 or 72 hours to allow for protein expression. Fixed cells were then imaged *via* confocal microscopy. As shown in **Figure 4.2 a**, similarly high Ack1 expression can be distinguished both at 24 and 48 hours post-transfection. Thus, the cells were incubated for 48 hours post-transfection to get optimal expression.

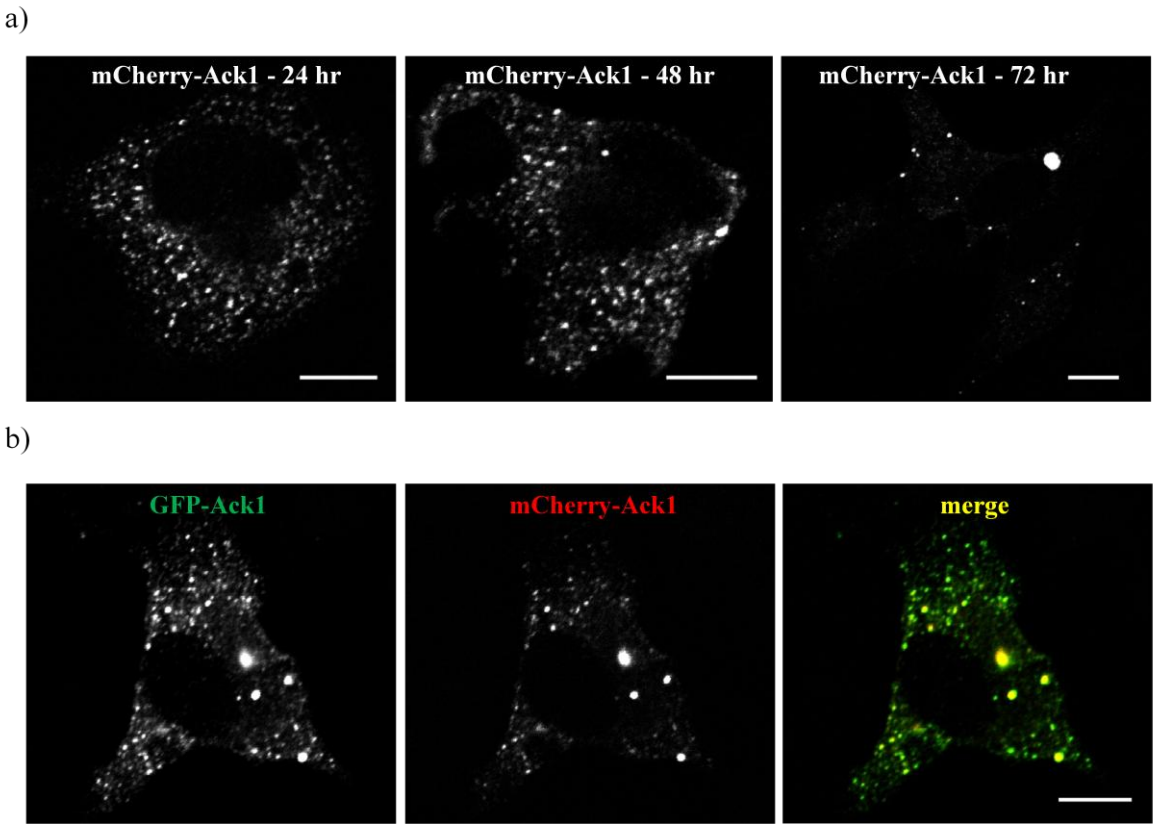

Figure 4.2. Optimising Ack1 transfections in HeLa cells

a) HeLa cells transfected with mCherry-Ack1 were fixed 24, 48 or 72 hours post-transfection and imaged *via* confocal microscopy; **b)** HeLa cells co-transfected with GFP-Ack1 and mCherry-Ack1 were fixed 48 hours post-transfection and imaged *via* confocal microscopy. Scale bars 10 µm.

Additionally, as different Ack1 constructs are available, it is important to validate whether they colocalize with each other. In particular in the case of mCherry-Ack1, which was constructed in our lab, verifying its functionality is crucial. For this purpose, mCherry- and GFP-tagged Ack1 were co-expressed in HeLa cells, and their colocalization was assessed *via* confocal microscopy. As shown in **Figure 4.2 b**, these two fusion proteins colocalize with each other. Although there is a possibility that the observed colocalization is due to dimerisation between mCherry- and GFP-tagged Ack1, since Ack1 has been shown to dimerise *via* N-terminal SAM domains (Prieto-Echaguee *et al.*, 2010), no major differences in subcellular distribution can be distinguished. Therefore, various Ack1 constructs were used interchangeably to provide the most optimal conditions for a particular experiment. Additionally, uptake of transferrin is not affected by low or moderate expression of Ack1, whilst it is inhibited in cells expressing high Ack1 levels (shown in **Chapter 5.3**) (Teo *et al.*, 2001). Thus, throughout the study presented in this thesis the cells expressing low or moderate levels of Ack1 have been employed.

4.2.3 Optimising conditions of EGF stimulation in LNCaP cells

Neither HeLa nor 293T cells are optimal for looking at endogenous Ack1, as detection of endogenous Ack1 within these two cell lines was very poor, both *via* biochemical studies and microscopy. Therefore, I searched for another the cell line that would be a good platform for studying endogenous Ack1 at the cellular level.

The membrane containing whole cell lysates from 13 various cancer cell lines was purchased and probed with antibodies against Ack1 and its phosphorylated form. As shown in **Figure 4.3**, total Ack1 is poorly distinguishable in the cell lines tested.

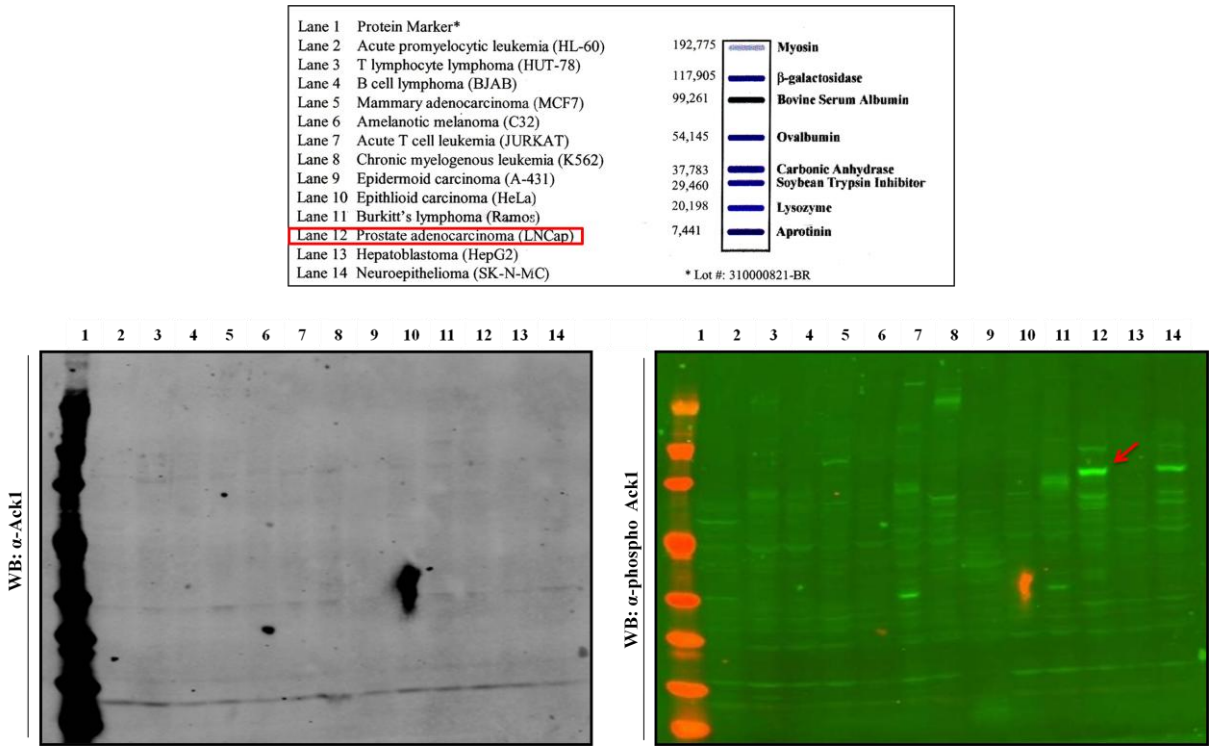

Figure 4.3. Identification of potentially phosphorylated Ack1 in LNCaP cells

The membrane purchased from G. Biosciences contains 50 µg of proteins from each cell line loaded, along with the protein marker. The membrane was incubated with α-Ack1 and α-phospho Ack1 (phospho Y284) antibodies. The arrow indicates potentially phosphorylated Ack1 in LNCaP cells. Predicted molecular weight of Ack1 is approximately 120 kDa.

Importantly, a relatively high level of potentially phosphorylated Ack1 can be found in prostate adenocarcinoma LNCaP cells, as the molecular weight of the protein identified is similar to Ack1. Additionally, Ack1 has been widely studied in LNCaP cells in the context of androgen receptor (AR) signalling (Mahajan *et al.*, 2005; Mahajan *et al.*, 2007). Therefore, this cell line has been chosen for studying endogenous Ack1. Interestingly, multiple phosphorylated proteins can be identified following incubation with an antibody against phosphorylated Ack1. The nature of those proteins is unknown: some of them are likely to be background proteins which are non-specifically recognised by the antibody, whereas others may be Ack1 isoforms or dimers.

To determine the optimal EGF concentration in LNCaP cells which promotes EGFR internalisation and degradation, the cells were stimulated with a range of different concentrations for up to three hours and EGFR degradation was assessed by Western blotting. As shown in **Figure 4.4**, the lowest concentration used (2 ng/ml) results in a delayed and decreased EGFR degradation compared to the other two concentrations employed (20 ng/ml and 50 ng/ml), both of which resulted in a similar level of EGFR degradation. This indicates that 20 ng/ml of EGFR is sufficient to promote EGFR internalisation and degradation. Additionally, a range of the EGF concentrations between 2 ng/ml and 20 ng/ml was applied to LNCaP cells ectopically expressing EGFR-GFP, and the cells were analysed *via* confocal microscopy using live-cell imaging to visualise EGFR endocytosis. As shown in **Figure 4.5**, the internalisation of EGFR is difficult to distinguish under these conditions, although EGF stimulation promotes cell movement and membrane 'blebbing'. Together with the data on EGFR degradation (**Figure 4.4**), the EGF concentration of 20 ng/ml was employed for further studies.

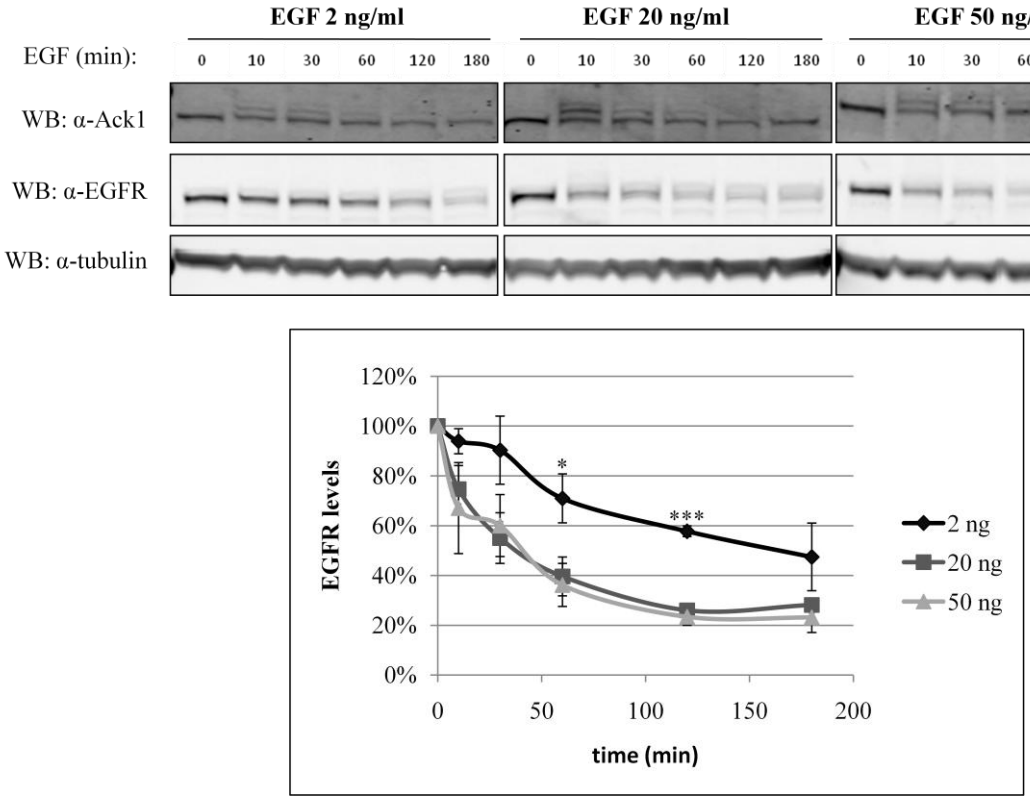

Figure 4.4. EGFR degradation upon treatment with various EGF concentrations

LNCaP cells were serum-starved for four hours and stimulated with various EGF concentrations for indicated times. The cells were lysed and cell lysates were subjected to SDS PAGE and Western blotting with α-Ack1, α-EGFR and α-tubulin antibodies. The densitometric analysis from three experiments is shown on the graph. The level of EGFR presented is obtained from a ratio of EGFR to tubulin.

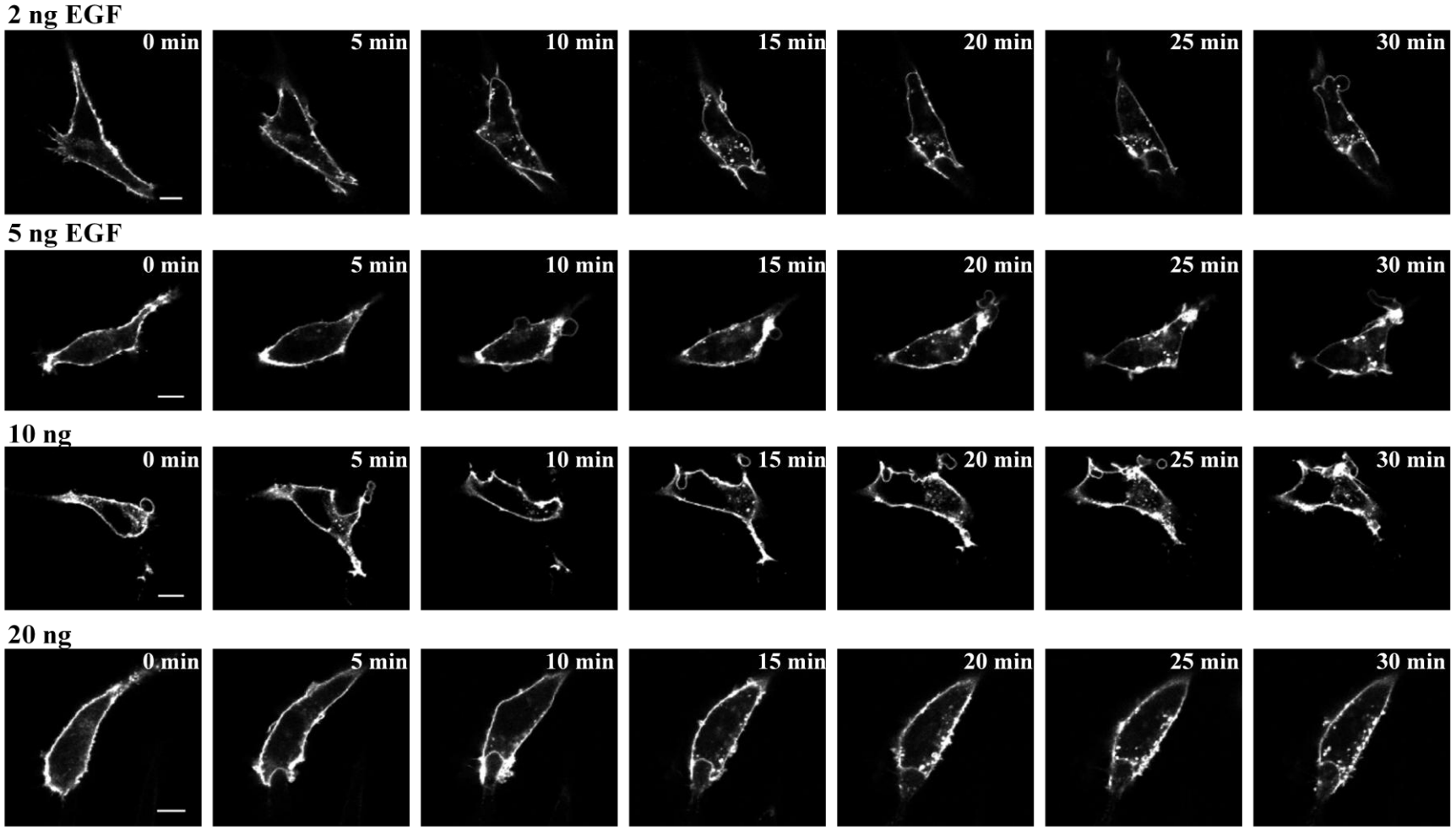

Figure 4.5. EGFR trafficking upon treatment with various EGF concentrations

LNCaP cells transfected with EGFR-GFP were serum-starved for four hours and imaged for 30 minutes (one frame every 30-60 seconds) upon stimulation with various EGF concentrations. Scale bars 10 µm.

4.3 Ack1 interacts with EGFR, but not FGFR2

The main aim of this chapter is to explore the potential roles of Ack1 in growth factor signalling and trafficking. As described in **Chapter 1.5.3**, it is well documented that Ack1 is involved in EGFR trafficking and degradation (Shen *et al.*, 2007; Grovdal *et al.*, 2008), yet the exact functions remain elusive. To investigate whether interaction of Ack1 with growth factor receptors is a general feature of the kinase, or whether it specifically binds EGFR and not other RTKs, I investigated a potential interaction between Ack1 and FGFR2. As shown in **Figure 4.6** upon Ack1 immunoprecipitation activated EGFR co-precipitates with Ack1, and this is not seen with FGFR2. These results are additionally validated when compared to the well described interaction between Ack1 and constitutively active Cdc42 (caCdc42) (Manser *et al.*, 1993). These data indicate that Ack1 specifically interacts with EGFR and not with FGFR2. This suggests that the interaction may be mediated through motifs within EGFR, which are absent in FGFR2, or through different binding proteins that recognise EGFR, but not FGFR2.

4.4 Ack1 colocalizes with EGFR, but not FGFR2

Consistent with the biochemical studies, Ack1 colocalizes with EGFR, but not with FGFR2, as shown in **Figure 4.7**. This colocalization has been quantified using Pearson's Correlation Coefficient (PCC). PCC is a relatively recent but very efficient method of quantification of colocalization between two channels (*e.g.* green and red) (Zinchuk *et al.*, 2007; Adler and Parmryd, 2010). Its values range from -1 to 1, with -1 indicating negative correlation, 0 showing no correlation and 1 designating complete colocalization. On the graph in **Figure 4.7**, the value of PCC for EGFR is relatively high and it decreases upon pixel movement, when one channel (*i.e.* green) has been shifted relatively to the other (*i.e.* red).

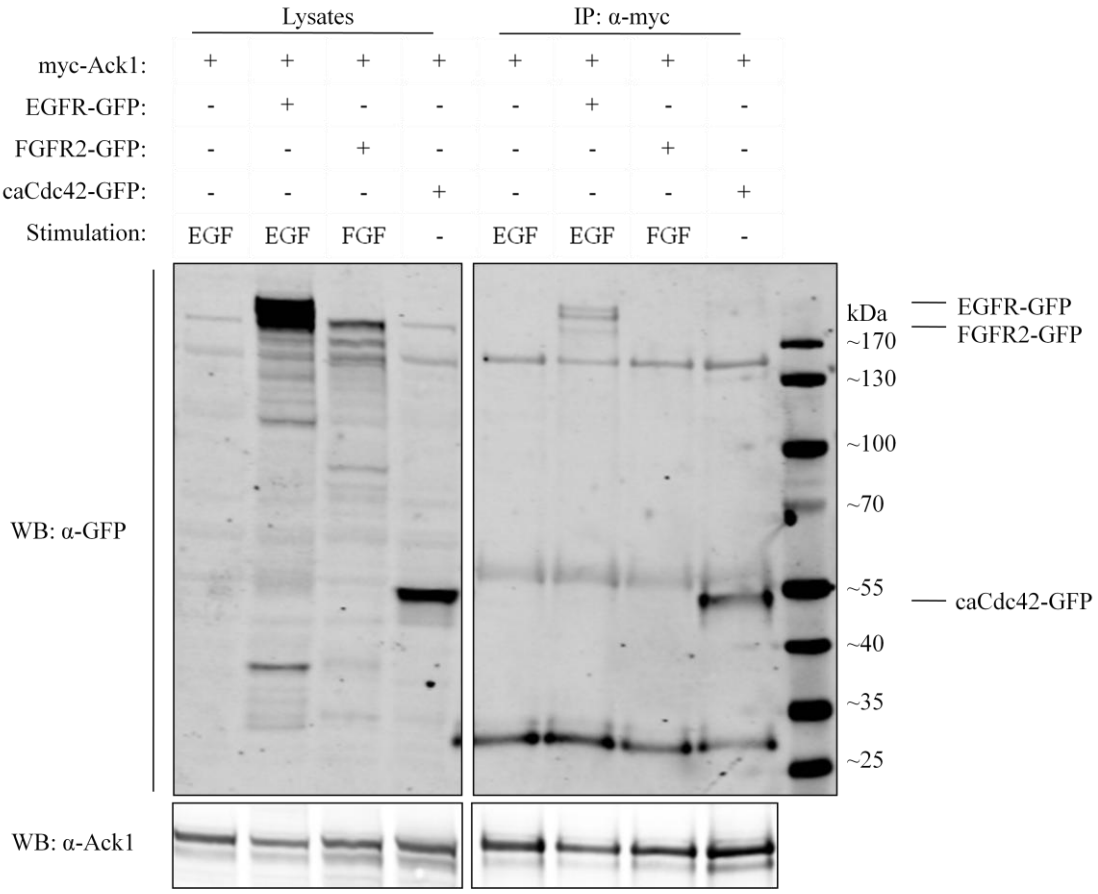

Figure 4.6.Ack1 interacts with EGFR and Cdc42, but not with FGFR2

293T cells transfected with myc-Ack1 and GFP-tagged EGFR, FGFR2 or caCdc42 were serum-starved for four hours (apart from cells transfected with Ack1 and caCdc42) and stimulated with EGF or FGF2 and heparin for 20 minutes, as indicated. The cells were lysed and cell lysates were incubated with α-myc antibody to imunoprecipitated Ack1. Immunoprecipitates were subjected to SDS PAGE and Western blotting with α-Ack1 and α-GFP antibodies.

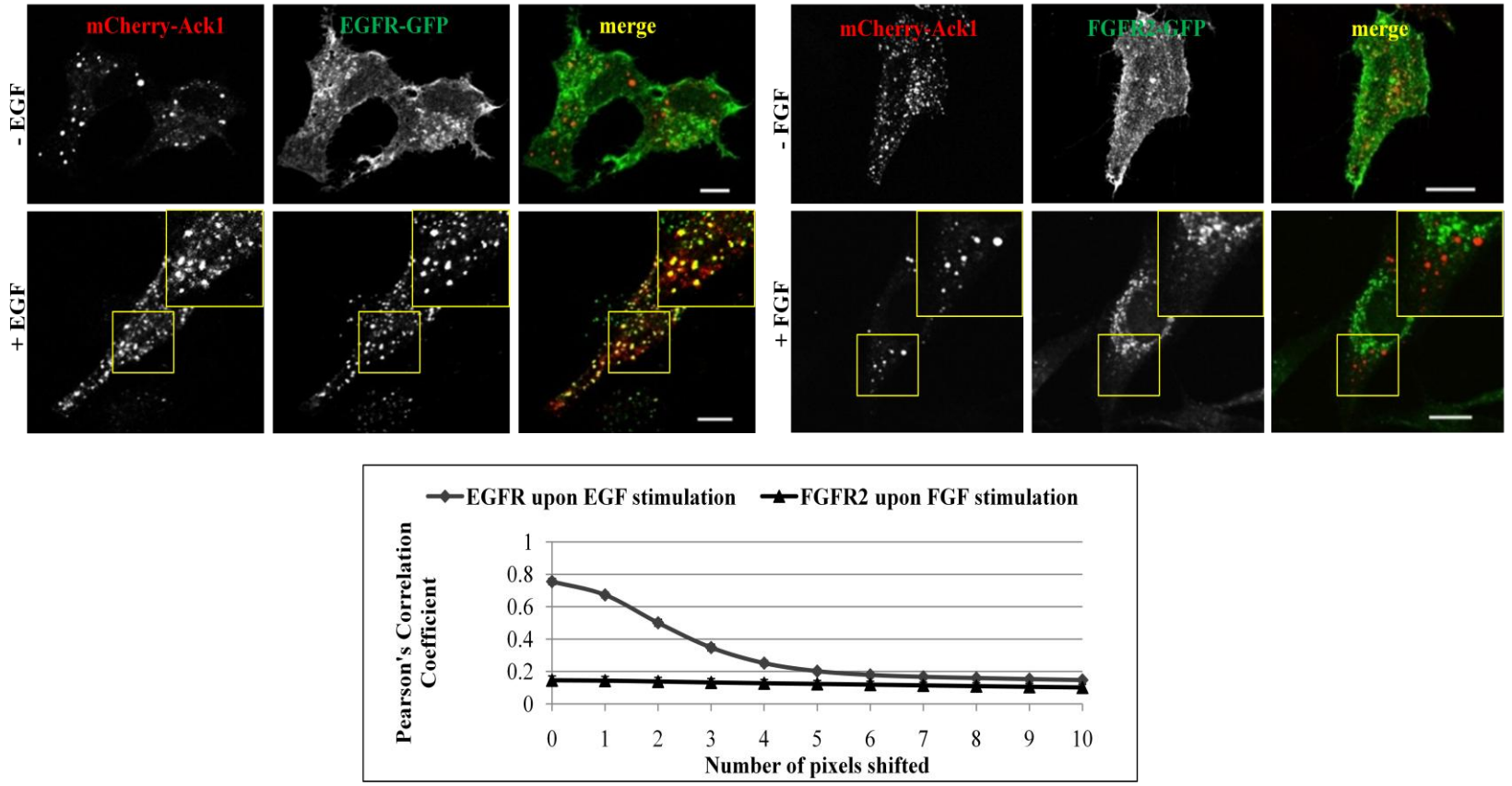

Figure 4.7. Ack1 colocalizes with EGFR, but not FGFR2

HeLa cells transfected with mCherry-Ack1 and EGFR-GFP or FGFR2-GFP were serum-starved for four hours and stimulated with EGF or FGF2 and heparin for 20 minutes, fixed and imaged *via* confocal microscopy. For quantification, the PCC values were obtained using *NIS Element* software and one channel was shifted relatively to the other, up to 10 pixels (explained in **Chapter 3.2.3**). The gradual decrease in PCC upon pixel movement is perceived as a genuine colocalization, whereas no change in PCC indicates lack of colocalization. Scale bars 10 µm. Error bars represent standard error of the mean (SEM).

Therefore, gradual decrease in PCC upon pixel movement as in the case of EGFR indicates genuine colocalization, rather than random alignment of pixels.

In the case of FGFR2, however, PCC is low and remains low irrespective of pixel movement, thus indicating the lack of colocalization between Ack1 and FGFR2. Similarly, the colocalization between Ack1 and EGFR can be seen in Cos7 cells following EGF stimulation, (**Figure 4.8**). Therefore, the association between Ack1 and EGFR is not cell type-specific and can be found in different cell lines. Altogether, these data indicate that Ack1 specifically colocalizes with EGFR and not with FGFR2, thus suggesting divergent endocytic pathways of EGFR and FGFR2.

4.5 Ack1 does not interact with FGFR1

Showing that Ack1 does not interact with FGFR2, I investigated whether it associates with other members of the FGFR family. 293T cells transfected with myc-Ack1 and FGFR1 were serum-starved and stimulated with FGF2, since FGF2 has been shown to activate FGFR1 (Lefevre *et al.*, 2009). Cell lysates were subjected to immunoprecipitation with α-myc antibody and analysed by immunoblotting. As shown in **Figure 4.9 a**, FGFR1 does not co-precipitate with Ack1, thus indicating that similarly to FGFR2, FGFR1 does not interact with Ack1. The experiment was duplicated, but the lysates were incubated with α-FGFR1 antibody rather than α-myc antibody. As shown in **Figure 4.9 b**, Ack1 does not co-precipitate with FGFR1 following FGF2 stimulation, further emphasizing that Ack1 and FGFR1 do not associate *in vitro*.

Furthermore, I used the FGFR1 constructs conjugated to the Fc fragment (Fragment, crystallizable) of the immunoglobulin G heavy chain.

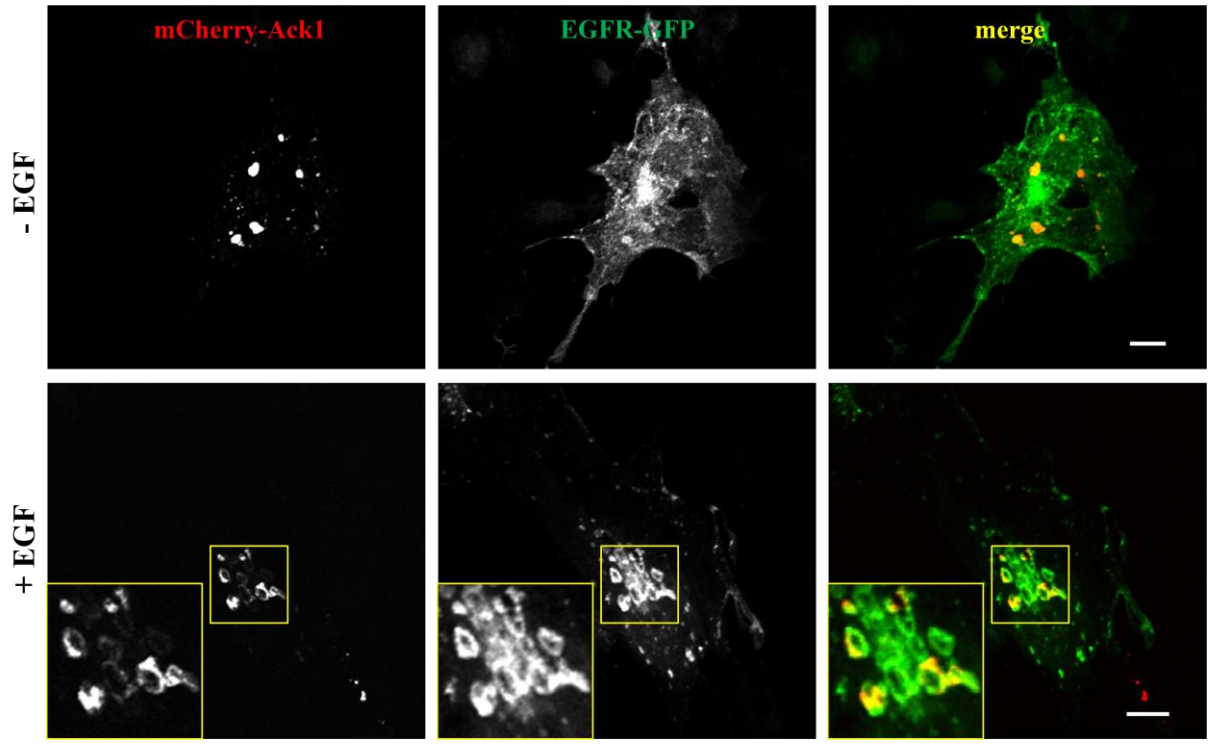

Figure 4.8. Ack1 colocalizes with EGFR in COS7 cells

Cos7 cells transfected with mCherry-Ack1 and EGFR-GFP were serum-starved for four hours and stimulated with EGF for 30 minutes, fixed and imaged *via* confocal microscopy. Scale bars 10 µm.

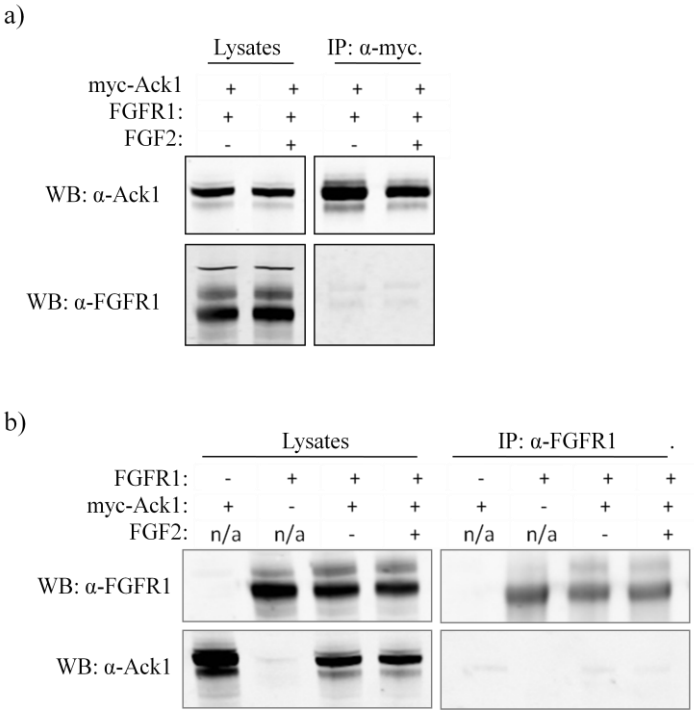

Figure 4.9. Ack1 does not interact with FGFR1 upon FGF2 stimulation

293T cells transfected with myc-Ack1 and FGFR1 were serum-starved for four hours and stimulated with FGF2 and heparin. The cells were lysed and cell lysates were incubated with α-myc **(a)** or α-FGFR1 **(b)** antibodies to immunoprecipitate Ack1 or FGFR1, respectively. Immunoprecipitates were subjected to SDS PAGE and Western blotting with α-Ack1 and α-FGFR1 antibodies.

Conjugation with Fc fragment enables direct binding to the beads during immunoprecipitation, without the requirement of an antibody (Burgar *et al.*, 2002), The following constructs were used: FcFGFR1 kinase active (KA), kinase dead (KD), transmembrane domain only (TM) and VT- (lacks two amino acids in its JM domain hence does not bind FGFR substrate 2, FRS2) (Burgar *et al.*, 2002). The receptors were co-expressed along with myc-tagged Ack1 in 293T cells. As a control, GFP was co-expressed along with myc-Ack1. The cells were serum-starved and lysed, and cell lysates were incubated with beads alone (in the case of FcFGFR1s) or with α-myc antibody (in a control). As shown in **Figure 4.10**, in the control sample Ack1 immunoprecipitates with α-myc antibody; howeve, it does not co-precipitate with either of the FcFGFR1 constructs. Additionally, the association between FGFR1s and phospholipase C gamma (PLCγ), which binds kinase active, but not kinase dead FGFR (Vecchione *et al.*, 2007), was veryfied. As expected, PLCγ co-precipitates with KA FGFR1, but not KD FGFR1, thus confirming that KA FcFGFR1 is functional. Altogether, these data further support the observation that Ack1 does not bind FGFR1 and suggest that Ack1 is not directly involved in FGFR1 trafficking.

4.6 Ack1 C-terminal truncation mutants

Ack1 is a relatively large protein with multiple domains which interact with various motifs within other proteins. In particular, the Mig6-homology domain has been previously shown to regulate the interaction with EGFR following EGF stimulation (Shen *et al.*, 2007; Lin *et al.*, 2012); however, other domains could potentially also contribute to this interaction. Therefore C-terminal truncation mutants of Ack1 were generated by Miss S. Brewer. These include the UBA domain deletion mutant (ΔUBA), the UBA and Mig6 domain deletion mutant (ΔMig6) and the UBA, Mig6 and proline rich domain deletion mutant (ΔPRD), as presented in **Figure 4.11 a** and **b**.

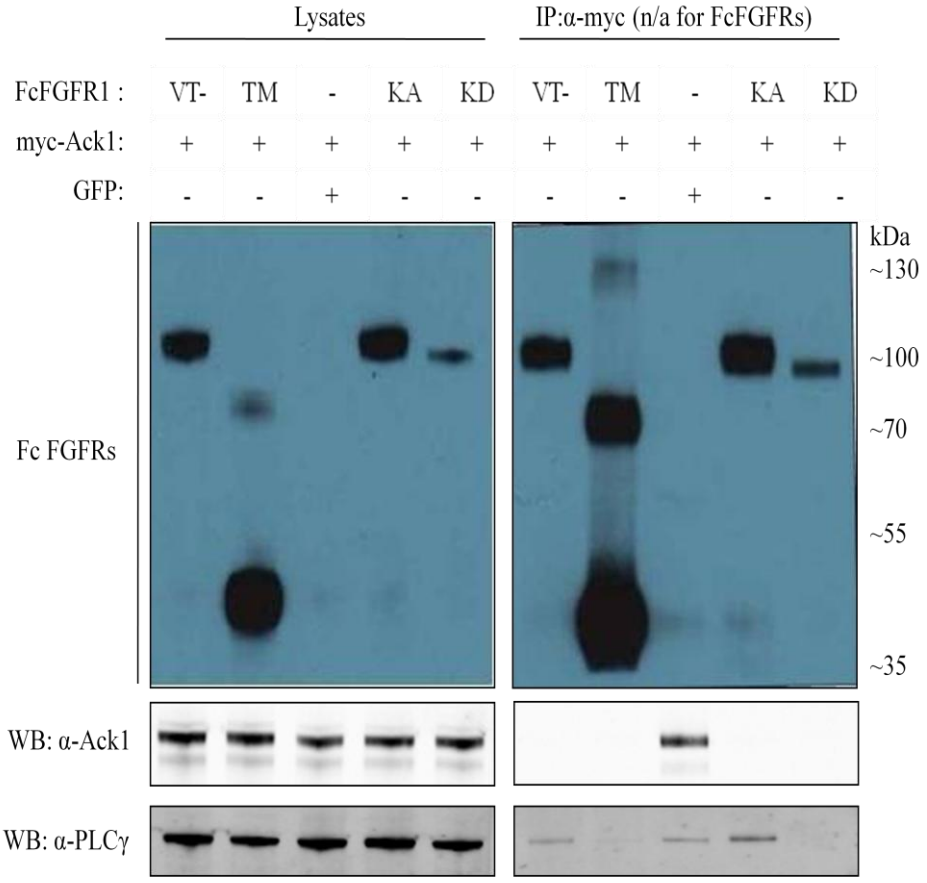

Figure 4.10. Ack1 does not co-precipitate with kinase-active FGFR1

293T cells transfected with myc-Ack1 and human IgG1 Fc-conjugated FGFR1 (VT-, TM, KA, KD) or GFP (control) were lysed and cell lysates were incubated with α-myc antibody (control) to immunoprecipitated Ack1, or with G protein agarose beads only (FcFGFR1 samples) to immunoprecipitate FcFGFRs. Immunoprecipitates were subjected to SDS PAGE and Western blotting with α-human IgG(Fc), α-Ack1 and α-PLCγ antibodies. n/a – non applicable; VT- – lacks two amino acids, valine and threonine, in its JM domain and does not bind FRS2; TM – truncated, transmembrane domain only; KA – kinase active; KD – kinase dead. From (Burgar *et al.*, 2002).

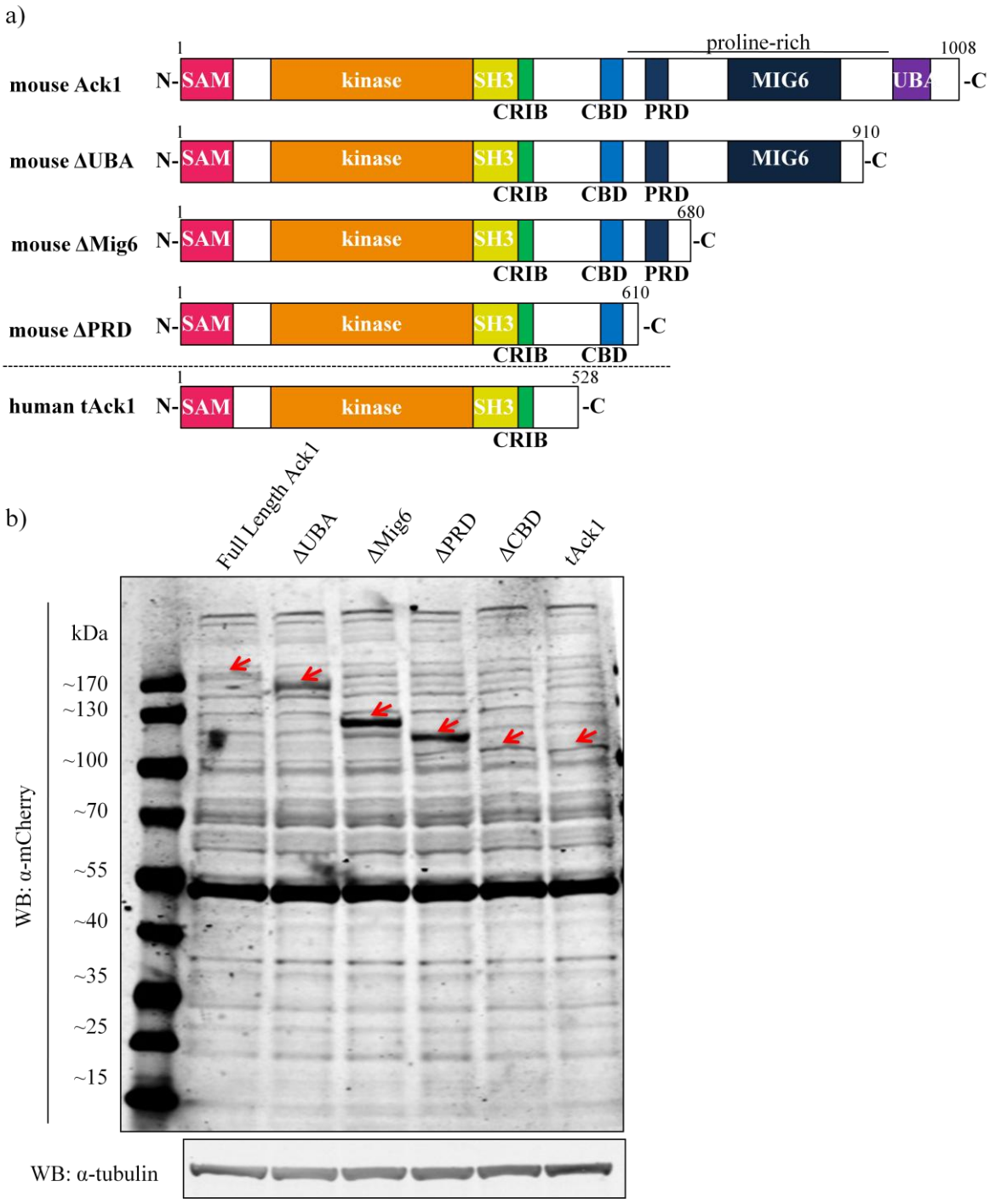

Figure 4.11. Ack1 C-terminal truncation mutants

a) Full-length mouse Ack1 (isoform 2) was amplified by polymerase chain reaction (PCR) with a common forward primer for all mutants and with different reverse primers constructed to omit particular domains (described in **Chapter 3.2.1**). The PCR product was linearised by digesting with restriction enzymes and ligated with pmCherry-C1 vector; **b)** 293T cells transfected with mCherry-tagged Ack1, tAck1 and Ack1 mutants were lysed and cell lysates were subjected to SDS PAGE and Western blotting with α-mCherry and α-tubulin antibodies.

The mutant lacking UBA, Mig6, PRD and clathrin binding domain (ΔCBD) was also constructed (**Figure 4.11 b**); however, for further experiments the truncated form of human Ack1 (tAck1) was used instead. The mutants were additionally N-terminally tagged to mCherry to facilitate imaging *via* confocal microscopy. These mutants were employed in several experiments to analyse the importance of the various domains in association between Ack1 and other proteins.

4.7 Mig6 and CBD both contribute to the colocalization with EGFR

It has been proposed that the UBA domain of Ack1 is required for EGFR degradation, whereas the Mig6 domain regulates EGFR binding (Shen *et al.*, 2007; Lin *et al.*, 2012). To analyse more precisely whether other Ack1 domains also contribute to the association with EGFR, I employed the mCherry-tagged C-terminal truncation mutants of Ack1 and human truncated Ack1. Using these constructs I carried out a series of colocalization studies with EGFR-GFP upon EGF stimulation. As shown in **Figure 4.12**, deletion of the UBA domain alone does not alter the colocalization between Ack1 and EGFR, which is similar to the full-length protein (~90%). In contrast, deletion of both UBA and Mig6 domains dramatically decreases this colocalization (~43%). Additional removal of the PRD does not have any further effects on the colocalization with EGFR; however, the absence of the clathrin binding domain, which is represented by tAck1, abolishes any remaining colocalization (**Figure 4.12**). These data emphasize the importance of the Mig6 domain in this context and suggest that Ack1 association with clathrin may also contribute to the colocalization between Ack1 and EGFR.

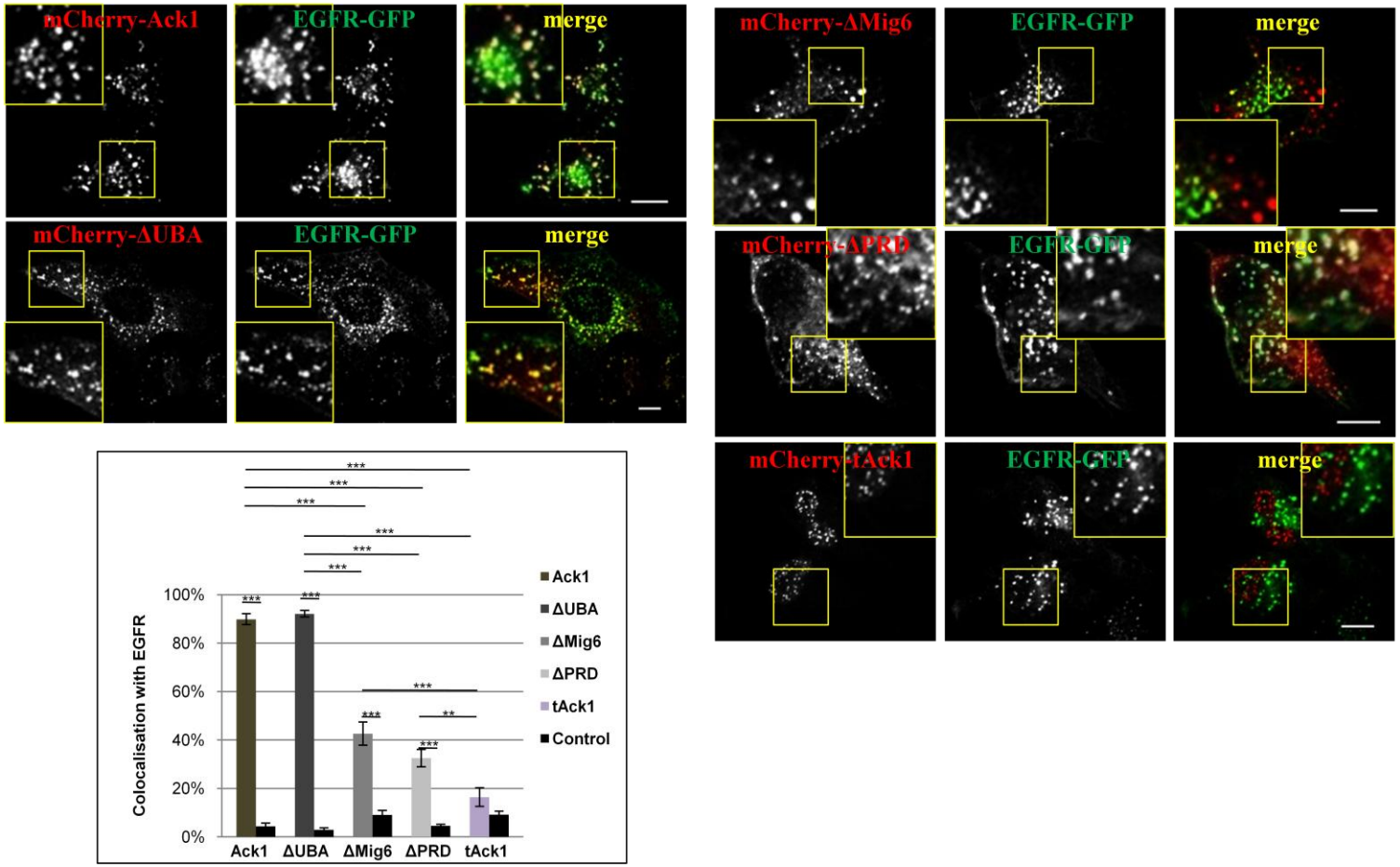

Figure 4.12. The Mig6 domain and CBD regulate colocalization with EGFR

HeLa cells transfected with mCherry-tagged Ack1, tAck1 and C-terminal truncation mutants and EGFR-GFP were serum-starved and stimulated with EGF for 30 minutes, fixed and imaged *via* confocal microscopy. For quantification, the Ack1, tAck1 or the Ack1 mutant puncta were circled and the colocalization with EGFR was quantified (described in **Chapter 3.2.3**). As a control, the circles were moved into the areas absent for Ack1, tAck1 or the Ack1 mutants and the random colocalization with EGFR was quantified. Scale bars 10 μm. Error bars represent SEM.

4.8 Endogenous Ack1 colocalizes with endogenous EGFR upon EGF stimulation

Showing that ectopically expressed Ack1 and EGFR colocalize in HeLa cells, I investigated this colocalization at the endogenous level in LNCaP cells, in which I identified endogenous Ack1 through immunostaining with α-Ack1 antibody (**Chapter 4.2.3**). As shown in **Figure 4.13**, endogenous Ack1 colocalizes with endogenous EGFR upon EGF stimulation. To my knowledge this is the first report of imaging the colocalization between Ack1 and EGFR at the endogenous level. These results validate that Ack1 and EGFR colocalize under physiological conditions.

4.9 Ack1 knockdown does not influence EGFR degradation

To further investigate the roles of Ack1 in EGFR trafficking, I investigated whether Ack1 influences EGFR degradation in LNCaP cells. A study by Grøvdal *et al.* shows that ectopically expressed Ack1 in HeLa cells inhibits EGFR sorting into the inner vesicles of late endosomes resulting in reduced EGFR degradation, whereas Ack1 knockdown increases EGFR recycling and thus decreases degradation (Grovdal *et al.*, 2008). Another study by Shen *et al.* also shows that EGFR degradation is inhibited following Ack1 knockdown in 293T cells (Shen *et al.*, 2007). Similarly in 1483 head and neck cancer cells, Ack1 knockdown inhibits EGFR degradation and ectopically expressed Ack1 in cells with downregulated Ack1 can rescue this inhibition (Kelley and Weed, 2012).

To determine whether Ack1 regulates EGFR signalling and degradation in LNCaP cells, the cells were treated with small interfering RNA (siRNA) against Ack1 or with non-targetting RNAi (control). The cells were then serum-starved for four hours and stimulated with EGF for up to three hours, and EGFR degradation was assessed by Western blotting, as shown in **Figure 4.14 a**.

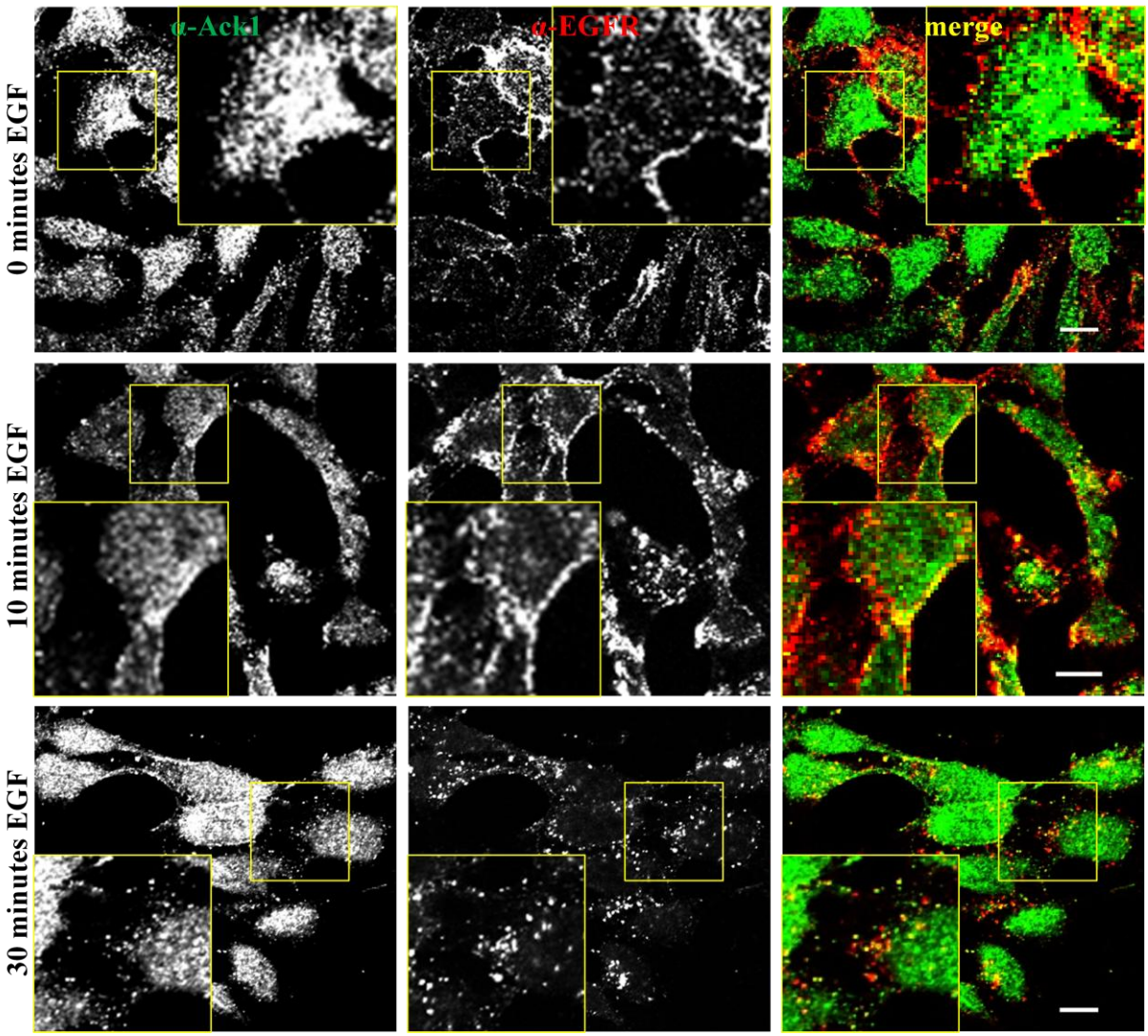

Figure 4.13. Endogenous Ack1 colocalizes with endogenous EGFR upon EGF treatment

LNCaP cells plated onto poly-D-lysine covered coverslips were serum-starved for four hours and stimulated with EGF for indicated times. The cells were fixed and immunostained with α-Ack1 and α-EGFR antibodies, and imaged *via* confocal microscopy. Scale bars 10 μm.

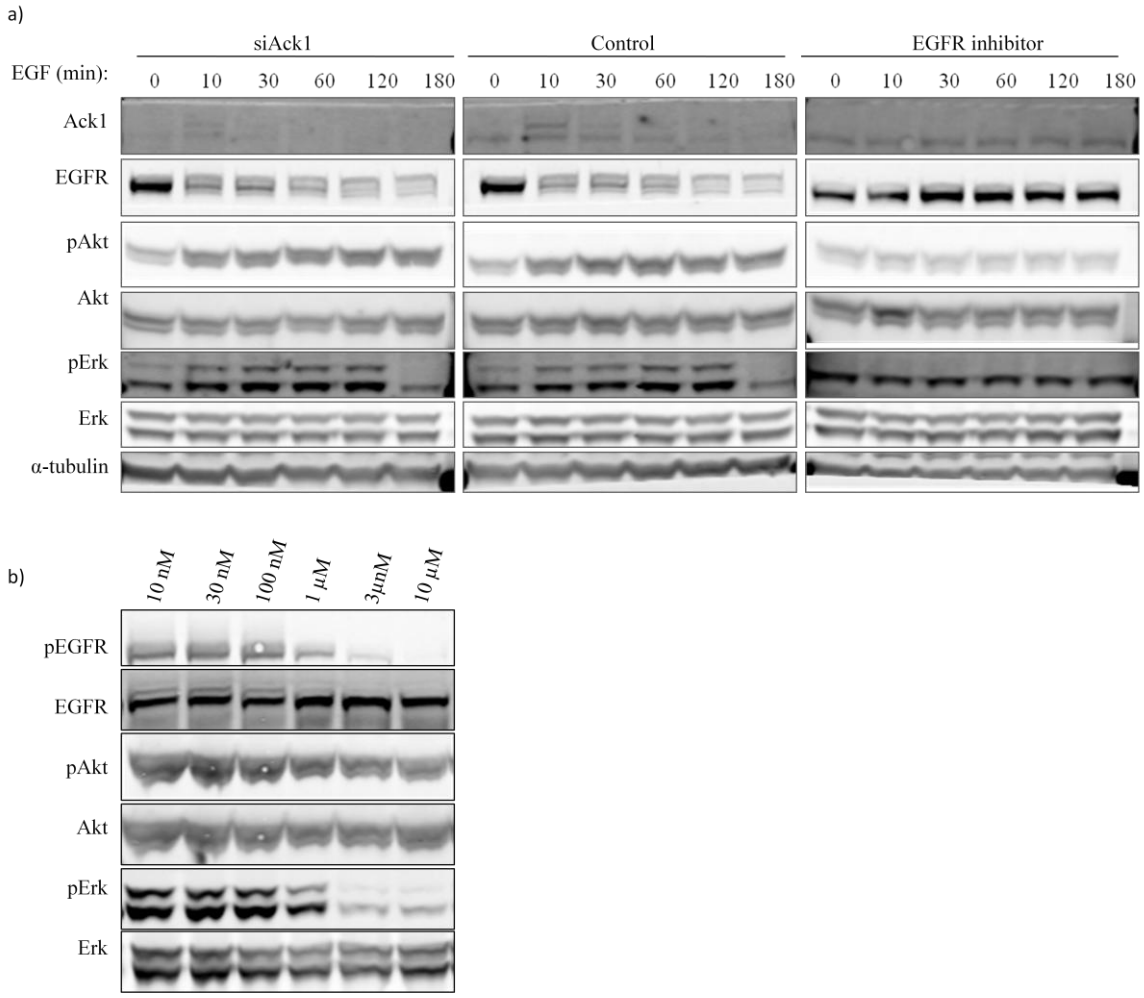

Figure 4.14. EGFR degradation in LNCaP cells following Ack1 knockdown

a) LNCaP cells transfected with siRNA against Ack1 or non-targeting RNAi (control) were serum-starved for four hours, the final hour in the presence or absence of the EGFR kinase inhibitor BIBX 1382, and stimulated with EGF for indicated times. The cells were lysed and cell lysates were subjected to SDS PAGE and Western blotting with α-Ack1, α-EGFR, α-phopsho Akt, α-Akt, α-phospho-Erk, α-Erk and α-tubulin antibodies; **b)** LNCaP cells were serum-starved for four hours, the final hour in the presence of BIBX 1382 at the indicated concentrations and stimulated with EGF for 30 minutes. The cells were lysed and cell lysates were subjected to SDS PAGE and Western blotting with α-phospho EGFR, α-EGFR, α-phospho Akt, α-Akt, α-phopsho-Erk and α-Erk antibodies.

As an additional control, cells were pre-treated with EGFR kinase inhibitor to prevent EGF-dependent EGFR degradation. Prior to this experiment, the optimal concentration of the EGFR inhibitor was tested and 10 µM has been found to sufficiently inhibit EGFR activation, as shown in **Figure 4.14 b**. Surprisingly, Ack1 knockdown does not influence EGFR degradation, as compared to control cells (**Figure 4.14 a**). Additionally, downstream signalling cascades are not affected by Ack1 knockdown, as represented by Erk and Akt phosphorylation which is similar to control cells. Therefore, these data indicate that in LNCaP cells, unlike in other cell lines, EGFR degradation is not affected by Ack1 depletion. Interestingly, although in the control Ack1 is degraded following EGF stimulation, this is not the case in the presence of the EGFR inhibitor (**Figure 4.14 a**). These data suggests that EGFR kinase activity is important for EGF-mediated Ack1 degradation.

4.10 Ack1 knockdown results in accelerated lysosomal localization of EGFR

Since Ack1 does not appear to influence EGFR signalling and degradation in LNCaP cells, I hypothesized that Ack1 may function in EGFR trafficking. Therefore I investigated whether EGFR localization to lysosomes is affected in cells depleted of Ack1. Thus, LNCaP cells expressing EGFR-GFP and treated with siRNA against Ack1 or with non-targetting RNAi (control) were serum-starved in the presence of lysotracker, a fluorescent dye that stains lysosomes (Chazotte, 2011). The cells were then imaged for 30 minutes upon EGF stimulation. As shown in **Figure 4.15 a**, when compared to the control, Ack1 knockdown promotes enhanced colocalization of EGFR and lysotracker following EGF stimulation. Additionally, average Ack1 knockdown in these conditions is approximately 80 %, as verified by real-time quantitative polymerase chain reaction (**Figure 4.15 b**).

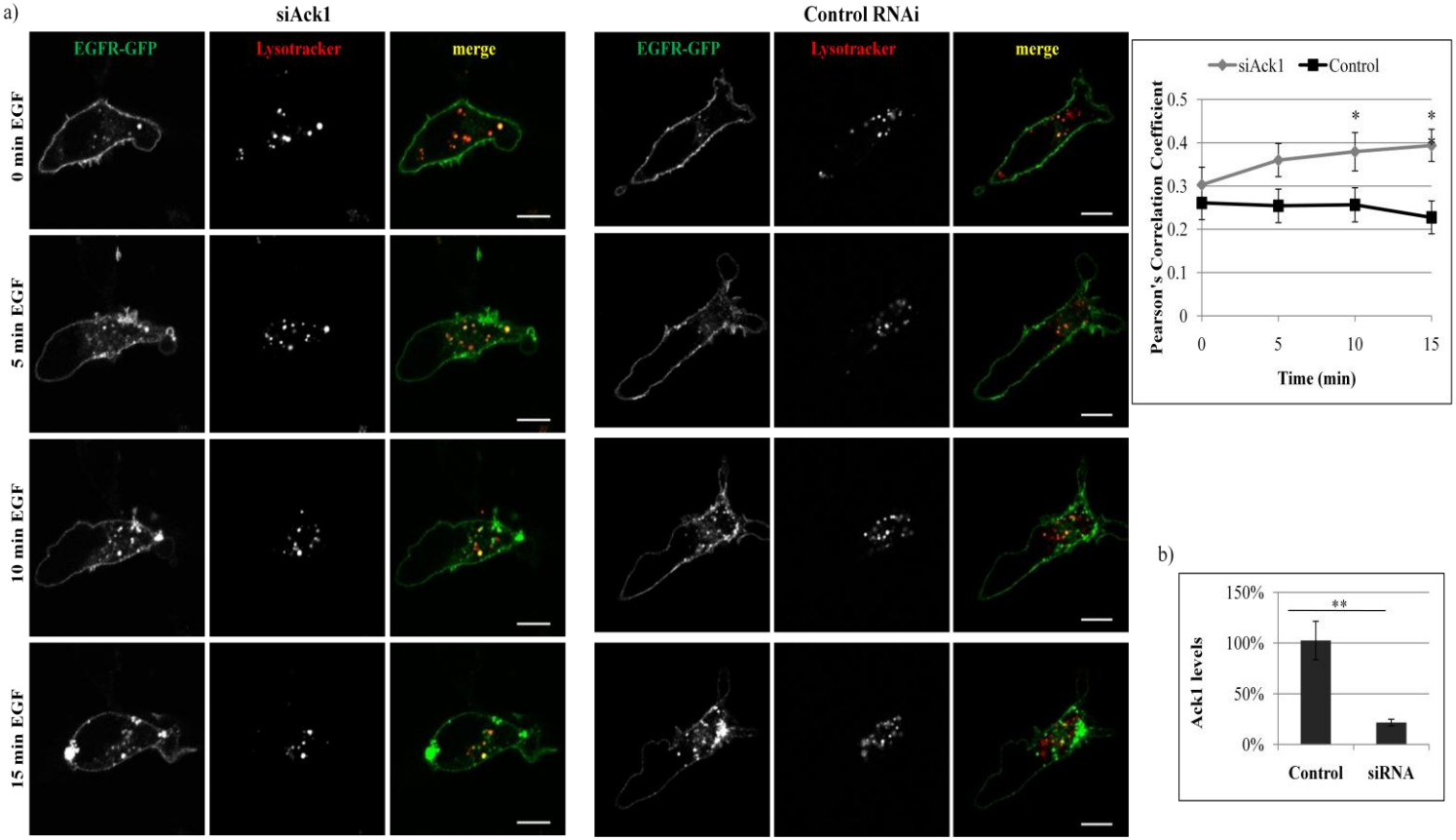

Figure 4.15. Ack1 knockdown increases EGFR lysosomal localization

a) LNCaP cells transfected with siRNA against Ack1 or non-targetting RNAi (control) and EGFR-GFP were serum-starved for four hours, the final 30 minutes in the presence of lysotracker (100 nM). The cells were washed with PBS and placed in cell imaging medium to enable live-cell imaging. Images were acquired upon 30 minutes of EGF treatment (one frame every 30-60 seconds). PCC was quantified at indicated times following EGF treatment; **b)** LNCaP cells transfected with siRNA against Ack1 or with non-targetting RNAi (control) were trypsinised and total RNA was isolated and used to synthesize cDNA. RT-qPCR was performed using primers for TNK2 or control r18S (**Chapter 3.2.5**).

Therefore, these results indicate that in the presence of Ack1, EGFR recruitment to lysosomes in reduced, thus suggesting that Ack1 functions in EGFR trafficking by preventing EGFR targetting to lysosomes following EGF stimulation.

4.11 Conclusions

The main aim of this chapter was to investigate the functions of Ack1 in RTK signalling and trafficking. So far numerous studies identified an involvement of Ack1 in signalling and trafficking of several RTKs. In particular, multiple lines of evidence implied on involvement of Ack1 implication in EGFR signalling, trafficking and degradation, and describe association between PDGFR, Axl, LTK and ALK (Shen *et al.*, 2007; Grovdal *et al.*, 2008; Pao-Chun *et al.*, 2009; Lin *et al.*, 2012). Interestingly, a screen for Ack1 interacting proteins showed that the C-terminal proline-rich portion of Ack1, including Mig6 domain, does not bind FGFR1 nor FGFR2 (Pao-Chun *et al.*, 2009). Therefore, the specificity of the interactions between Ack1 and EGFR, PDGFR and other RTKs is likely to depend on the motifs present within these RTKs, on interacting proteins or on the proximal subcellular localization.

The data presented in this chapter further characterise the association between Ack1 and EGFR. Immunoprecipitation of Ack1 results in co-precipitation of EGFR following EGF stimulation, whereas FGFR2 does not co-precipitate with Ack1 following FGF2 stimulation. Similar results are observed in the case of Fc-conjugated FGFR1 constructs, since Ack1 does not co-precipitate with any of these proteins, including kinase-active FcFGFR1. Furthermore, although an interaction between endogenous Ack1 and EGFR has been previously shown *via* biochemical approaches (Shen *et al.*, 2007), I believe that the imaging of the Ack1 and EGFR colocalization is shown for the first time at the physiological, endogenous level. Investigating the association between proteins at the cellular level can be very challenging, as some proteins

may not be very abundant and therefore difficult to identify. This often results in shifting towards the ectopically expressed proteins, which are usually easier to detect; however, this approach raises the question of the physiological relevance of identified associations. Therefore, detecting EGF-dependent colocalization between Ack1 and EGFR at the cellular level adds further evidence for their association *in vivo* and opens up the possibility of further research in these conditions. In summary, I conclude that Ack1 specifically interacts with EGFR, but not with FGFR, which potentially indicates the divergence in the endocytic trafficking of these RTKs.

Another outcome of the studies presented in this chapter comes from the work on the Ack1 C-terminal truncation mutants. This particular work has been performed to characterise the association between Ack1 and EGFR more precisely. Previous studies defined the regions within the Mig6 domain of Ack1 that interact with EGFR following EGF stimulation (Shen *et al.*, 2007) and in the presence of an adaptor protein Grb2 (Lin *et al.*, 2012). Mig6 has been shown to bind directly to activated EGFR and inhibit EGFR autophosphorylation, thus acting as a feedback EGFR inhibitor (Zhang *et al.*, 2007). Nevertheless, to my knowledge and according to the data presented in this chapter, Ack1 does not inhibit EGFR activation. The reason may be that another region within Mig6 is required for EGFR inhibition, and this region is absent in Ack1 (Zhang *et al.*, 2007). In this chapter I confirm the importance of the Mig6 domain in the association between Ack1 and EGFR. I also identify the clathrin binding domain as another region that contributes to this association. This is likely to be an indirect effect of EGFR being present within clathrin-coated vesicles and Ack1 association with clathrin through CBD.

Although other studies demonstrate that Ack1 regulates EGFR degradation, my work fails to demonstrate Ack1 function in this context. One of the reasons for this discrepancy may be that this function of Ack1 is cell-type specific, as my work was performed on prostate cancer cells, whereas the other studies employed cervical adenocarcinoma, head and neck cancer cells and human embryonic kidney cells (Shen *et al.*, 2007; Grovdal *et al.*, 2008; Kelley and Weed, 2012). As each cell line has its own specific proteome, EGFR degradation may be affected in different ways depending on cell context. In particular, I observe that in LNCaP cells the amount of endogenous EGFR is relatively high, whereas there is very little Ack1 (**Figure 4.14 a**). Therefore, it is possible that this discrepancy between the amount of endogenous Ack1 and EGFR may prevent observation of any influence of Ack1 depletion on EGFR degradation. In other cells, the difference may be smaller and thus Ack1 depletion could potentially exert a much more striking effect in this context. Additionally, other studies have shown that Ack1 is involved in Akt and Erk activation, *e.g.* Ack1 has been found to promote Erk phosphorylation downstream of activation of Axl RTK in Cos7 cells, and purified Ack1 has been shown to phosphorylate purified Akt (Pao-Chun *et al.*, 2009; Mahajan *et al.*, 2010). In contrast, I do not observe dramatic changes in Erk or Akt phosphorylation upon Ack1 knockdown. The reason may similarly be the cell-type specific differences; however, it is possible that activation of other signalling cascades may be affected by Ack1, *e.g.* those involved in autophagosomal degradation (described in **Chapter 6**). Interestingly, I show that Ack1 functions in EGFR trafficking and demonstrate that Ack1 knockdown promotes accelerated lysosomal localization of EGFR. Therefore, I propose that Ack1 interaction with EGFR following EGF stimulation may prevent EGFR trafficking through the classical endo-lysosomal pathway.

5 Ack1 endo-lysosomal localization

5.1 Introduction

The subcellular localization of a protein can potentially be very informative and shed a light on protein functions. For example receptor tyrosine kinases, such as EGFR, which are located at the plasma membrane, sense the extracellular environment and translate the signals from the outside into the cell (Lemmon and Schlessinger, 2010). Non-receptor tyrosine kinases are predominantly cytoplasmic, although some can associate with membranes, *e.g.* Src, and transduce signals upon RTKs activation (Blume-Jensen and Hunter, 2001; Roskoski, 2004; Mahajan and Mahajan, 2010). Other protein kinases, such as Akt, translocate to the nucleus to activate transcription factors, whereas STATs are themselves transcription factors and translocate to the nucleus to regulate gene expression (Blume-Jensen and Hunter, 2001).

Ack1 is a non-receptor tyrosine kinase and therefore is expected to be predominantly cytoplasmic. Consistently, the reports show that Ack1 partially localizes to early endosomes following EGF stimulation (Shen *et al.*, 2007; Grovdal *et al.*, 2008). Apart from the endosomal localization, reports exist suggesting that Ack1 translocates to the nucleus following activation (Ahmed *et al.*, 2004; Mahajan *et al.*, 2010). The N-terminal SAM domain has been found to promote plasma membrane localization; however, the other domains present within full-length protein prevent membrane localization (Prieto-Echaguee *et al.*, 2010). Other structures found to partially colocalize with Ack1 include clathrin-containing vesicles and AP2 complexes (Teo *et al.*, 2001), as well as amorphous intracellular structures (Prieto-Echaguee *et al.*, 2010) or a tubulo-reticular membrane compartments (Grovdal *et al.*, 2008). Nevertheless, the precise Ack1 subcellular localization has not yet been characterised.

In this chapter I investigate Ack1 localization in serum-starved cells and upon EGF stimulation. Consistently with previous reports, I find that Ack1 partially colocalizes to early, but not late or recycling, endosomes following EGF treatment; however, in contrast to other studies, I show that Ack1 does not translocate to the nucleus following EGF stimulation, even when nuclear export is inhibited. I also find association between Ack1 and Rab5, which localizes to early endosomes, but can also be found at the plasma membrane and in other intracellular structures, *e.g.* early autophagosomes (Stenmark, 2009).

5.2 Cytoplasmic localization of Ack1

Since Ack1 subcellular localization is poorly characterised and inconclusive, I investigated this more precisely. As mentioned above, some proteins and protein kinases translocate to the nucleus following activation and they regulate gene expression, *e.g.* it has been shown that Akt translocates to the nucleus upon phosphorylation, to activate downstream proteins and transcription factors (Nguyen *et al.*, 2006). In contrast the endocytic protein Eps15, which contains an identified nuclear export signal (NES), has been found to shuttle between the cytoplasm and nucleus in a phosphorylation-independent manner. In particular, when nuclear export was inhibited by treatment with leptomycin B, ectopically expressed Eps15 accumulated within the nucleus in both serum-starved and EGF treated cells (Vecchi *et al.*, 2001). Ack1 has been proposed to interact with androgen receptor (AR) and translocate to the nucleus to promote DNA binding of AR and regulate gene transcription in prostate cancer cells (Mahajan *et al.*, 2007). Additionally, Ack1 has been proposed to translocate to the nucleus in semi-confluent, but not confluent, glioblastoma cells through interaction with Cdc4, and a putative NES sequence has been identified within the N-terminal portion of Ack1 (Ahmed *et al.*, 2004).

In order to determine whether Ack1 translocates to the nucleus following EGF stimulation, HeLa cells expressing GFP-Ack1 were serum-starved for four hours followed by an overnight incubation with EGF in the presence of leptomycin B. Additionally, truncated Ack1 has been employed to determine whether the C-terminal portion, which is present in full-length but not tAck1, is important for a potential nuclear localization. Eps15 was used as a positive control. As shown in **Figure 5.1**, Ack1 does not accumulate within the nucleus following EGF treatment, even in the presence of leptomycin B. In contrast, Eps15 exhibits strong nuclear localization when nuclear export is inhibited. This possibly indicates that although the putative NES motif may be present within the N-terminus of Ack1, additional features, *e.g.* conformation of a full-length protein or interacting partners, prevent Ack1 nuclear translocation. Surprisingly, tAck1 shows leptomycin-independent nuclear localization. These results suggest that the N-terminal portion of Ack1 does not comprise NES sequence, as tAck1 would accumulate within the nucleus in the presence of leptomycin B. Although it is possible that nuclear localization of tAck1 is an artefact, the molecular size of GFP-tagged tAck1 (approximately 100 kDa) prevents it from diffusing freely through nuclear pores (Marfori *et al.*, 2011). Therefore, the nuclear localization potentially indicates that tAck1 may play a role within the nucleus, *e.g.* in a process of DNA replication or gene transcription.

Additionally, to exclude the possibility that aquired images do not focus entirely on the nucleus and thus the observed nuclear localization of Eps15 and tAck1 may be the result of imaging of the perinuclear region rather than nucleus, the images were taken at various depths within the sample (*Z*-stack). As shown in **Figure 5.2**, the nuclear localization of both Eps15 and tAck1 can be distinguished. In contrast, no Ack1 can be found within the nucleus. Therefore I conclude that in HeLa cells, ectopically expressed Ack1 does not translocate to the nucleus following EGF treatment, even when nuclear export is inhibited.

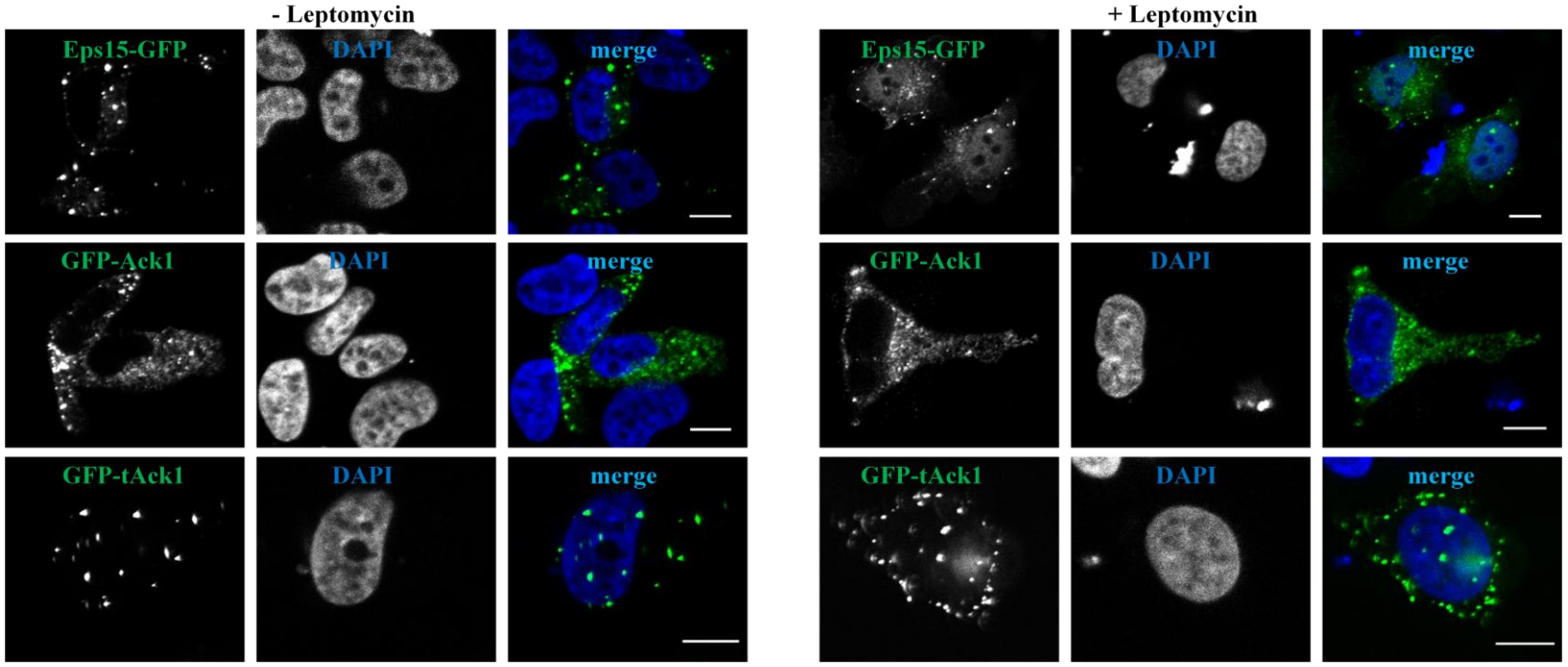

Figure 5.1. Ack1 does not translocate the nucleus

HeLa cells transfected with Eps15-GFP, GFP-Ack1 or GFP-tAck1 were serum-starved for four hours and stimulated overnight with EGF in the presence of leptomycin B (10 ng/ml). The cells were fixed and mounted with Vectashield with DAPI, which stains the nucleus. The cells were imaged *via* confocal microscopy. Scale bars 10 µm.

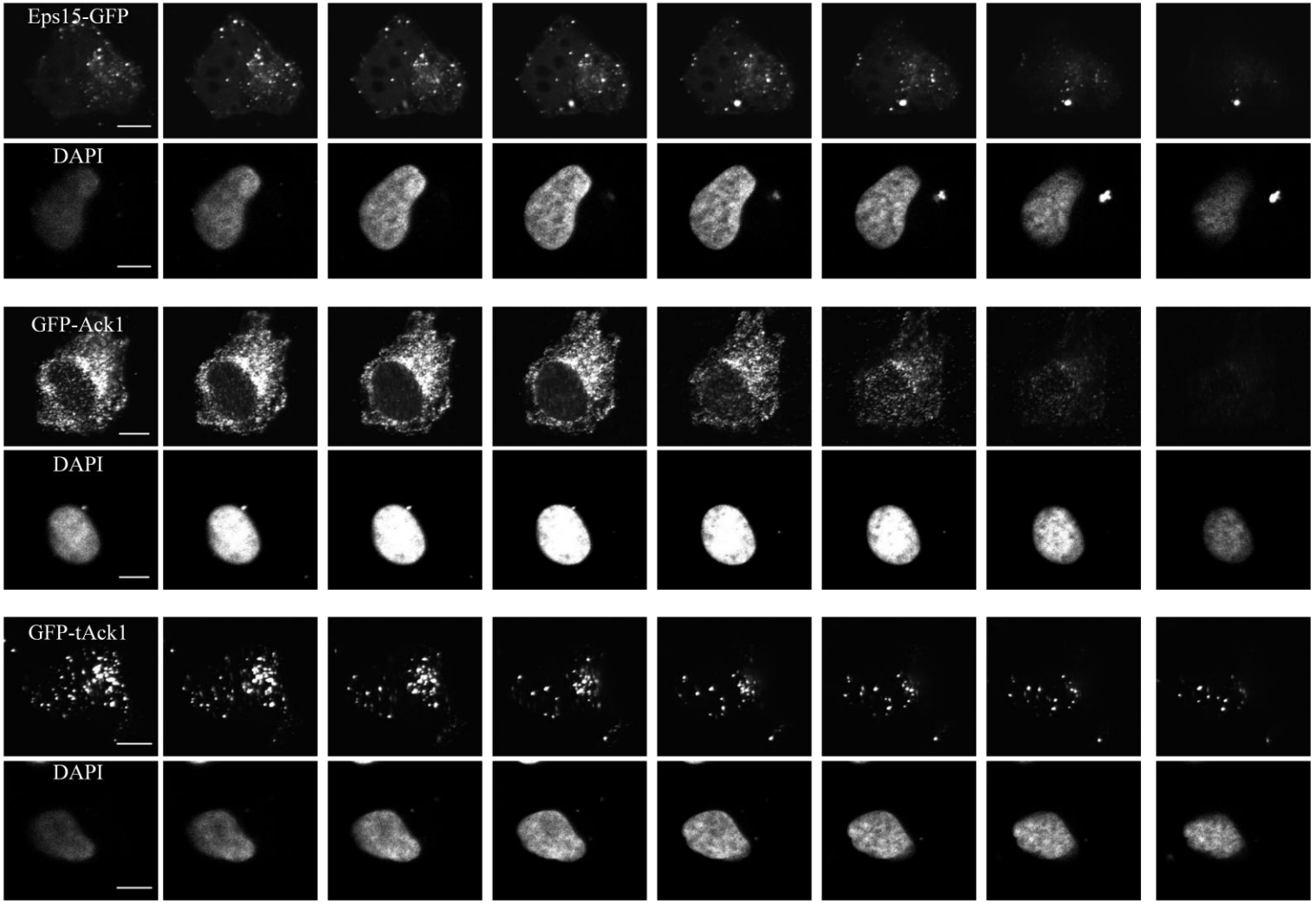

Figure 5.2. *Z*-stack of cells expressing Eps15-GFP, GFP-Ack1 and GFP-tAck1

The cells were treated as in **Figure 5.1**. Presented *Z*-stack cover 5.6 µm of the cell (each frame every 0.8 µm). Scale bars 10 µm.

5.3 Ack1 partially colocalizes with transferrin

Considering that Ack1 does not localize within the nucleus, I investigated other potential intracellular localizations. Firstly, I assessed Ack1 colocalization with transferrin (Tf), an iron-binding protein that undergoes clathrin-mediated endocytosis following binding to Tf receptor (TfR). Tf-TfR traffics to early endosomes to deliver iron and then recycles back to the plasma membrane (Mayle *et al.*, 2012). HeLa cells expressing GFP-Ack1 were briefly serum-starved and incubated with Tf for 30 min, fixed and imaged. As shown in **Figure 5.3 a**, partial colocalization between Ack1 and Tf can be distinguished suggesting that Ack1 may localize to clathrin-coated vesicles, early endosomes or recycling endosomes, all of which are characterised by Tf; however, a substantial portion of Ack1 is present within structures devoid of Tf, indicating that Ack1 also localizes to compartments other than early or recycling endosomes. Interestingly and consistently with previous reports, I find that high levels of Ack1 expression inhibit Tf uptake, shown in **Figure 5.3 b**, likely as a result of perturbation of clathrin distribution (Teo *et al.*, 2001). Therefore, for all studies presented, low or moderate levels of Ack1 expression were employed.

I also investigated the colocalization between Ack1 and acidic compartments, such as late endosomes and lysosomes using lysotracker, which permeates plasma membrane and accumulates within acidic compartments (Chazotte, 2011). HeLa cells expressing GFP-Ack1 and incubated with lysotracker were fixed and imaged *via* confocal microscopy. As shown in **Figure 5.3 c**, no colocalization can be distinguished suggesting that Ack1 does not localize to acidic compartments; however, the fluorescence of GFP has been shown to decrease in low pH (Patterson *et al.*, 1997). Since this study employed GFP-tagged Ack1, it is possible that the fluorescence of GFP-Ack1 was decreased in acidic compartments.

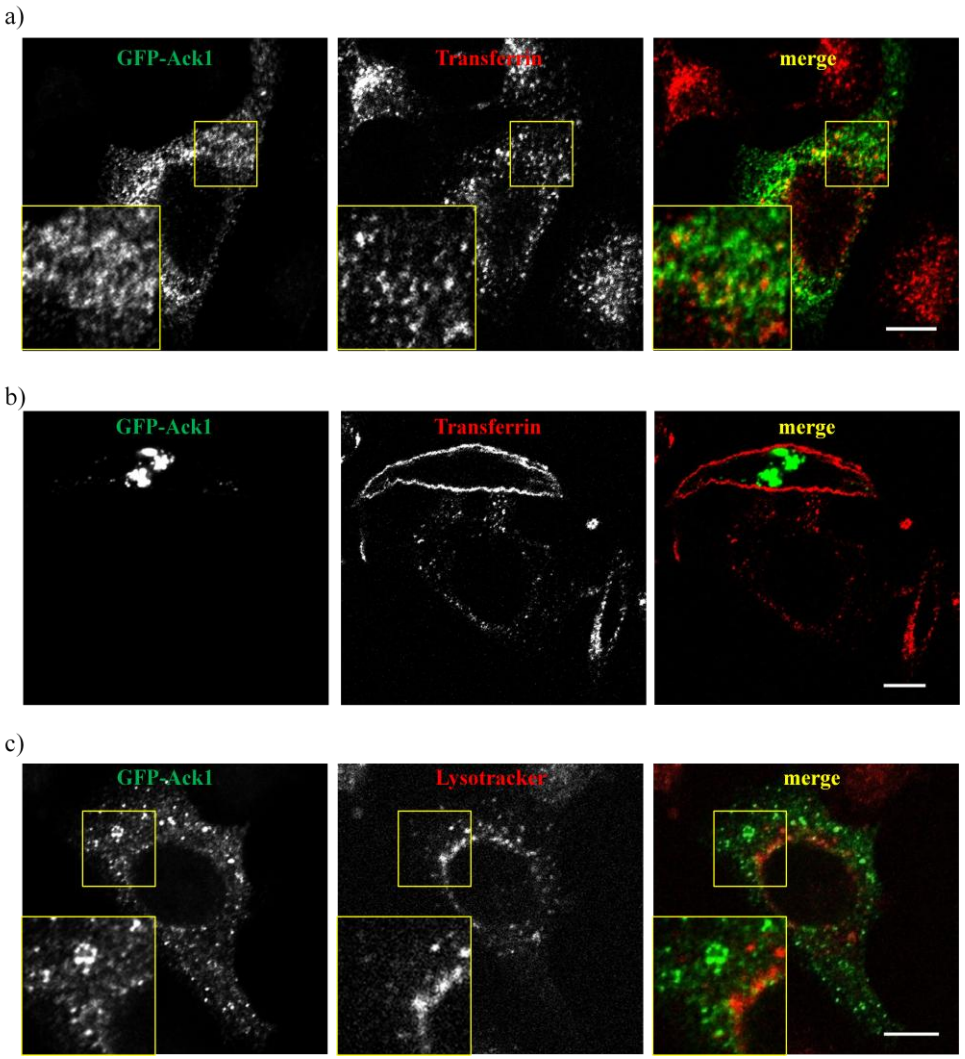

Figure 5.3. Ack1 partially colocalizes with transferrin

HeLa cells transfected with GFP-Ack1 were serum-starved for 10 minutes and incubated with Alexa Fluor-568 transferrin for 30 minutes **(a)** or 5 minutes **(b)**. The cells were fixed and imaged *via* confocal microscopy, c) HeLa cells transfected with GFP-Ack1 were incubated with lysotracker for two hours, fixed and imaged *via* confocal microscopy. Scale bars 10 µm.

Therefore the late endosomal or lysosomal localization of Ack1 cannot be excluded on the basis of this experiment

5.4 Ack1 partially localizes to early endosomes upon EGF stimulation

Previous reports demonstrate that upon EGF treatment, Ack1 partially colocalizes with EGF on early endosomes which are the initial delivery sites for membrane proteins upon endocytosis (Maxfield and McGraw, 2004; Grovdal *et al.*, 2008). Early endosome antigen 1 (EEA1) is a peripheral membrane protein that localizes to early endosomes (Mu *et al.*, 1995). I therefore employed α-EEA1 antibody to confirm the previous reports on early endosomal localization of Ack1. HeLa cells expressing mCherry-Ack1 were serum-starved followed by incubation with EGF for various times, fixed and immunostained with α-EEA1 antibody. As shown in **Figure 5.4**, Ack1 poorly colocalizes with EEA1 in serum-starved cells (0 minutes EGF), which is manifested by a very low PCC (**Figure 5.4**, **graph**). Consistently with the previous reports, upon EGF stimulation Ack1 colocalization with EEA1 significantly increases. These results confirm that Ack1 partially translocates to early endosomes following EGF treatment.

5.5 Ack1 partially colocalizes with Rab5 upon EGF stimulation

In addition to early endosomes, I also investigated whether Ack1 may localize to other subcellular compartments. As explained in **Chapter 1.3.4**, Rab GTPases localize to various endocytic compartments, *e.g.* Rab4 predominantly to early and recycling endosomes, Rab5 to early endosomes, autophagosomes and clathrin-coated pits, Rab7 to late endosomes, autophagosomes and autolysosomes and Rab11 to recycling endosomes (Stenmark, 2009). Therefore I investigated the colocalization between Ack1 and these Rab GTPases.

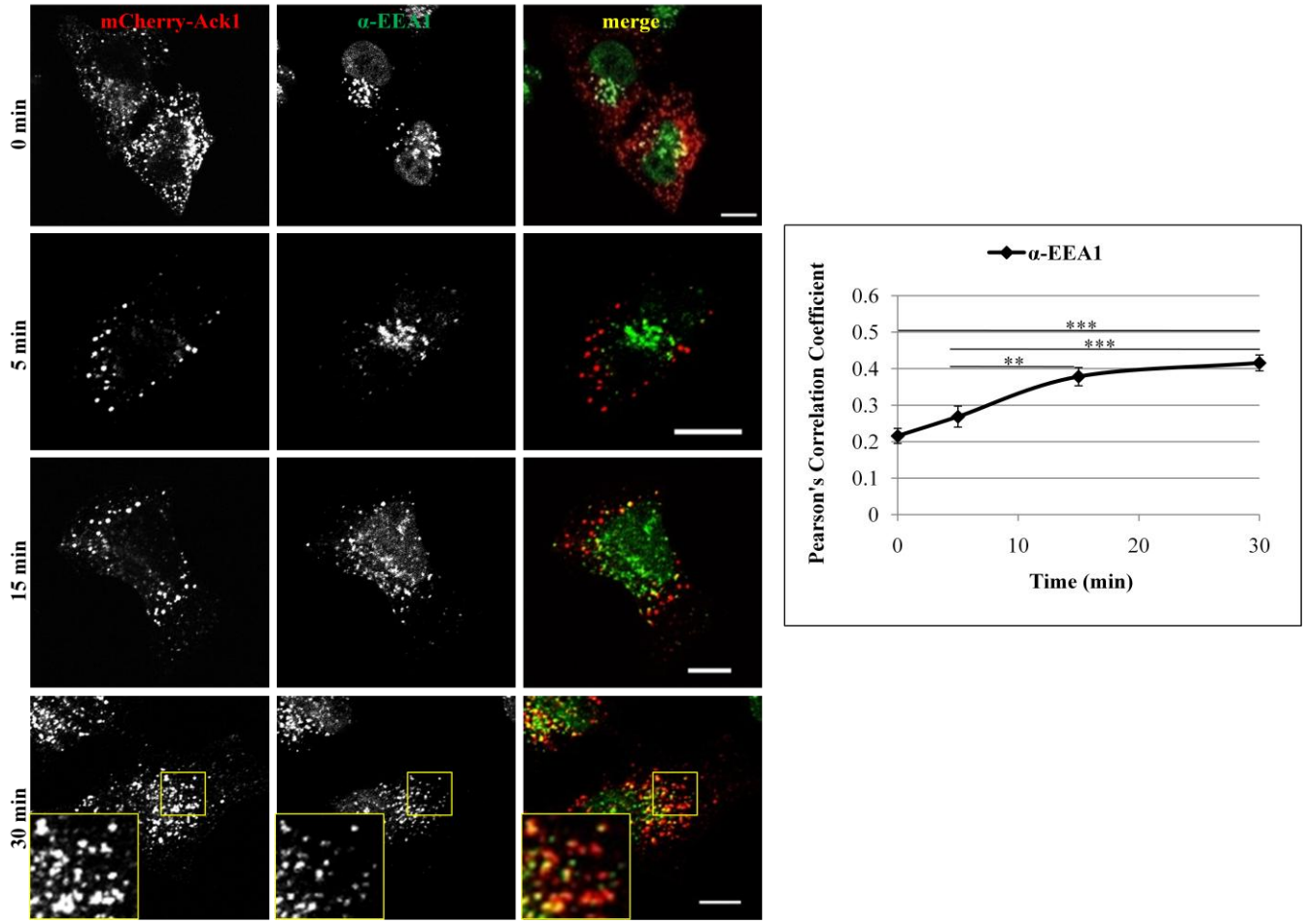

Figure 5.4. Ack1 partially localizes to early endosomes upon EGF stimulation

HeLa cells transfected with mCherry-Ack1 were serum-starved for four hours and stimulated with EGF for indicated times, fixed and immunostained with α-EEA1 antibody. The cells were imaged *via* confocal microscopy, and the colocalization was quantified. Scale bars 10 µm. Error bars represent SEM.

Firstly, I examined the association between Ack1 and Rab5. HeLa cells expressing mCherry-Ack1 and Rab5-GFP were serum-starved and stimulated with EGF for various times, fixed and imaged. As shown in **Figure 5.5 a**, Ack1 only marginally colocalizes with Rab5 in starved cells; however, the colocalization between Ack1 and Rab5 significantly increases following EGF stimulation. Additionally, I employed a mutant Rab5aQ79L-GFP, which is constitutively active and GTP-bound. This mutant has been shown to promote early endosomal fusion and its expression led to the accumulation of enlarged endosomes (Stenmark *et al.*, 1994). As shown in **Figure 5.5 b**, mCherry-Ack1 colocalizes with Rab5aQ79L-GFP mutant following EGF stimulation. These results support the finding that Ack1 partially colocalizes with Rab5 upon EGF treatment.

Subsequently, I examined whether Ack1 colocalizes with Rab4 and Rab11. These two Rab GTPases are found on recycling endosomes: Rab4 on vesicles derived from early endosomes, whereas Rab11 on vesicles trafficking through the perinuclear recycling compartment (PNRC) (Stenmark, 2009). As shown in **Figure 5.6 a** and **b**, very little colocalization between mCherry-Ack1 and GFP-tagged Rab4 or Rab11 can be distinguished in serum-starved cells. Following EGF stimulation, some colocalization can be found at 15 and 30 minutes post-EGF treatment in the case of Rab4 (**Figure 5.6 a**), and at 30 minutes post-EGF in the case Rab11 (**Figure 5.6 b**). These data potentially suggest that Ack1 may regulate recycling following EGF stimulation.

I also examined the colocalization between Ack1 and Rab7, which has been found enriched in late endosomes, lysosomes and autophagosomes (Stenmark, 2009). As shown in **Figure 5.7**, Ack1 does not colocalize with Rab7 in serum-starved cells. Following EGF stimulation, some level of colocalization can be distinguished at 15 and 30 minutes of EGF treatment.

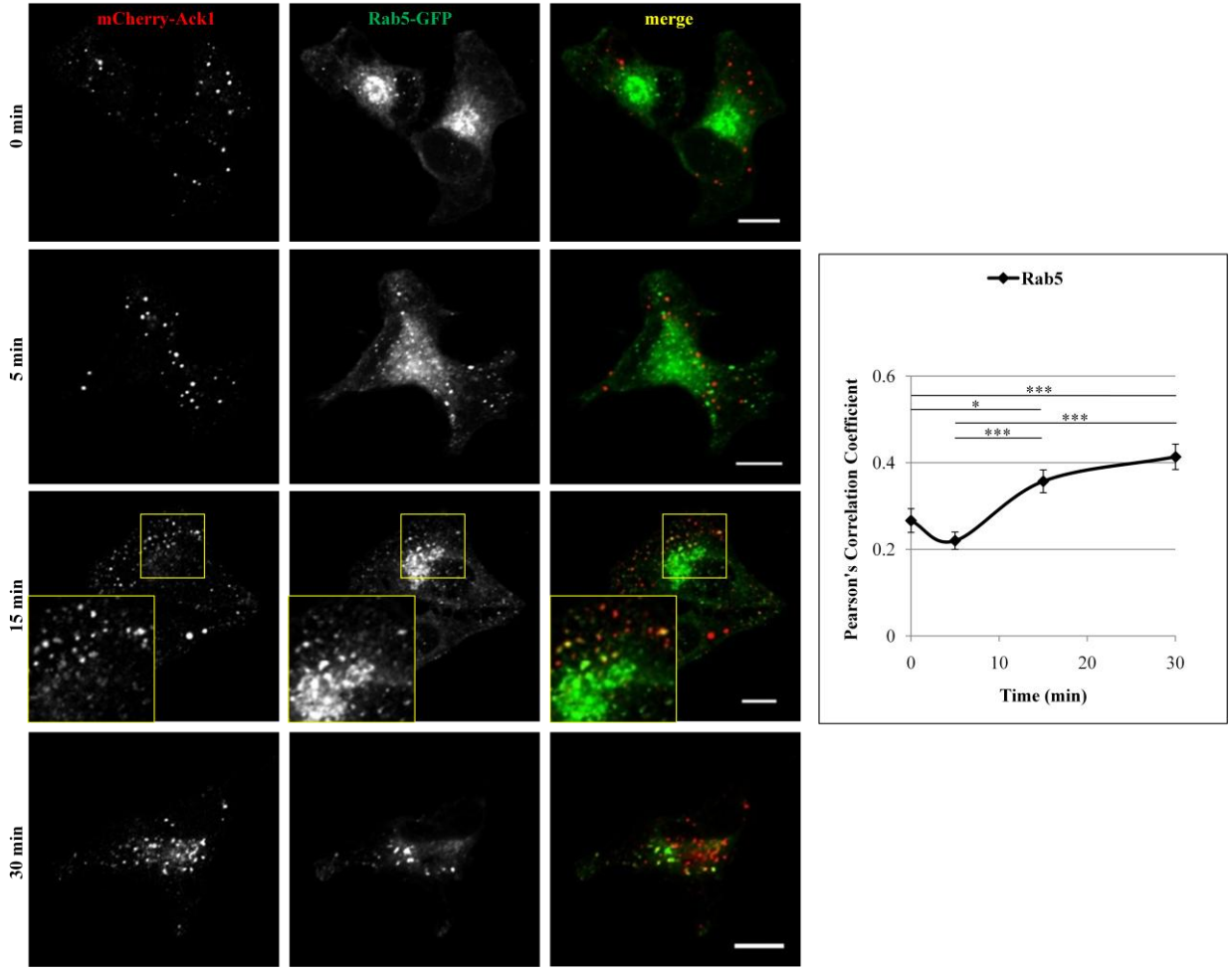

Figure 5.5 Ack1 partially localizes to Rab5 upon EGF stimulation (a) and (b)

a) HeLa cells transfected with mCherry-Ack1 and Rab5-GFP were serum-starved for four hours and stimulated with EGF for indicated times, and fixed. The cells were imaged *via* confocal microscopy, and the colocalization was quantified. Scale bars 10 µm. Error bars represent SEM.

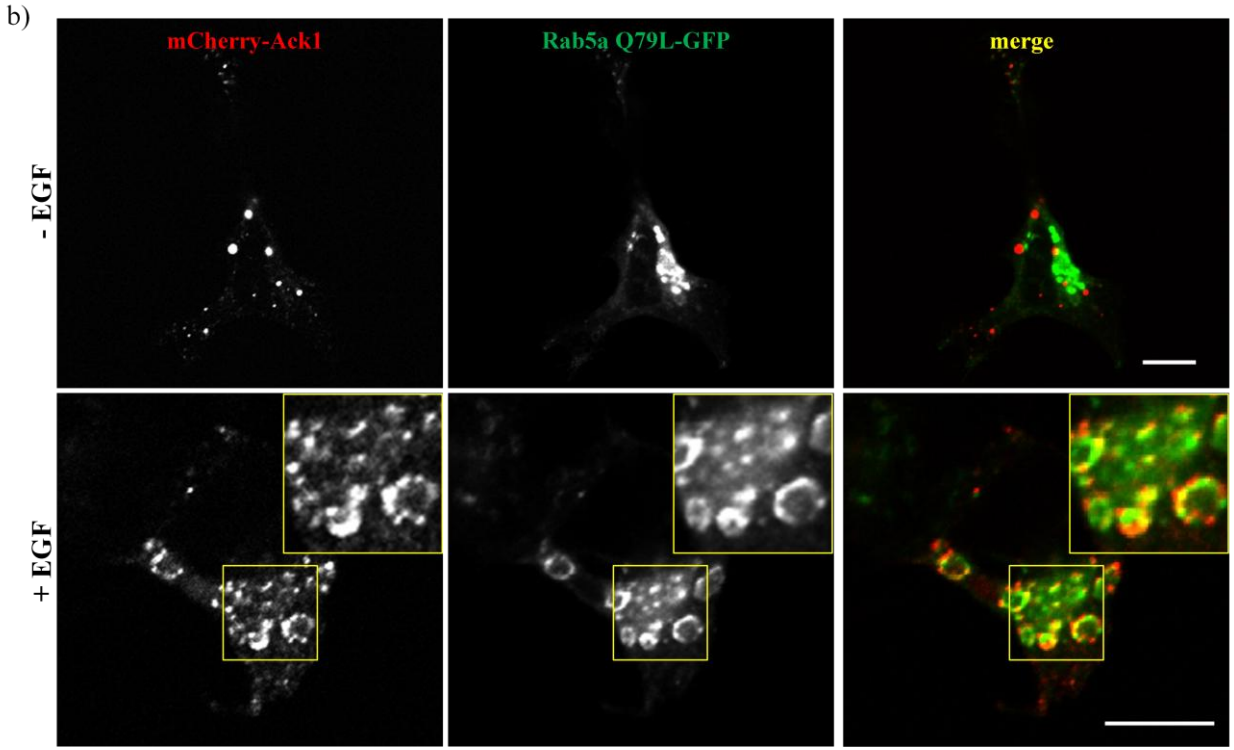

Figure 5.5 Ack1 partially localizes to Rab5 upon EGF stimulation (a) and (b)

b) HeLa cells transfected with mCherry-Ack1 and Rab5aQ79L-GFP mutant were serum-starved for four hours and stimulated with EGF for 30 minutes, fixed and imaged *via* confocal microscopy. Scale bars 10 µm.

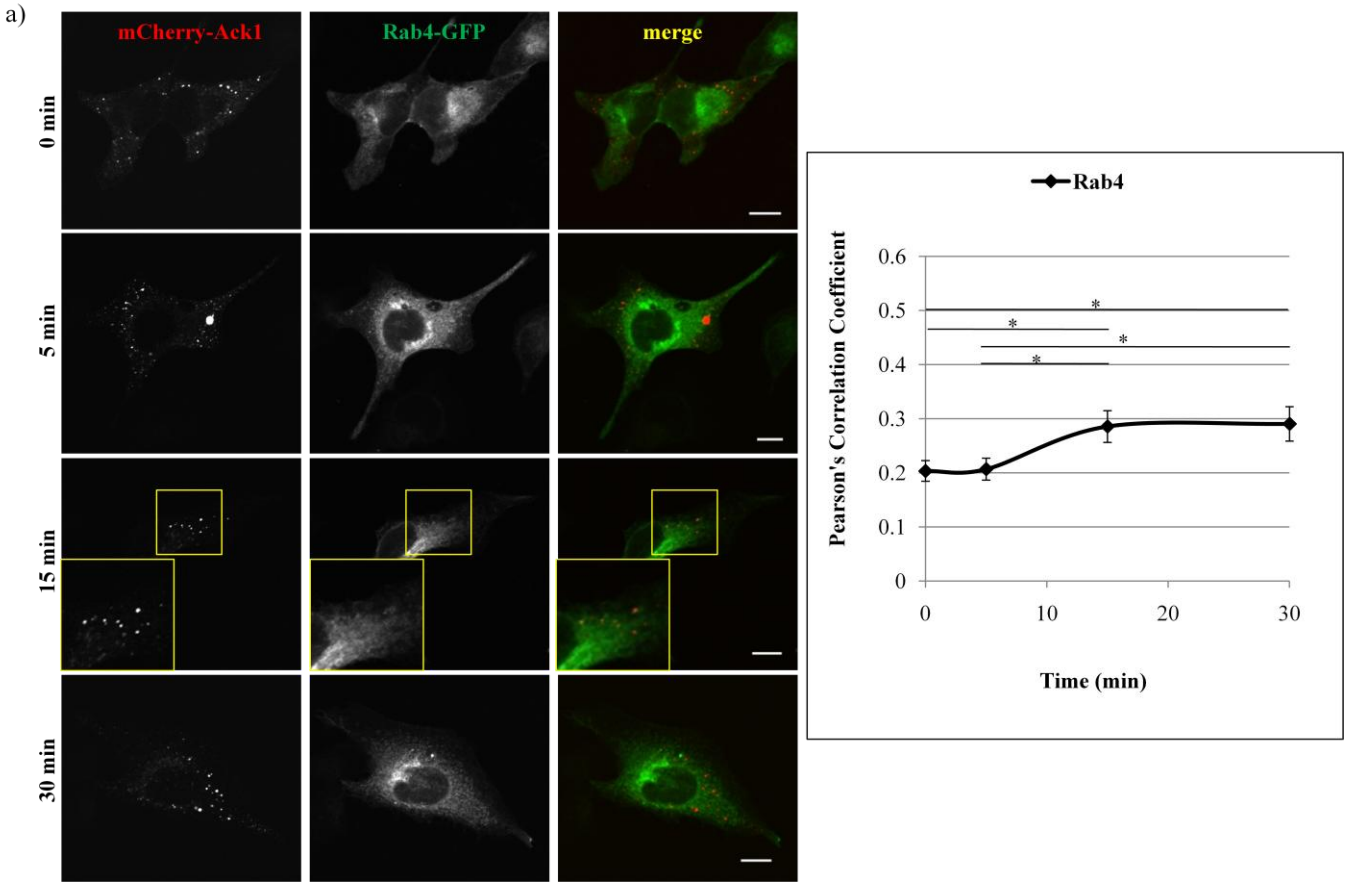

Figure 5.6. Ack1 partially colocalizes with Rab4 and Rab11 post-EGF treatment (a) and (b)

a) HeLa cells transfected with mCherry-Ack1 and Rab4-GFP were serum-starved for four hours and stimulated with EGF for indicated times, and fixed. The cells were imaged *via* confocal microscopy, and the colocalization was quantified. Scale bars 10 µm. Error bars represent SEM.

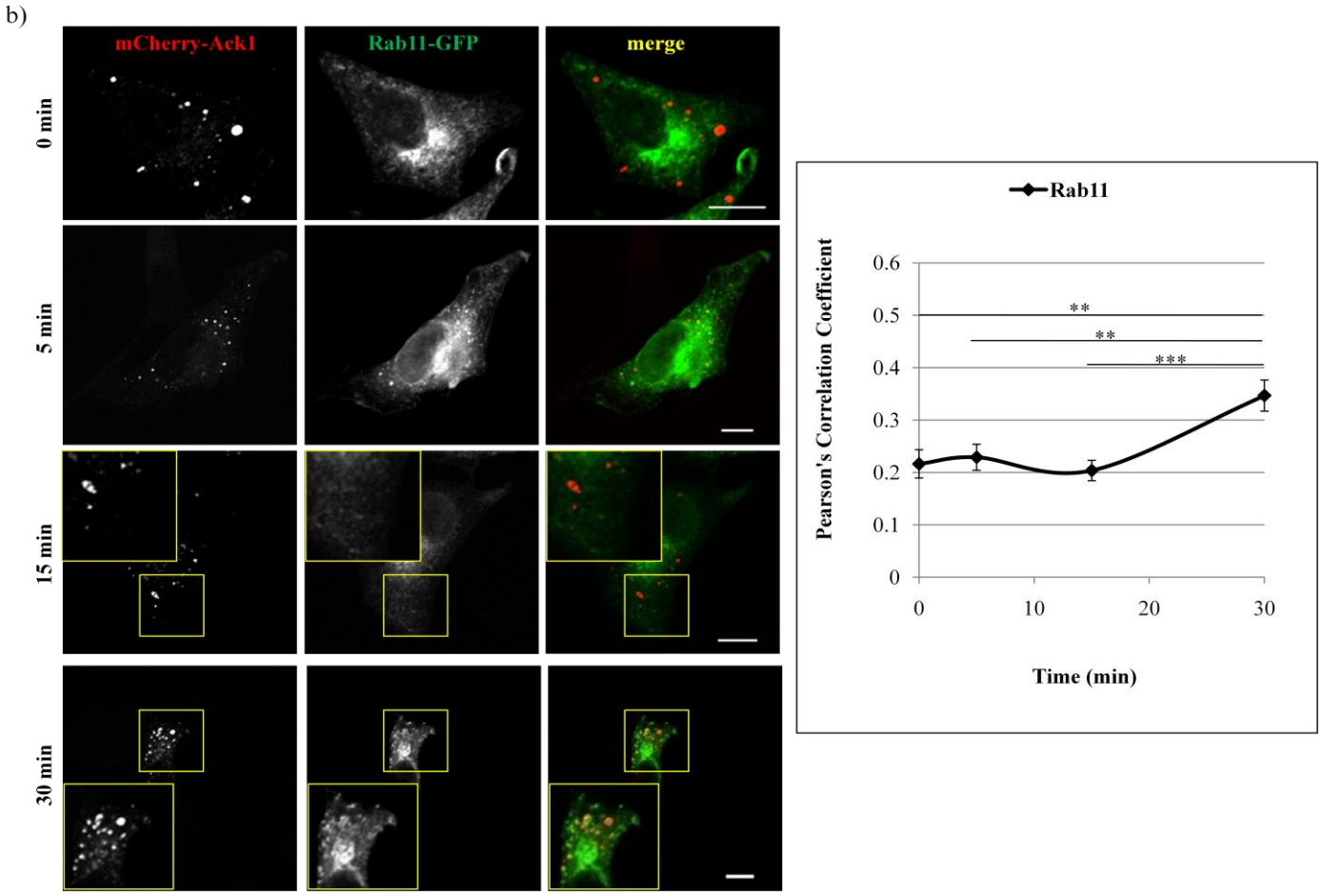

Figure 5.6. Ack1 partially colocalizes with Rab4 and Rab11 post-EGF treatment (a) and (b)

b) HeLa cells transfected with mCherry-Ack1 and Rab11-GFP were serum-starved for four hours and stimulated with EGF for indicated times, and fixed. The cells were imaged *via* confocal microscopy, and the colocalization was quantified. Scale bars 10 µm. Error bars represent SEM.

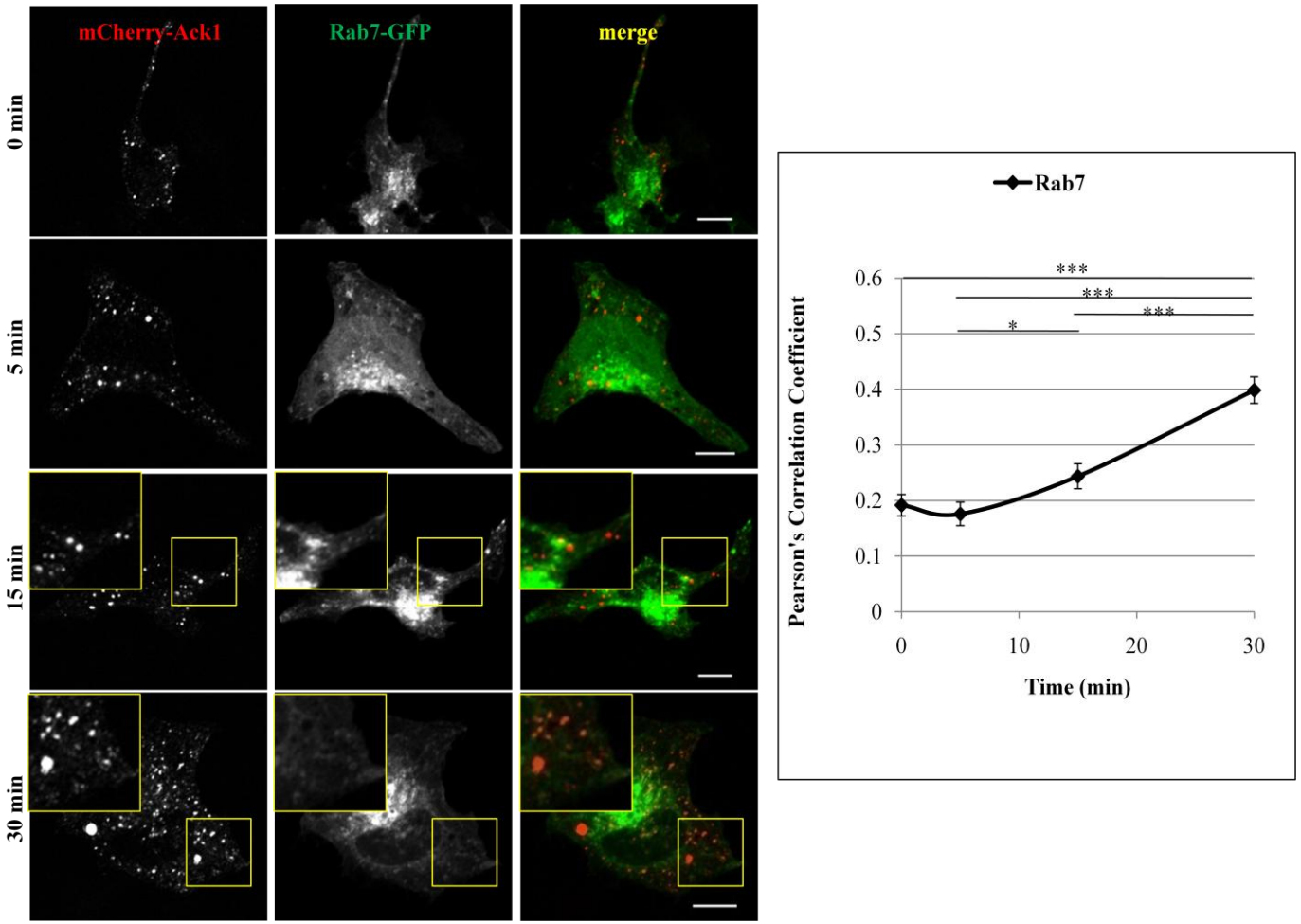

Figure 5.7. Ack1 partially colocalizes with Rab7 post-EGF treatment

HeLa cells transfected with mCherry-Ack1 and Rab7-GFP were serum-starved for four hours and stimulated with EGF for indicated times, and fixed. The cells were imaged *via* confocal microscopy, and the colocalization was quantified. Scale bars 10 µm. Error bars represent SEM.

Therefore, these results indicate that following EGF treatment, a portion of Ack1 translocates to Rab7-enriched compartments. Taken together, these data raise the possibility that Ack1 may partially regulate recycling through its association with Rab4 and Rab11, and degradation through association with Rab7. Nevertheless, these studies have been completed on ectopically expressed Rab GTPases, which may potentially disturb subcellular trafficking. Therefore, subsequent experiments have been carried out without ectopically expressed Rab GTPases.

5.6 Ack1 does not localize to late endosomes or recycling endosome

Following studies with ectopically expressed Rab GTPases, I further investigated Ack1 localization to late endosomes and recycling compartment taking advantage of the specific characteristics of these compartments, *i.e.* late endosomes being enriched in lysobisphosphatidic acid (LBPA), whereas PNRC in Rab11 (Kobayashi *et al.*, 1998; Kobayashi *et al.*, 1999; Galve-de Rochemonteix *et al.*, 2000; Stenmark, 2009). Therefore, I performed the colocalization studies between Ack1 and endogenous LBPA and Rab11. HeLa cells expressing mCherry-Ack1 were serum-starved and stimulated with EGF for various times. The cells were fixed and immunostained with α-LBPA or α-Rab11 antibodies. As shown in **Figure 5.8** and **Figure 5.9**, Ack1 does not colocalize with endogenous LBPA or Rab11 in serum-starved cells or upon EGF stimulation. This is inconsistent with my data on ectopically expressed Rab GTPases, where Ack1 partially colocalized with GFP-tagged Rab4, Rab7 and Rab11 upon EGF treatment (**Chapter 5.5**). This discrepancy may reflect the differences between experiments completed at the physiological levels to those employing ectopically expressed proteins. Additionally, subcellular distribution of Rab7 may slightly differ from LBPA, which could additionally explain observed differences.

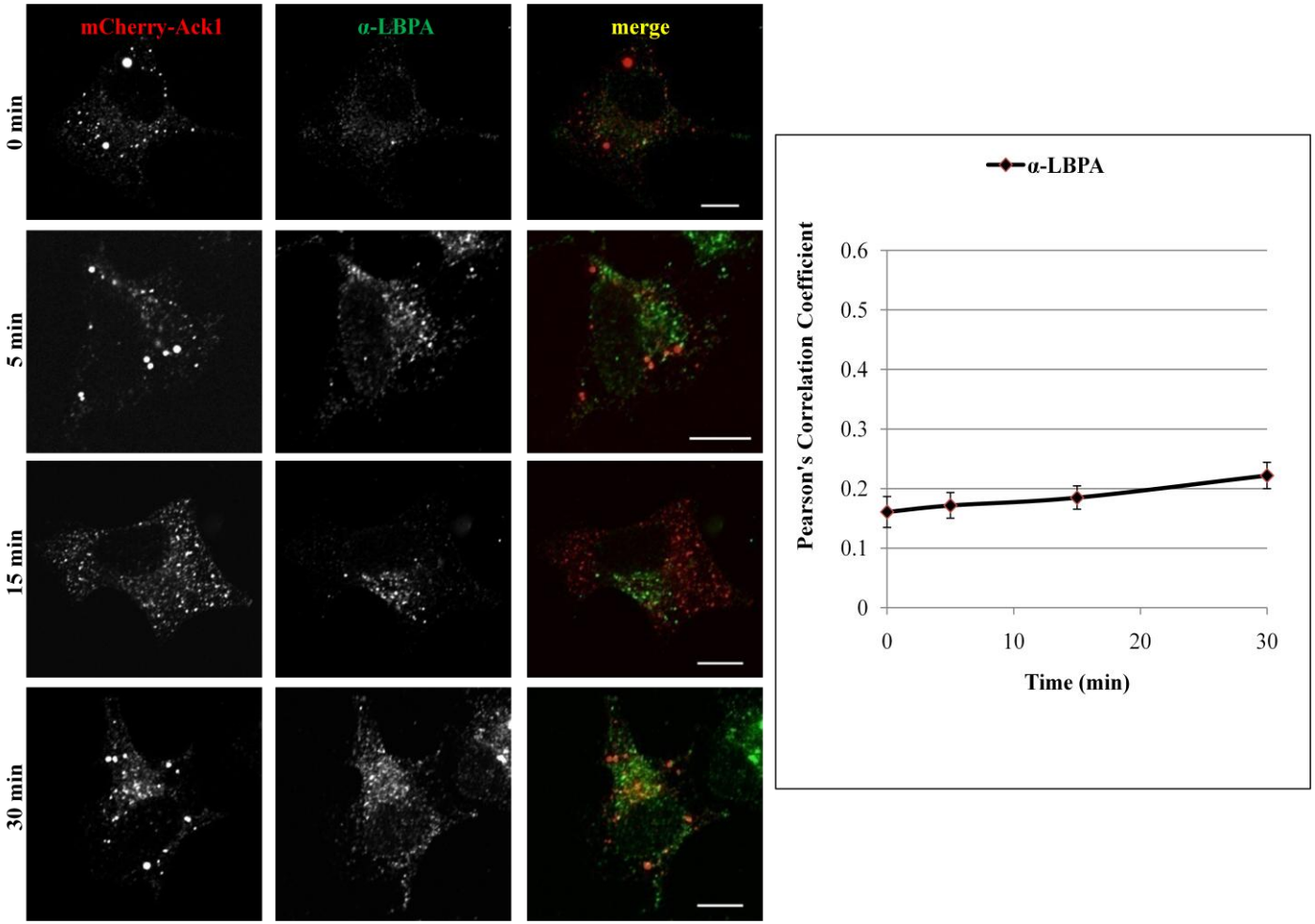

Figure 5.8. Ack1 does not localize to late endosomes post-EGF treatment

HeLa cells transfected with mCherry-Ack1 were serum-starved for four hours and stimulated with EGF for indicated times, and fixed. The cells were immunostained with α-LBPA antibody and imaged *via* confocal microscopy, and the colocalization was quantified. Scale bars 10 μm. Error bars represent SEM.

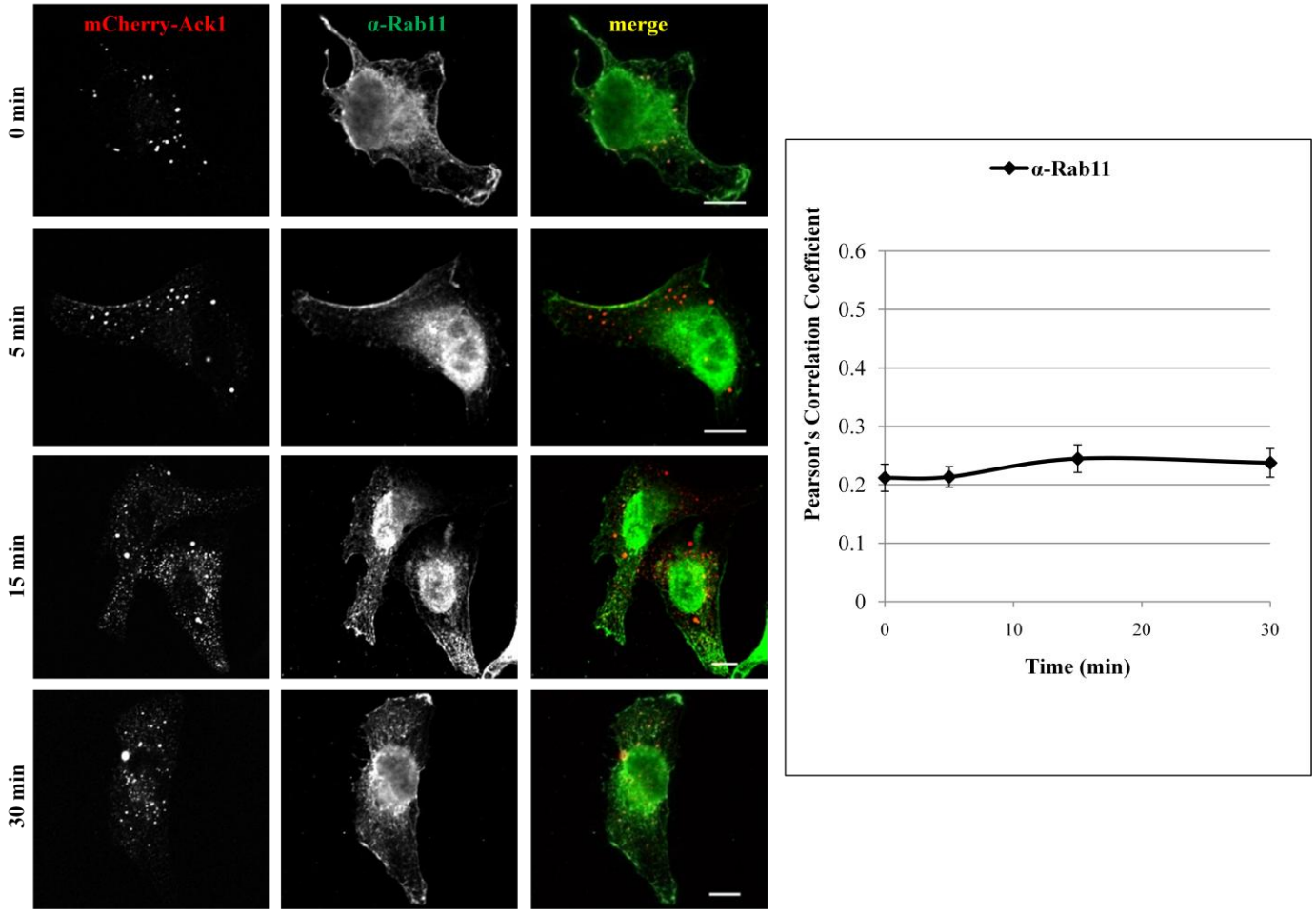

Figure 5.9. Ack1 does not localize to recycling endosomes post-EGF treatment

HeLa cells transfected with mCherry-Ack1 were serum-starved for four hours and stimulated with EGF for indicated times, and fixed. The cells were immunostained with α-Rab11 antibody and imaged *via* confocal microscopy, and the colocalization was quantified. Scale bars 10 μm. Error bars represent SEM.

It seems reasonable that a portion of Ack1 may partially localize to late or recycling endosomes following EGF stimulation; however, taking into consideration the data on endogenous LBPA and Rab11, it is likely the minority of the Ack1 molecules. Importantly, the concordance of results obtained with GFP-Rab5 and anti-EEA1 suggest that the localization of Ack1 to early endosomes is genuine.

5.7 Conclusions

The study presented within this chapter explores Ack1 subcellular localization in more detail. To date the characterisation of the Ack1 location is rather limited, with indication on partial endosomal localization upon EGF treatment; Ack1 has also been found within uncharacterised tubulo-reticular compartments (Grovdal *et al.*, 2008; Prieto-Echaguee *et al.*, 2010).

In this study I confirm that Ack1 partially translocates to early endosomes following EGF stimulation. This is shown by an increase in colocalization between Ack1 and EEA1. Interestingly, early endosomes have also been shown to be essential during autophagy (Razi *et al.*, 2009; Tooze and Razi, 2009). In particular, the fusion of early endosomes with autophagosomes has been found required for autophagosome maturation. Therefore, although Ack1 exhibits endosomal localization, this does not necessarily exclude the potential association between Ack1 and the autophagosomal compartments.

Similar to the results on EEA1, an increased EGF-dependent colocalization can be seen between Ack1 and Rab5. This association has been further confirmed through studies with constitutively active Rab5 mutant, in which strong colocalization between Ack1 and Rab5 mutant can be observed upon EGF treatment. As explained in **Chapter 1.3.4**, Rab5 is found

on several distinctive intracellular compartments; these include early endosomes, early and late phagosomes and clathrin-coated pits (Stenmark, 2009). Therefore an increase in colocalization between Ack1 and Rab5 following EGF stimulation suggests that Ack1 partially translocates towards Rab5-enriched compartments, *e.g.* early endosomes or autophagosomes.

I show that when investigating endosomal localization of Ack1, the outcomes of the studies vary depending on the experimental design. In particular, I can distinguish a partial colocalization between Ack1 and the ectopically expressed Rab4, Rab7 and Rab11 upon EGF treatment. More precisely, the colocalization with Rab4 increases at 15 minutes post-EGF, with Rab7 at 15 minutes and further at 30 minutes, and with Rab11 at 30 minutes post-EGF treatment. Therefore, it seems reasonable to interpret these data that following EGF stimulation, Ack1 partially translocates to early endosomes at 15 minutes of the EGF stimulation, from where a portion of Ack1 remains within endosomes which mature into late endosomes and another portion recycles *via* recycling endosomes. In contrast, the data on endogenous Rab11 and LBPA indicate no colocalization between Ack1 and late or recycling endosomes upon EGF treatment. Partial explanation may come from the possible influence of ectopically expressed proteins on cell functions. Additionally, non-physiological expression of proteins may promote the colocalization that does not occur in physiological conditions. For example, ectopically expressed Rab5 has been found to promote enlargement of endosomes and their mislocalization to the cell periphery (Trim, 2009). Finally, the differences in Ack1 colocalization with Rab7 and LBPA may be the result of slight differences in their subcellular distribution.

6 Ack1 autophagosomal localization

6.1 Introduction

I and others have shown that Ack1 partially localizes to early endosomes following EGF stimulation (Shen *et al.*, 2007; Grovdal *et al.*, 2008); however, Ack1 does not display endosomal localization in serum-starved cells. Additionally, uncharacterised tubulo-reticular compartments have also been identified where Ack1 resides (Shen *et al.*, 2007; Grovdal *et al.*, 2008). Nevertheless, more precise Ack1 subcellular localization, in particular pre-EGF stimulation, is elusive. This chapter investigates Ack1 subcellular localization more precisely and with focus on the compartments outside the classical endo-lysosomal pathway, as I did not find Ack1 present within endosomes in serum-starved cells.

Firstly I investigate Ack1 association with ubiquitin, which is an important regulator of protein degradation and ubiquitylated proteins typically undergo proteasomal, lysosomal or autophagosomal degradation (Kraft *et al.*, 2010; Lemmon and Schlessinger, 2010). Previous reports show that Ack1 interacts with mono- and polyubiquitin and with ubiquitylated proteins (Shen *et al.*, 2007). Ack1 contains a UBA domain, which in other proteins recognises ubiquitylated cargo targeted for degradation (Lamark *et al.*, 2009). Therefore I studied a potential localization of Ack1 to degradative compartments marked by the presence of ubiquitin.

6.2 Ack1 localizes to ubiquitin-rich compartments

Since my attempts to identify Ack1 endosomal localization in serum-starved cells were unsuccessful, I searched for other compartments not directly connected to the endosomal pathway. As explained in **Chapter 1.3.3**, protein ubiquitylation is a common factor targeting proteins for degradation *via* several degradative pathways, *e.g.* ubiquitylated cargo is enriched and enclosed within double membranes during selective autophagy (Kraft *et al.*, 2010). Since Ack1 has been previously shown to bind both mono- and polyubiquitin (Shen *et al.*, 2007), I therefore examined the colocalization between ectopically expressed Ack1 and ubiquitin in HeLa cells. As shown in **Figure 6.1 a**, there is a striking colocalization between Ack1 and ubiquitin in steady-state cells and this is not the case for truncated Ack1 or GFP. This is particularly relevant considering that truncated Ack1 lacks the C-terminal portion, including the UBA domain. Therefore the C-terminus of Ack1 promotes the colocalization with ubiquitin. Since Ack1 has also been found to be ubiquitylated (Chan *et al.*, 2009; Lin *et al.*, 2010), this may also reflect Ack1 ubiquitylation. Interestingly, I commonly observe large ubiquitin-rich structures to which Ack1 localizes, hereafter referred to as ubiquitin-rich compartments (**Figure 6.1 b**). I also observe that the subcellular distribution of ubiquitin is affected by the presence of ectopically expressed Ack1 when compared to truncated Ack1 or GFP. In the case of truncated Ack1 and GFP, a disperse staining for ubiquitin typically can be distinguished, whereas in the presence of full-length Ack1 ubiquitin often forms larger structures. These data indicate that Ack1 influences subcellular distribution of ubiquitin and promotes formation of condensed ubiquitin and ubiquitin-rich compartments.

Consistently with the colocalization studies, ubiquitin associates only with the full-length protein following Ack1 or tAck1 immunoprecipitation, as shown in **Figure 6.2**, and this is independent of EGF treatment.

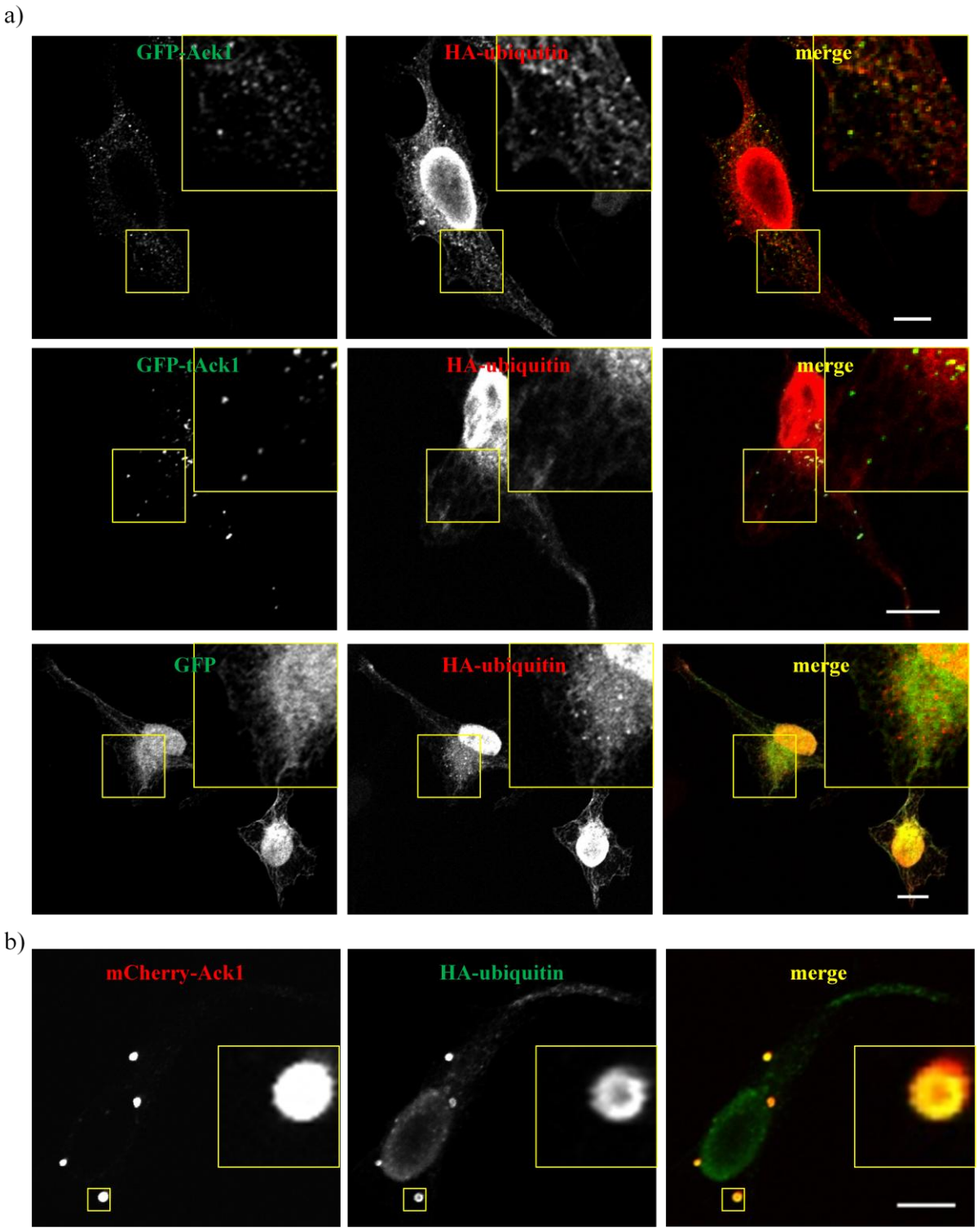

Figure 6.1. Ack1 localizes to ubiquitin-rich compartments

a) and **b)** HeLa cells transfected with GFP-Ack1, GFP-tAck1 or GFP and HA-ubiquitin were serum-starved for four hours and stimulated with EGF for 30 minutes. The cells were fixed and immunostained with α-HA antibody, and imaged *via* confocal microscopy. Scale bars 10 μm.

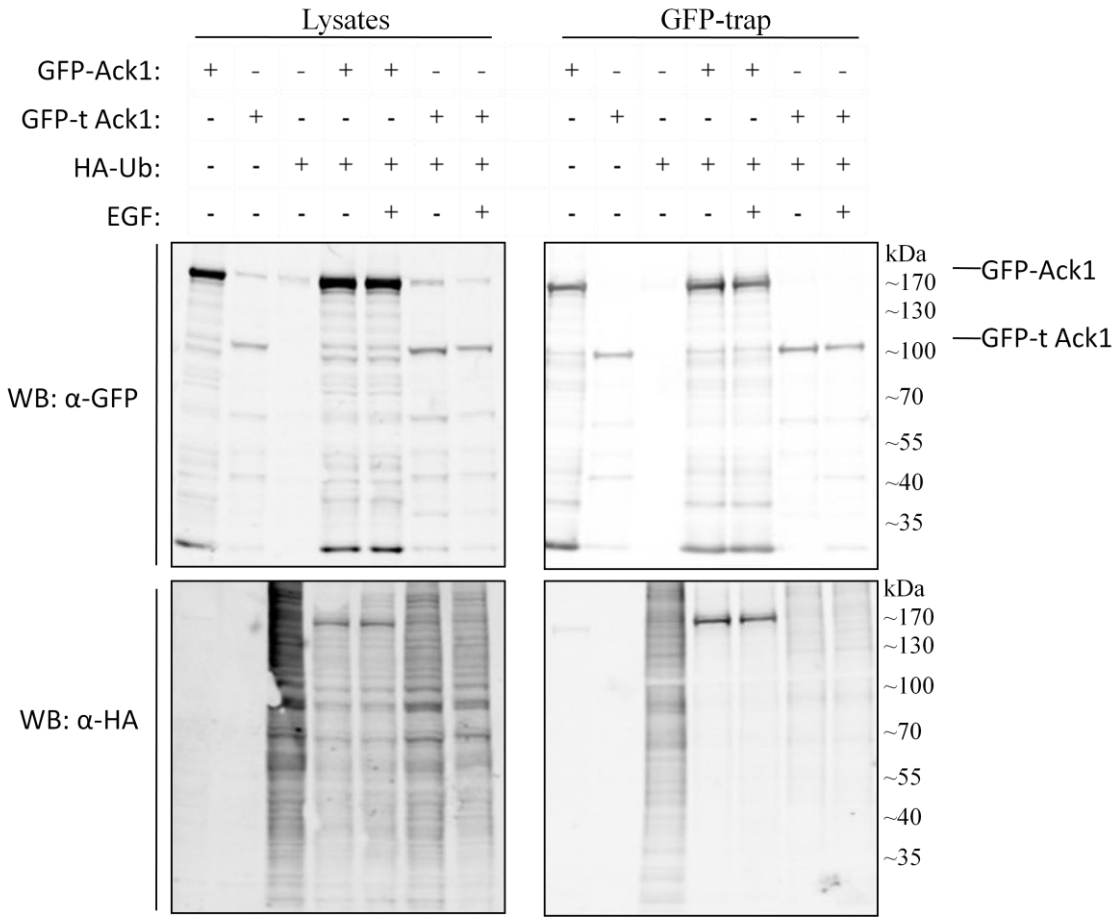

Figure 6.2. Ack1 binds ubiquitin

293T cells transfected with GFP-Ack1 or GFP-tAck1 and HA-ubiquitin were serum-starved for four hours and stimulated with EGF for 30 minutes. The cells were lysed and cell lysates were incubated with GFP-trap to immunoprecipitate GFP-tagged proteins. Immunoprecipitates were subjected to SDS PAGE and Western blotting with α-GFP and α-HA antibodies.

These results indicate that Ack1 constitutively associates with ubiquitin, or is constitutively ubiquitylated, and confirm that the C-terminus is required for this association.

Showing that Ack1 localizes to ubiquitin-rich compartments, and that EGFR colocalizes with Ack1 upon EGF treatment, I examined whether EGFR localizes with Ack1 to ubiquitin-rich compartments. HeLa cells expressing EGFR-GFP, mCherry-Ack1 and HA-ubiquitin were serum-starved and stimulated with EGF, fixed and immunostained with α-HA antibody. The cells were imaged *via* confocal microscopy. As shown in **Figure 6.3**, in starved cells EGFR is mainly present at the plasma membrane, whereas Ack1 colocalizes with ubiquitin. Following EGF stimulation, EGFR moves away from the plasma membrane and localizes with Ack1 to ubiquitin-rich compartments. These data further support the association between Ack1 and ubiquitin, which may be important for EGFR trafficking, and may reflect the ubiquitylation of Ack1 and/or EGFR.

Subsequently, I examined the colocalization between ubiquitin and the C-terminal truncation mutants of Ack1 to determine more precisely which of the Ack1 domains promote association with ubiquitin. HeLa cells expressing mCherry-tagged Ack1, truncated Ack1 or the Ack1 mutants and HA-ubiquitin were serum-starved and stimulated with EGF, fixed and immunostained with α-HA antibody. The cells were imaged *via* confocal microscopy. As shown in **Figure 6.4 a**, **b** and **c**, there is a striking colocalization between Ack1 and ubiquitin (approximately 70-80 %) and this is independent of EGF stimulation. This colocalization dramatically decreases upon deletion of the UBA domain (to approximately 40-50 %); however, the colocalization is not completely abrogated thus indicating that other domains also contribute to this colocalization.

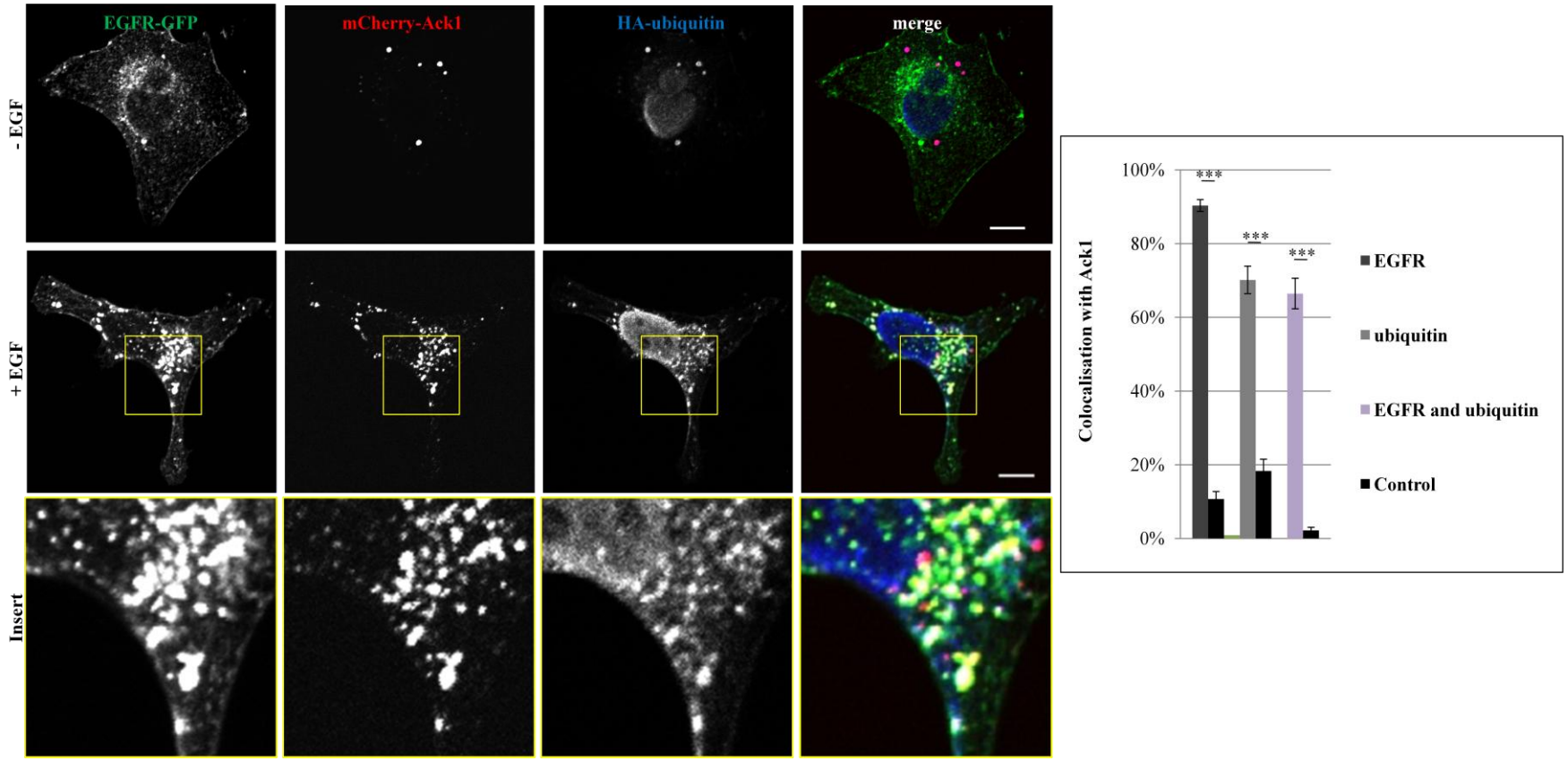

Figure 6.3. EGFR colocalizes with Ack1 and ubiquitin post-EGF treatment

HeLa cells transfected with mCherry-Ack1, EGFR-GFP and HA-ubiquitin were serum-starved for four hours and stimulated with EGF for 30 minutes. The cells were fixed and immunostained with α-HA antibody, and imaged *via* confocal microscopy. For quantification, the Ack1 puncta were circled and the colocalization with EGFR and ubiquitin was quantified. As a control, the circles were moved into the areas absent for Ack1, and the random colocalization with EGFR and/or ubiquitin was quantified. Nuclear localization was excluded from analysis. Scale bars 10 µm. Error bars represent SEM.

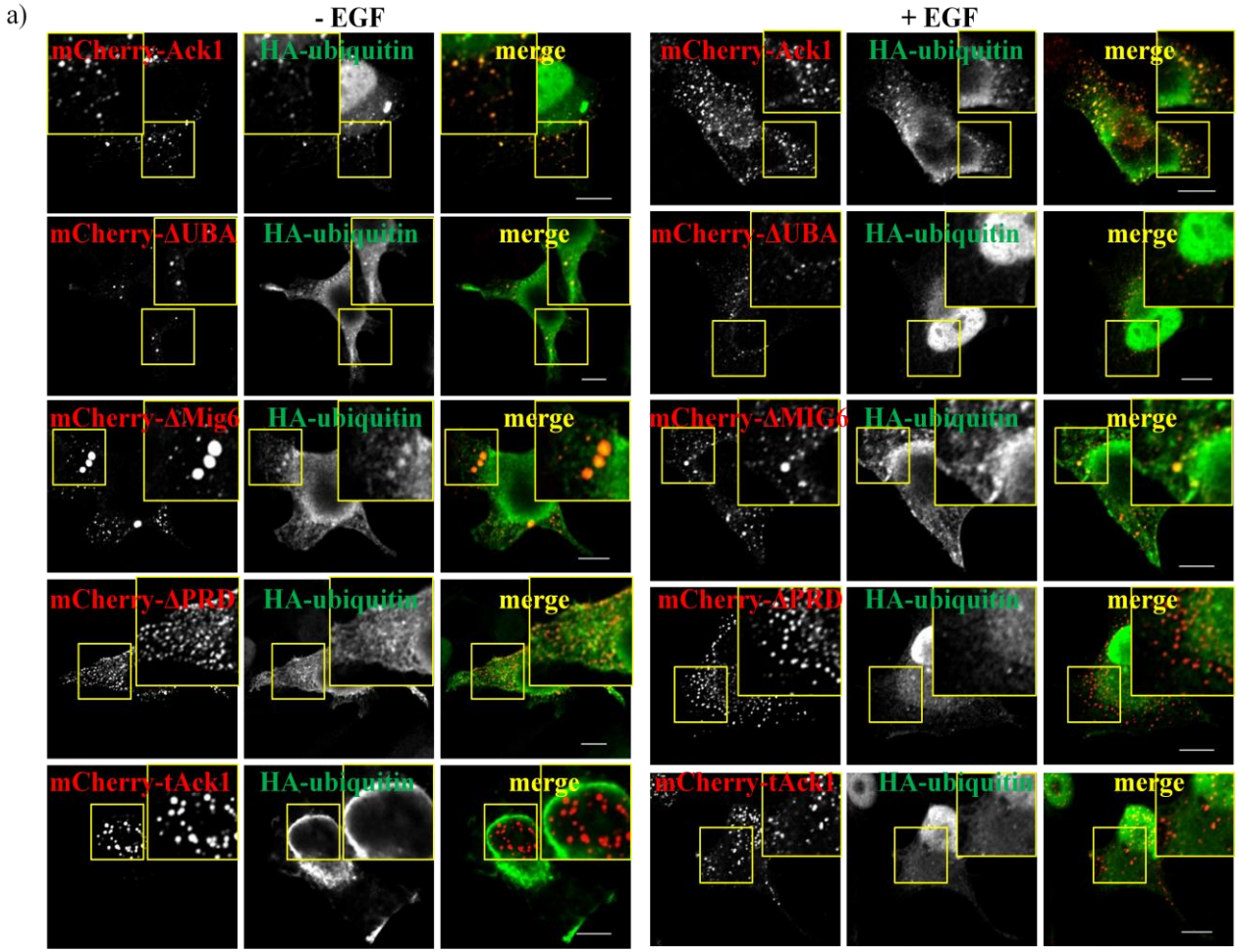

Figure 6.4. Ack1 domains required for colocalization with ubiquitin (a), (b) and (c)

a) HeLa cells transfected with mCherry-tagged Ack1, tAck1 or the Ack1 mutants and HA-ubiquitin were serum-starved for four hours and stimulated with EGF for 30 minutes. The cells were fixed and immunostained with α-HA antibody, and imaged *via* confocal microscopy. Scale bars 10 µm.

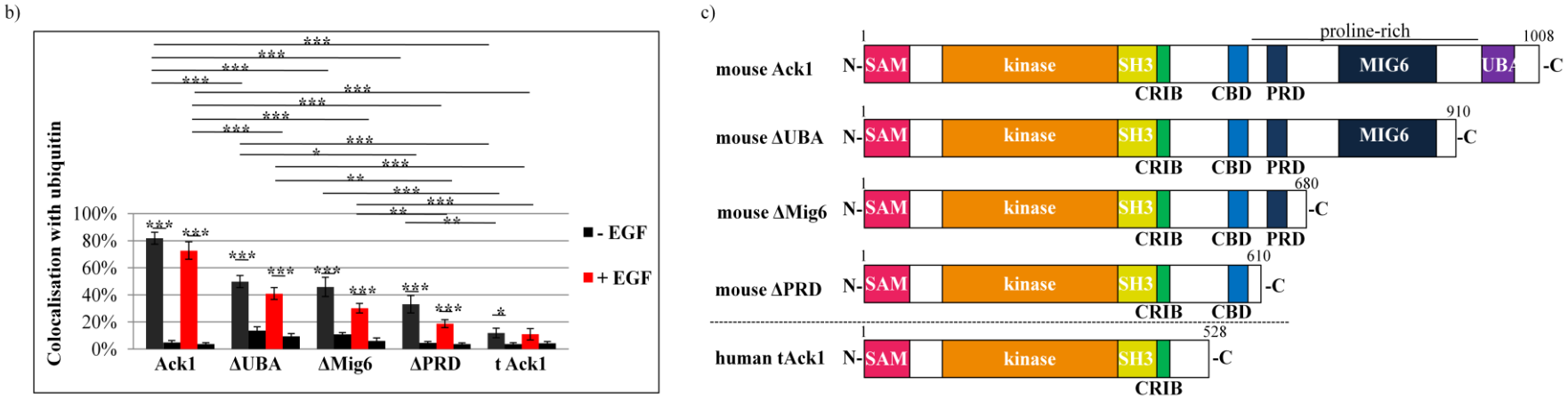

Figure 6.4. Ack1 domains required for colocalization with ubiquitin (a), (b) and (c)

b) For quantification (**Figure 6.4 a**), the Ack1, tAck1 or Ack1 mutant puncta were circled and the colocalization with ubiquitin was quantified. As a control, circles were moved into the areas absent for Ack1, tAck1 or the Ack1 mutants and the random colocalization with ubiquitin was quantified. Error bars represent SEM; **c)** schematic structure of Ack1, tAck1 and the Ack1 mutants employed.

Deletion of the Mig6 domain does not have any influence on this colocalization, whereas deletion of the PRD further decreases the colocalization between Ack1 and ubiquitin (approximately 20-30 %). In the case of truncated Ack1, only minute colocalization can be distinguished (approximately 10 %). Interestingly, although no significant EGF-dependence can be found, a trend can be recognised that EGF stimulation slightly decreases the colocalization between Ack1 and ubiquitin. In conclusion, the UBA domain, PRD and CBD all contribute to the colocalization between Ack1 and ubiquitin.

6.3 Ack1 associates with Eps15 and Hrs

As explained in **Chapter 1.3.1**, Hrs is a component of the ESCRT-0 complex, which regulates incorporation of ubiquitylated cargo, such as RTKs, into the internal vesicles of late endosomes (Clague *et al.*, 2012). I find that ectopically expressed Ack1 and Hrs colocalize with each other both in serum-starved and in EGF-treated HeLa cells, as presented in **Figure 6.5 a**. Interestingly, ectopically expressed Hrs has been found to retain EGFR at the limiting membranes of early endosomes and thus inhibit EGFR degradation, whereas a UIM-deletion Hrs mutant with reduced ability to interact with ubiquitylated proteins failed to do so (Urbe *et al.*, 2003). This could potentially indicate that Hrs overexpression prevents EGFR degradation *via* a classical endo-lysosomal pathway, and that the UIM is important for this function. Additionally, Hrs has been found to localize to autophagosomes and regulate autophagosomal maturation, which was impaired in cells depleted of Hrs (Tamai *et al.*, 2007). These data suggest that Hrs potentially plays a role in autophagosomal degradation.

Eps15 is another ubiquitin-binding protein with well-established role in endo-lysosomal trafficking that has also been proposed to regulate autophagosomal degradation. Eps15 activation upon EGF stimulation is required for EGFR endocytosis (Confalonieri *et al.*, 2000).

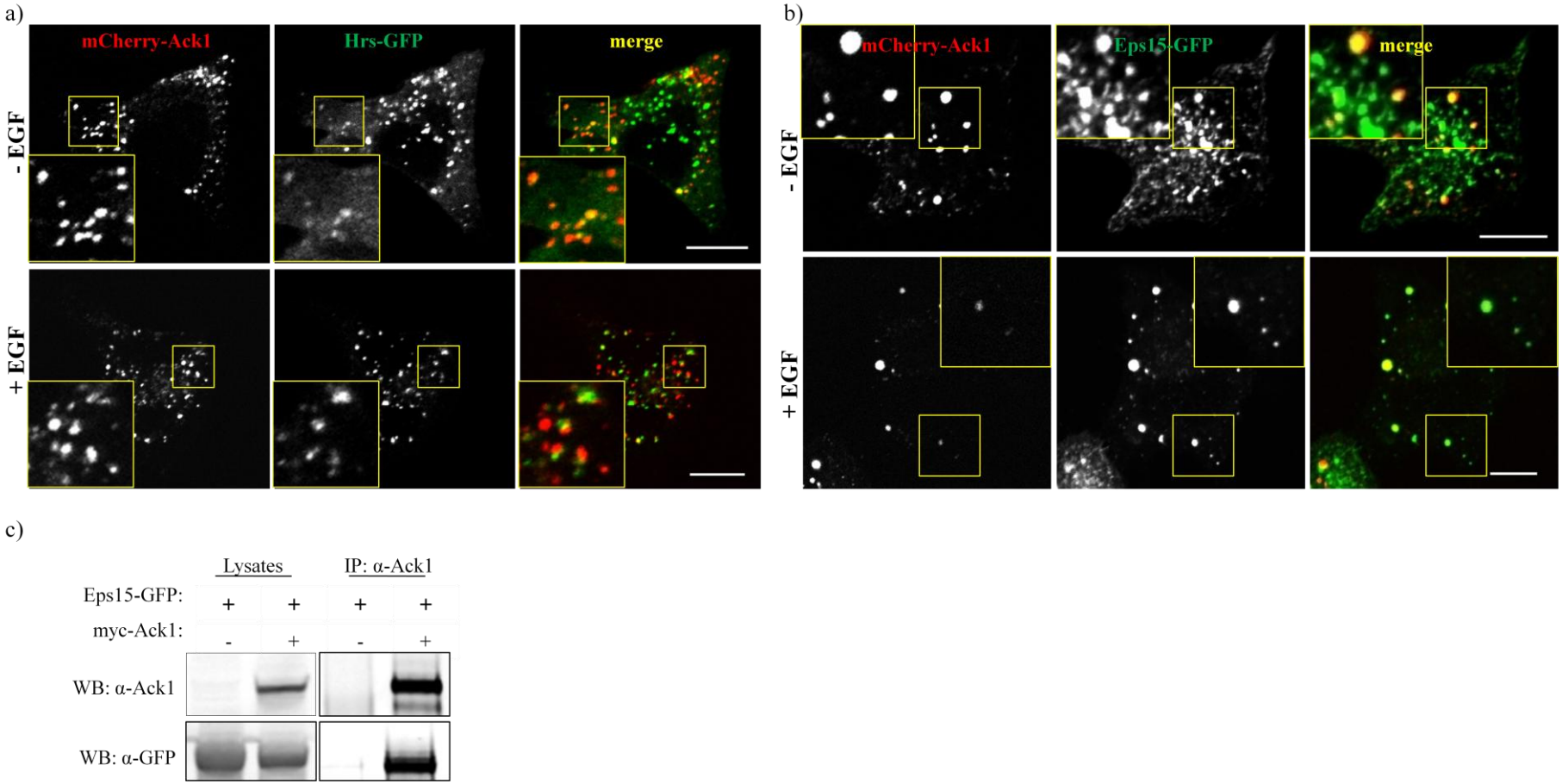

Figure 6.5. Ack1 colocalizes with Hrs and Eps15

HeLa cells transfected with mCherry-Ack1 and Hrs-GFP **(a)** or mCherry-Ack1 and Eps15-GFP **(b)** were serum-starved for four hours and stimulated with EGF for 30 minutes. The cells were fixed and imaged *via* confocal microscopy. Scale bars 10 µm; **c)** 293T cells transfected with myc-Ack1 and Eps15-GFP were lysed and cell lysates were incubated with α-Ack1 antibody to immunoprecipitate Ack1. Immunoprecipitates were subjected to SDS PAGE and Western blotting with α-Ack1 and α-GFP antibodies.

Ubiquilin, a ubiquitin-like protein that localizes to ubiquitin-rich structures, has been found to associate with endogenous Eps15 and Hrs. Additionally, this association has been found dependent on UIMs of Eps15 and Hrs, as the UIM-deletion mutants did not associate with ubiquilin (Regan-Klapisz *et al.*, 2005). I show that ectopically expressed Ack1 and Eps15 colocalize in HeLa cells in EGF-independent manner, as shown in **Figure 6.5 b**. Furthermore, I found that Ack1 and Eps15 interact with each other, and Eps15-GFP co-precipitates with myc-Ack1 in steady-state 293T cells (**Figure 6.5 c**).

6.4 Ack1 interacts and colocalizes with p62/SQSTM1 and NBR1

The data presented so far on Ack1 subcellular localization suggest that Ack1 may be involved in ubiquitin-dependent degradation. Furthermore, Ack1 association with Hrs and Eps15 supports this suggestion, since both Hrs and Eps15 have proposed roles in autophagosomal degradation (Regan-Klapisz *et al.*, 2005; Tamai *et al.*, 2007). Therefore, my studies have focused on the non-canonical degradative pathways.

Sequestosome 1 (p62/SQSTM1) has been shown to target ubiquitylated proteins for degradation through selective autophagy, as explained in more detail in **Chapter 1.4.2**. In particular, the UBA domain of p62/SQSTM1 recognises ubiquitylated cargo, whereas the LC3-interacting region (LIR) binds LC3 which is associated with autophagosomal membranes (Lamark *et al.*, 2009).

Thus, I examined whether Ack1 interacts with p62/SQSTM1. 293T cells expressing myc-Ack1 and p62/SQSTM1-flag were lysed and cell lysates were subjected to immunoprecipitation with α-Ack1 antiobody. As shown in **Figure 6.6 a**, p62/SQSTM1 co-precipitates with Ack1, thus indicating that Ack1 and p62/SQSTM1 interact in these conditions.

Subsequently, I investigated whether Ack1 and p62/SQSTM1 colocalize with each other. HeLa cells expressing GFP-Ack1 and p62/SQSTM-flag were serum-starved and stimulated with EGF, fixed and immunostained with α-SQSTM1 antibody. The cells were imaged *via* confocal microscopy. As shown in **Figure 6.6 b**, a strong colocalization can be distinguished particularly in serum-starved cells, whereas upon EGF stimulation the colocalization partially decreases. Therefore Ack1 and p62/SQSTM1 colocalize predominantly in serum-starved cells and EGF stimulation partially reduces this colocalization.

Finally, I analysed whether the interaction between Ack1 and p62/SQSTm1 takes place at the physiological level. LNCaP cells were serum-starved in the presence or absence of bafilomycin, an inhibitor of lysosomal acidification and thus autophagy, and stimulated with EGF. The cells were lysed and cell lysates were incubated with α-Ack1. As a negative control, cell lystes were incubated with non-specific IgG. As shown in **Figure 6.6 c**, endogenous p62/SQSTM1 co-precipitates with Ack1 in serum-starved cells, but not in the control. This indicates that the interaction between Ack1 and p62/SQSTM1 is physiologically relevant. Furthermore, this interaction decreases following EGF treatment and this is consistent with my studies on colocalization between ectopically expressed Ack1 and p62/SQSTM1 in HeLa cells.

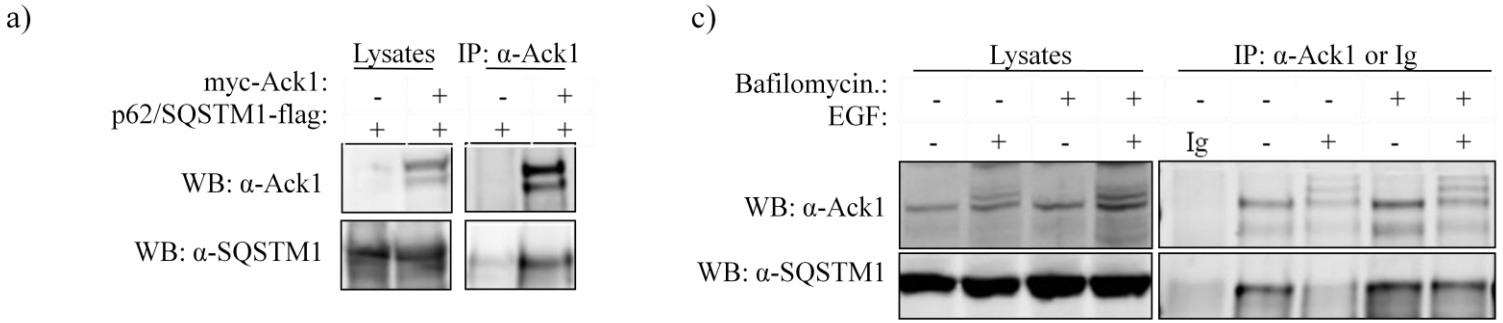

Figure 6.6. Ack1 interacts and colocalizes with p62/SQSTM1 (a), (b) and (c)

a) 293T cells transfected with myc-Ack1 and p62/SQSTM1-flag were lysed and cell lysates were incubated with α-Ack1 antibody previously cross-linked to the beads, to immunoprecipitate Ack1. Immunoprecipitates were subjected to SDS PAGE and Western blotting with α-Ack1 and α-SQSTM1 antibodies; **c)** LNCaP cells were serum-starved for four hours in the presence or absence of bafilomycin A (400 nM). The cells were stimulated with EGF for 10 minutes, lysed and cell lysates were incubated with α-Ack1 antibody previously cross-linked to the beads, to immunoprecipitate endogenous Ack1. Immunoprecipitates were subjected to SDS PAGE and Western blotting with α-Ack1 and α-SQSTM1 antibodies.

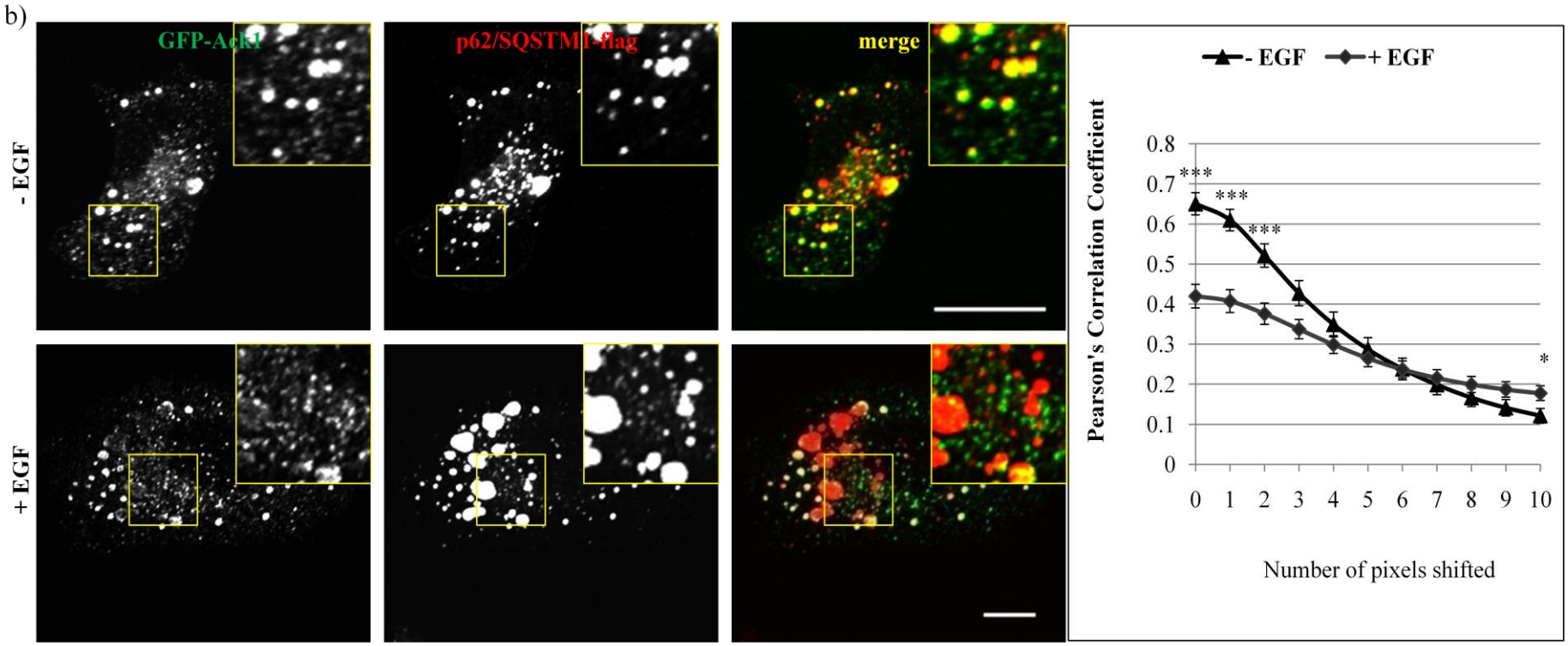

Figure 6.6. Ack1 interacts and colocalizes with p62/SQSTM1 (a), (b) and (c)

b) HeLa cells transfected with GFP-Ack1 and p62/SQSTM1-flag were serum-starved for four hours and stimulated with EGF for 30 minutes. The cells were fixed and immunostained with α-SQSTM1 antibody. The cells were imaged *via* confocal microscopy, and the colocalization was quantified. Scale bars 10 μm. Error bars represent SEM.

Interestingly, the interaction between Ack1 and p62/SQSTM1 is retained upon EGF stimulation in bafilomycin treated cells, suggesting that this interaction may take place at the stages involving acidic lysosomes.

NBR1 is another autophagic receptor that has been proposed to play a similar role to p62/SQSTM1. Although nearly twice the size of p62/SQSTM1, it shares a similar domain structure with a UBA domain recognising ubiquitylated proteins and a LIR motif interacting with LC3, as explained in more detail in **Chapter 1.4.2**. Additionally, NBR1 and p62/SQSTM1 interact with each other *via* their PB1 domains (Lamark *et al.*, 2009). To examine whether Ack1 colocalizes with NBR1, HeLa cells expressing mCherry-Ack1 and NBR1-GFP were serum-starved and stimulated with EGF, fixed and imaged *via* confocal microscopy. As shown in **Figure 6.7**, partial colocalization between Ack1 and NBR can be seen; however, it is not as striking as in the case of p62/SQSTM1. When quantified, approximately 20-25 % of the Ack1 puncta colocalize with NBR1 (**Figure 6.7**, **graph**), but the colocalization between Ack1 and NBR1 is EGF-independent. This is in contrast with the data on the interaction between Ack1 and p62/SQSTM1, which decreases upon EGF treatment.

6.5 p62/SQSTM1 promotes colocalization between Ack1 and NBR1

As explained in **Chapter 1.4.2** and **Chapter 1.4.3**, p62/SQSTM1 and NBR1 interact with each other *via* their PB1 domains (Lamark *et al.*, 2003; Lamark *et al.*, 2009). They also colocalize with each other within ubiquitin-rich compartments in autophagy-deficient cells; however, NBR1 has been shown to be degraded by autophagy independently of p62/SQSTM1 (Kirkin *et al.*, 2009).

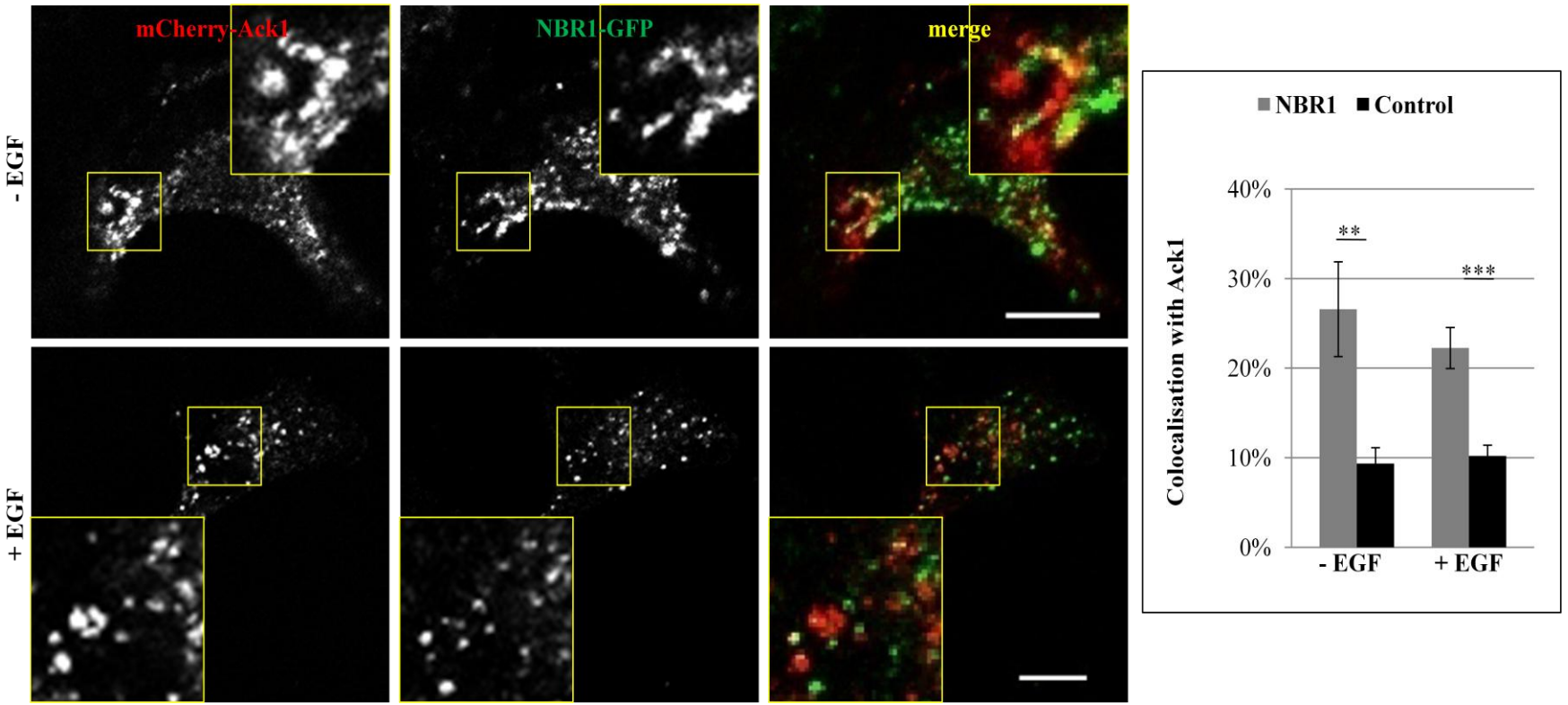

Figure 6.7. Ack1 only partially colocalizes with NBR1

HeLa cells transfected with mCherry-Ack1 and NBR1-GFP were serum-starved for four hours and stimulated with EGF for 30 minutes, fixed and imaged *via* confocal microscopy. For quantification, the Ack1 puncta were circled and colocalization with NBR was quantified. As a control, the circles were moved into the areas absent for Ack1 and the random colocalization with NBR1 was quantified. Scale bars 10 µm. Error bars represent SEM.

Additionally, the late endosomal and autophagosomal localization of NBR1 have been shown to be independent of each other, suggesting that NBR1 may play different roles in each context (Mardakheh *et al.*, 2010).

When comparing the colocalization between Ack1 and NBR1 to the colocalization between Ack1 and p62/SQSTM1, it is apparent that the latter is more striking. This suggests that Ack1 may preferably interact with p62/SQSTM1. To compare the interaction between Ack1, NBR1 and p62/SQSTM1, 293T cells expressing myc-Ack1, NBR1-GFP and p62/SQSTM1-flag were serum-starved followed by stimulation with EGF. The cells were lysed and cell lysates were incubated with α-Ack1 antibody. As shown in **Figure 6.8**, in these conditions Ack1 interacts with both NBR1 and p62/SQSTM1 to a similar level and independently of EGF treatment. This is suprising, since previous data on HeLa and LNCaP cells show that Ack1 association with p62/SQSTM1 decreases following EGF treatment. This discrepancy is likely to reflect the differences between different cell lines. Thus, subsequent experiments were designed to further explore the association between Ack1, NBR and p62/SQSTM1.

To examine the colocalization between Ack1, NBR1 and p62/SQSTM1, HeLa cells expressing mCherry-Ack1, NBR1-GFP and p62/SQSTM1-flag were serum-starved and stimulated with EGF. The cells were fixed and immunostained with α-SQSTM1 antibody, and imaged *via* confocal microscopy. As shown in **Figure 6.9 a** and **b**, relatively strong colocalization between Ack1, NBR1 and p62/SQSTM1 can be distinguished in serum-starved cells (approximately 50 %), which decreases following EGF treatment (approximately 30 %). Additionally, when examining the colocalization between NBR1 and p62/SQSTM1 within the Ack1 puncta, it is strong both in serum-starved and in EGF-treated cells (approximately 80 %) (**Figure 6.9 c**).

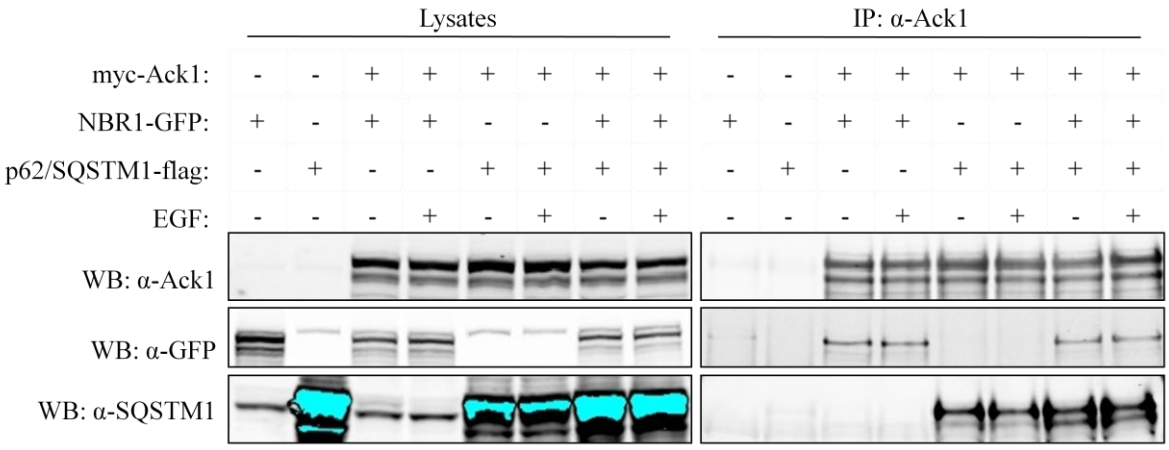

Figure 6.8. p62/SQSTM1 and NBR1 co-precipitate with Ack1

293T cells transfected with myc-Ack1, NBR1-GFP and p62/SQSTM1-flag were serum-starved for four hours and stimulated with EGF for 30 minutes. The cells were lysed and cell lysates were incubated with α-Ack1 antibody to immunoprecipitate Ack1. Immunoprecipitates were subjected to SDS PAGE and Western blotting with α-Ack1, α-GFP and α-SQSTM1 antibodies.

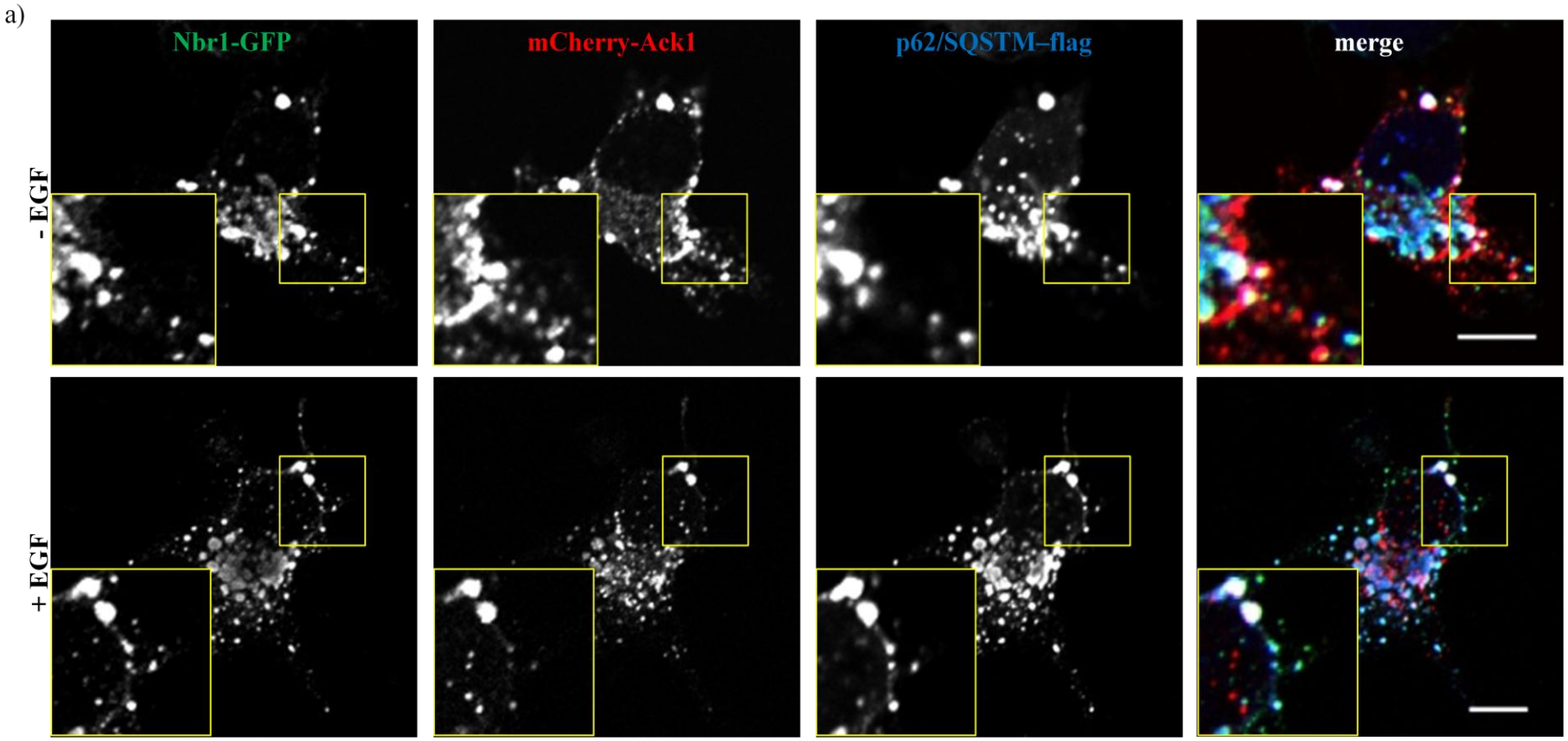

Figure 6.9. The colocalization between Ack1, p62/SQSTM1 and NBR1 (a), (b) and (c)

a) HeLa cells transfected with mCherry-Ack1, NBR1-GFP and p62/SQSTM1-flag were serum starved for four hours and stimulated with EGF for 30 minutes, fixed and immunostained with α-SQSTM1 antibody. The cells were imaged *via* confocal microscopy. Scale bars 10 µm.

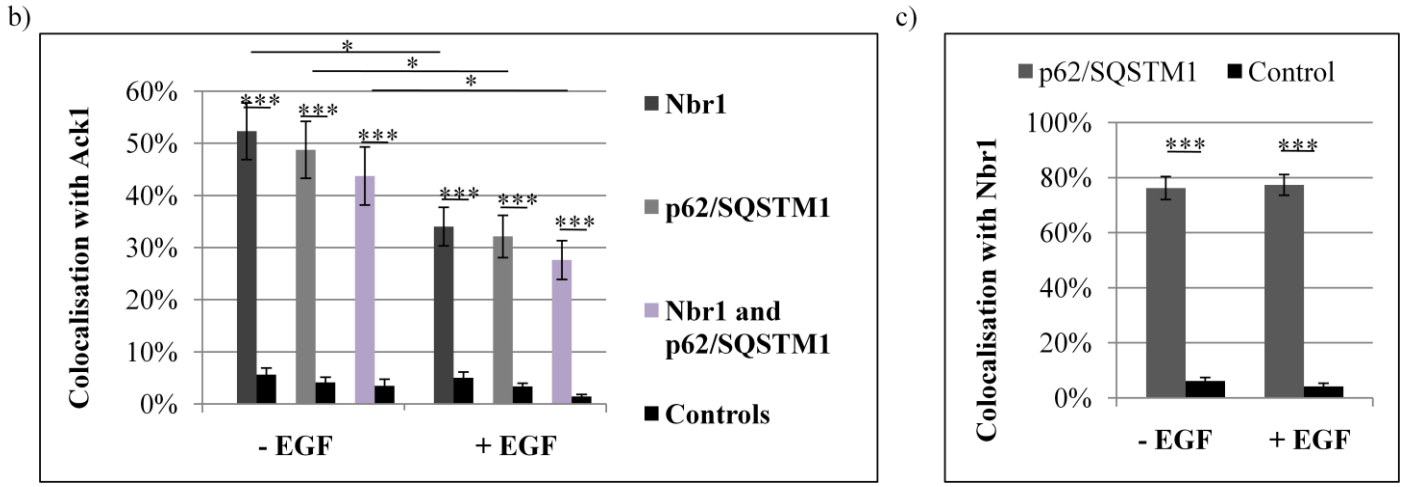

Figure 6.9. The colocalization between Ack1, p62/SQSTM1 and NBR1 (a), (b) and (c)

b) For quantification (**Figure 6.9 a**), the Ack1 puncta were circled and the colocalization with NBR1 and p62/SQSTM1 was quantified. As a control, the circles were moved into the areas absent for Ack1 and the random colocalization with NBR1 or p62/SQSTM1 was quantified; **c)** For quantification (**Figure 6.9 a**), the Ack1 puncta were circled and the colocalization between NBR1 and p62/SQSTM1 within Ack1 puncta was quantified (bottom right graph). As a control, the circles were moved into the areas absent for Ack1 and the random colocalization between NBR1 and p62/SQSTM1 was quantified. Error bars represent SEM.

Therefore, the colocalization between Ack1 and NBR1 is nearly doubled in the presence of ectopically expressed p62/SQSTM1 and acquires EGF sensitivity (**Figure 6.9 a** and **b** compared to **Figure 6.7**). Thus, p62/SQSTM1 promotes the association between Ack1 and NBR1 in serum-starved HeLa cells.

6.6 The UBA domain regulates association with p62/SQSTM1, but not NBR1

Showing that Ack1 colocalizes with p62/SQSTM1, I further examined which of the Ack1 domains regulate this colocalization. HeLa cells expressing mCherry-tagged Ack1, truncated Ack1 or the C-terminal truncation mutants and p62/SQSTM1-flag were serum-starved and stimulated with EGF. The cells were fixed and immunostained with α-SQSTM1 antibody, and imaged *via* confocal microscopy. As shown in **Figure 6.10 a** and **b**, the colocalization between full-length Ack1 and p62/SQSTM1 is strong in serum-starved cells (approximately 55 %) and decreases significantly following EGF stimulation (approximately 30 %). Deletion of the UBA domain dramatically reduces the colocalization between Ack1 and p62/SQSTM1 (approximately 20 %) and desensitizes it to EGF treatment. Further deletion of the Mig6 domain or PRD does not influence the colocalization between Ack1 and p62/SQSTM1, whereas any remaining colocalization is abrogated in the case of truncated Ack1. Therefore the UBA domain mediates the colocalization between Ack1 and p62/SQSTM1.

Subsequently, I examined whether the UBA domain similarly promotes the association between Ack1 and NBR1. HeLa cells transfected with mCherry- tagged Ack1 or the UBA domain-deletion mutant and NBR1-GFP were serum-starved and stimulated with EGF. The cells were fixed and imaged *via* confocal microscopy.

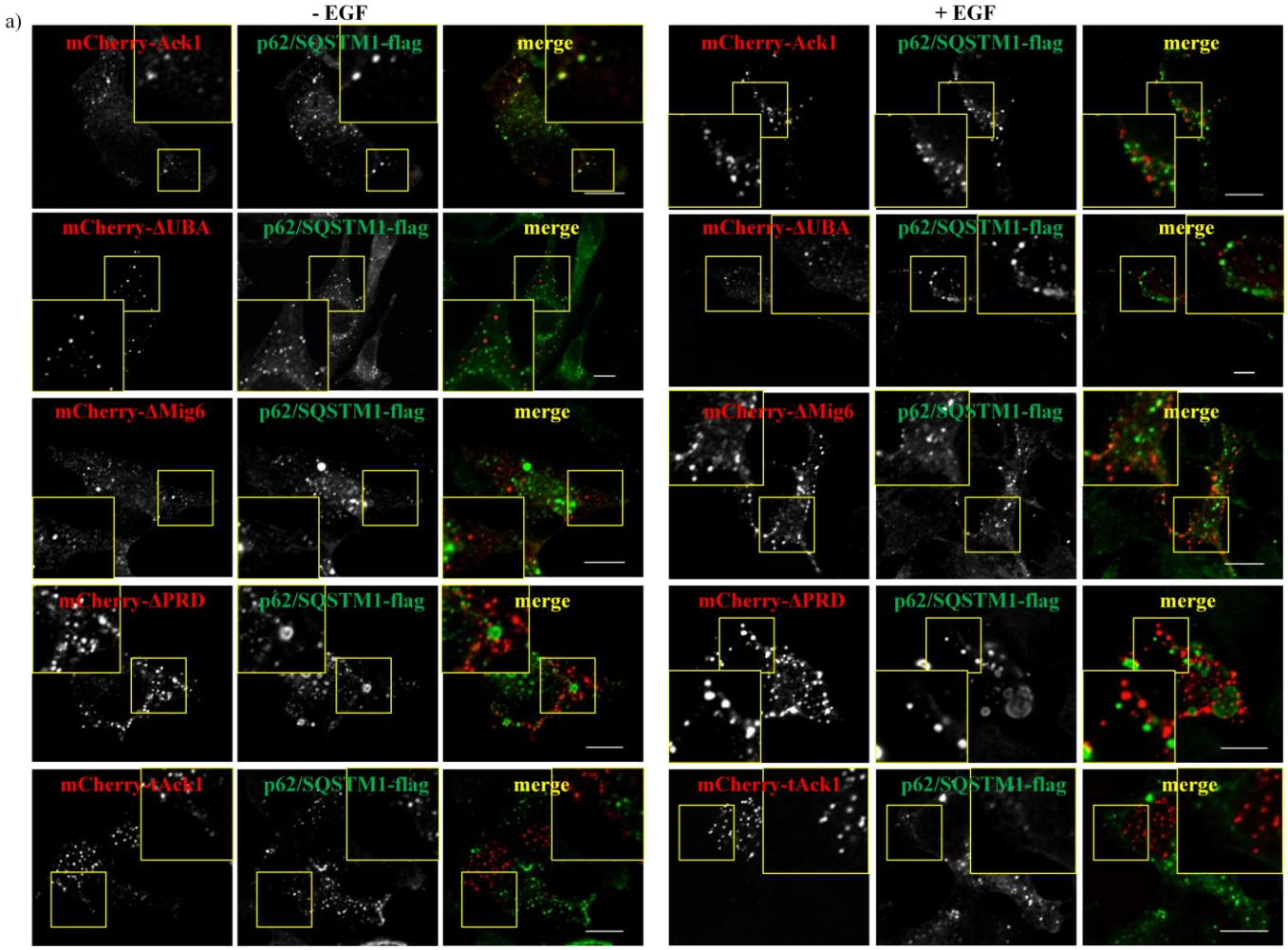

Figure 6.10. The UBA domain mediates the colocalization with p62/SQSTM1 (a) and (b)

a) HeLa cells transfected with mCherry-tagged Ack1, truncated Ack1 or the Ack1 mutants were serum-starved for four hours and stimulated with EGF for 30 minutes, fixed and immunostained with α-SQSTM1 antibody. Scale bars 10 µm.

b)

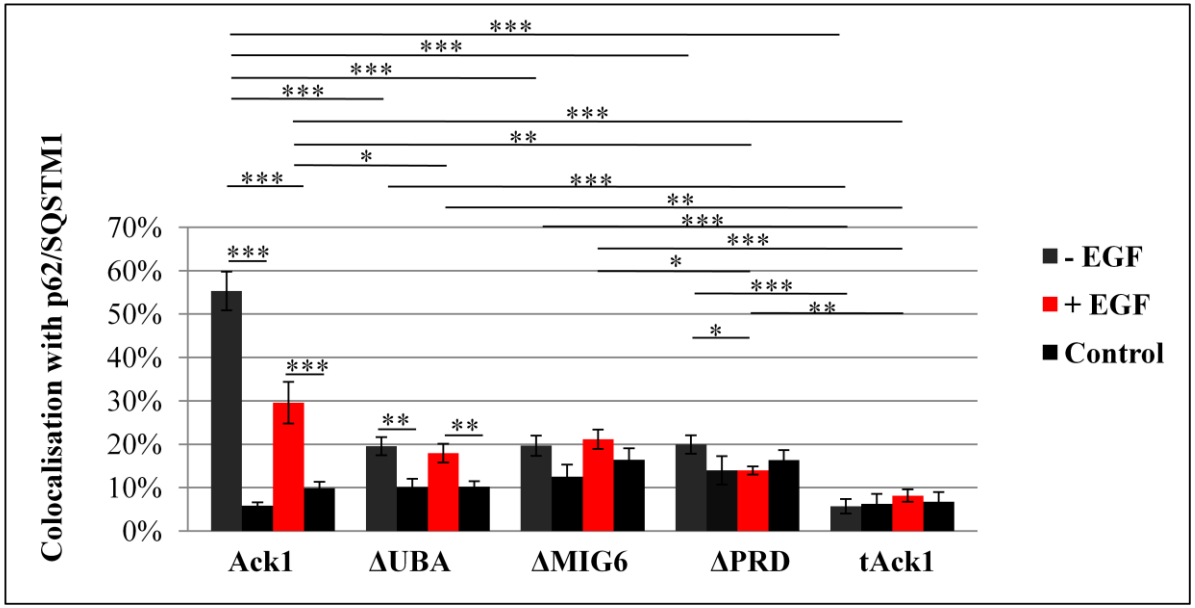

Figure 6.10. The UBA domain mediates the colocalization with p62/SQSTM1 (a) and (b)

b) For quantification (**Figure 6.10 a**), the Ack1, tAck1 or Ack1 mutant puncta were circled and the colocalization with p62/SQSTM1 was quantified. As a control, the circles were moved into the areas absent for Ack1, tAck1 or the Ack1 mutants and the random colocalization with p62/SQSTM1 was quantified. Error bars represent SEM.

As shown in **Figure 6.11**, deletion of the UBA domain does not influence the colocalization between Ack1 and NBR1, nor alters its EGF-independence. Thus, the UBA domain specifically mediates the colocalization between Ack1 and p62/SQSTM1.

6.7 EGFR partially colocalizes with Ack1 and p62/SQSTM1 post-EGF treatment

I and others show that Ack1 colocalizes with EGFR following EGF stimulation (Shen *et al.*, 2007; Grovdal *et al.*, 2008). I also identify the association between Ack1 and the autophagy receptors, *i.e.* NBR1 and p62/SQSTM1. Therefore I examined whether EGFR colocalizes with Ack1 and p62/SQSTM1 upon EGF treatment. HeLa cells expressing mCherry-Ack1, EGFR-GFP and p62/SQSTM1-flag were serum-starved and stimulated with EGF. The cells were fixed and immunostained with α-SQSTM1 antibody, and imaged *via* confocal microscopy. As shown in **Figure 6.12**, upon EGF treatment approximately 90 % of the Ack1 puncta colocalize with EGFR, whereas approximately 30 % colocalize with p62/SQSTM1. This relatively low colocalization with p62/SQSTM1 is expected, since EGF stimulation decreases the colocalization between Ack1 and p62/SQSTM1. Importantly, the majority of the Ack1 puncta which colocalize with p62/SQSTM1 also colocalize with EGFR (approximately 20 %). Therefore EGFR partially colocalizes with Ack1 and p62/SQSTM1 following EGF stimulation.

6.8 Ack1 partially localizes to early phagophores upon EGF stimulation

Since I identified the interaction between Ack1 and the autophagy receptors, I examined whether Ack1 colocalizes with pre-autophagosomes. As explained in more detail in **Chapter 1.4.1**, the Atg proteins are essential for autophagy as they are required for initiation and maturation of autophagosomes (Mizushima *et al.*, 2011).

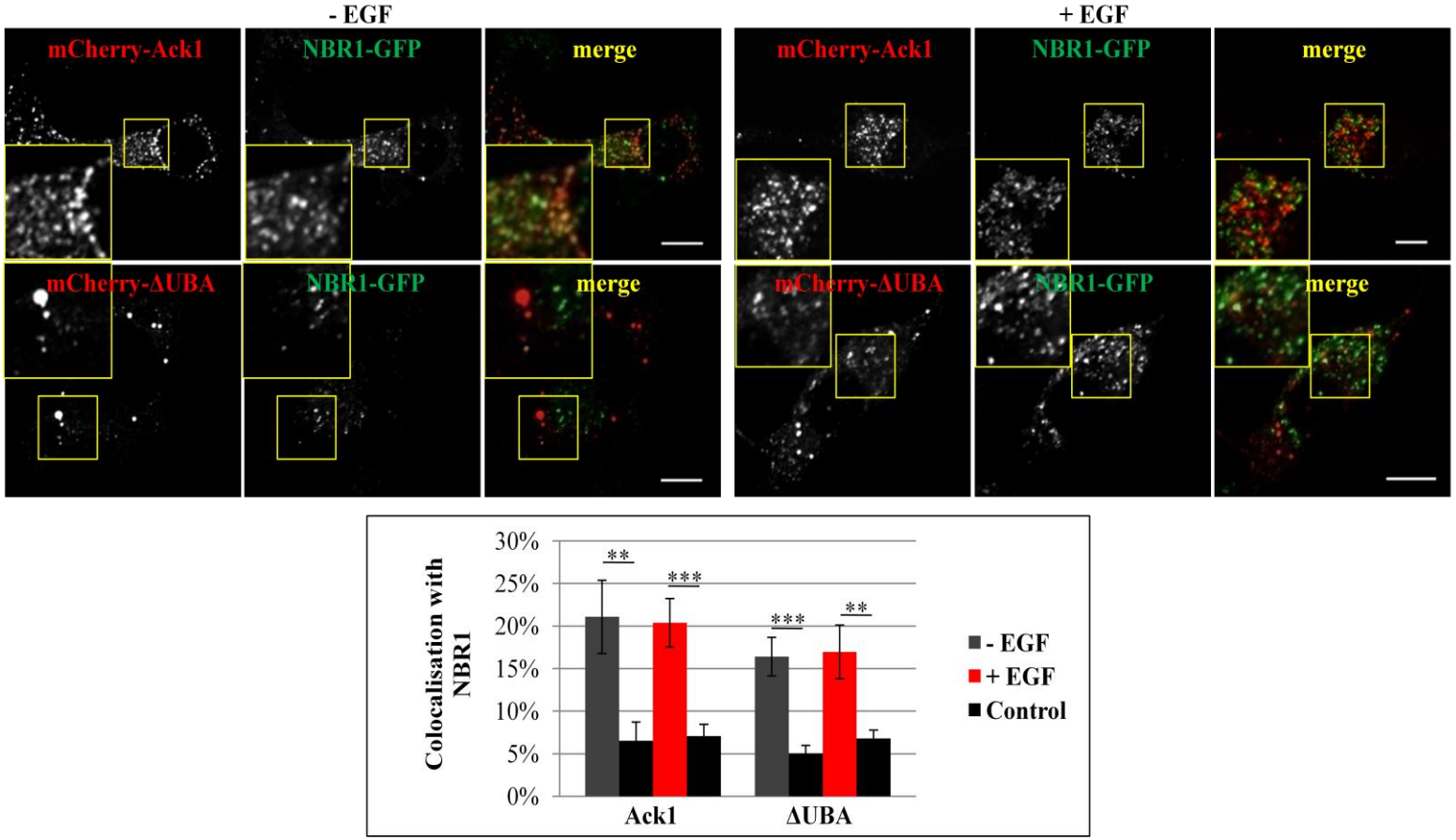

Figure 6.11. The UBA domain does not mediate the colocalization with NBR1

HeLa cells transfected with mCherry-tagged Ack1 or ΔUBA Ack1 mutant and NBR1-GFP were serum-starved for four hours and stimulated with EGF for 30 minutes, fixed and imaged *via* confocal microscopy. For quantification, the Ack1 or ΔUBA Ack1 mutant puncta were circled and the colocalization with NBR1 was quantified. As a control, the circles were moved into the areas absent for Ack1 or ΔUBA Ack1 mutant and the random colocalization with NBR1 was quantified. Scale bars 10 µm. Error bars represent SEM.

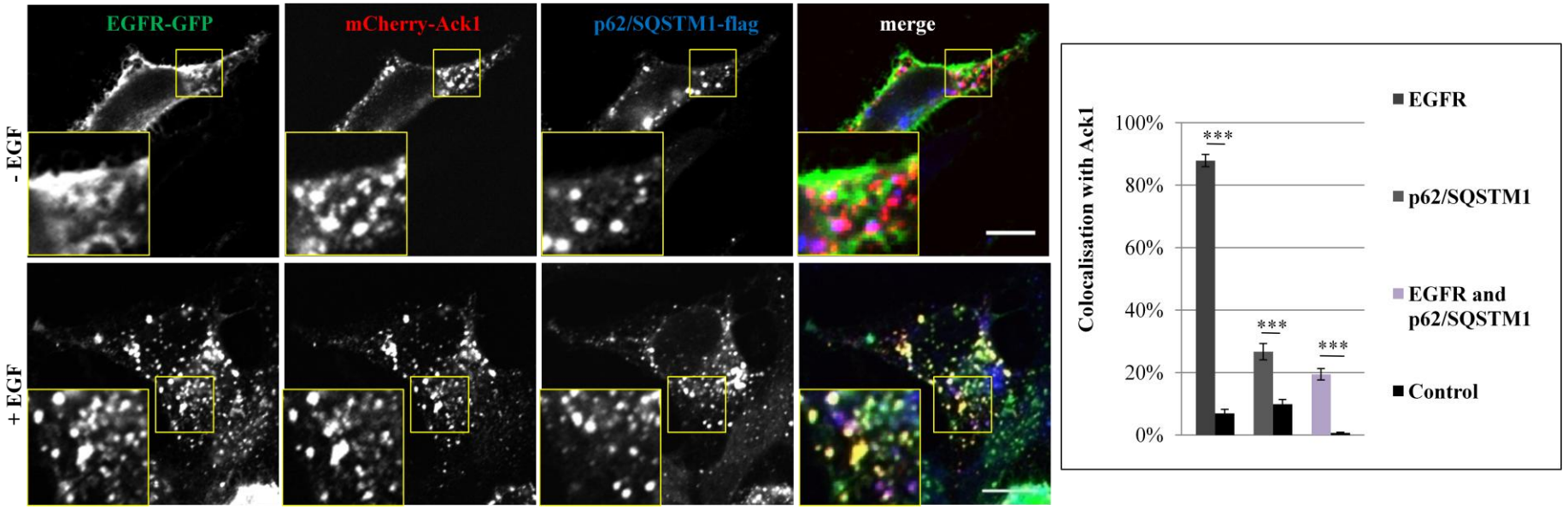

Figure 6.12. EGFR partially colocalizes with Ack1 and p62/SQSTM1 post-EGF treatment

Hela cells transfected with mCherry-Ack1, EGFR-GFP and p62/SQSTM1-flag were serum-starved for four hours and stimulated with EGF for 30 minutes, fixed and immunostained with α-SQSTM1 antibody. The cells were imaged *via* confocal microscopy. For quantification, the Ack1 puncta were circled and the colocalization with EGFR and p62/SQSTM1 was quantified. As a control, the circles were moved into the areas absent for Ack1, and the random colocalization with EGFR and p62/SQSTM1 was quantified. Scale bars 10 µm. Error bars represent SEM.

For example, Atg16 forms a multimeric complex with Atg5 and Atg12 at the initial stages of autophagosome formation, which dissociates when the autophagosome is formed, and disruption of the *Atg16* gene decreases cell viability upon nitrogen starvation in yeast (Mizushima *et al.*, 1999; Mizushima *et al.*, 2011).

To examine whether Ack1 colocalizes with Atg16, HeLa cells expressing GFP-Ack1 were serum-starved and stimulated with EGF for various times. The cells were fixed and immunostained with α-Atg16L antibody, and imaged *via* confocal microscopy. As shown in **Figure 6.13 a**, in serum-starved cells the antibody exhibits rather diffused staining, although some punctual staining can also be observed. Following EGF stimulation, the Atg16-positive structures can be distinguished, and Ack1 colocalizes to these structures upon EGF treatment. When quantified at 15 minutes post-EGF, approximately 25 % of the Ack1 puncta colocalizes with Atg16 (**Figure 6.13 a**, **top right graph**). Additional quantification with PCC shows a significant increase in colocalization between Ack1 and Atg16 at 15 and 30 minutes of EGF treatment (**Figure 6.13 a**, **bottom right graph**). Thus, EGF stimulation promotes colocalization between Ack1 and Atg16.

To verify whether the interaction between Ack1 and Atg16 takes place at the physiological level, LNCaP cells were serum-starved and stimulated with EGF for various times. The cells were lysed and cell lysates were incubated with α-Atg16L antibody. Consistenly with the data from HeLa cells, endogenous Ack1 co-precipitates with endogenous Atg16 in LNCaP cells, as shown in **Figure 6.13 b**. Additionally endogenous LC3, another member of the Atg family crucial for autophagy (described in **Chapter 1.4.1**) (Mizushima *et al.*, 2011) also co-precipitates with Atg16, suggesting formation of a complex is formed between Ack1, Atg16 and LC3.

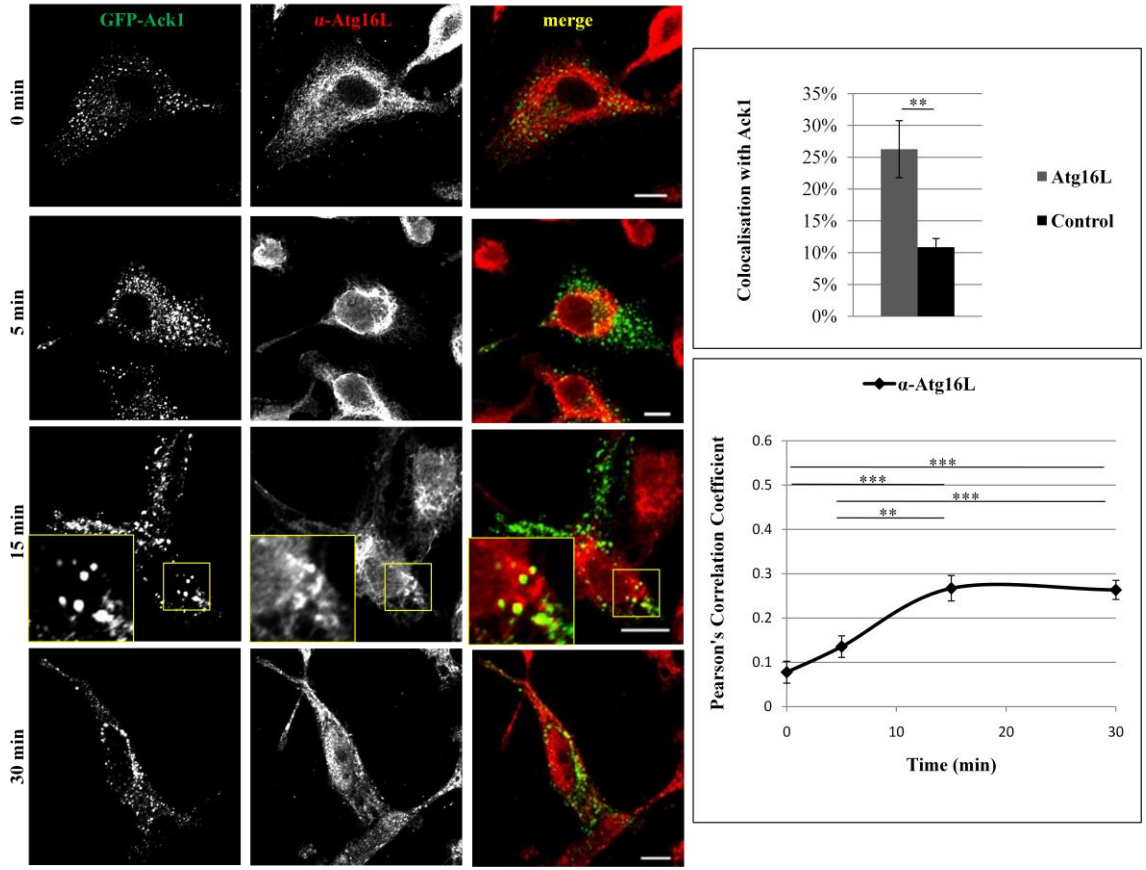

Figure 6.13. Ack1 partially localizes to early phagosomes upon EGF stimulation (a) and (b)

a) HeLa cells transfected with GFP-Ack1 were serum-starved for four hours and stimulated with EGF for indicated times, fixed and immunostained with α-Atg16L antibody. The cells were imaged *via* confocal microscopy. For quantification, top right graph: the Ack1 puncta at 15 minutes post-EGF were circled and the colocalization with Atg16L was quantified. As a control, the circles were moved into the areas absent for Ack1 and the random colocalization with Atg16L was quantified. The PCC quantification was also completed, shown on the bottom right graph. Scale bars 10 µm. Error bars represent SEM.

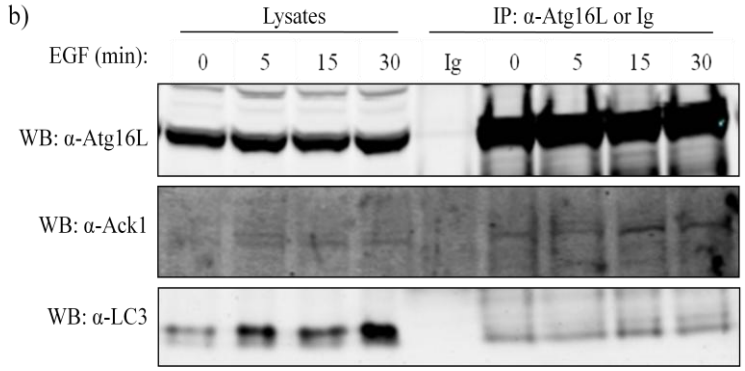

Figure 6.13. Ack1 partially localizes to early phagoosomes upon EGF stimulation (a) and (b)

b) LNCaP cells were serum-starved for four hour and stimulated with EGF for 10 minutes. The cells were lysed and cell lysates were incubated with α-Atg16L antibody to immunoprecipitate endogenous Atg16. Immunoprecipitates were subjected to SDS PAGE and. Western blotting with α-Atg16L, α-Ack1 and α-LC3B antibodies.

6.9 Ack1 colocalizes with LC3

LC3, a mammalian homologue of yeast Atg8, associates with isolation membranes downstream of Atg16 and remains within autophagosomes to undergo degradation, as described in **Chapter 1.4.1** (Mizushima *et al.*, 2011). LC3 association with autophagosomes is critical for the isolation membrane elongation and closure (Sou *et al.*, 2008). To examine the colocalization between Ack1 and LC3, HeLa cells expressing mCherry-Ack1 and GFP-LC3 (Kabeya *et al.*, 2000) were serum-starved in the presence or absence of bafilomycin, which inhibits autophagy. The cells were stimulated with EGF and fixed, and imaged *via* confocal microscopy. As shown in **Figure 6.14 a**, the colocalization between ectopically expressed Ack1 and LC3 can be distinguished in serum-starved cells and upon EGF treatment; however, EGF stimulation may partially reduce this colocalization. Additionally, treatment with bafilomycin appears to positively influence the colocalization between Ack1 and LC3, which may indicate that it takes place prior to fusion of autophagosomes with lysosomes.

Subsequently, I tested the association between GFP-Ack1 and endogenous LC3 in the presence of bafilomycin to inhibit autophagosomal degradation of LC3 (Ravikumar *et al.*, 2010). As shown in **Figure 6.14 b**, nearly 30 % of the Ack1 puncta colocalize with endogenous LC3; however, in the case of endogenous LC3 the colocalization with Ack1 is EGF-independent.

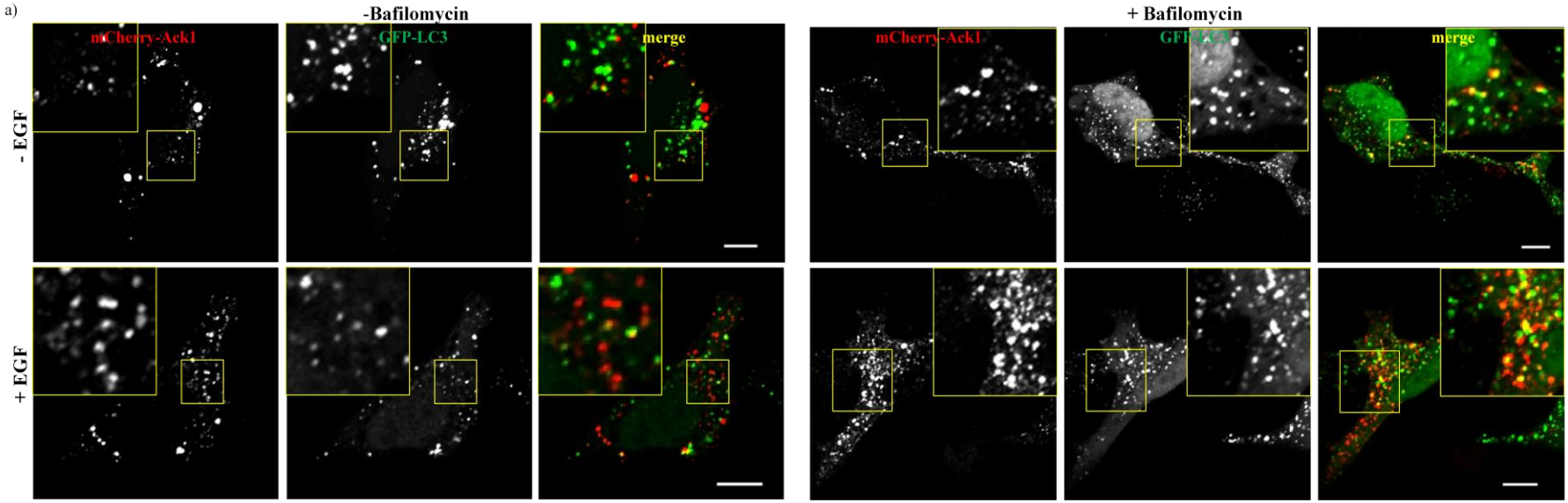

Figure 6.14. Ack1 colocalizes with LC3 (a) and (b)

a) HeLa cells transfected with mCherry-Ack1 and GFP-LC3 were serum-starved for four hours in the presence or absence of bafilomycin A (400 nM) and stimulated with EGF for 30 minutes. The cells were fixed and imaged *via* confocal microscopy. Scale bars 10 µm.

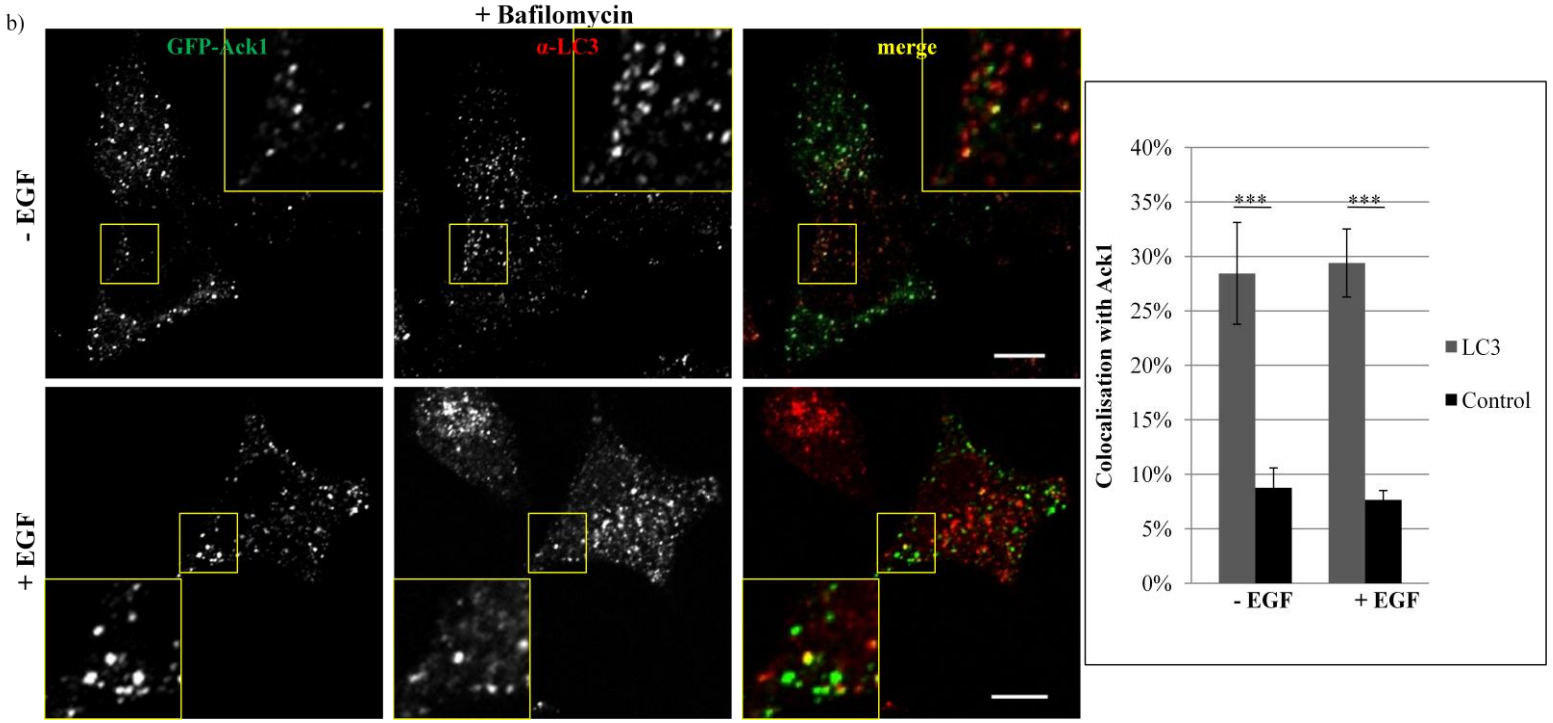

Figure 6.14. Ack1 colocalizes with LC3 (a) and (b)

b) HeLa cells transfected with GFP-Ack1 were serum-starved for four hours in the presence of bafilomycin A (400 nM) and stimulated with EGF for 30 minutes. The cells were fixed and immunostained with α-LC3B antibody. For quantification, the Ack1 puncta were circled and the colocalization with LC3B was quantified. As a control, the circles were moved into the areas absent for Ack1 and the random colocalization with LC3B was quantified. Scale bars 10 μm. Error bars represent SEM.

6.10 Conclusions

The studies completed in this chapter suggest Ack1 implication in the autophagic machinery. The first indication of possible functions of Ack1 in selective autophagy is its association with ubiquitin, a protein commonly involved in several degradative pathways (Kraft *et al.*, 2010). Previously Ack1 has been shown to bind mono- and polyubiquitin and interact with ubiquitylated proteins (Shen *et al.*, 2007). Additionally, Ack1 has also been shown to be ubiquitylated (Chan *et al.*, 2009; Lin *et al.*, 2010). I show that Ack1 localizes to ubiquitin-rich compartments and the C-terminal portion of Ack1 is critical for this localization, as truncated Ack1 fails to do so. Additionally, through employing the C-terminal truncation mutants of Ack1 I identify several domains which regulate the association between Ack1 and ubiquitin; these include the UBA domain, the proline-rich domain and the clathrin-binding domain. These data further emphesize that Ack1 may interact with ubiquitylated proteins and/or may be ubiquitylated by ubiquitin ligases.

I also find association between Ack1 and p62/SQSTM1, an autophagic receptor which recognises ubiquitylated cargo during autophagosomal degradation (Lamark *et al.*, 2009). This association is enhanced in serum-starved cells and partially decreases following EGF stimulation. These data indicate that EGF treatment results in Ack1 translocation from p62/SQSTM1 compartments. Importantly, the UBA domain is critical for this association. Therefore, it appears that the ubiquitin binding mediated *via* the UBA domain contributes to the association between Ack1 and p62/SQSTM1. Interestingly, Ack1 association with NBR1, which plays a similar function to p62/SQSTM1 (Lamark *et al.*, 2009), is much less evident and is independent on EGF treatment. Thus, it is likely that the interaction between Ack1 and p62/SQSTM1 is specific. Finally, ectopically expressed p62/SQSTM1 promotes association between Ack1 and NBR1 and confers EGF sensitivity to this association. This is likely due to

an interaction between NBR1 and p62/SQSTM1 *via* their PB1 domains (Lamark *et al.*, 2009). This is schematically presented in **Table 6.1**.

I also show that Ack1 interacts and colocalizes with Atg16, a protein that regulates the early stages of the autophagosome formation (Mizushima *et al.*, 1999; Mizushima *et al.*, 2011) and this is enhanced in EGF-treated cells. Interestingly, EGF treatment appears to stimulate the formation of the Atg16-positive structures thus suggesting that Atg16-positive phagophores (isolation membranes) are formed in these conditions. In addition to the interaction with Atg16, I find an association between Ack1 and LC3, which plays a critical role in autophagosomal membranes elongation (Sou *et al.*, 2008). Interestingly, the colocalization between Ack1 and ectopically expressed LC3 appears to decrease upon EGF stimulation, whereas colocalization between Ack1 and endogenous LC3 is EGF-independent. These data again suggest that the colocalization studies at the physiological levels may differ from that on ectopically expressed proteins. In summary, the association between Ack1 and Atg16 is promoted upon EGF treatment, the colocalization between Ack1 and ectopically expressed LC3 appears to decrease upon EGF stimulation, whereas the colocalization between Ack1 and endogenous LC3 is independent of EGF stimulation. This is schematically presented in **Table 6.1**.

Colocalization between Ack1 and:	Colocalization (approximate)		EGF sensitivity	Colocalization post-EGF
	-EGF	+EGF		
NBR1	25 %	20 %	No	No change
p62/SQSTM1	55 %	30 %	Yes	Decreases
NBR1 and p62/SQSTM1	50 % and 50 %	35 % and 30 %	Yes	Decreases
LC3 (endogenous)	30 %	30 %	No	No change
Atg16 (endogenous)	Less	More	Yes	Increases

Table 6.1. Summary of the studies on Ack1 colocalization with autophagic proteins

The table presents the results of the studies performed to evaluate the association between Ack1 and the autophagic proteins, including the level of colocalization and the EGF sensitivity of a particular association.

7 Identification of novel PTMs and Ack1 interactors *via* mass spectrometry

7.1 Introduction

Posttranslational modification (PTM) of proteins is a ubiquitous mechanism for regulation of cellular functions, as described in more detail in **Chapter 1.3.2** and **Chapter 1.3.3**. PTMs provide a very efficient way for controlling cellular physiology, are important aspects of protein folding, structure and function, and allow the cell to rapidly react to an extracellular signal *via* transmitting the message throughout the cell (Deribe *et al.*, 2010). PTMs involve attachment of a chemical group (*e.g.* phosphate in phosphorylation), a protein (*e.g.* ubiquitin in ubiquitylation), lipid (*i.e.* lipidation), sugar (*i.e.* glycosylation) or other molecules to amino acid residues within the modified protein and these modifications result in alteration of protein properties (Deribe *et al.*, 2010).

There are many different types of PTMs; some are stable and regulate protein folding and maturation (*e.g.* glycosylation and formation of disulfide bridges), others are reversible and control cellular signalling (*e.g.* phosphorylation, nitrosylation, ubiquitylation) (Hess *et al.*, 2005; Hjerpe and Rodriguez, 2008; Deribe *et al.*, 2010). Among the latter, phosphorylation is ubiquitous and is considered central for correct cellular function (Cohen, 2002; Deribe *et al.*, 2010). In eukaryotic cells, phosphorylation is a process in which a phosphate group is attached to tyrosine, serine or threonine residue (Deribe *et al.*, 2010). Phosphorylation is regulated by the enzymatic function of protein kinases, which add phosphate groups, and phosphatases, which remove phosphate groups (Deribe *et al.*, 2010), as described in **Chapter 1.3.2**. Therefore, identification of novel phosphorylation sites allows for better understanding of protein regulation. Mass spectrometry is currently one of the most used techniques for the

identification of phosphorylation and other PTMs within the protein, due to a change in mass upon protein modification.

Apart from identification of PTMs there are many other areas, in which mass spectrometry has been applied, *e.g.* identification of binding partners of a protein of interest. Typically, a particular protein is immunoprecipitated and the co-precipitating proteins are characterised by mass spectrometry. Additionally, in this context, stable isotope labelling of amino acids in cell culture (SILAC) may be used in order to quantitatively analyse the interactors that bind in response to a particular treatment.

SILAC was first described by Ong *et al.* in 2002 (Ong *et al.*, 2002). They used mouse myoblast cells which have a potential to differentiate into myotubes, and cultured the uninduced cells in normal medium ("light"), whereas cells undergoing differentiation induced by reduced concentration of serum, in medium with isotypically labelled leucine ("heavy"). Using mass spectrometry, they quantitatively compared the proteins obtained from uninduced cells to those obtained from differentiating cells and identified upregulation of several proteins in cells undergoing differentiation. This study opened up the possibility to employ the SILAC technique to study the quantitative changes in protein levels in cells in response to a particular treatment.

7.2 Novel phosphorylation sites

To identify potential novel phosphorylation sites within Ack1, 293T cells expressing myc-Ack1 were lysed and cell lysates were subjected to immunoprecipitation with α-myc antibody. The immunoprecipitated proteins were resolved by SDS PAGE (**Chapter 3.2.4**) and the gel was stained with Coomassie in order to visualise separated proteins (**Chapter 3.2.7**).

(**Figure 7.1**). The section of the gel identified as containing myc-Ack1 (approximately 140 kDa) was cut out along with a very thin section directly above myc-Ack1, at approximately 150 kDa, which could potentially include modified Ack1, *i.e.* phosphorylated or ubiquitylated. These sections of the gel were cut into pieces, which were further destained and subjected to trypsin digestion and desalting (**Chapter 3.2.7**), and the samples were subjected to liquid chromatography (LC) mass spectrometry (MS/MS) (**Chapter 3.2.7**). The mass spectrometry-obtained data were analysed by Dr. A. J. Creese using Proteome Discoverer, as described in **Chapter 3.2.7**. In particular, phosphorylation of serine, threonine and tyrosine, and ubiquitylation of lysine were set as variable modifications. The experiment was repeated several times to improve Ack1 sequence coverage. The data from all experiments were collated resulting in 52.28 % protein sequence coverage, shown in **Figure 7.2**. Green regions indicate the sequences identified with high confidence and yellow indicate the sequences with medium confidence. The coverage obtained allows for confident identification of Ack1 within the sample; however, parts of Ack1 have not been characterised. These include the N-terminus containing the SAM domain, some regions in the kinase domain, a large region containing the clathrin binding domain, a region containing the EGFR binding domain and the C-terminus with the UBA domain.

Three novel phosphorylation sites of serine residues have been identified, which are shown in **Figure 7.3 a** and **b** and **Figure 7.4 a**. These modifications are defined as novel, since they are not described in an online database containing a comprehensive information on proteins phosphorylation sites (www.phosphosite.org) (Hornbeck *et al.*, 2012). The identified novel PTMs include serine 102 (Ser102), Ser761 and Ser936. These novel PTMs along with known phosphorylation sites within mouse Ack1 (isoform 2) are shown in **Figure 7.5**.

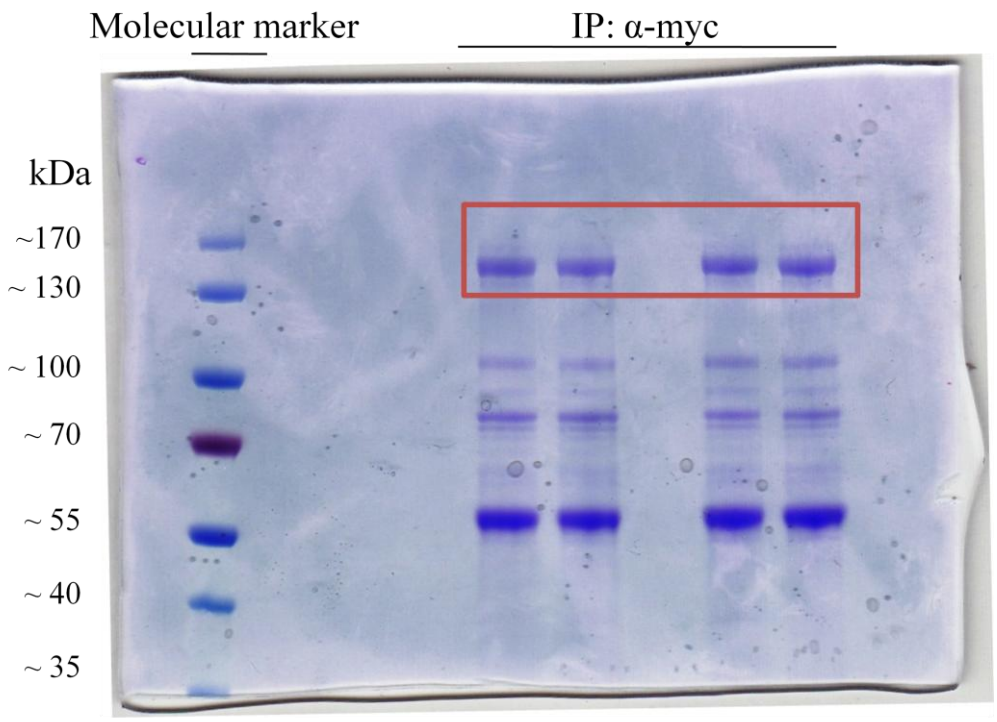

Figure 7.1. Coomassie-stained gel with immunoprecipitated Ack1

293T cells transfected with myc-Ack1 were lysed and cell lysates were incubated with α-myc antibody to immunoprecipitate Ack1. Immunoprecipitates were subjected to SDS PAGE followed by the staining of the gel with Coomassie. The red rectangle indicates the section of the gel containing myc-Ack1 (approximately 140 kDa) and potentially modified myc-Ack1 (approximately 150 kDa), which was cut out and subjected to trypsin digestion and further mass spectrometric analysis (**Chapter 3.2.7**).

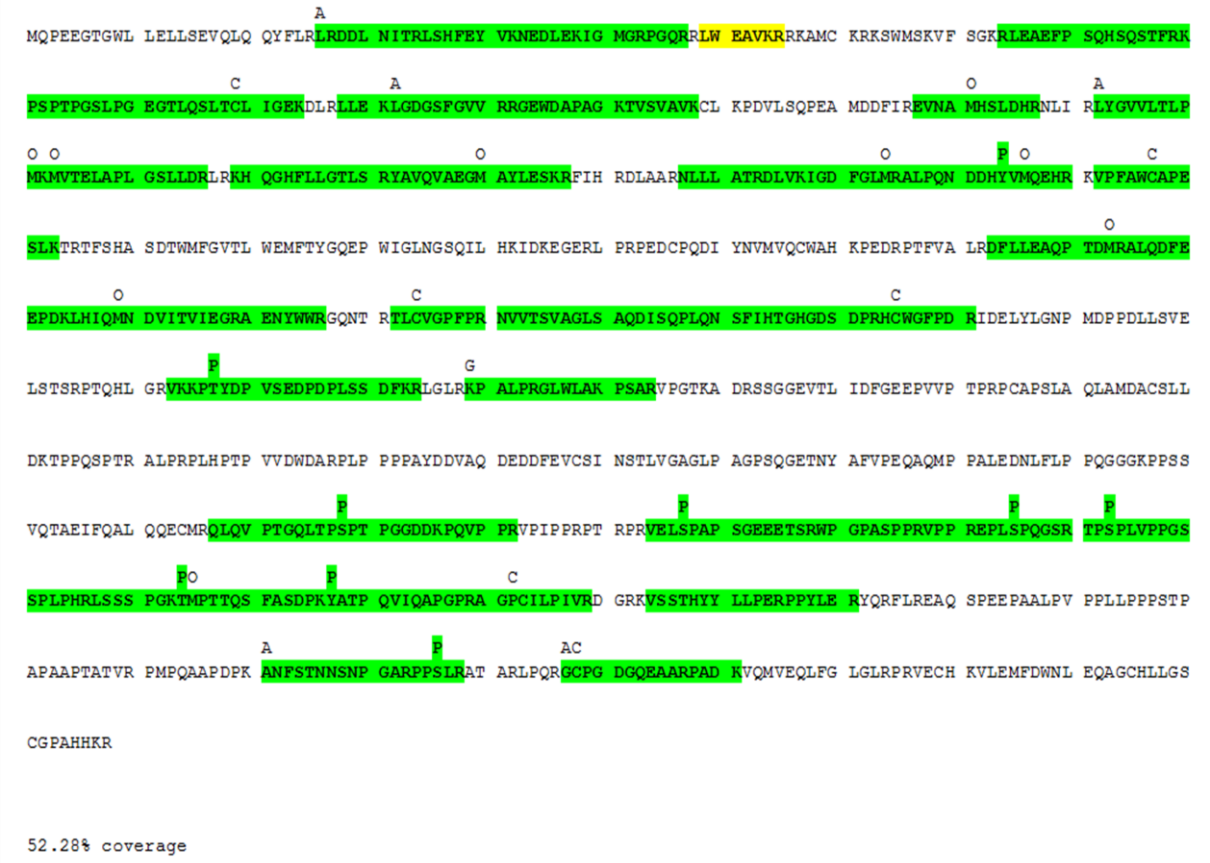

Figure 7.2. Ack1 sequence coverage

The primary sequence of Ack1 identified by LC-MS/MS with 52.28 % sequence coverage. Green colour indicates the regions identified with high confidence, yellow colour with medium confidence. The following PTMs are indicated: A-acetylation ($COCH_3$ addition to N-terminus); C-carbamidomethylation (CH_2CONH_2 addition to Cys); G-ubiquitylation (Gly-Gly addition to Lys); O-oxidation (O addition to Met); P-phosphorylation (H_2PO_3 addition to Ser, Thr or Tyr).

a)

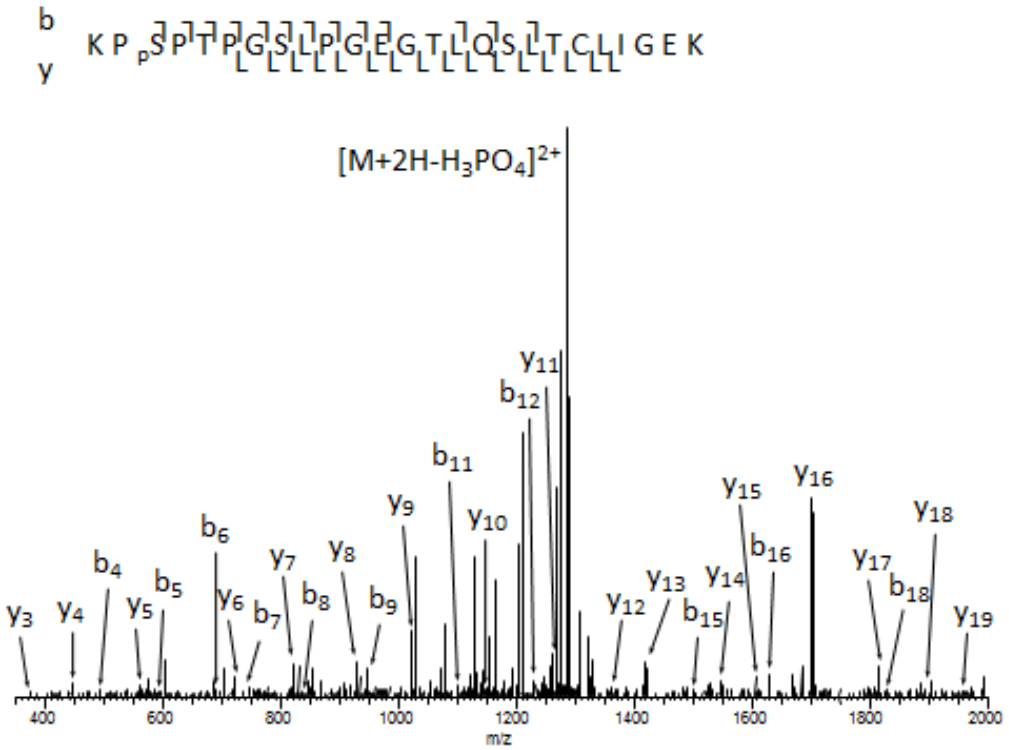

b)

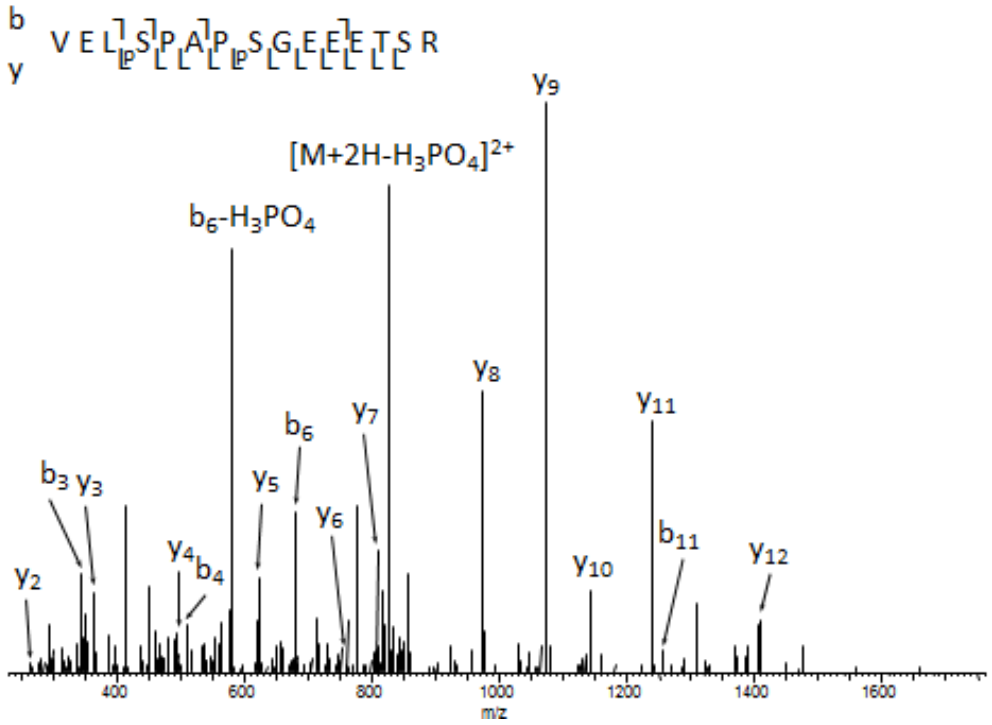

Figure 7.3. Novel phosphorylation sites at Ser102 and Ser761

Mass spectra of the peptides comprising novel phosphorylation sites identified by LC-MS/MS: phospho-serine 102 **(a)** and phospho-serine 761 **(b)**. The sequence of each peptide is shown above the spectrum, with *b* and *y* fragment ions.

a)

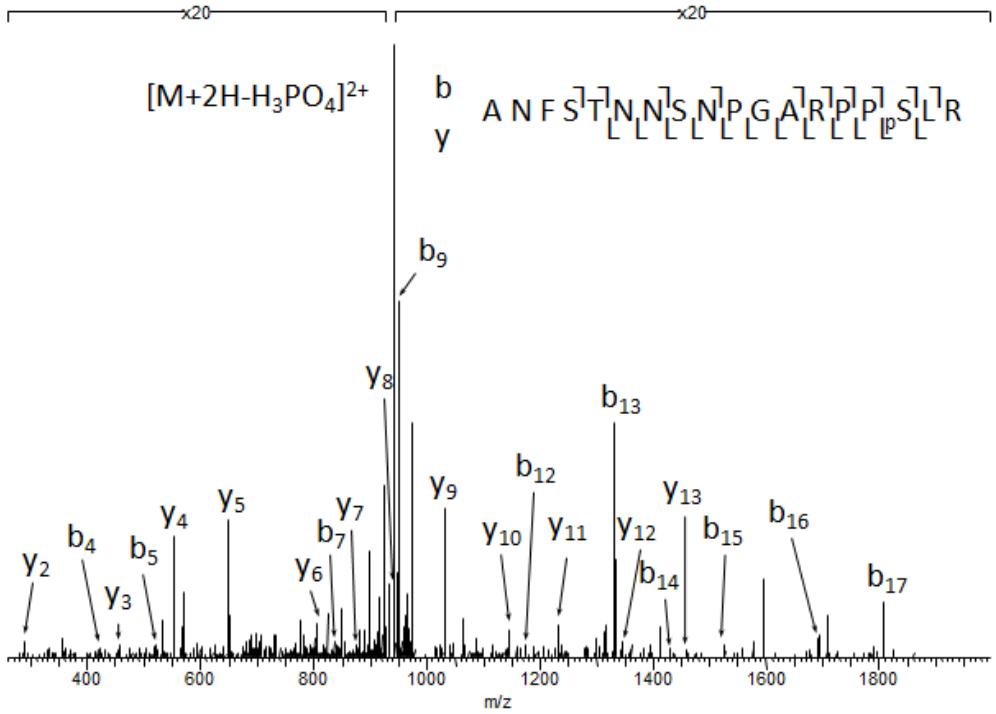

b)

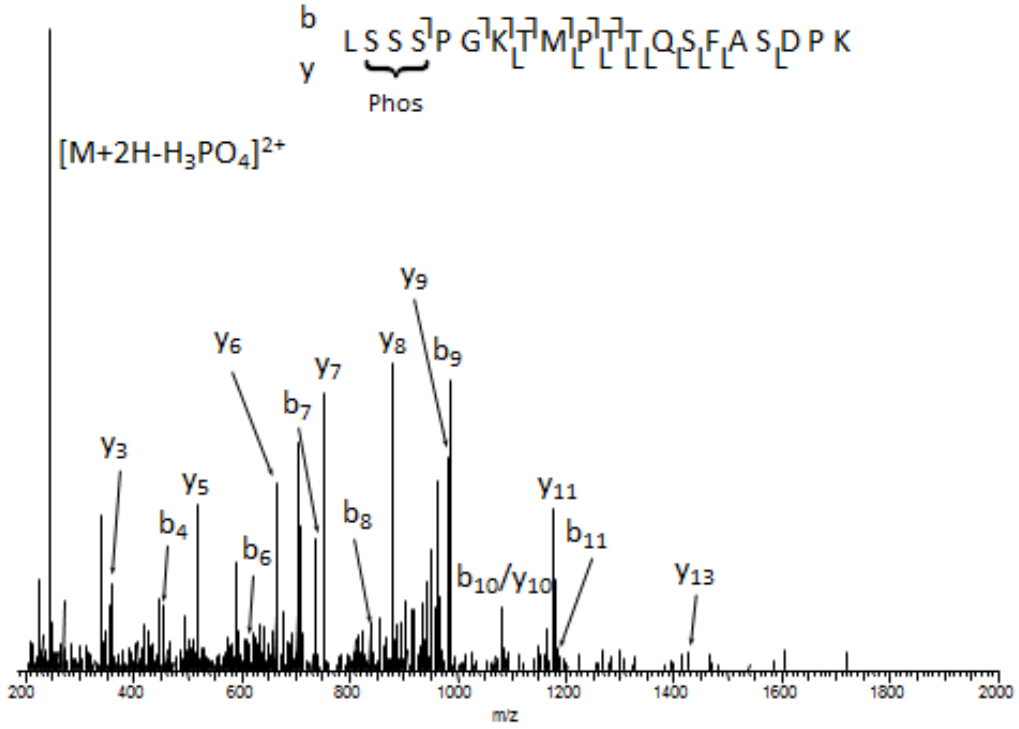

Figure 7.4. Novel phosphorylation sites at Ser936 and the SSS region

Mass spectra of a peptide comprising novel phosphorylation site identified by LC-MS/MS: phospho-serine 936 **(a)** and of a peptide comprising three consecutive serines (Ser808, Ser809, Ser810), one of which has been identified as phosphorylated **(b)**. The sequence of each peptide is shown above the spectrum, with *b* and *y* fragment ions.

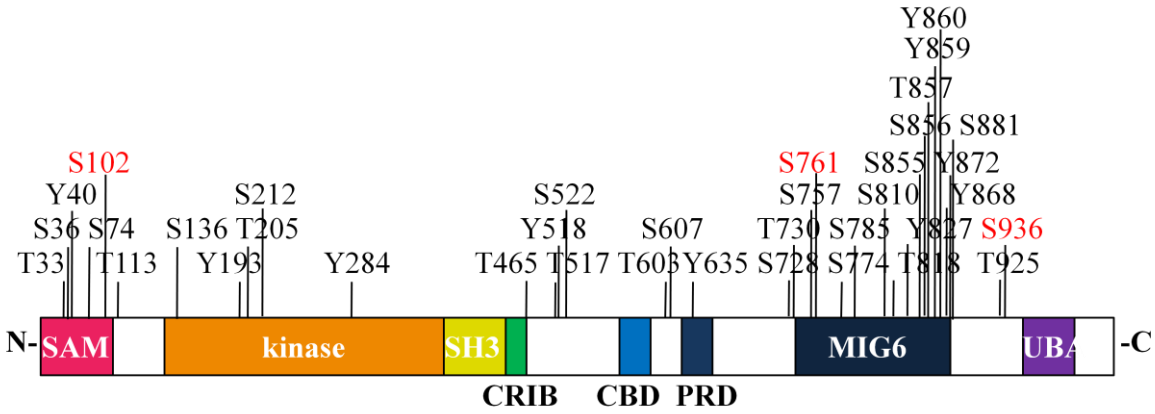

Figure 7.5. Known and novel phosphorylation sites within mouse Ack1 (isoform 2)

Known phosphorylation sites are shown in black, whereas three novel phosphorylation sites identified are shown in red. T-Thr, S-Ser, Y-Tyr. From PhosphoSitePlus (www.phosphosite.org).

Ser102 does not localize within any specific domain within Ack1 and is located between the SAM and the kinase domains (Mahajan and Mahajan, 2010), Ser936 is located within the C-terminal proline-rich region and is adjacent to two proline residues (Mahajan and Mahajan, 2010), whereas Ser761 is located within the Mig6-homology domain (the EGFR binding domain) (Shen *et al.*, 2007). This phosphoprylation may be important for the interaction with EGFR and a point mutation of Ser761 may potentially influence EGFR binding. Additionally, a region with three consecutive serine residues (SSS) is found to be phosphorylated, as shown in **Figure 7.4 b**. The precise identification of a specific phospho-serine in this case is not possible due to a lack of peptide fragmentation in this region. These serines (Ser808, Ser809, Ser810) are also localized within the EGFR binding domain.

As described above, the 52.28 % sequence coverage indicates that 47.72 % of the Ack1 sequence is not characterised. These uncharacterised regions are likely to be modified, as they contain numerous tyrosine, serine and threonine residues which could potentially be phosphorylated, and multiple lysine residues that could be ubiquitylated. Although trypsin is a highly efficient enzyme for protein digestion and cleaves the amide bond at the C-terminus of lysine and arginine, it does not cleave this bond when lysine or arginine is followed by a proline residue. The uncharacterised regions appear to have a great amount of Lys-Pro and Arg-Pro motifs, and therefore would not be cleaved. This would result in very large peptides which may be difficult to detect. The peptide coverage could potentially be improved by using a different enzyme for digestion rather than, or additionally to, trypsin.

Having identified three novel phosphorylation sites within Ack1, it is possible to predict which kinases could potentially phosphorylate these sites using software available online.

This information may be further used for investigation of the signalling pathways upstream of Ack1 phosphorylation. An integrative computational approach NetworKIN (www.networkin.info) has been developed in order to predict relationships between kinases and their substrates. It combines the information on the motifs that are preferentially targeted by a specific family of kinases with the protein network described in STRING database (string-db.org), an online database of known and predicted protein interactions. This should enhance the likelihood of identifying the kinase that targets a particular phosphorylation site (Linding *et al.*, 2007). This approach allowed us to predict the potential kinases that phosphorylate Ack1 at the three novel phosphorylation sites identified. As shown in **Table 7.1**, Ser102 is predicted to be phosphorylated by the cell-division protein kinases (CDKs) or by MAP kinases, Ser761 by casein kinases 2 (CK2), whereas Ser936 by PIM2 kinase. These can be further verified, *e.g*. through Western blotting and if confirmed, could potentially lead to characterisation of signalling cascades comprising Ack1 and the identified kinases.

7.3 Novel ubiquitylation site

Ubiquitylation is another common PTM which regulates cell signalling. Attachment of ubiquitin to a lysine residue is mediated by the subsequent action of E1, E2 and E3 ubiquitin ligases, described in more detail in **Chapter 1.3.3** (Deribe *et al.*, 2010). The proteins can be modified by attachment of a single ubiquitin (monoubiquitylation) or a chain of ubiquitin molecules (polyubiquitylation). Within Ack1, SAM and UBA domains have been proposed to contain potential ubiquitylation sites (Chan *et al.*, 2009; Lin *et al.*, 2010); however, the precise localization remains uncovered.

Phosphosite	Kinase Family	Post. Prob.	String Score	Kinase Gene
S102	CDK2_CDK3_group	0.2084	0.992	CDK2
S102	CDK2_CDK3_group	0.2084	0.964	CDK3
S102	p38_group	0.2602	0.993	MAPK14
S102	p38_group	0.2602	0.993	MAPK11
S102	p38_group	0.2602	0.99	MAPK13
S102	p38_group	0.2602	0.98	MAPK12
S761	CK2_group	0.5139	0.979	CSNK2A2
S761	CK2_group	0.5139	0.979	CK2A1
S936	Pim2	0.2047	0.98	PIM2

Table 7.1. Prediction of the kinases which phosphorylate novel sites within Ack1

Prediction of the kinases which phosphorylate Ack1 at Ser102, Ser761 and Ser 936 using NetworKIN. Additional information include NetPhorest posterior probability (probability that a phosphorylation site is a substrate of a kinase/phospho-binding domain) and string score (probability of the best association path between a kinase and substrate in string database).

The peptides extracted from the gel directly above Ack1 (potentially ubiquitylated Ack1) (**Figure 7.1**) were subjected to LC-MS/MS. This led to the identification of a potentially ubiquitylated peptide, whose spectrum is shown in **Figure 7.6**. A potential ubiquitylation (Lys539) is recognised as a presence of two consecutive glycine residues attached to a lysine residue (Gly-Gly-Lys; GGK). Surprisingly this potential ubiquitylation site is not localized within either the SAM nor the UBA domains, nor does it localize within any other characterised domain, but it is in close proximity to the clathrin binding domain (Teo *et al.*, 2001). The mass spectrum presented in **Figure 7.6** shows 100 % peptide backbone sequence coverage for the identified peptide. Unfortunately, this ubiquitylated peptide was identified only once in one of the samples, possibly due to its low abundance, and therefore further confirmation of this PTM is required. Additionally, since the modified lysine residue is located at the N-terminus of the peptide (K in KPALPR) it is possible that the peptide sequence is GGKPALPR rather than KPALPR with GG-modified lysine residue. Nevertheless, searching of a database with known mouse proteins was unsuccessful in identifying a protein containing a GGKPALPR sequence. Therefore the identified peptide is likely to be ubiquitylated. Two other ubiquitylation sites have previously been identified within mouse Ack1, which are shown along with the site identified in this study, in **Figure 7.7**. Importantly, Lys539 is not present within truncated Ack1, which is consistent with the observation that only full-length Ack1 associates with ubiquitin and/or is ubiquitylated (**Chapter 6.2**). This finding therefore may be useful for further characterisation of the precise functions of Ack1 ubiquitylation in cell signalling and trafficking.

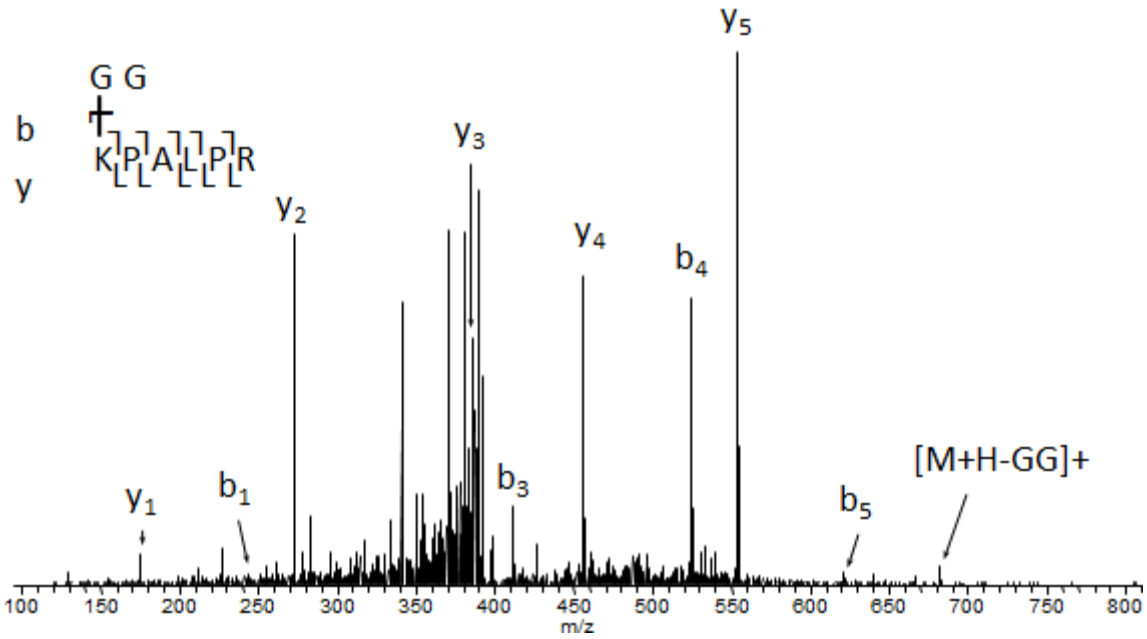

Figure 7.6. Novel ubiquitylation site at Lys539

Mass spectrum of a peptide comprising novel ubiquitylation site identified by LC-MS/MS at Lys539. The sequence of the peptide is shown abouve the spectrum, with *b* and *y* fragment ions.

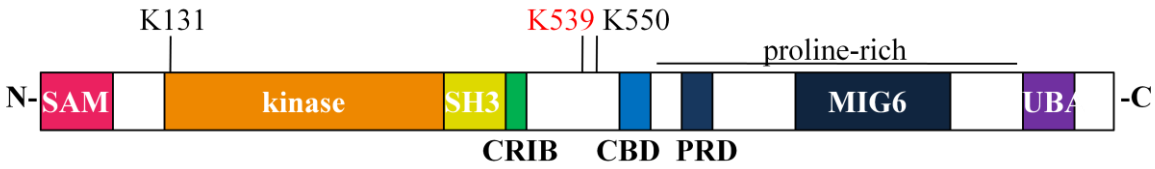

Figure 7.7. Known and novel ubiquitylation sites within mouse Ack1 (isoform 2)

Known ubiquitylation sites are shown in black, whereas the novel ubiquitylation site identified is shown in red. K-Lys. From Mammalian Ubiquitination Site Database (http://222.193.31.35:8000/mUbiSiDa.php).

7.4 Ack1 binding partners identified by SILAC

In order to identify the proteins interacting with Ack1 in an EGF-dependent manner, 293T cells were first cultured for at least five doubling times in SILAC "light", "medium" or "heavy" media (described in **Chapter 3.2.6**). This allowed the cells to fully incorporate the labelled amino acids into the proteins during protein synthesis (Cunningham *et al.*, 2010). Subsequently, "medium" and "heavy" cells were transfected with myc-Ack1, whereas "light" cells were untransfected and later used as control. The cells were serum-starved, and the "heavy" cells were stimulated with EGF for 15 minutes (+EGF sample), whereas "light" (control) and "medium" (-EGF sample) cells were left untreated. The cells were lysed and cell lysates were subjected to immunoprecipitation with α-myc antibody, or with α-myc antibody previously cross-linked to the beads. Antibody cross-linking is useful as it allows a formation of a covalent bond between antibody chains and the beads, and thus the antibody chains are not eluted into the sample (Sousa *et al.*, 2011). On the other hand, I find that it may result in a decreased amount of immunoprecipitated proteins. For example, as shown in **Figure 7.8**, antibody cross-linking dramatically reduces the amount of endogenous Ack1 immunoprecipitated from LNCaP cell lysates**.** Therefore, for optimal results each experiment was carried in both conditions, *i.e.* with and without antibody cross-linking. Following immunoprecipitation, the beads were washed extensively, mixed ("light". "medium" and "heavy") and washed again. Precipitated proteins were eluted and separated through SDS PAGE. The antibody cross-linking largely prevented coelution of antibody chains shown in **Figure 7.9**; however, fewer proteins were found co-precipitated with Ack1, as visualised following gel staining with Coomassie. Separated proteins were digested with trypsin and subjected to LC-MS/MS by Dr. A. J. Creese (described in **Chapter 3.2.7**).

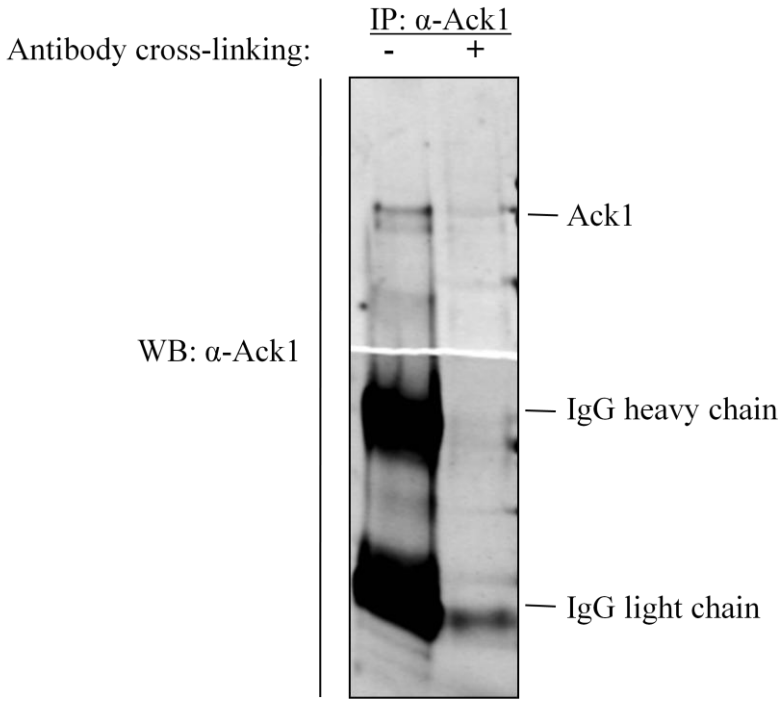

Figure 7.8. Antibody cross-linking reduces the amount of immunoprecipitated proteins

LNCaP cells were lysed and cell lysates were subjected to immunoprecipitation with α-Ack1 antibody, which had been previously cross-linked to the beads (+), or with the antibody alone (-). The same amounts of proteins, antibody and beads were used in both experiments. Immunoprecipitates were subjected to SDS PAGE and Western blotting with α-Ack1 antibody.

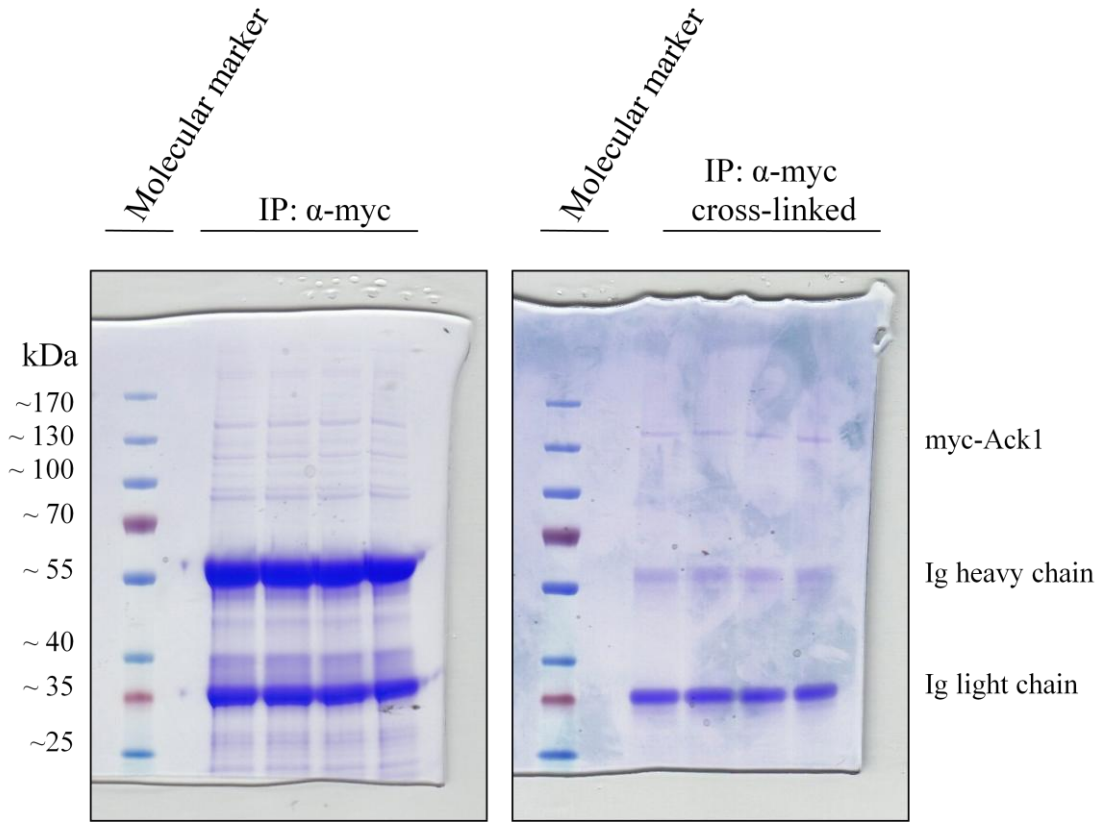

Figure 7.9. Immunoprecipitation of myc-Ack1

SILAC labelled 293T cells transfected with myc-Ack1 were serum-starved for four hours and the "heavy" cells were stimulated with EGF for 15 minutes. The cells were lysed and cell lysates were incubated with α-myc antibody (either alone or previously cross-linked to the beads) to immunoprecipitate Ack1. Immunoprecipitates were mixed and subjected to SDS PAGE following by the staining of the gel with Coomassie. Ack1 and co-precipitated proteins were cut out off the gel and subjected to trypsin digestion and further mass spectrometric analysis (**Chapter 3.2.7**).

The data were analysed using MaxQuant and Perseus (**Chapter 3.2.7**). MaxQuant recognises sets of isotope patterns and compares them to the theoretical isotope patterns, and if the mass differences are within the accepted error, and if the intensity correlation of the patterns is sufficient, then the peaks are recognised as a SILAC set (Cox and Mann, 2008).

As explained in **Chapter 3.2.7**, the data were searched against a human protein database containing the reverse peptides and common contaminants, both of which were removed from the dataset. The protein ratios were normalised, so that the median of log-transformed peptide ratios equals zero (Cox and Mann, 2008). The normalised protein ratios ("medium"/"light" (M/L), "heavy"/"light" (H/L) and "heavy"/"medium" (H/M)) were subsequently log-transformed to ensure the equal treatment of up- and downregulation. As shown in **Figure 7.10**, the majority of the log-transformed ratios spread around zero, which indicates that their ratios have a value of, or close to, one (natural logarithm of one is zero). Therefore, the majority of the proteins are background proteins which co-precipitate in a control ("light"), as well as in -EGF ("medium") and +EGF ("heavy") samples. Additionally, since the experiment was performed four times (two independent experiments, each performed with and without antibody crosslinking), as shown in **Figure 7.10**, only the proteins identified in at least two samples were considered as potential binding partners for Ack1. Using Perseus, the proteins enriched in -EGF or +EGF samples were identified. For every protein, the p-value is adjusted with Benjamini Hochberg false discovery rate (FDR) to correct for the false positives due to multiple hypothesis testing (Cox and Mann, 2012). The threshold value for FDR is 0.05. Importantly, there are proteins identified only in one or two samples (*e.g.* in "medium" and/or "heavy", and not in "light"), resulting in ratios of infinity as they cannot be calculated (*e.g.* M/L and H/L"). These proteins may potentially be novel interactors; however, in the study presented in this thesis they were omitted due to a lack of validation.

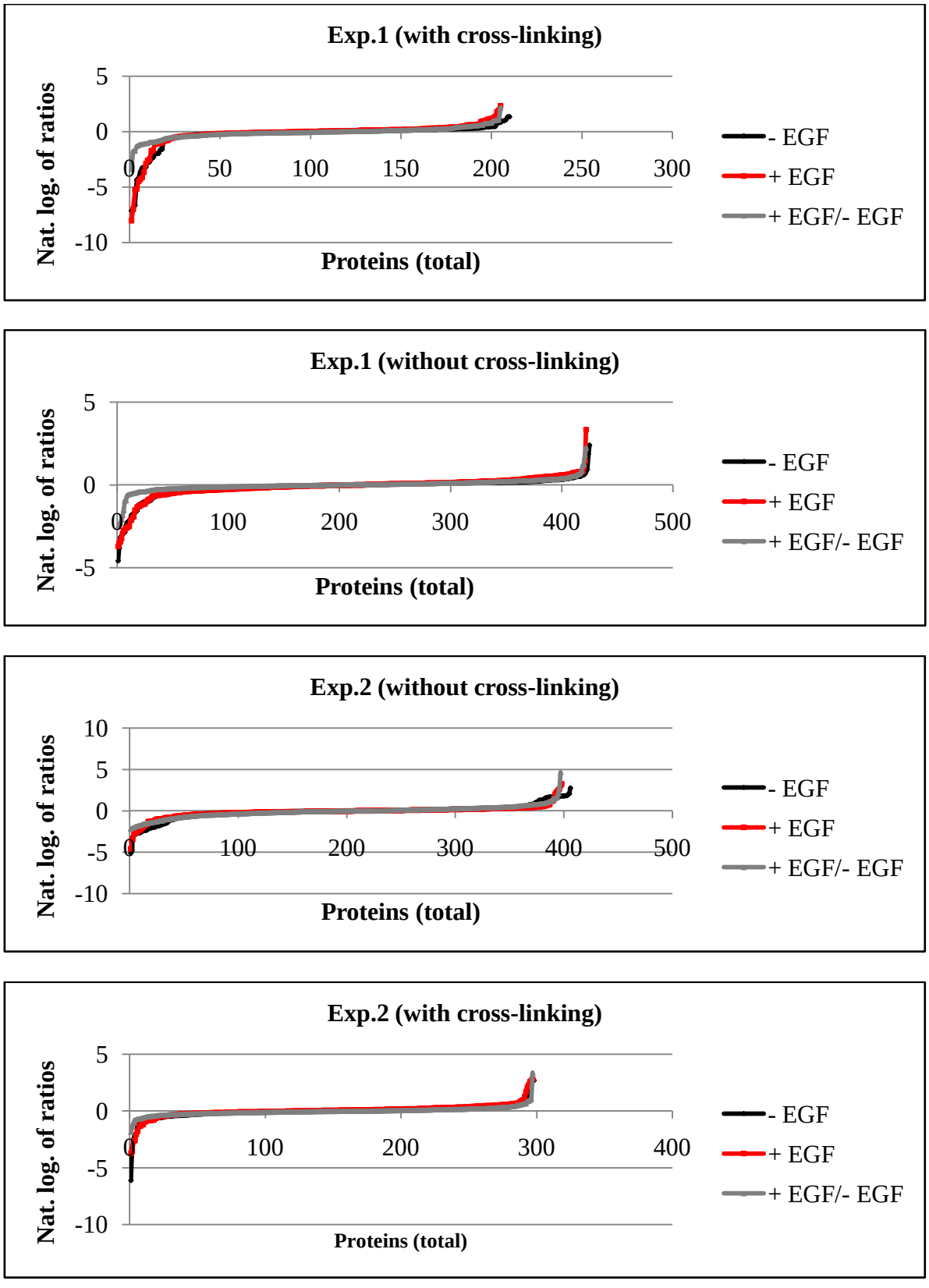

Figure 7.10.Natural logarithm of ratios from two independent experiments

Natural logarithm of the ratios M/L (-EGF), H/L (+EGF) and H/M (+EGF/-EGF) from two independent experiments (each performed with or without antibody cross-linking to the beads).

Additionally, some proteins which are known Ack1 interactors (*e.g.* clathrin) were not retained using the parameters described above, indicating that these parameters appear strict and conservative. Therefore, due to these restrictions, any proteins significantly enriched in "medium" or "heavy" samples are likely to be genuine Ack1 interactors.

Using these parameters, the graphs have been plotted, as presented in **Figure 7.11**. The graphs show the log-transformed ratios of proteins identified in -EGF to control sample (H/L) on *x* axis, and +EGF to control sample (M/L) on *y* axis. The gene names of the proteins which have been significantly enriched in -EGF or +EGF sample, as compared to the control sample, are shown in **Figure 7.12** and **Figure 7.13**, respectively. The proteins whose H/M ratio was significantly increased or decreased are shown in **Figure 7.14**. Additional information, including protein names, the ratios and the p-values for the proteins enriched in -EGF or +EGF sample is shown in **Table 7.2**. Among the identified proteins, some are characterised as binding independently of EGF treatment (high M/L and H/L ratio), some which preferably bind Ack1 following EGF treatment (high H/M ratio), whereas others preferably interact with Ack1 in untreated cells (high M/L and low H/M ratio). This is shown in **Table 7.3**.

As shown in **Table 7.2** and **Table 7.3**, some proteins are enriched in both -EGF and +EGF samples, as their M/L and H/L ratios are significantly increased, *i.e.* Cdc42, Nck1 and Nck2, TCEB2 and HSP90-α. These proteins therefore can interact with Ack1 both under serum starvation and following EGF stimulation. Other proteins are enriched in the -EGF sample, as their M/L ratio is significantly increased, *i.e.* CPSF3, MCM7, CANX and KAT7. Another group of proteins interacts with Ack1 upon EGF stimulation, as their H/L ratio is significantly increased, *i.e.* PFKL, HSP90-β, ARHGEF12 and Cdc37.

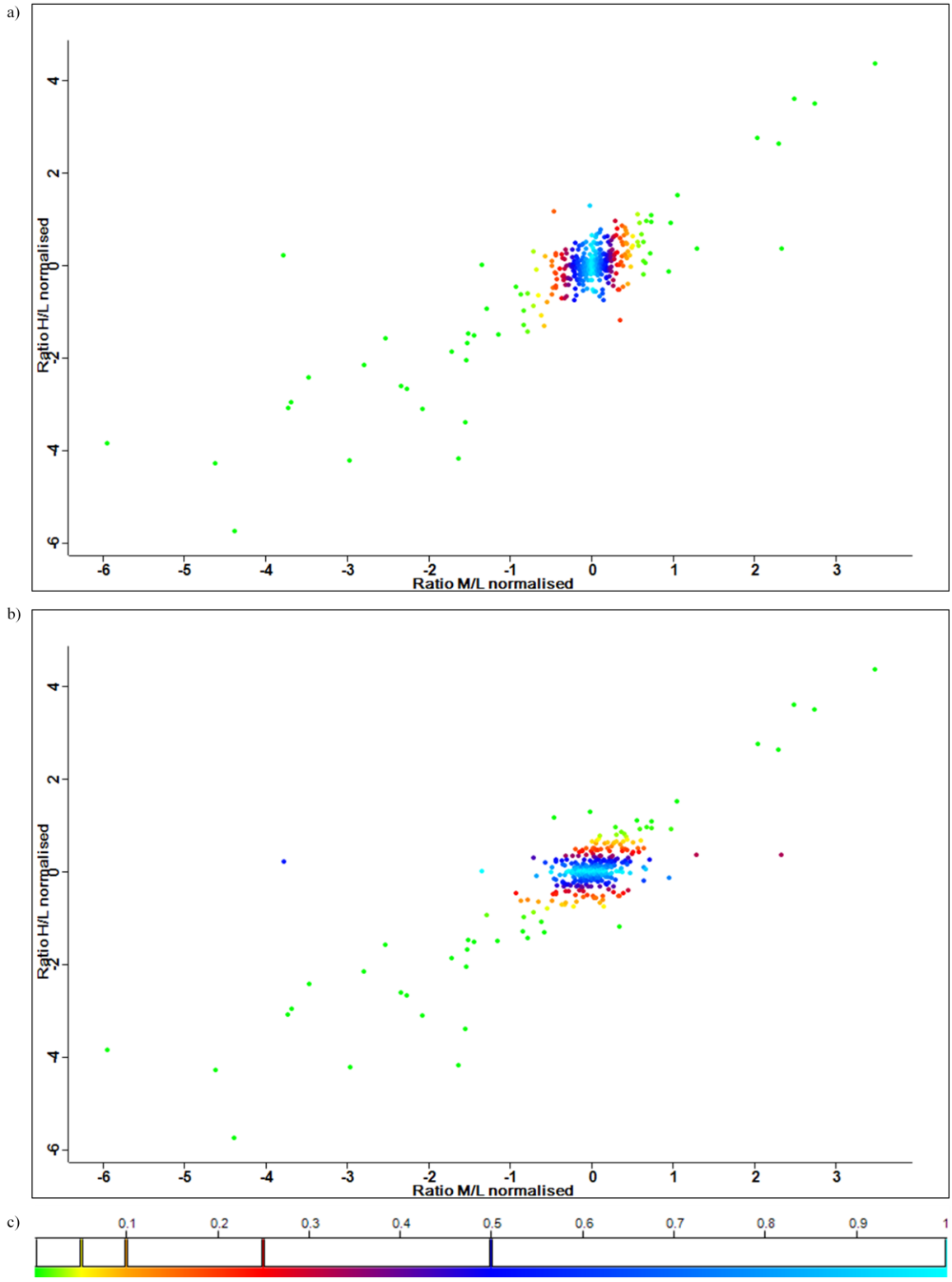

Figure 7.11. Proteins enriched or depleted in -EGF or +EGF sample

The distribution of the log-transformed ratios of -EGF to control (M/L) **(a)** and +EGF to control (H/L) **(b)**; **c)** the colour scheme of the p-values (which have been further adjusted with Benjamini Hochberg FDR) (Cox and Mann, 2012).

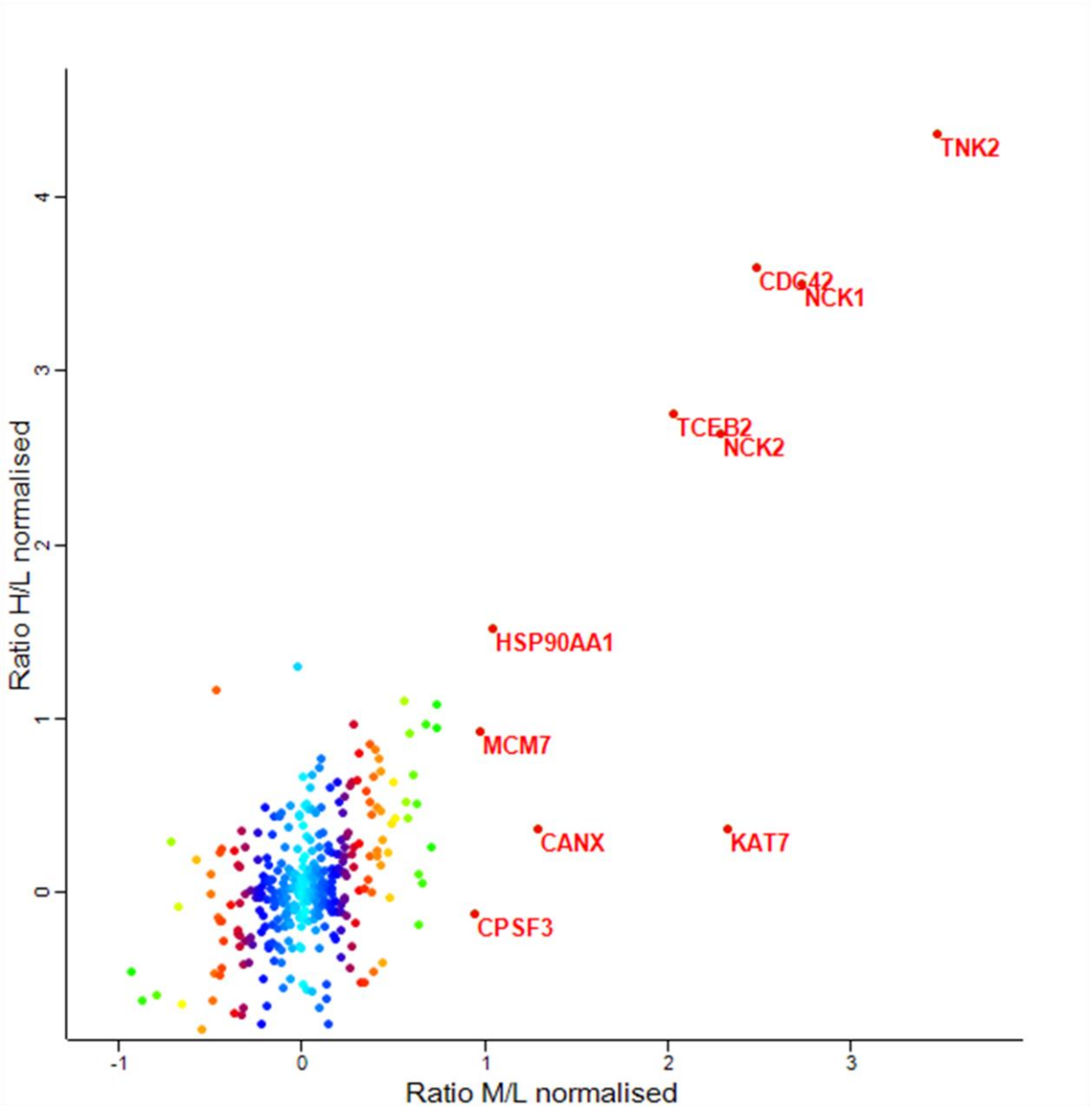

Figure 7.12. Proteins enriched in -EGF sample

The graph shows the gene names of the proteins enriched in -EGF sample as compared to the control (the M/L ratio increased).

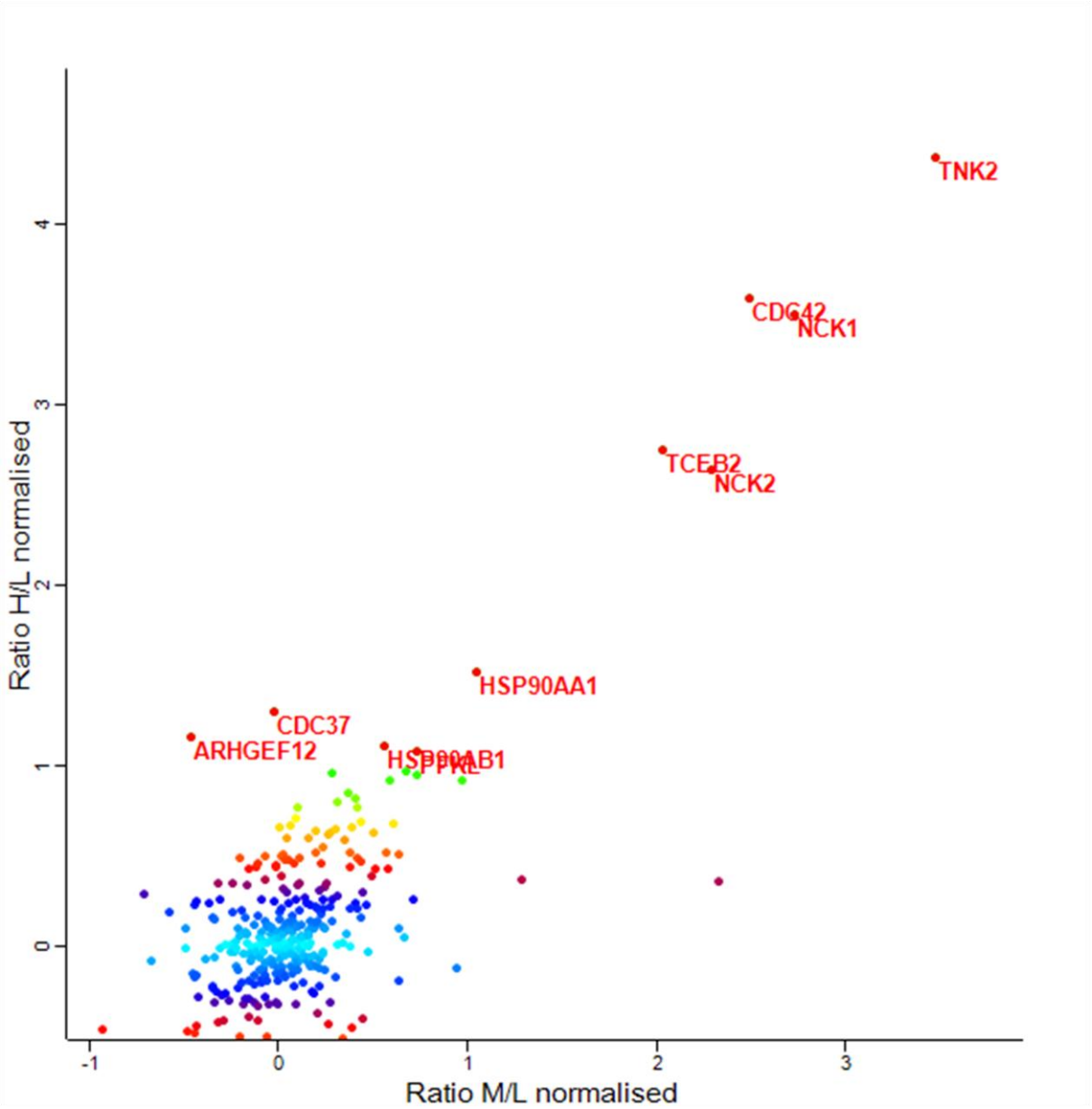

Figure 7.13. Proteins enriched in +EGF sample

The graph shows the gene names of the proteins enriched in +EGF sample as compared to the control (the H/L ratio increased).

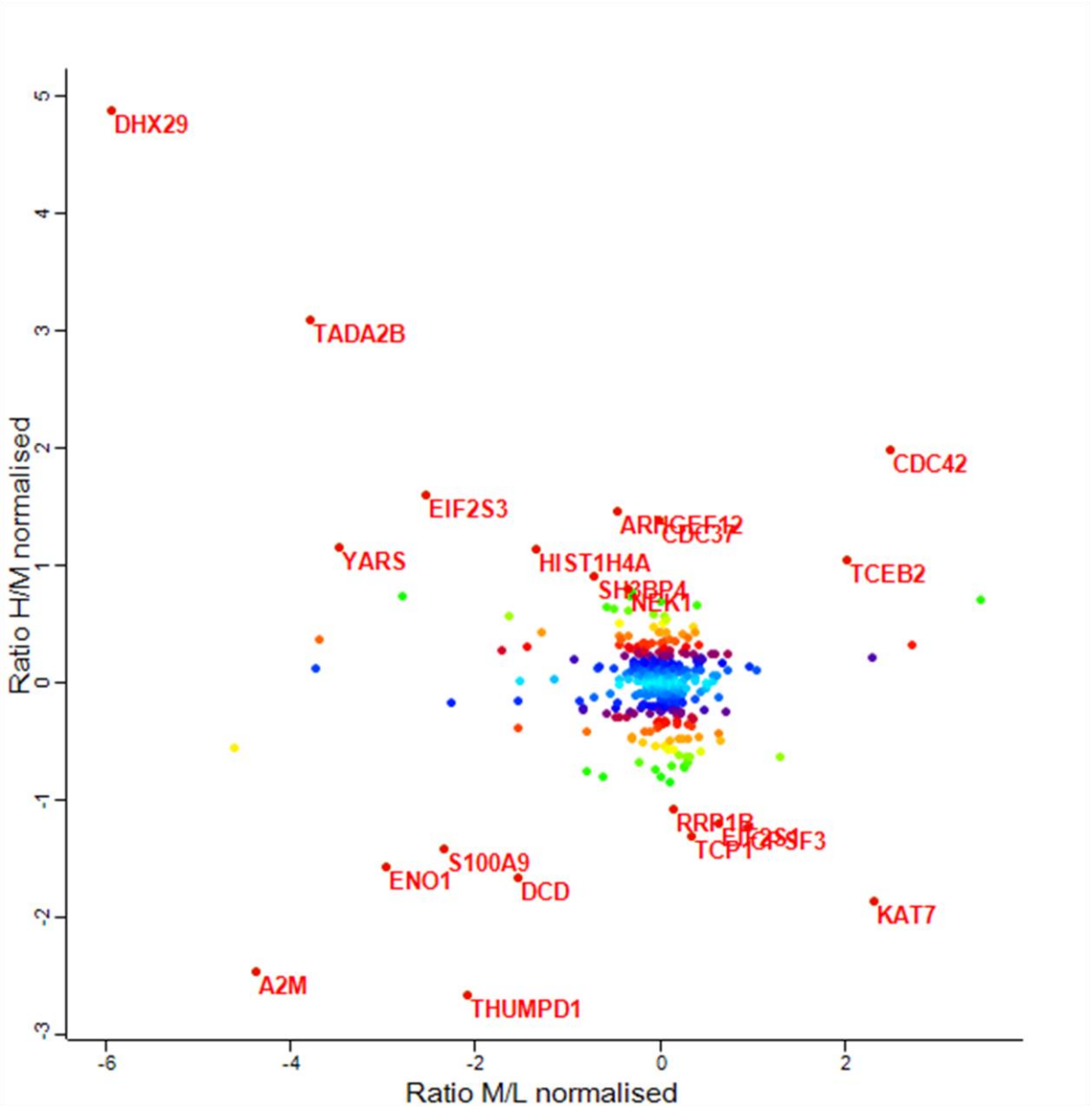

Figure 7.14. Proteins enriched in +EGF vs. –EGF sample and –EGF vs. +EGF sample

The graph shows the gene names of the proteins enriched in +EGF vs. -EGF sample and -EGF vs. +EGF sample (the H/M ratio increased or decreased, respectively).

Proteins enriched in -EGF sample	**Gene names**	**Ratio M/L**	**Significance**
Cleavage and polyadenylation specificity factor subunit 3	CPSF3	1.925	0.0003
DNA replication licensing factor MCM7	MCM7	1.962	0.0002
Heat shock protein HSP 90-alpha	HSP90AA1	2.067	0.0001
Calnexin	CANX	2.447	0.0000
Transcription elongation factor B polypeptide 2	TCEB2	4.096	0.0000
Cytoplasmic protein NCK2	NCK2	4.888	0.0000
Histone acetyltransferase KAT7	KAT7*	5.016	0.0000
Cell division control protein 42 homolog;Rho-related GTP-binding protein RhoQ	CDC42;RHOQ	5.607	0.0000
Cytoplasmic protein NCK1	NCK1	6.651	0.0000
Activated CDC42 kinase 1	TNK2	11.103	0.0000
Proteins enriched in +EGF sample	**Gene names**	**Ratio H/L**	**Significance**
6-phosphofructokinase, liver type	PFKL	2.111	0.0031
Heat shock protein HSP 90-beta;Putative heat shock protein HSP 90-beta-3	HSP90AB1;HSP 90AB3P	2.154	0.0024
Rho guanine nucleotide exchange factor 12	ARHGEF12*	2.240	0.0014
Hsp90 co-chaperone Cdc37	CDC37*	2.460	0.0004
Heat shock protein HSP 90-alpha	HSP90AA1	2.863	0.0000
Cytoplasmic protein NCK2	NCK2	6.231	0.0000
Transcription elongation factor B polypeptide 2	TCEB2*	6.728	0.0000
Cytoplasmic protein NCK1	NCK1	11.355	0.0000
Cell division control protein 42 homolog;Rho-related GTP-binding protein RhoQ	CDC42;RHOQ*	12.082	0.0000
Activated CDC42 kinase 1	TNK2	20.687	0.0000

Table 7.2. Proteins enriched in –EGF or +EGF sample

The table presents the proteins enriched in –EGF or +EGF sample as compared to the control. Gene names, the ratios (M/L or H/L) and the p-values are shown. Stars indicate proteins, whose binding to Ack1 is EGF-dependent, as assessed by significantly low or high H/M ratios; these proteins are presented in **Table 7.3**.

Proteins showing EGF sensitivity	**Gene names**	**Ratio H/M**	**Significance**
Histone acetyltransferase KAT7	KAT7	0.276	0.0000
Rho guanine nucleotide exchange factor 12	ARHGEF12	2.759	0.0000
Hsp90 co-chaperone Cdc37	CDC37	2.611	0.0000
Transcription elongation factor B polypeptide 2	TCEB2	2.060	0.0001
Cell division control protein 42 homolog;Rho-related GTP-binding protein RhoQ	CDC42;RHOQ	3.974	0.0000

Table 7.3. The proteins identified to bind Ack1 in an EGF-dependent manner

The table presents the proteins preferably binding Ack1 in untreated cells (H/M ratio < 1) or in EGF-treated cells (H/M ratio > 1). Gene names, the H/M ratio and the p-values are shown.

Several proteins are identified as binding preferentially to Ack1 following EGF stimulation compared to serum-starved conditions, since their H/M ratio is significantly increased, *i.e.* ARHGEF12, Cdc37, TCEB and Cdc42. Interestingly, KAT7 is the only protein identified to specifically interact with Ack1 in serum-starved cells rather than upon EGF stimulation, and its H/M ratio is significantly reduced. Importantly, as explained below, some proteins identified are known Ack1 interactors, *i.e.* Cdc42, Nck and HSP90-β. This indicates that the employed method is reliable and that the identified novel Ack1 interactors are likely to be accurate.

Additionally, clustering all of the proteins from **Table 7.2** using STRING database (string-db.org) allowed for identification with medium confidence a group of interactors, shown in **Figure 7.15 a**. Some of the interactions have been shown experimentally, whereas others are based on databases or textmining. Identification of this major protein network (**Figure 7.15 a**) strongly support the reliability of the results obtained, as the proteins involved in common signalling networks are likely to interact and co-precipitate with one another. Additionally, knwon and/or predicted Ack1 interactors described in STRING database are shown for comparison in **Figure 7.15 b**.

Ack1 has been shown to bind GTP-bound Cdc42 and to regulate Cdc42-dependent migration of breast cancer cells (Manser *et al.*, 1993; Modzelewska *et al.*, 2006). Similarly, the interaction between Ack1 and Nck has been suggested (Teo *et al.*, 2001; Galisteo *et al.*, 2006). Nck is an adaptor protein comprised of three SH3 domains and one SH2 domain (Lettau *et al.*, 2009). In human two members of the Nck family have been identified: Nck1 and Nck2. Nck has been found to be phosphorylated following EGF treatment, and the SH2 domain of Nck has been shown to interact with activated EGFR (Li *et al.*, 1992).

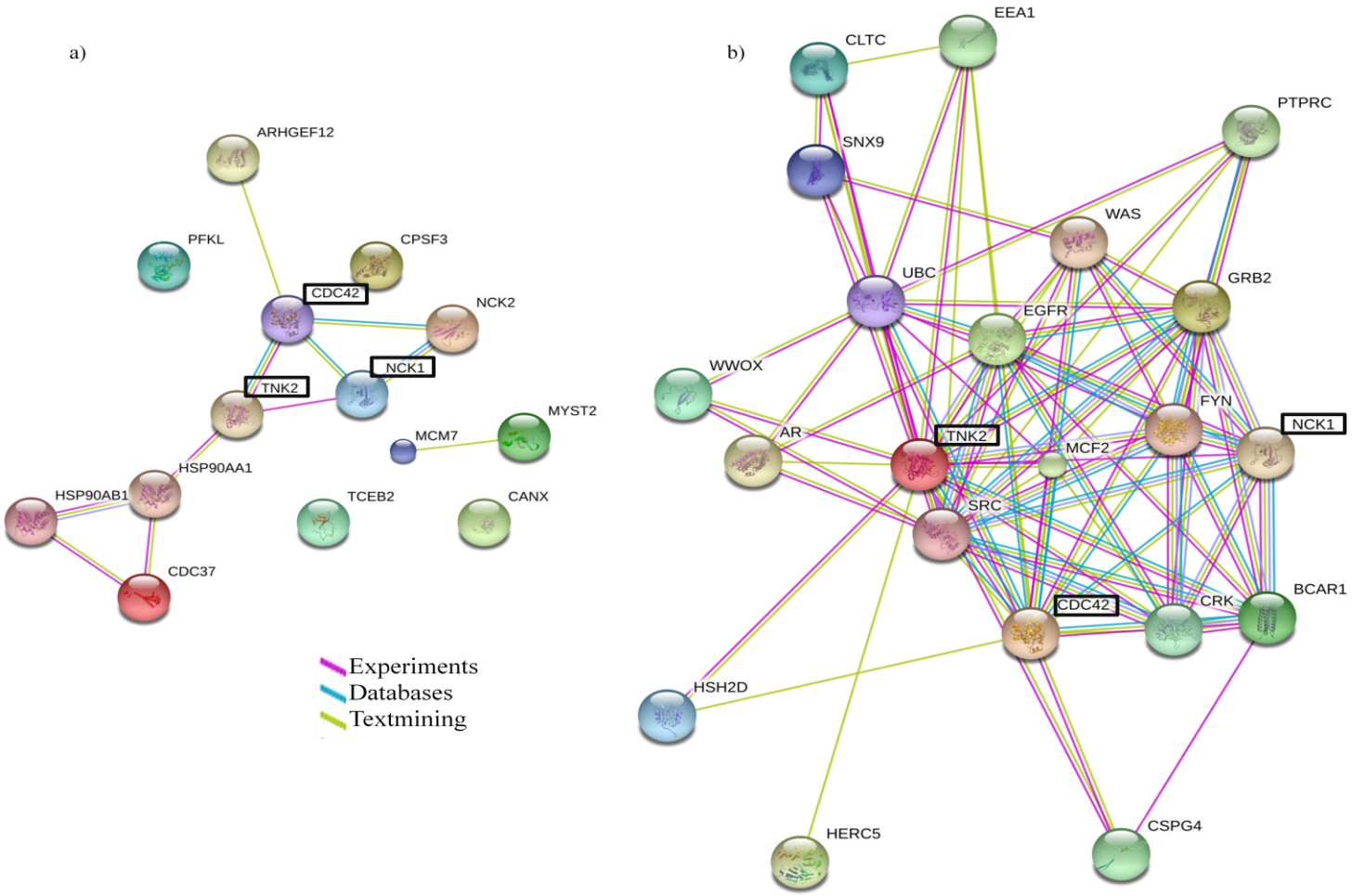

Figure 7.15. Protein clustering using STRING database

Proteins identified as Ack1 (TNK2) interactors (**Table 7.2**) **(a)** and known/predicted Ack1 (TNK2) interactors from STRING database (no more than 20 interactors) **(b)**, both identified with medium confidence. Proteins present in both **(a)** and **(b)** are shown in black rectangles.

Therefore it is unlikely that Nck mediates an interaction between Ack1 and EGFR, since the SH2 domain of Nck has been similarly shown to bind phosphorylated Ack1 (Galisteo *et al.*, 2006). Nevertheless, through interaction with adaptor proteins such as Nck and GTPases such as Cdc42, Ack1 is a proposed to coordinate multiple signalling pathways (Galisteo *et al.*, 2006).

HSP90 is a chaperone which regulates protein folding, stabilisation and degradation (Vaughan *et al.*, 2010). HSP90-β has been found to associate with Ack1, in particular with constitutively active Ack1 (caAck1) (Mahajan *et al.*, 2005). Treatment of cells with geldanamycin, an HSP90 inhibitor, reduced the kinase activity of caAck1, indicating that HSP90 is involved in maintaining Ack1 activity. Cdc37 is a HSP90 cochaperone that facilitates substrate recognition and binding (MacLean and Picard, 2003). Since Cdc37 is found enriched in +EGF sample as compared to -EGF sample, this suggests that EGF treatment enhances the interaction between Ack1 and the HSP90 co-chaperone Cdc37, and potentially with HSP90 itself. CANX, or calnexin, is a lectin chaperone that resides in endoplasmic reticulum (ER) and assists maturation and folding of newly synthesised proteins (Hebert and Molinari, 2007). An interaction between Ack1 and calnexin in serum-starved cells may indicate that Ack1 is being synthesised by ribosomes and targeted to ER, where calnexin assists in correct Ack1 folding.

ARHGEF12, or LARG (leukemia-associated RhoGEF) is a member of the Dbl family of GEFs (Zheng, 2001). They all share a conserved motif of Dbl homology (DH) domain followed immediately by a tandem pleckstrin homology (PH) domain. These domains are required for their GEF activity, and the DH domain is proposed to regulate the GDP to GTP exchange, whereas the PH domain is proposed to control intracellular targetting of the DH

domain and membrane association. ARHGEF12/LARG has been shown to specifically interact with and activate RhoA, but not Rac1 or Cdc42 (Reuther *et al.*, 2001). In contrast, as explained above, Ack1 interacts with GTP-bound Cdc42, but not Rac1 or RhoA. Therefore, co-precipitation of ARHGEF12/LARG with Ack1 is surprising. The study completed on human squamous carcinoma cells revealed that EGFR is in complex with ARHGEF12/LARG and CD44 (hyaluronan receptor), and stimulation with hyaluronan promotes the association between EGFR, ARHGEF12/LARG and CD44, and activates EGFR and downstream signalling cascades (Bourguignon *et al.*, 2006). Therefore, it is possible that EGF stimulation promotes an interaction between ARHGEF12/LARG and EGFR, as between Ack1 and EGFR, leading to an indirect association between Ack1 and ARHGEF12/LARG.

PFKL, or phosphofructokinase, is an enzyme that catalyses phosphorylation of fructose-6-phosphate to fructose-1,6-biphosphate in the process of glycolysis (Pelicano *et al.*, 2006). Addition of serum, which contains growth factors, to quiescent (non-dividing) cells induces glycolysis, and the homogenates obtained from quiescent cells treated with serum or with EGF show increased glycolytic activity compared to untreated cells (Diamond *et al.*, 1978). In addition, purified EGFR has been shown to phosphorylate PFK, with suggestion that PFK may be an EGFR substrate *in vivo* (Reiss *et al.*, 1986). An interaction between Ack1 and PFKL observed in cells treated with EGF may therefore indicate that EGFR phosphorylates PFKL and PFKL is in the complex with EGFR and Ack1.

K (lysine) acetyltransferase KAT7 (MYST2/HBO1) has been proposed to acetylate histone H4 at the origin of replication, which then facilitates loading of MCM2-7 helicase complex and DNA replication (Chadha and Blow, 2010). Co-precipitation of KAT7MYST2/HBO1 and

MCM7 with Ack1 in -EGF sample could potentially indicate Ack1 implication in DNA replication process.

TCEB2, or elongin, has been characterised as a transcription elongation factor (Aso *et al.*, 1995). Co-precipitation of TCEB2/elongin with Ack1, which is additionally enhanced upon EGF treatment, may indicate that Ack1 is implicated in RNA synthesis. CPSF3, or CPSF73 (cleavage and polyadenylation specificity factor 73-kDa subunit), which also co-precipitates with Ack1, is an endonuclease that has been proposed to assemble in a precleavage complex to cleave newly synthesised precursor messenger RNA at the 3' end, in the process of mRNA maturation (Ryan *et al.*, 2004; Mandel *et al.*, 2006). This further supports a potential function of Ack1 in RNA synthesis. Alternatively, TCEB2/elongin has been found associated with von Hippel-Lindau tumour suppressor (VHL), cullin-2 and RING-box protein 1 (RBX1) in an E3 ubiquitin ligase complex which marks proteins for proteasomal degradation (Pugh and Ratcliffe, 2003). Therefore, this potentially suggests that Ack1 associates with this complex and therefore Ack1 may play a role, either positive or negative, in ubiquitin-mediated degradation of proteins *via* proteasome.

7.5 Conclusions

The employment of the mass spectrometric techniques allowed for identification of novel PTMs within Ack1. These include three phosphorylation sites on serine residues (Ser102, Ser761 and Ser936), one ubiquitylation site (Lys539), as well as a phosphorylation of a serine residue within the SSS motif (Ser808, Ser809 and Ser810); in this case, the exact localization of the phosphorylation site is limited due to insufficient sequence coverage of this region. As described in **Chapter 1.3.2** and **Chapter 1.3.3**, protein phosphorylation and ubiquitylation play major roles in trafficking and signalling, and identification of PTMs within a protein is

likely to further the knowledge on protein functions. Using an online available resource (NetworKIN) I identify several kinases which may potentially phosphorylate the identified phosphorylated serine residues. These include cell-division protein kinases (CDKs), MAP kinases, casein kinases 2 (CK2) and PIM2 kinase. These results provide an input into the understanding of the Ack1 functions, as it may be involved in signalling pathways mediated by these kinases. Identification of the ubiquitylation site within Ack1 may provide further knowledge of the proposed functions of Ack1 in ubiquitin-mediated degradation, and mutation of the identified lysine residue may lead to characterisation Ack1 functions in this context more precisely.

In adition to characterisation of novel PTMs within Ack1, using mass spectrometry I also identify several proteins that interact with Ack1, some of which are well-known Ack1 interactors, *e.g.* Cdc42 and Nck1/Nck2, whereas others are novel, *e.g.* ARHGEF12/LARG, MCM7 or PFKL. I employed the SILAC technique to analyse the binding in the presence or absence of EGF treatment. This led to identification of proteins that bind Ack1 independently of EGF stimulation: adaptor proteins Nck1 and Nck2 and chaperone HSP90α; proteins that bind Ack1 upon serum-starvation: histone acetyltransferase KAT7/MYST2/HBO1, endonuclease CPSF3/CPSF73, helicase MCM7 and lectin chaperone CANX/calnexin; proteins that bind Ack1 following EGF treatment: RhoGEF ARHGEF12/LARG, HSP90 co-chaperone Cdc37, phosphofructokinase PFKL, and chaperone HSP90β; and proteins that bind Ack1 both in the absence and presence of EGF treatment, but their binding is enhanced following EGF stimulation: transcription elongation factor TCEB2 and a small GTPase Cdc42 (described in **Chapter 7.4**). To verify these interactions, further experiments may be employed, including biochemical studies and microscopy, to validate whether they take place at the physiological level.

8 Discussion and future plans

The scientific field of growth factors has evolved significantly since their discovery in the 1950s (Garfield, 1987). Novel growth factors and growth factor receptors are being frequently discovered, as are the mechanisms underlying growth factor functions; however, many of these still remain unresolved. Therefore, more research is still required in order to fully understand the mechanisms underlying growth factor roles within the cell.

The implication of Ack1 in growth factor signalling and trafficking has been developing for the past two decades. It is well documented that Ack1 plays a role in RTK trafficking and degradation (Galisteo *et al.*, 2006; Shen *et al.*, 2007; Grovdal *et al.*, 2008), but the precise mechanism remains elusive. In the work presented within this thesis, I have investigated the molecular mechanisms underlying Ack1 involvement in growth factor signalling and in RTK trafficking. The schematic representation of the function of Ack1 in EGFR trafficking is presented in **Figure 8.1**.

In **Chapter 4**, the implication of Ack1 in RTK trafficking is investigated. The immunoprecipitation studies reveal that activated FGFR2 does not interact with Ack1. In contrast, both activated EGFR and constitutively active Cdc42 co-precipitate with Ack1. Further studies also reveal that activated FGFR2 does not colocalize with Ack1, thus Ack1 and active FGFR2 are likely located within distinct compartments/microdomains within the same compartment. In the study presented in **Chapter 4**, the colocalization of Ack1 with EGFR upon EGF stimulation is further confirmed. In addition to studies on FGFR2, the work was carried out with another member of the FGFR family, *i.e.* FGFR1. From these studies it emerges that active FGFR1, similarly to FGFR2, does not interact with Ack1.

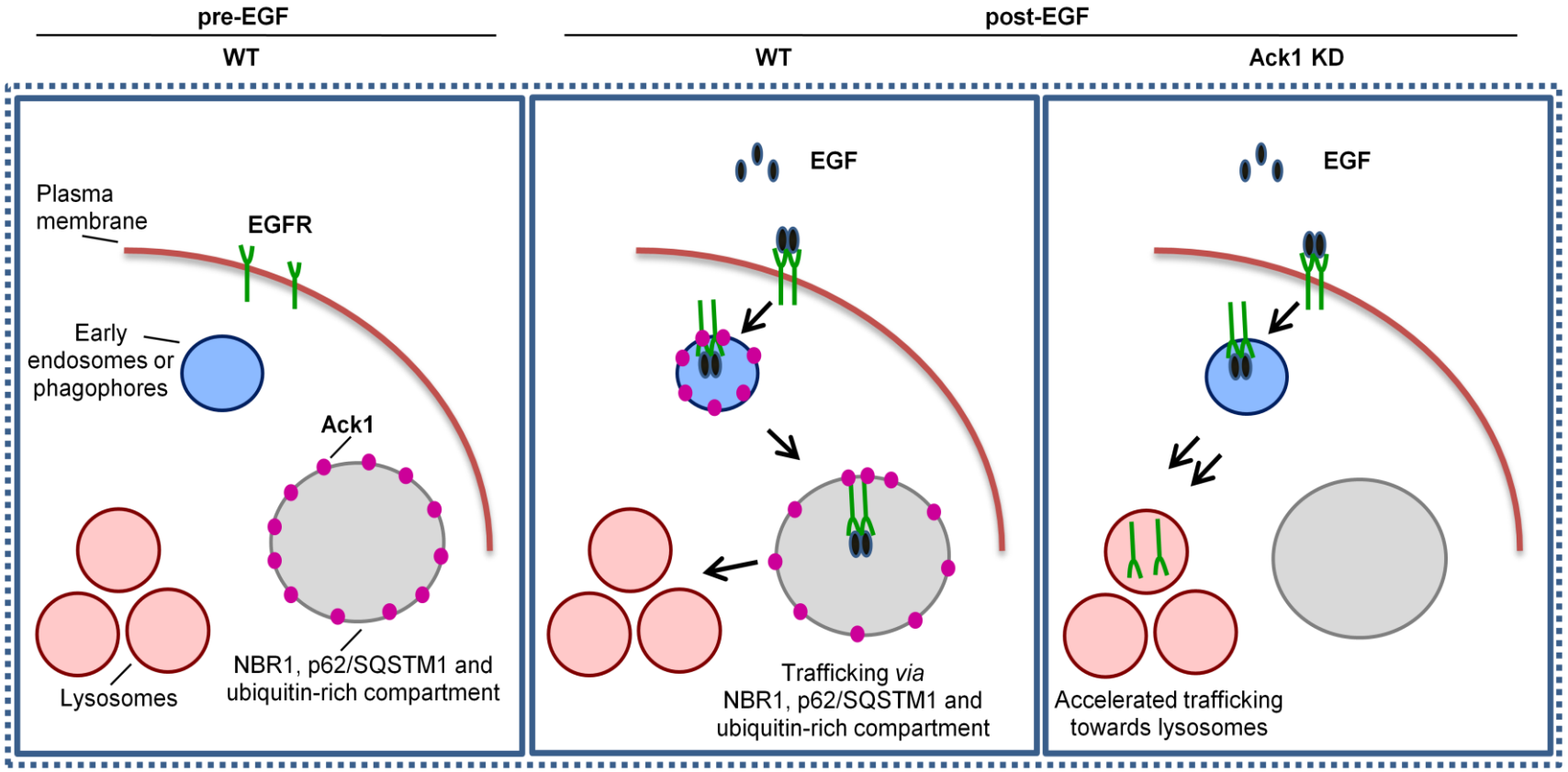

Figure 8.1. Proposed mechanism for the role of Ack1 in EGFR trafficking

Ack1 predominantly associates within p62/SQSTM1-rich compartments in serum-starved cells. Upon EGF stimulation, a portion of Ack1 translocates away from these compartments towards early-endosomes where it colocalizes with EGFR and diverts EGFR trafficking into a non-canonical degradative pathway. In Ack1 knockdown (KD) cells, EGFR is free to traffic *via* a canonical endo-lysosomal pathway.

Thus, Ack1 may have a specific function in EGF signalling pathway and not in FGF signalling. The interaction between Ack1 and EGFR is likely dependent on the motifs that are absent in FGFRs. Additionally, this work emphasizes the divergence in the endocytic pathways of EGFR and FGFR2. Since Ack1 colocalizes with active EGFR, and not FGFR2, this suggests that these RTKs traffic through different endocytic compartments. Interestingly, NBR1 has been found to inhibit degradation of EGFR and FGFR upon ligand stimulation; however, through its interaction with Sprouty related with EVH1 domain 2 (Spred2), NBR1 has also been shown to promote FGFR degradation (Mardakheh *et al.*, 2009; Mardakheh *et al.*, 2010). Additionally, Spred2 has been found in complex with NBR1 and p62/SQSTM1, the autophagic receptors. Therefore, it is possible that NBR1 interacts with Spred2 to target FGFR to p62/SQSTM1 compartments, whereas in the case of EGFR, Ack1 plays a role similar to NBR1 and Spred2.

In **Chapter 5**, Ack1 subcellular localization is explored. The previous reports show that Ack1 partially colocalizes with EGF on early endosomes following EGF stimulation (Shen *et al.*, 2007; Grovdal *et al.*, 2008); however, the localization starved cells has not been reported. Additionally, nuclear localization for Ack1 has been proposed (Ahmed *et al.*, 2004; Mahajan *et al.*, 2007). In the work presented in **Chapter 5**, Ack1 exhibits cytoplasmic localization and is not detected within the nucleus following EGF stimulation. In contrast, truncated Ack1 which lacks the C-terminal portion can be found within the nucleus and independently of EGF treatment. Therefore, this indicates that the domains located within Ack1 C-terminal portion prevent nuclear localization of Ack1. This could be the result of differences in conformation between full-length and truncated Ack1, or in the interactions with other proteins which would prevent Ack1 translocation to the nucleus.

Further colocalization studies described in **Chapter 5** confirm previously published data on Ack1 partial localization to EEA1-positive early endosomes following EGF stimulation, in particular at 15 and 30 minutes post-EGF (**Chapter 5.4**) (Shen *et al.*, 2007; Grovdal *et al.*, 2008). Interestingly, similar EGF-dependent colocalization can be seen between Ack1 and ectopically expressed Rab5 (**Chapter 5.5**). Rab5 has been shown to localize to early endosomes and other structures, including autophagosomes (Stenmark, 2009). Similar to Rab5, partial increase in colocalization between Ack1 and ectopically expressed Rab4, Rab11 and Rab7 can be found following EGF treatment. In particular, in the case of Rab4 an increase is noted at 15 minutes of EGF treatment, in the case of Rab11 at 30 minutes of EGF stimulation, whereas in the case of Rab7 at 15 and even more at 30 minutes of EGF stimulation. As explained in **Chapter 1.3.4**, Rab4 has been shown to promote fast recycling from early endosomes, whereas Rab11 controls slow recycling from the PNRC. Additionally, Rab11 has been proposed to regulate fusion of early endosomes with autophagosomes (Fader *et al.*, 2008). Therefore, it is possible that Ack1 may play a role in endocytic recycling pathways *via* its association with Rab4 and Rab11, or in fusion of endosomes with autophagosomes *via* its association with Rab11. Rab7, as explained in **Chapter 1.3.4**, has been found to localize to late endosomes and autophagosomes, and has been proposed to regulate trafficking to lysosomes and to promote fusion between autophagosomes and lysosomes (Gutierrez *et al.*, 2004; Stenmark, 2009). An increase in colocalization between Ack1 and Rab7 following EGF stimulation may suggest a potential role for Ack1 in trafficking through the late endosomal or autophagosomal compartments. However, the colocalization studies between Ack1 and the endogenous Rab11 and LBPA, a lipid enriched in late endosomal membranes (Kobayashi *et al.*, 1998; Kobayashi *et al.*, 1999; Galve-de Rochemonteix *et al.*, 2000), reveal that Ack1 does not localize to recycling or late endosomes following EGF treatment (**Chapter 5.6**). This discrepancy may be due to the differences in

the experimental design (*e.g.* endogenous *verus* ectopically expressed Rab11), or in subcellular distribution (*i.e.* Rab7 *verus* LBPA). Since ectopically expressed proteins may perturb some cellular functions, or mislocalize within the cell, the studies employing endogenous proteins or molecules can be more reliable.

In **Chapter 6** Ack1 subcellular localization is further characterized. Since Ack1 does not strikingly localize to early, late or recycling endosomes particularly in serum-starved conditions (**Chapter 5**), Ack1 localization to other compartments has been examined. Previous reports indicate that Ack1 is ubiquitylated and interacts with mono- and polyubiquitin, and that the UBA domain of Ack1 binds ubiquitylated proteins (Shen *et al.*, 2007; Chan *et al.*, 2009; Lin *et al.*, 2010). I show that Ack1 localizes to ubiquitin-rich compartments and that the UBA domain contributes to this localization, which may reflect binding of ubiquitylated proteins by Ack1, as well as Ack1 ubiquitylation (**Chapter 6.2**). Protein ubiquitylation is an important signal for degradation *via* several degradative pathways, *e.g.* selective autophagy (Kraft *et al.*, 2010). In this process, ubiquitylated cargo is concentrated within the double membrane autophagosomes. I find that Ack1 colocalizes and interacts with p62/SQSTM1, an autophagic receptor (**Chapter 6.4**). This is particularly enhanced in serum-starved conditions and decreases following EGF treatment. Thus, Ack1 partially moves away from p62/SQSTM1 upon activation with EGF. The UBA domain is critical for the colocalization with p62/SQSTM1, indicating that binding of ubiquitylated proteins by the UBA domain is required for this to occur. Since Ack1 does not dramatically colocalize with NBR1, another autophagic receptor (**Chapter 6.4**), this suggests that the interaction with p62/SQSTM1 is highly specific. Interestingly, the presence of ectopically expressed p62/SQSTM1 promotes the colocalization between Ack1 and NBR1 (**Chapter 6.5**). Since p62/SQSTM1 and NBR1 interact *via* their PB1 domains (Lamark *et al.*, 2003;

Lamark *et al.*, 2009), it is likely that ectopically expressed p62/SQSTM1 interacts with NBR1 and thus indirectly enhances the colocalization between Ack1 and NBR1.

In **Chapter 6** I also identify an interaction between Ack1 and Atg16, which is an important regulator of autophagosome biogenesis (Mizushima *et al.*, 1999; Mizushima *et al.*, 2003). This interaction is enhanced following EGF treatment (**Chapter 6.8**). Growth factor stimulation has been shown to inhibit autophagy *via* mTOR activation, *i.e.* activation of mTOR downstream of RTKs has been proposed to phosphorylate Atg13 and thus disrupt its interaction with Atg1 during autophagosome formation (Kamada *et al.*, 2000; Stephan *et al.*, 2009; Jung *et al.*, 2010). Nevertheless, studies exist showing that clathrin-mediated endocytosis may provide membranes for autophagosome formation and inhibition of CME reduces autophagy (Ravikumar *et al.*, 2010). Additionally, Atg16 has been shown to interact with clathrin and inhibition of CME resulted in decreased formation of Atg16-positive structures. Thus, since EGF stimulation promotes CME (Sigismund *et al.*, 2005; Sigismund *et al.*, 2008) it may also promote autophagosome formation. In addition, Ack1 partially colocalizes with LC3, a protein required at later stages of autophagosome formation and maturation (**Chapter 6.9**) (Ichimura *et al.*, 2000; Mizushima *et al.*, 2011). This, however, does not seem to be dependent on EGF treatment. Taken together, the results presented in **Chapter 6** identify a novel implication of Ack1 in the autophagic pathway marked by its association with p62/SQSTM1, Atg16 and LC3.

Chapter 7 describes the identification of novel phosphorylation and ubiquitylation sites within Ack1. The mass spectrometry technique used in the study allowed for identification of three novel phospho-serine residues and the SSS motif with one phosphorylated serine residue (**Chapter 7.2**). Through an online resource (NetworKIN) I identify potential kinases that

phosphorylate these three novel sites. In particular, Ser102 is suggested to be a target of CDK2, CDK3 or MAPK11-14, Ser761 to be phosphorylated by CSNK2A2 or CK2A1 and Ser936 by PIM2. These data may be further verified and potentially identify signalling cascades that comprise Ack1 and these kinases. Additionally, a potential novel ubiquitylation site within Ack1 has been identified (**Chapter 7.3**). This site may be mutated and the phenotype of the mutant may help in understanding the functions of Ack1 ubiquitylation in cell signalling and trafficking.

I also combine SILAC technique with mass spectrometry to identify the proteins that interact with Ack1 in serum-starved cells and upon EGF stimulation (**Chapter 7.4**). This approached led to the characterization of known Ack1 interactors, such as Cdc42 and Nck1, as well as several novel binding partners. The identified interactors include the proteins that bind Ack1 independently on EGF stimulation (*e.g.* Nck1, Nck2, HSP90α), proteins that preferentially interact with Ack1 upon serum-starvation (e.g. KAT7MYST2/HBO1, MCM7) and others whose binding is enhanced following EGF treatment (e.g. Cdc37, ARHGEF12/LARG). Interestingly, two of these proteins are implicated in DNA replication (MCM7 and KAT7) which potentially indicates that Ack1 may be involved in this process. Another two interactors (CPSF3 and TCEB2) are required for transcription, which may also suggests that Ack1 is implicated in some stages of the RNA synthesis and/or maturation process. Although the work presented in this thesis fails to identify nuclear localization of full-length Ack1 in HeLa cells (**Chapter 5.2**), other studies suggest Ack1 nuclear translocation and function in AR-mediated gene expression (Ahmed *et al.*, 2004; Mahajan *et al.*, 2007). Therefore, characterisation of Ack1 interaction with nuclear proteins is not surprising and further supports Ack1 functions in this context.

Finally, future plans would include investigations of the precise Ack1 functions in selective autophagy and how this affects EGFR signalling and trafficking. In particular, an understanding of the association between Ack1, p62/SQSTM1, Atg16L and LC3 would be of a highest priority. Does the UBA domain of Ack1 bind p62/SQSTM1 directly? Is Ack1 ubiquitylation required for this interaction? Would the p62/SQSTM1 mutant that lacks the UBA domain still interact with Ack1? All these questions could be addressed using available approaches. For assessing the potential direct interaction between Ack1 and p62/SQSTM1, the yeast two-hybrid technique could be used. In this technique, the direct binding of the two proteins results in the activation of the transcription of the reporter gene (Bruckner *et al.*, 2009). Similar techniques could be used for assessing the interactions between Ack1 and Atg16, and possibly Ack1 and LC3. Additionally, since Ack1 colocalizes with both Atg16 (**Chapter 6.8**) and EEA1 (**Chapter 5.4**), it is interesting to analyse whether a colocalization may be detected between Atg16 and EEA1. It has been shown previously that Atg16 does not colocalize with EEA1 (Ravikumar *et al.*, 2010), and therefore it is expected that following EGF treatment, a portion of Ack1 colocalizes with EEA1, and another portion colocalizes with Atg16. Another interesting question is whether the Ack1 puncta that colocalize with LC3 (**Chapter 6.9**) also colocalize with EEA1. Early endosomes have been shown to be required for autophagosome maturation (Razi *et al.*, 2009) and therefore it is expected that a portion of the EEA1-positive Ack1 puncta would also colocalize with LC3. In addition, more precise characterization of the Ack1 functions in EGFR trafficking is required. Since approximately 20 % of the EGFR puncta colocalize with Ack1 and p62/SQSTM1 following EGF treatment (**Chapter 6.7**), it is tempting to speculate that approximately one in five EGFR molecules is targeted by Ack1 into autophagosomes. Therefore, triple colocalization studies could also be applied in this instance, tracing the colocalization between Ack1, EGFR and LC3 following EGF treatment. Another interesting issue is how EGF stimulation affects interaction between

p62/SQSTM1 and LC3. All of these studies could be performed in order to understand the mechanisms underlying precise Ack1 involvement in the non-canonical trafficking of EGFR. Another set of future experiments would be aimed at investigation of the potential novel interactions between Ack1 and the proteins identified through SILAC and mass spectrometry techniques. These interactions would be confirmed at the endogenous level, *i.e.* through immunoprecipitation and microscopy. Confirmation of these associations would open a new area of research on an implication of Ack1 in the identified processes and pathways.

References

Adams, J. A. and Taylor, S. S. (1992). Energetic limits of phosphotransfer in the catalytic subunit of cAMP-dependent protein-kinase as measured by viscosity experiments. *Biochemistry* **31**, 8516-8522.

Adler, J. and Parmryd, I. (2010). Quantifying colocalization by correlation: The Pearson correlation coefficient is superior to the Mander's overlap coefficient. *Cytometry Part A* **77A**, 733-742.

Aguilar, R. C. and Wendland, B. (2005). Endocytosis of membrane receptors: Two pathways are better than one. *Proceedings of the National Academy of Sciences of the United States of America* **102**, 2679-2680.

Ahmed, I., Calle, Y., Sayed, M. A., Kamal, J. M., Rengaswamy, P., Manser, E., Meiners, S. and Nur-E-Kamal, A. (2004). Cdc42-dependent nuclear translocation of non-receptor tyrosine kinase, ACK. *Biochemical and Biophysical Research Communications* **314**, 571-579.

An, Y., Shao, Y., Alory, C., Matteson, J., Sakisaka, T., Chen, W., Gibbs, R. A., Wilson, I. A. and Balch, W. E. (2003). Geranylgeranyl switching regulates GDI-Rab GTPase recycling. *Structure* **11**, 347-357.

Andl, C. D., Mizushima, T., Oyama, K., Bowser, M., Nakagawa, H. and Rustgi, A. K. (2004). EGFR-induced cell migration is mediated predominantly by the JAK-STAT pathway in primary esophageal keratinocytes. *American Journal of Physiology-Gastrointestinal and Liver Physiology* **287**, G1227-G1237.

Arora, S., Gonzales, I. M., Hagelstrom, R. T., Beaudry, C., Choudhary, A., Sima, C., Tibes, R., Mousses, S. and Azorsa, D. O. (2010). RNAi phenotype profiling of kinases identifies potential therapeutic targets in Ewing's sarcoma. *Molecular Cancer* **9**, 218-229.

Aso, T., Lane, W. S., Conaway, J. W. and Conaway, R. C. (1995). Elongin (SIII) - a multisubunit regulator of elongation by RNA-polymerase-II. *Science* **269**, 1439-1443.

Auciello, G., Cunningham, D. L., Tatar, T., Heath, J. K. and Rappoport, J. Z. (2013). Regulation of fibroblast growth factor receptor signalling and trafficking by Src and Eps8. *Journal of Cell Science* **126**, 613-624.

Avraham, R. and Yarden, Y. (2011). Feedback regulation of EGFR signalling: decision making by early and delayed loops. *Nature Reviews Molecular Cell Biology* **12**, 104-117.

Bai, D., Ueno, L. and Vogt, P. K. (2009). Akt-mediated regulation of NF kappa B and the essentialness of NF kappa B for the oncogenicity of PI3K and Akt. *International Journal of Cancer* **125**, 2863-2870.

Bao, J., Alroy, I., Waterman, H., Schejter, E. D., Brodie, C., Gruenberg, J. and Yarden, Y. (2000). Threonine phosphorylation diverts internalized epidermal growth factor receptors from a degradative pathway to the recycling endosome. *Journal of Biological Chemistry* **275**, 26178-26186.

Barford, D., Das, A. K. and Egloff, M. P. (1998). The structure and mechanism of protein phosphatases: Insights into catalysis and regulation. *Annual Review of Biophysics and Biomolecular Structure* **27**, 133-164.

Beguinot, L., Lyall, R. M., Willingham, M. C. and Pastan, I. (1984). Down-regulation of epidermal growth-factor receptor in KB cells is due to receptor internalization and subsequent degradation in lysosomes. *Proceedings of the National Academy of Sciences of the United States of America-Biological Sciences* **81**, 2384-2388.

Biscardi, J. S., Maa, M. C., Tice, D. A., Cox, M. E., Leu, T. H. and Parsons, S. J. (1999). c-Src-mediated phosphorylation of the epidermal growth factor receptor on Tyr(845) and Tyr(1101) is associated with modulation of receptor function. *Journal of Biological Chemistry* **274**, 8335-8343.

Bjorkoy, G., Lamark, T., Brech, A., Outzen, H., Perander, M., Overvatn, A., Stenmark, H. and Johansen, T. (2005). p62/SQSTM1 forms protein aggregates degraded by autophagy and has a protective effect on huntingtin-induced cell death. *Journal of Cell Biology* **171**, 603-614.

Blume-Jensen, P. and Hunter, T. (2001). Oncogenic kinase signalling. *Nature* **411**, 355-365.

Boname, J. M., Thomas, M., Stagg, H. R., Xu, P., Peng, J. M. and Lehner, P. J. (2010). Efficient internalization of MHC I requires lysine-11 and lysine-63 mixed linkage polyubiquitin chains. *Traffic* **11**, 210-220.

Bourguignon, L. Y. W., Gilad, E., Brightman, A., Diedrich, F. and Singleton, P. (2006). Hyaluronan-CD44 interaction with leukemia-associated RhoGEF and epidermal growth factor receptor promotes Rho/Ras co-activation, phospholipase C epsilon-Ca2+ signaling, and cytoskeleton modification in head and neck squamous cell carcinoma cells. *Journal of Biological Chemistry* **281**, 14026-14040.

Bruckner, A., Polge, C., Lentze, N., Auerbach, D. and Schlattner, U. (2009). Yeast two-hybrid, a powerful tool for systems biology. *International Journal of Molecular Sciences* **10**, 2763-2788.

Bucci, C., Parton, R. G., Mather, I. H., Stunnenberg, H., Simons, K., Hoflack, B. and Zerial, M. (1992). The small GTPase Rab5 functions as a regulatory factor in the early endocytic pathway. *Cell* **70**, 715-728.

Burgar, H. R., Burns, H. D., Elsden, J. L., Lalioti, M. D. and Heath, J. K. (2002). Association of the signaling adaptor FRS2 with fibroblast growth factor receptor 1 (Fgfr1) is mediated by alternative splicing of the juxtamembrane domain. *Journal of Biological Chemistry* **277**, 4018-4023.

Burgess, A. W. (2008). EGFR family: Structure physiology signalling and therapeutic targets. *Growth Factors* **26**, 263-274.

Calamandrei, G. and Alleva, E. (1989). Epidermal growth-factor has both growth-promoting and growth-inhibiting effects on physical and neuro-behavioral development of neonatal mice. *Brain Research* **477**, 1-6.

Campbell, I. G., Nicolai, H. M., Foulkes, W. D., Senger, G., Stamp, G. W., Allan, G., Boyer, C., Jones, K., Bast, R. C., Solomon, E., et al. (1994). A novel gene encoding a B-box protein within the BRCA1 region at 17q21.1. *Human Molecular Genetics* **3**, 589-594.

Cantalupo, G., Alifano, P., Roberti, V., Bruni, C. B. and Bucci, C. (2001). Rab-interacting lysosomal protein (RILP): the Rab7 effector required for transport to lysosomes. *Embo Journal* **20**, 683-693.

Cantor, S. B., Urano, T. and Feig, L. A. (1995). Identification and characterization of Ral-binding protein-1, a potential downstream target of Ral GTPases. *Molecular and Cellular Biology* **15**, 4578-4584.

Carpenter, G. and Cohen, S. (1976). I125 labeled human epidermal growth-factor - binding, internalization, and degradation in human fibroblasts. *Journal of Cell Biology* **71**, 159-171.

Carpenter, G. and Cohen, S. (1979). Epidermal growth-factor. *Annual Review of Biochemistry* **48**, 193-216.

Carpenter, G., Lembach, K. J., Morrison, M. M. and Cohen, S. (1975). Characterization of binding of I-125-labeled epidermal growth-factor to human fibroblasts. *Journal of Biological Chemistry* **250**, 4297-4304.

Carroll, K. S., Hanna, J., Simon, I., Krise, J., Barbero, P. and Pfeffer, S. R. (2001). Role of Rab9 GTPase in facilitating receptor recruitment by TIP47. *Science* **292**, 1373-1376.

Cartwright, C. A., Eckhart, W., Simon, S. and Kaplan, P. L. (1987). Cell-transformation by pp60C-Src mutated in the carboxy-terminal regulatory domain. *Cell* **49**, 83-91.

Casanova, M. L., Larcher, F., Casanova, B., Murillas, R., Fernandez-Acenero, M. J., Villanueva, C., Martinez-Palacio, J., Ullrich, A., Conti, C. J. and Jorcano, J. L. (2002). A critical role for ras-mediated, epidermal growth factor receptor-dependent angiogenesis in mouse skin carcinogenesis. *Cancer Research* **62**, 3402-3407.

Chadha, G. S. and Blow, J. J. (2010). Histone acetylation by HBO1 tightens replication licensing. *Molecular Cell* **37**, 5-6.

Chalhoub, N. and Baker, S. J. (2009). PTEN and the PI3-kinase pathway in cancer. *Annual Review of Pathology-Mechanisms of Disease* **4**, 127-150.

Chamberlain, M. D., Berry, T. R., Pastor, M. C. and Anderson, D. H. (2004). The p85 alpha subunit of phosphatidylinositol 3 '-kinase binds to and stimulates the GTPase activity of rab proteins. *Journal of Biological Chemistry* **279**, 48607-48614.

Chan, R., Hardy, W. R., Laing, M. A., Hardy, S. E. and Muller, W. J. (2002). The catalytic activity of the ErbB-2 receptor tyrosine kinase is essential for embryonic development. *Molecular and Cellular Biology* **22**, 1073-1078.

Chan, W., Tian, R., Lee, Y. F., Sit, S. T., Lim, L. and Manser, E. (2009). Down-regulation of active Ack1 is mediated by association with the E3 ubiquitin ligase Nedd4-2. *Journal of Biological Chemistry* **284**, 8185-8194.

Chau, V., Tobias, J. W., Bachmair, A., Marriott, D., Ecker, D. J., Gonda, D. K. and Varshavsky, A. (1989). A multiubiquitin chain is confined to specific lysine in a targeted short-lived protein. *Science* **243**, 1576-1583.

Chavrier, P., Parton, R. G., Hauri, H. P., Simons, K. and Zerial, M. (1990). Localization of low-molecular-weight GTP binding-proteins to exocytic and endocytic compartments. *Cell* **62**, 317-329.

Chazotte, B. (2011). Labeling lysosomes in live cells with LysoTracker. *Cold Spring Harbor protocols* **2011**,

Chen, P., MurphyUllrich, J. E. and Wells, A. (1996). Role for gelsolin in actuating epidermal growth factor receptor-mediated cell motility. *Journal of Cell Biology* **134**, 689-698.

Chen, P., Xie, H., Sekar, M. C., Gupta, K. and Wells, A. (1994). Epidermal growth-factor receptor-mediated cell motylity - phospholipase-C activity is required, but mitogen-activated protein-kinase activity is not sufficient for induced cell-movement. *Journal of Cell Biology* **127**, 847-857.

Chen, Z. J. J. and Sun, L. J. J. (2009). Nonproteolytic functions of ubiquitin in cell signaling. *Molecular Cell* **33**, 275-286.

Cho, H. S. and Leahy, D. J. (2002). Structure of the extracellular region of HER3 reveals an interdomain tether. *Science* **297**, 1330-1333.

Cho, H. S., Mason, K., Ramyar, K. X., Stanley, A. M., Gabelli, S. B., Denney, D. W. and Leahy, D. J. (2003). Structure of the extracellular region of HER2 alone and in complex with the Herceptin Fab. *Nature* **421**, 756-760.

Christoforidis, S., McBride, H. M., Burgoyne, R. D. and Zerial, M. (1999). The Rab5 effector EEA1 is a core component of endosome docking. *Nature* **397**, 621-625.

Chua, B. T., Lim, S. J., Tham, S. C., Poh, W. J. and Ullrich, A. (2010). Somatic mutation in the ACK1 ubiquitin association domain enhances oncogenic signaling through EGFR regulation in renal cancer derived cells. *Molecular Oncology* **4**, 323-334.

Clague, M. J. (1998). Molecular aspects of the endocytic pathway. *Biochemical Journal* **336**, 271-282.

Clague, M. J., Liu, H. and Urbe, S. (2012). Governance of endocytic trafficking and signaling by reversible ubiquitylation. *Developmental Cell* **23**, 457-467.

Cohen, P. (2002). The origins of protein phosphorylation. *Nature Cell Biology* **4**, E127-E130.

Cohen, S. (1962). Isolation of a mouse submaxillary gland protein accelerating incisor eruption and eyelid opening in new-born animal. *Journal of Biological Chemistry* **237**, 1555-1562.

Cohen, S., Carpenter, G. and King, L. (1980). Epidermal growth factor-receptor-protein kinase interactions - co-purification of receptor and epidermal growth factor-enhanced phosphorylation activity. *Journal of Biological Chemistry* **255**, 4834-4842.

Cohen, S. and Fava, R. A. (1985). Internalization of functional epidermal growth-factor - receptor kinase complexes in A-431 cells. *Journal of Biological Chemistry* **260**, 2351-2358.

Cohen, S., Ushiro, H., Stoscheck, C. and Chinkers, M. (1982). A native 170,000 epidermal growth-factor receptor-kinase complex from shed plasma-membrane vesicles. *Journal of Biological Chemistry* **257**, 1523-1531.

Confalonieri, S., Salcini, A. E., Puri, C., Tacchetti, C. and Di Fiore, P. P. (2000). Tyrosine phosphorylation of Eps15 is required for ligand-regulated, but not constitutive, endocytosis. *Journal of Cell Biology* **150**, 905-911.

Courtney, K. D., Corcoran, R. B. and Engelman, J. A. (2010). The PI3K pathway as drug target in human cancer. *Journal of Clinical Oncology* **28**, 1075-1083.

Cox, J. and Mann, M. (2008). MaxQuant enables high peptide identification rates, individualized p.p.b.-range mass accuracies and proteome-wide protein quantification. *Nature Biotechnology* **26**, 1367-1372.

Cox, J. and Mann, M. (2012). 1D and 2D annotation enrichment: a statistical method integrating quantitative proteomics with complementary high-throughput data. *Bmc Bioinformatics* **13**, S12-S23.

Cuif, M. H., Possmayer, F., Zander, H., Bordes, N., Jollivet, F., Couedel-Courteille, A., Janoueix-Lerosey, I., Langsley, G., Bornens, M. and Goud, B. (1999). Characterization of GAPCenA, a GTPase activating protein for Rab6, part of which associates with the centrosome. *Embo Journal* **18**, 1772-1782.

Cunningham, D. L., Sweet, S. M. M., Cooper, H. J. and Heath, J. K. (2010). Differential pPhosphoproteomics of fibroblast growth factor signaling: Identification of Src family kinase-mediated phosphorylation events. *Journal of Proteome Research* **9**, 2317-2328.

Damke, H., Baba, T., Warnock, D. E. and Schmid, S. L. (1994). Induction of mutant dynamin specifically blocks endocytic coated vesicle formation. *Journal of Cell Biology* **127**, 915-934.

Datta, S. R., Dudek, H., Tao, X., Masters, S., Fu, H. A., Gotoh, Y. and Greenberg, M. E. (1997). Akt phosphorylation of BAD couples survival signals to the cell-intrinsic death machinery. *Cell* **91**, 231-241.

Dawson, J. P., Berger, M. B., Lin, C. C., Schlessinger, J., Lemmon, M. A. and Ferguson, K. M. (2005). Epidermal growth factor receptor dimerization and activation require ligand-induced conformational changes in the dimer interface. *Molecular and Cellular Biology* **25**, 7734-7742.

Dawson, J. P., Bu, Z. M. and Lemmon, M. A. (2007). Ligand-induced structural transitions in ErbB receptor extracellular domains. *Structure* **15**, 942-954.

Deribe, Y. L., Pawson, T. and Dikic, I. (2010). Post-translational modifications in signal integration. *Nature Structural & Molecular Biology* **17**, 666-672.

Deshaies, R. J. and Joazeiro, C. A. P. (2009). RING domain E3 ubiquitin ligases. *Annual Review of Biochemistry* **78**, 399-434.

Diamond, I., Legg, A., Schneider, J. A. and Rozengurt, E. (1978). Glycolysis in quiescent cultures of 3T3 cells - stimulation by serum, epidermal growth-factor, and insulin in intact-cells and persistence of stimulation after cell homogenization. *Journal of Biological Chemistry* **253**, 866-871.

Dimitrov, S. D., Matouskova, E. and Forejt, J. (2001). Expression of BRCA1, NBR1 and NBR2 genes in human breast cancer cells. *Folia Biologica* **47**, 120-127.

Duan, L., Miura, Y., Dimri, M., Majumder, B., Dodge, I. L., Reddi, A. L., Ghosh, A., Fernandes, N., Zhou, P. C., Mullane-Robinson, K., et al. (2003). Cbl-mediated ubiquitinylation is required for lysosomal sorting of epidermal growth factor receptor but is dispensable for endocytosis. *Journal of Biological Chemistry* **278**, 28950-28960.

Duran, A., Serrano, M., Leitges, M., Flores, J. M., Picard, S., Brown, J. P., Moscat, J. and Diaz-Meco, M. T. (2004). The atypical PKC-interacting protein p62 is an important mediator of RANK-activated osteoclastogenesis. *Developmental Cell* **6**, 303-309.

Eden, E. R., Huang, F. T., Sorkin, A. and Futter, C. E. (2012). The role of EGF receptor ubiquitination in regulating its intracellular traffic. *Traffic* **13**, 329-337.

El-Aneed, A., Cohen, A. and Banoub, J. (2009). Mass spectrometry, review of the basics: Electrospray, MALDI, and commonly used mass analyzers. *Applied Spectroscopy Reviews* **44**, 210-230.

Endicott, J. A., Noble, M. E. M. and Johnson, L. N. (2012). The structural basis for control of eukaryotic protein kinases. *Annual Review of Biochemistry* **81**, 587-613.

Fader, C. M., Sanchez, D., Furlan, M. and Colombo, M. I. (2008). Induction of autophagy promotes fusion of multivesicular bodies with autophagic vacuoles in K562 cells. *Traffic* **9**, 230-250.

Ferby, I., Reschke, M., Kudlacek, O., Knyazev, P., Pante, G., Amann, K., Sommergruber, W., Kraut, N., Ullrich, A., Fassler, R., et al. (2006). Mig6 is a negative regulator of EGF receptor-mediated skin morphogenesis and tumor formation. *Nature Medicine* **12**, 568-573.

Ferguson, K. M. (2008). Structure-based view of epidermal growth factor receptor regulation. *Annual Review of Biophysics* **37**, 353-373.

Ferguson, K. M., Berger, M. B., Mendrola, J. M., Cho, H. S., Leahy, D. J. and Lemmon, M. A. (2003). EGF activates its receptor by removing interactions that autoinhibit ectodomain dimerization. *Molecular Cell* **11**, 507-517.

Finley, D., Sadis, S., Monia, B. P., Boucher, P., Ecker, D. J., Crooke, S. T. and Chau, V. (1994). Inhibition of proteolysis and cell-cycle progression in a multiubiquitination-deficient yeast mutant. *Molecular and Cellular Biology* **14**, 5501-5509.

Flynn, D. C. (2001). Adaptor proteins. *Oncogene* **20**, 6270-6272.

Francavilla, C., Cattaneo, P., Berezin, V., Bock, E., Ami, D., de Marco, A., Christofori, G. and Cavallaro, U. (2009). The binding of NCAM to FGFR1 induces a specific cellular response mediated by receptor trafficking. *Journal of Cell Biology* **187**, 1101-1116.

Friend, D. S. and Farquhar, M. G. (1967). Functions of coated vesicles during protein absorption in rat vas deferens. *Journal of Cell Biology* **35**, 357-376.

Fujita, N., Sato, S., Katayama, K. and Tsuruo, T. (2002). Akt-dependent phosphorylation of p27(Kip1) promotes binding to 14-3-3 and cytoplasmic localization. *Journal of Biological Chemistry* **277**, 28706-28713.

Fukui, K., Sasaki, T., Imazumi, K., Matsuura, Y., Nakanishi, H. and Takai, Y. (1997). Isolation and characterization of a GTPase activating protein specific for the Rab3 subfamily of small G proteins. *Journal of Biological Chemistry* **272**, 4655-4658.

Galisteo, M. L., Yang, Y., Urena, J. and Schlessinger, J. (2006). Activation of the nonreceptor protein tyrosine kinase Ack by multiple extracellular stimuli. *Proceedings of the National Academy of Sciences of the United States of America* **103**, 9796-9801.

Galve-de Rochemonteix, B., Kobayashi, T., Rosnoblet, C., Lindsay, M., Parton, R. G., Reber, G., de Maistre, E., Wahl, D., Kruithof, E. K. O., Gruenberg, J., et al. (2000). Interaction of anti-phospholipid antibodies with late endosomes of human endothelial cells. *Arteriosclerosis Thrombosis and Vascular Biology* **20**, 563-574.

Garfield, E. (1987). Stanley Cohen's and Rita Levi-Montalcini's discoveries of growth-factors lead to 1986 Nobel in Medicine. *Current Contents* 3-9.

Garrett, T. P. J., McKern, N. M., Lou, M. Z., Elleman, T. C., Adams, T. E., Lovrecz, G. O., Kofler, M., Jorissen, R. N., Nice, E. C., Burgess, A. W., et al. (2003). The crystal structure of a truncated ErbB2 ectodomain reveals an active conformation, poised to interact with other ErbB receptors. *Molecular Cell* **11**, 495-505.

Garrett, T. P. J., McKern, N. M., Lou, M. Z., Elleman, T. C., Adams, T. E., Lovrecz, G. O., Zhu, H. J., Walker, F., Frenkel, M. J., Hoyne, P. A., et al. (2002). Crystal structure of a truncated epidermal growth factor receptor extracellular domain bound to transforming growth factor alpha. *Cell* **110**, 763-773.

Gassmann, M., Casagranda, F., Orioli, D., Simon, H., Lai, C., Klein, R. and Lemke, G. (1995). Aberrant neural and cardiac development in mice lacking the ErbB4 neuregulin receptor. *Nature* **378**, 390-394.

Geetha, T. and Wooten, M. W. (2002). Structure and functional properties of the ubiquitin binding protein p62. *Febs Letters* **512**, 19-24.

Goh, L. K., Huang, F. T., Kim, W., Gygi, S. and Sorkin, A. (2010). Multiple mechanisms collectively regulate clathrin-mediated endocytosis of the epidermal growth factor receptor. *Journal of Cell Biology* **189**, 871-883.

Gotoh, N. (2009). Feedback inhibitors of the epidermal growth factor receptor signaling pathways. *International Journal of Biochemistry & Cell Biology* **41**, 511-515.

Gotoh, N., Tojo, A., Hino, M., Yazaki, Y. and Shibuya, M. (1992). A highly conserved tyrosine residue at codon 845 within the kinase domain is not required for the transforming activity of human epidermal growth-factor receptor. *Biochemical and Biophysical Research Communications* **186**, 768-774.

Grandis, J. R. and Sok, J. C. (2004). Signaling through the epidermal growth factor receptor during the development of malignancy. *Pharmacology & Therapeutics* **102**, 37-46.

Greenman, C., Stephens, P., Smith, R., Dalgliesh, G. L., Hunter, C., Bignell, G., Davies, H., Teague, J., Butler, A., Edkins, S., et al. (2007). Patterns of somatic mutation in human cancer genomes. *Nature* **446**, 153-158.

Griffiths, G. and Gruenberg, J. (1991). The arguments for pre-existing early and late endosomes. *Trends in Cell Biology* **1**, 5-9.

Grimes, M. L., Zhou, J., Beattie, E. C., Yuen, E. C., Hall, D. E., Valletta, J. S., Topp, K. S., LaVail, J. H., Bunnett, N. W. and Mobley, W. C. (1996). Endocytosis of activated TrkA: Evidence that nerve growth factor induces formation of signaling endosomes. *Journal of Neuroscience* **16**, 7950-7964.

Grovdal, L. M., Johannessen, L. E., Rodland, M. S., Madshus, I. H. and Stang, E. (2008). Dysregulation of Ack1 inhibits down-regulation of the EGF receptor. *Experimental Cell Research* **314**, 1292-1300.

Gschwind, A., Fischer, O. M. and Ullrich, A. (2004). Timeline - The discovery of receptor tyrosine kinases: targets for cancer therapy. *Nature Reviews Cancer* **4**, 361-370.

Gu, F., Crump, C. M. and Thomas, G. (2001). Trans-Golgi network sorting. *Cellular and Molecular Life Sciences* **58**, 1067-1084.

Gur, G., Rubin, C., Katz, M., Amit, I., Citri, A., Nilsson, J., Amariglio, N., Henriksson, R., Rechavi, G., Hedman, H., et al. (2004). LRIG1 restricts growth factor signaling by enhancing receptor ubiquitylation and degradation. *Embo Journal* **23**, 3270-3281.

Gutierrez, M. G., Munafo, D. B., Beron, W. and Colombo, M. I. (2004). Rab7 is required for the normal progression of the autophagic pathway in mammalian cells. *Journal of Cell Science* **117**, 2687-2697.

Haglund, K., Sigismund, S., Polo, S., Szymkiewicz, I., Di Fiore, P. P. and Dikic, I. (2003). Multiple monoubiquitination of RTKs is sufficient for their endocytosis and degradation. *Nature Cell Biology* **5**, 461-466.

Hailey, D. W., Rambold, A. S., Satpute-Krishnan, P., Mitra, K., Sougrat, R., Kim, P. K. and Lippincott-Schwartz, J. (2010). Mitochondria supply membranes for autophagosome biogenesis during starvation. *Cell* **141**, 656-667.

Hales, C. M., Vaerman, J. P. and Goldenring, J. R. (2002). Rab11 family interacting protein 2 associates with myosin Vb and regulates plasma membrane recycling. *Journal of Biological Chemistry* **277**, 50415-50421.

Hall, J. M., Lee, M. K., Newman, B., Morrow, J. E., Anderson, L. A., Huey, B. and King, M. C. (1990). Linkage of early-onset familial breast-cancer to chromosome-17q21. *Science* **250**, 1684-1689.

Hara, T. and Mizushima, N. (2009). Role of ULK-FIP200 complex in mammalian autophagy FIP200, a counterpart of yeast Atg 17? *Autophagy* **5**, 85-87.

Harris, R. C., Chung, E. and Coffey, R. J. (2003). EGF receptor ligands. *Experimental Cell Research* **284**, 2-13.

Harrison, R. E., Bucci, C., Vieira, O. V., Schroer, T. A. and Grinstein, S. (2003). Phagosomes fuse with late endosomes and/or lysosomes by extension of membrane protrusions along microtubules: Role of Rab7 and RILP. *Molecular and Cellular Biology* **23**, 6494-6506.

Hayashi-Nishino, M., Fujita, N., Noda, T., Yamaguchi, A., Yoshimori, T. and Yamamoto, A. (2009). A subdomain of the endoplasmic reticulum forms a cradle for autophagosome formation. *Nature Cell Biology* **11**, 1433-1438.

He, C. C., Baba, M., Cao, Y. and Klionsky, D. J. (2008). Self-interaction is critical for Atg9 transport and function at the phagophore assembly site during autophagy. *Molecular Biology of the Cell* **19**, 5506-5516.

Hebert, D. N. and Molinari, M. (2007). In and out of the ER: Protein folding, quality control, degradation, and related human diseases. *Physiological Reviews* **87**, 1377-1408.

Hess, D. T., Matsumoto, A., Kim, S. O., Marshall, H. E. and Stamler, J. S. (2005). Protein S-nitrosylation: Purview and parameters. *Nature Reviews Molecular Cell Biology* **6**, 150-166.

Heuser, J. E. and Anderson, R. G. W. (1989). Hypertonic media inhibit receptor-mediated endocytosis by blocking clathrin-coated pit formation. *Journal of Cell Biology* **108**, 389-400.

Hirsch, F. R., Varella-Garcia, M., Bunn, P. A., Di Maria, M. V., Veve, R., Bremnes, R. M., Baron, A. E., Zeng, C. and Franklin, W. A. (2003). Epidermal growth factor receptor in non-small-cell lung carcinomas: Correlation between gene copy number and protein expression and impact on prognosis. *Journal of Clinical Oncology* **21**, 3798-3807.

Hjerpe, R. and Rodriguez, M. S. (2008). Efficient approaches for characterizing ubiquitinated proteins. *Biochemical Society Transactions* **36**, 823-827.

Hoare, S., Hoare, K., Reinhard, M. K., Lee, Y. J., Oh, S. P. and May, W. S., Jr. (2008). Tnk1/Kos1 Knockout Mice Develop Spontaneous Tumors. *Cancer Research* **68**, 8723-8732.

Hoepfner, S., Severin, F., Cabezas, A., Habermann, B., Runge, A., Giilooly, D., Stenmark, H. and Zerial, M. (2005). Modulation of receptor recycling and degradation by the endosomal kinesin KIF16B. *Cell* **121**, 437-450.

Honegger, A. M., Kris, R. M., Ullrich, A. and Schlessinger, J. (1989). Evidence that autophosphorylation of solubilized receptors for epidermal growth-factor is mediated by intermolecular cross-phosphorylation. *Proceedings of the National Academy of Sciences of the United States of America* **86**, 925-929.

Hornbeck, P. V., Kornhauser, J. M., Tkachev, S., Zhang, B., Skrzypek, E., Murray, B., Latham, V. and Sullivan, M. (2012). PhosphoSitePlus: a comprehensive resource for investigating the structure and function of experimentally determined post-translational modifications in man and mouse. *Nucleic Acids Research* **40**, D261-D270.

Howlin, J., Rosenkvist, J. and Andersson, T. (2008). TNK2 preserves epidermal growth factor receptor expression on the cell surface and enhances migration and invasion of human breast cancer cells. *Breast Cancer Research* **10**, 36-48.

Huang, F. T., Goh, L. K. and Sorkin, A. (2007). EGF receptor ubiquitination is not necessary for its internalization. *Proceedings of the National Academy of Sciences of the United States of America-Biological Sciences* **104**, 16904-16909.

Huang, F. T., Kirkpatrick, D., Jiang, X. J., Gygi, S. and Sorkin, A. (2006a). Differential regulation of EGF receptor internalization and degradation by multiubiquitination within the kinase domain. *Molecular Cell* **21**, 737-748.

Huang, L., Watanabe, M., Chikamori, M., Kido, Y., Yamamoto, T., Shibuya, M., Gotoh, N. and Tsuchida, N. (2006b). Unique role of SNT-2/FRS2 beta/FRS3 docking/adaptor protein for negative regulation in EGF receptor tyrosine kinase signaling pathways. *Oncogene* **25**, 6457-6466.

Hynes, N. E., Horsch, K., Olayioye, M. A. and Badache, A. (2001). The ErbB receptor tyrosine family as signal integrators. *Endocrine-Related Cancer* **8**, 151-159.

Ichimura, Y., Kirisako, T., Takao, T., Satomi, Y., Shimonishi, Y., Ishihara, N., Mizushima, N., Tanida, I., Kominami, E., Ohsumi, M., et al. (2000). A ubiquitin-like system mediates protein lipidation. *Nature* **408**, 488-492.

Itakura, E. and Mizushima, N. (2010). Characterization of autophagosome formation site by a hierarchical analysis of mammalian Atg proteins. *Autophagy* **6**, 764-776.

Jeffrey, P. D., Ruso, A. A., Polyak, K., Gibbs, E., Hurwitz, J., Massague, J. and Pavletich, N. P. (1995). Mechanism of CDK activation revealed by the structure of a cyclin A-CDK2 complex. *Nature* **376**, 313-320.

Jermy, A. (2010). Bacterial endocytosis uncovered. *Nature Reviews Microbiology* **8**, 534-534.

Jiang, X. J., Huang, F. T., Marusyk, A. and Sorkin, A. (2003). Grb2 regulates internalization of EGF receptors through clathrin-coated pits. *Molecular Biology of the Cell* **14**, 858-870.

Johansen, T. and Lamark, T. (2011). Selective autophagy mediated by autophagic adapter proteins. *Autophagy* **7**, 279-296.

Jones, A. W. and Cooper, H. J. (2011). Dissociation techniques in mass spectrometry-based proteomics. *Analyst* **136**, 3419-3429.

Jordens, I., Fernandez-Borja, M., Marsman, M., Dusseljee, S., Janssen, L., Calafat, J., Janssen, H., Wubbolts, R. and Neefjes, J. (2001). The Rab7 effector protein RILP controls lysosomal transport by inducing the recruitment of dynein-dynactin motors. *Current Biology* **11**, 1680-1685.

Jorissen, R. N., Walker, F., Pouliot, N., Garrett, T. P. J., Ward, C. W. and Burgess, A. W. (2003). Epidermal growth factor receptor: mechanisms of activation and signalling. *Experimental Cell Research* **284**, 31-53.

Jullienflores, V., Dorseuil, O., Romero, F., Letourneur, F., Saragosti, S., Berger, R., Tavitian, A., Gacon, G. and Camonis, J. H. (1995). Bridging Ral GTPase to Rho-pathways - RLIP76, a Ral effector with Cdc42/Rac GTPase-activating protein activity. *Journal of Biological Chemistry* **270**, 22473-22477.

Jung, C. H., Ro, S. H., Cao, J., Otto, N. M. and Kim, D. H. (2010). mTOR regulation of autophagy. *Febs Letters* **584**, 1287-1295.

Jura, N., Endres, N. F., Engel, K., Deindl, S., Das, R., Lamers, M. H., Wemmer, D. E., Zhang, X. W. and Kuriyan, J. (2009). Mechanism for Activation of the EGF Receptor Catalytic Domain by the Juxtamembrane Segment. *Cell* **137**, 1293-1307.

Kabeya, Y., Kawarnata, T., Suzuki, K. and Ohsumi, Y. (2007). Cis1/Atg31 is required for autophagosome formation in Saccharomyces cereviside. *Biochemical and Biophysical Research Communications* **356**, 405-410.

Kabeya, Y., Mizushima, N., Uero, T., Yamamoto, A., Kirisako, T., Noda, T., Kominami, E., Ohsumi, Y. and Yoshimori, T. (2000). LC3, a mammalian homologue of yeast Apg8p, is localized in autophagosome membranes after processing. *Embo Journal* **19**, 5720-5728.

Kabeya, Y., Mizushima, N., Yamamoto, A., Oshitani-Okamoto, S., Ohsumi, Y. and Yoshimori, T. (2004). LC3, GABARAP and GATE16 localize to autophagosomal membrane depending on form-II formation. *Journal of Cell Science* **117**, 2805-2812.

Kabeya, Y., Noda, N. N., Fujioka, Y., Suzuki, K., Inagaki, F. and Ohsumi, Y. (2009). Characterization of the Atg17-Atg29-Atg31 complex specifically required for starvation-induced autophagy in Saccharomyces cerevisiae. *Biochemical and Biophysical Research Communications* **389**, 612-615.

Kamada, Y., Funakoshi, T., Shintani, T., Nagano, K., Ohsumi, M. and Ohsumi, Y. (2000). Tor-mediated induction of autophagy via an Apg1 protein kinase complex. *Journal of Cell Biology* **150**, 1507-1513.

Kario, E., Marmor, M. D., Adamsky, K., Citri, A., Amit, I., Amariglio, N., Rechavi, G. and Yarden, Y. (2005). Suppressors of cytokine signaling 4 and 5 regulate epidermal growth factor receptor signaling. *Journal of Biological Chemistry* **280**, 7038-7048.

Kato, M., Miyazawa, K. and Kitamura, N. (2000). A deubiquitinating enzyme UBPY interacts with the Src homology 3 domain of Hrs-binding protein via a novel binding motif PX(V/I)(D/N)RXXKP. *Journal of Biological Chemistry* **275**, 37481-37487.

Kawamata, T., Kamada, Y., Suzuki, K., Kuboshima, N., Akimatsu, H., Ota, S., Ohsumi, M. and Ohsumi, Y. (2005). Characterization of a novel autophagy-specific gene, ATG29. *Biochemical and Biophysical Research Communications* **338**, 1884-1889.

Kelley, G. G., Reks, S. E., Ondrako, J. M. and Smrcka, A. V. (2001). Phospholipase C epsilon: a novel Ras effector. *Embo Journal* **20**, 743-754.

Kelley, L. C. and Weed, S. A. (2012). Cortactin is a substrate of activated Cdc42-associated kinase 1 (ACK1) during ligand-induced epidermal growth factor receptor downregulation. *Plos One* , 44363-44374.

Kinsella, B. T. and Maltese, W. A. (1992). Rab GTP-binding proteins with 3 different carboxyl-terminal cysteine motifs are modified invivo by 20-carbon isoprenoids. *Journal of Biological Chemistry* **267**, 3940-3945.

Kirisako, T., Ichimura, Y., Okada, H., Kabeya, Y., Mizushima, N., Yoshimori, T., Ohsumi, M., Takao, T., Noda, T. and Ohsumi, Y. (2000). The reversible modification regulates the membrane-binding state of Apg8/Aut7 essential for autophagy and the cytoplasm to vacuole targeting pathway. *Journal of Cell Biology* **151**, 263-275.

Kirkin, V., Lamark, T., Sou, Y. S., Bjorkoy, G., Nunn, J. L., Bruun, J. A., Shvets, E., McEwan, D. G., Clausen, T. H., Wild, P., et al. (2009). A role for NBR1 in autophagosomal degradation of ubiquitinated substrates. *Molecular Cell* **33**, 505-516.

Klionsky, D. J. (2008). Autophagy revisited. *Autophagy* **4**, 740-743.

Klionsky, D. J., Cregg, J. M., Dunn, W. A., Emr, S. D., Sakai, Y., Sandoval, I. V., Sibirny, A., Subramani, S., Thumm, M., Veenhuis, M., et al. (2003). A unified nomenclature for yeast autophagy-related genes. *Developmental Cell* **5**, 539-545.

Klos, K. S., Wyszomierski, S. L., Sun, M. H., Tan, N., Zhou, X. Y., Li, P., Yang, W. T., Yin, G. S., Hittelman, W. N. and Yui, D. H. (2006). ErbB2 increases vascular endothelial growth factor protein synthesis via activation of mammalian target of rapamycin/p70S6K leading to increased angiogenesis and spontaneous metastasis of human breast cancer cells. *Cancer Research* **66**, 2028-2037.

Kmiecik, T. E. and Shalloway, D. (1987). Activation and suppression of pp60c-Src transforming ability by mutation of its primary sites of tyrosine phosphorylation. *Cell* **49**, 65-73.

Knowlden, J. M., Jones, H. E., Barrow, D., Gee, J. M. W., Nicholson, R. I. and Hutcheson, I. R. (2008). Insulin receptor substrate-1 involvement in epidermal growth factor receptor and insulin-like growth factor receptor signalling: implication for Gefitinib ('Iressa') response and resistance. *Breast Cancer Research and Treatment* **111**, 79-91.

Kobayashi, S., Boggon, T. J., Dayaram, T., Janne, P. A., Kocher, O., Meyerson, M., Johnson, B. E., Eck, M. J., Tenen, D. G. and Halmos, B. (2005). EGFR mutation and resistance of non-small-cell lung cancer to gefitinib. *New England Journal of Medicine* **352**, 786-792.

Kobayashi, T., Beuchat, M. H., Lindsay, M., Frias, S., Palmiter, R. D., Sakuraba, H., Parton, R. G. and Gruenberg, J. (1999). Late endosomal membranes rich in lysobisphosphatidic acid regulate cholesterol transport. *Nature Cell Biology* **1**, 113-118.

Kobayashi, T., Stang, E., Fang, K. S., de Moerloose, P., Parton, R. G. and Gruenberg, J. (1998). A lipid associated with the antiphospholipid syndrome regulates endosome structure and function. *Nature* **392**, 193-197.

Komada, M. and Kitamura, N. (1995). Growth factor-induced tyrosine phosphorylation of Hrs, a novel 115-kilodalton protein with a structurally conserved putative zinc-finger domain. *Molecular and Cellular Biology* **15**, 6213-6221.

Kraft, C., Peter, M. and Hofmann, K. (2010). Selective autophagy: ubiquitin-mediated recognition and beyond. *Nature Cell Biology* **12**, 836-841.

Kuan, C. T., Wikstrand, C. J. and Bigner, D. D. (2001). EGF mutant receptor vIII as a molecular target in cancer therapy. *Endocrine-Related Cancer* **8**, 83-96.

Kulathu, Y. and Komander, D. (2012). Atypical ubiquitylation - the unexplored world of polyubiquitin beyond Lys48 and Lys63 linkages. *Nature Reviews Molecular Cell Biology* **13**, 508-523.

Kuznetsov, S. A. and Gelfand, V. I. (1987). 18 kDa mictrotubule-associated protein - identification as a new light chain (LC-3) of microtubul-associated protein (Map-1). *Febs Letters* **212**, 145-148.

Kyriakis, J. M. (2009). Thinking outside the box about Ras. *Journal of Biological Chemistry* **284**, 10993-10994.

Lai, W. H., Cameron, P. H., Doherty, J. J., Posner, B. I. and Bergeron, J. J. M. (1989). Ligand-mediated autophosphorylation activity of the epidermal growth-factor receptor during internalization. *Journal of Cell Biology* **109**, 2751-2760.

Lamark, T., Kirkin, V., Dikic, I. and Johansen, T. (2009). NBR1 and p62 as cargo receptors for selective autophagy of ubiquitinated targets. *Cell Cycle* **8**, 1986-1990.

Lamark, T., Perander, M., Outzen, H., Kristiansen, K., Overvatn, A., Michaelsen, E., Bjorkoy, G. and Johansen, T. (2003). Interaction codes within the family of mammalian Phox and Bem1p domain-containing proteins. *Journal of Biological Chemistry* **278**, 34568-34581.

Lamb, C. A., Yoshimori, T. and Tooze, S. A. (2013). The autophagosome: origins unknown, biogenesis complex. *Nature Reviews Molecular Cell Biology* **14**, 759-774.

Lange, S., Xiang, F. Q., Yakovenko, A., Vihola, A., Hackman, P., Rostkova, E., Kristensen, J., Brandmeier, B., Franzen, G., Hedberg, B., et al. (2005). The kinase domain of titin controls muscle gene expression and protein turnover. *Science* **308**, 1599-1603.

Lauwers, E., Jacob, C. and Andre, B. (2009). K63-linked ubiquitin chains as a specific signal for protein sorting into the multivesicular body pathway. *Journal of Cell Biology* **185**, 493-502.

Le Roy, C. and Wrana, J. L. (2005). Clathrin- and non-clathrin-mediated endocytic regulation of cell signalling. *Nature Reviews Molecular Cell Biology* **6**, 112-126.

Leahy, D. J. (2004). Structure and function of the epidermal growth factor (EGF/ERBB) family of receptors. *Cell Surface Receptors* **68**, 1-27.

Lefevre, G., Babchia, N., Calipel, A., Mouriaux, F., Faussat, A.-M., Mrzyk, S. and Mascarelli, F. (2009). Activation of the FGF2/FGFR1 autocrine loop for cell proliferation and survival in uveal melanoma cells. *Investigative Ophthalmology & Visual Science* **50**, 1047-1057.

Lemmon, M. A. and Schlessinger, J. (2010). Cell signaling by receptor tyrosine kinases. *Cell* **141**, 1117-1134.

Lemmon, S. K. (2001). Clathrin uncoating: Auxilin comes to life. *Current Biology* **11**, R49-R52.

Lettau, M., Pieper, J. and Janssen, O. (2009). Nck adapter proteins: functional versatility in T cells. *Cell Communication and Signaling* **7**, 1-13.

Levimontalcini, R., Meyer, H. and Hamburger, V. (1954). In-vitro experiments on the effects of mouse sarcomas 180 and 37 on the spinal and sympathetic ganglia of the chick embryo. *Cancer Research* **14**, 49-57.

Levine, B. and Yuan, J. Y. (2005). Autophagy in cell death: an innocent convict? *Journal of Clinical Investigation* **115**, 2679-2688.

Levkowitz, G., Waterman, H., Zamir, E., Kam, Z., Oved, S., Langdon, W. Y., Beguinot, L., Geiger, B. and Yarden, Y. (1998). c-Cbl/Sli-1 regulates endocytic sorting and ubiquitination of the epidermal growth factor receptor. *Genes & Development* **12**, 3663-3674.

Li, W., Hu, P., Skolnik, E. Y., Ullrich, A. and Schlessinger, J. (1992). The SH2 and SH3 domain-containing Nck protein is oncogenic and a common target for phosphorylation by different surface receptors. *Molecular and Cellular Biology* **12**, 5824-5833.

Libermann, T. A., Nusbaum, H. R., Razon, N., Kris, R., Lax, I., Soreq, H., Whittle, N., Waterfield, M. D., Ullrich, A. and Schlessinger, J. (1985). Amplification, enhanced expression and possible rearrangement of EGF receptor gene in primary human-brain tumors of glial origin. *Nature* **313**, 144-147.

Lin, Q., Lo, C. G., Cerione, R. A. and Yang, W. (2002). The Cdc42 target ACK2 interacts with sorting nexin 9 (SH3PX1) to regulate epidermal growth factor receptor degradation. *Journal of Biological Chemistry* **277**, 10134-10138.

Lin, Q., Wang, J., Childress, C., Sudol, M., Carey, D. J. and Yang, W. N. A. (2010). Hect E3 ubiquitin ligase Nedd4-1 ubiquitinates Ack and regulates epidermal growth factor (EGF)-induced degradation of EGF receptor and Ack. *Molecular and Cellular Biology* **30**, 1541-1554.

Lin, Q., Wang, J., Childress, C. and Yang, W. (2012). The activation mechanism of Ack1 (activated Cdc42-associated tyrosine kinase 1). *Biochemical Journal* **445**, 255-264.

Linding, R., Jensen, L. J., Ostheimer, G. J., van Vugt, M., Jorgensen, C., Miron, I. M., Diella, F., Colwill, K., Taylor, L., Elder, K., et al. (2007). Systematic discovery of in vivo phosphorylation networks. *Cell* **129**, 1415-1426.

Lipkowitz, S. (2003). The role of the ubiquitination-proteasome pathway in breast cancer - Ubiquitin mediated degradation of growth factor receptors in the pathogenesis and treatment of cancer. *Breast Cancer Research* **5**, 8-15.

Lombardi, D., Soldati, T., Riederer, M. A., Goda, Y., Zerial, M. and Pfeffer, S. R. (1993). Rab9 functions in transport between late endosomes and the trans Golgi network. *Embo Journal* **12**, 677-682.

Lougheed, J. C., Chen, R. H., Mak, P. and Stout, T. J. (2004). Crystal structures of the phosphorylated and unphosphorylated kinase domains of the Cdc42-associated tyrosine kinase ACK1. *Journal of Biological Chemistry* **279**, 44039-44045.

Luetteke, N. C., Phillips, H. K., Qiu, T. H., Copeland, N. G., Earp, H. S., Jenkins, N. A. and Lee, D. C. (1994). The mouse waved-2 phenotype results from a point mutation in the EGF receptor tyrosine kinase. *Genes & Development* **8**, 399-413.

Lynch, T. J., Bell, D. W., Sordella, R., Gurubhagavatula, S., Okimoto, R. A., Brannigan, B. W., Harris, P. L., Haserlat, S. M., Supko, J. G., Haluska, F. G., et al. (2004). Activating mutations in the epidermal growth factor receptor underlying responsiveness of non-small-cell lung cancer to gefitinib. *New England Journal of Medicine* **350**, 2129-2139.

MacLean, M. and Picard, D. (2003). Cdc37 goes beyond Hsp90 and kinases. *Cell Stress & Chaperones* **8**, 114-119.

Madshus, I. H. and Stang, E. (2009). Internalization and intracellular sorting of the EGF receptor: a model for understanding the mechanisms of receptor trafficking. *Journal of Cell Science* **122**, 3433-3439.

Mahajan, K., Coppola, D., Challa, S., Fang, B., Chen, Y. A., Zhu, W. W., Lopez, A. S., Koomen, J., Engelman, R. W., Rivera, C., et al. (2010). Ack1 mediated AKT/PKB tyrosine 176 phosphorylation regulates its activation. *Plos One* **5**, e9646-e9662.

Mahajan, K. and Mahajan, N. P. (2010). Shepherding Akt and androgen receptor by Ack1 tyrosine kinase. *Journal of Cellular Physiology* **224**, 327-333.

Mahajan, N. P., Liu, Y., Majumder, S., Warren, M. R., Parker, C. E., Mohler, J. L., Earp, H. S. and Whang, Y. E. (2007). Activated Cdc42-associated kinase Ack1 promotes prostate cancer progression via androgen receptor tyrosine phosphorylation. *Proceedings of the National Academy of Sciences of the United States of America* **104**, 8438-8443.

Mahajan, N. P., Whang, Y. E., Mohler, J. L. and Earp, H. S. (2005). Activated tyrosine kinase Ack1 promotes prostate tumorigenesis: Role of Ack1 in polyubiquitination of tumor suppressor Wwox. *Cancer Research* **65**, 10514-10523.

Maity, A., Pore, N., Lee, J., Solomon, D. and O'Rourke, D. M. (2000). Epidermal growth factor receptor transcriptionally up-regulates vascular endothelial growth factor expression in human glioblastoma cells via a pathway involving phosphatidylinositol 3 '-kinase and distinct from that induced by hypoxia. *Cancer Research* **60**, 5879-5886.

Mandel, C. R., Kaneko, S., Zhang, H. L., Gebauer, D., Vethantham, V., Manley, J. L. and Tong, L. (2006). Polyadenylation factor CPSF-73 is the pre-mRNA 3 '-end-processing endonuclease. *Nature* **444**, 953-956.

Manser, E., Leung, T., Salihuddin, H., Tan, L. and Lim, L. (1993). A nonreceptor tyrosine kinase that inhibits the GTPase activity of p21 (Cdc42). *Nature* **363**, 364-367.

Mao, W. G., Irby, R., Coppola, D., Fu, L., Wloch, M., Turner, J., Yu, H., Garcia, R., Jove, R. and Yeatman, T. J. (1997). Activation of c-Src by receptor tyrosine kinases in human colon cancer cells with high metastatic potential. *Oncogene* **15**, 3083-3090.

Mardakheh, F. K., Auciello, G., Dafforn, T. R., Rappoport, J. Z. and Heath, J. K. (2010). Nbr1 is a novel inhibitor of ligand-mediated receptor tyrosine kinase degradation. *Molecular and Cellular Biology* **30**, 5672-5685.

Mardakheh, F. K., Yekezare, M., Machesky, L. M. and Heath, J. K. (2009). Spred2 interaction with the late endosomal protein NBR1 down-regulates fibroblast growth factor receptor signaling. *Journal of Cell Biology* **187**, 265-277.

Marfori, M., Mynott, A., Ellis, J. J., Mehdi, A. M., Saunders, N. F. W., Curmi, P. M., Forwood, J. K., Boden, M. and Kobe, B. (2011). Molecular basis for specificity of nuclear import and prediction of nuclear localization. *Biochimica Et Biophysica Acta-Molecular Cell Research* **1813**, 1562-1577.

Mattoon, D., Klein, P., Lemmon, M. A., Lax, I. and Schlessinger, J. (2004). The tethered configuration of the EGF receptor extracellular domain exerts only a limited control of receptor function. *Proceedings of the National Academy of Sciences of the United States of America* **101**, 923-928.

Maxfield, F. R. and McGraw, T. E. (2004). Endocytic recycling. *Nature Reviews Molecular Cell Biology* **5**, 121-132.

Mayle, K. M., Le, A. M. and Kamei, D. T. (2012). The intracellular trafficking pathway of transferrin. *Biochimica Et Biophysica Acta-General Subjects* **1820**, 264-281.

Mayor, S. and Pagano, R. E. (2007). Pathways of clathrin-independent endocytosis. *Nature Reviews Molecular Cell Biology* **8**, 603-612.

McCubrey, J. A., Steelman, L. S., Chappell, W. H., Abrams, S. L., Wong, E. W. T., Chang, F., Lehmann, B., Terrian, D. M., Milella, M., Tafuri, A., et al. (2007). Roles of the Raf/MEK/ERK pathway in cell growth, malignant transformation and drug resistance. *Biochimica Et Biophysica Acta-Molecular Cell Research* **1773**, 1263-1284.

McCullough, J., Clague, M. J. and Urbe, S. (2004). AMSH is an endosome-associated ubiquitin isopeptidase. *Journal of Cell Biology* **166**, 487-492.

Menzo, S., Clementi, M., Alfani, E., Bagnarelli, P., Iacovacci, S., Manzin, A., Dandri, M., Natoli, G., Levrero, M. and Carloni, G. (1993). Transactivation of epidermal growth-factor receptor gene by the hepatitis-B virus x-gene product. *Virology* **196**, 878-882.

Metz, H. E. and Houghton, A. M. (2011). Insulin receptor substrate regulation of phosphoinositide 3-kinase. *Clinical Cancer Research* **17**, 206-211.

Miaczynska, M., Christoforidis, S., Giner, A., Shevchenko, A., Uttenweiler-Joseph, S., Habermann, B., Wilm, M., Parton, R. G. and Zerial, M. (2004a). APPL proteins link Rab5 to nuclear signal transduction via an endosomal compartment. *Cell* **116**, 445-456.

Miaczynska, M., Pelkmans, L. and Zerial, M. (2004b). Not just a sink: endosomes in control of signal transduction. *Current Opinion in Cell Biology* **16**, 400-406.

Miettinen, P. J., Berger, J. E., Meneses, J., Phung, Y., Pedersen, R. A., Werb, Z. and Derynck, R. (1995). Epithelial immaturity and multiorgan failure in mice lacking epidermal growth-factor receptor. *Nature* **376**, 337-341.

Miller, V. P.-E. a. W. T. (2011). Regulation of Ack-family nonreceptor tyrosine kinases. *Journal of Signal Transduction* **2011**, 1-9.

Miller, W. E., Earp, H. S. and Raabtraub, N. (1995). The Epstein-Barr-virus latent membrane-protein-1 induced expression of the epidermal growth-factor receptor. *Journal of Virology* **69**, 4390-4398.

Mizushima, N. (2007). Autophagy: process and function. *Genes & Development* **21**, 2861-2873.

Mizushima, N., Kuma, A., Kobayashi, Y., Yamamoto, A., Matsubae, M., Takao, T., Natsume, T., Ohsumi, Y. and Yoshimori, T. (2003). Mouse Apg16L, a novel WD-repeat protein, targets to the autdphagic isolation membrane with the Apg12-Apg5 conjugate. *Journal of Cell Science* **116**, 1679-1688.

Mizushima, N., Noda, T. and Ohsumi, Y. (1999). Apg16p is required for the function of the Apg12p-Apg5p conjugate in the yeast autophagy pathway. *Embo Journal* **18**, 3888-3896.

Mizushima, N., Noda, T., Yoshimori, T., Tanaka, Y., Ishii, T., George, M. D., Klionsky, D. J., Ohsumi, M. and Ohsumi, Y. (1998). A protein conjugation system essential for autophagy. *Nature* **395**, 395-398.

Mizushima, N., Yamamoto, A., Hatano, M., Kobayashi, Y., Kabeya, Y., Suzuki, K., Tokuhisa, T., Ohsumi, Y. and Yoshimori, T. (2001). Dissection of autophagosome formation using Apg5-deficient mouse embryonic stem cells. *Journal of Cell Biology* **152**, 657-667.

Mizushima, N., Yoshimori, T. and Ohsumi, Y. (2011). The role of Atg proteins in autophagosome formation. *Annual Review of Cell and Developmental Biology* **27**, 107-132.

Modzelewska, K., Newman, L. P., Desai, R. and Keely, P. J. (2006). Ack1 mediates Cdc42-dependent cell migration and signaling to p130(Cas). *Journal of Biological Chemistry* **281**, 37527-37535.

Montesano, R., Roth, J., Robert, A. and Orci, L. (1982). Non-coated membrane invaginations are involved in binding and internalization of cholera and tetanus toxins. *Nature* **296**, 651-653.

Moscat, J. and Diaz-Meco, M. T. (2009). p62 at the crossroads of autophagy, apoptosis, and cancer. *Cell* **137**, 1001-1004.

Moscat, J. and Diaz-Meco, M. T. (2012). p62: a versatile multitasker takes on cancer. *Trends in Biochemical Sciences* **37**, 230-236.

Mosesson, Y., Shtiegman, K., Katz, M., Zwang, Y., Vereb, G., Szollosi, J. and Yarden, Y. (2003). Endocytosis of receptor tyrosine kinases is driven by monoubiquitylation, not polyubiquitylation. *Journal of Biological Chemistry* **278**, 21323-21326.

Moyer, B. D., Allan, B. B. and Balch, W. E. (2001). Rab1 interaction with a GM130 effector complex regulates COPII vesicle cis-Golgi tethering. *Traffic* **2**, 268-276.

Mu, F. T., Callaghan, J. M., Steelemortimer, O., Stenmark, H., Parton, R. G., Campbell, P. L., McCluskey, J., Yeo, J. P., Tock, E. P. C. and Toh, B. H. (1995). EEA1, an early endosome-associated protein - EEA1 is a conserved alpha-helical peripheral membrane-protein flanked by cysteine fingers and contains a calmodulin-binding IQ motif. *Journal of Biological Chemistry* **270**, 13503-13511.

Murphy, R. F. (1991). Maturation models for endosome and lysosome biogenesis. *Trends in Cell Biology* **1**, 77-82.

Nakatogawa, H., Suzuki, K., Kamada, Y. and Ohsumi, Y. (2009). Dynamics and diversity in autophagy mechanisms: lessons from yeast. *Nature Reviews Molecular Cell Biology* **10**, 458-467.

Nguyen, T. L. X., Choi, J. W., Lee, S. B., Ye, K., Woo, S.-D., Lee, K.-H. and Ahn, J.-Y. (2006). Akt phosphorylation is essential for nuclear translocation and retention in NGF-stimulated PC12 cells. *Biochemical and Biophysical Research Communications* **349**, 789-798.

Nielsen, E., Christoforidis, S., Uttenweiler-Joseph, S., Miaczynska, M., Dewitte, F., Wilm, M., Hoflack, B. and Zerial, M. (2000). Rabenosyn-5, a novel Rab5 effector, is complexed with hVPS45 and recruited to endosomes through a FYVE finger domain. *Journal of Cell Biology* **151**, 601-612.

Noda, T., Kim, J., Huang, W. P., Baba, M., Tokunaga, C., Ohsumi, Y. and Klionsky, D. J. (2000). Apg9p/Cvt7p is an integral membrane protein required for transport vesicle formation in the Cvt and autophagy pathways. *Journal of Cell Biology* **148**, 465-479.

Normanno, N., De Luca, A., Bianco, C., Strizzi, L., Mancino, M., Maiello, M. R., Carotenuto, A., De Feo, G., Caponigro, F. and Salomon, D. S. (2006). Epidermal growth factor receptor (EGFR) signaling in cancer. *Gene* **366**, 2-16.

Ogawara, Y., Kishishita, S., Obata, T., Isazawa, Y., Suzuki, T., Tanaka, K., Masuyama, N. and Gotoh, Y. (2002). Akt enhances Mdm2-mediated ubiquitination and degradation of p53. *Journal of Biological Chemistry* **277**, 21843-21850.

Ogiso, H., Ishitani, R., Nureki, O., Fukai, S., Yamanaka, M., Kim, J. H., Saito, K., Sakamoto, A., Inoue, M., Shirouzu, M., et al. (2002). Crystal structure of the complex of human epidermal growth factor and receptor extracellular domains. *Cell* **110**, 775-787.

Ohno, H. (2006). Clathrin-associated adaptor protein complexes. *Journal of Cell Science* **119**, 3719-3721.

Okamoto, S. and Oka, T. (1984). Evidence for physiological-function of epidermal growth-factor - pregestational sialoadenectomy of mice decreases milk-production and increases offspring mortality during lactation period. *Proceedings of the National Academy of Sciences of the United States of America* **81**, 6059-6063.

Olayioye, M. A., Beuvink, I., Horsch, K., Daly, J. M. and Hynes, N. E. (1999). ErbB receptor-induced activation of Stat transcription factors is mediated by Src tyrosine kinases. *Journal of Biological Chemistry* **274**, 17209-17218.

Omerovic, J., Hammond, D. E., Prior, I. A. and Clague, M. J. (2012). Global snapshot of the influence of endocytosis upon EGF receptor signaling output. *Journal of Proteome Research* **11**, 5157-5166.

Ong, S. E., Blagoev, B., Kratchmarova, I., Kristensen, D. B., Steen, H., Pandey, A. and Mann, M. (2002). Stable isotope labeling by amino acids in cell culture, SILAC, as a simple and accurate approach to expression proteomics. *Molecular & Cellular Proteomics* **1**, 376-386.

Ostman, A. and Bohmer, F. D. (2001). Regulation of receptor tyrosine kinase signaling by protein tyrosine phosphatases. *Trends in Cell Biology* **11**, 258-266.

Ouyang, L., Shi, Z., Zhao, S., Wang, F. T., Zhou, T. T., Liu, B. and Bao, J. K. (2012). Programmed cell death pathways in cancer: a review of apoptosis, autophagy and programmed necrosis. *Cell Proliferation* **45**, 487-498.

Pankiv, S., Clausen, T. H., Lamark, T., Brech, A., Bruun, J. A., Outzen, H., Overvatn, A., Bjorkoy, G. and Johansen, T. (2007). p62/SQSTM1 binds directly to Atg8/LC3 to facilitate degradation of ubiquitinated protein aggregates by autophagy. *Journal of Biological Chemistry* **282**, 24131-24145.

Pao-Chun, L., Chan, P. M., Chan, W. and Manser, E. (2009). Cytoplasmic Ack1 interaction with multiple receptor tyrosine kinases is mediated by Grb2 - an analysis of Ack1 effects on Axl signaling. *Journal of Biological Chemistry* **284**, 34954-34963.

Pap, M. and Cooper, G. M. (1998). Role of glycogen synthase kinase-3 in the phosphatidylinositol 3-kinase/Akt cell survival pathway. *Journal of Biological Chemistry* **273**, 19929-19932.

Park, I., Chung, J., Walsh, C. T., Yun, Y. D., Strominger, J. L. and Shin, J. (1995). Phosphotyrosine-independent binding of a 62-kDa protein to the src homology 2 (SH2) domain of p56(lck) and its regulation by phosphorylation of Ser-59 in the lck unique N-terminal region. *Proceedings of the National Academy of Sciences of the United States of America* **92**, 12338-12342.

Patterson, G. H., Knobel, S. M., Sharif, W. D., Kain, S. R. and Piston, D. W. (1997). Use of the green fluorescent protein and its mutants in quantitative fluorescence microscopy. *Biophysical Journal* **73**, 2782-2790.

Pearse, B. M. F. (1976). Clathrin - unique protein associated with intracellular transfer of membrane by coated vesicles. *Proceedings of the National Academy of Sciences of the United States of America* **73**, 1255-1259.

Pelicano, H., Martin, D. S., Xu, R. H. and Huang, P. (2006). Glycolysis inhibition for anticancer treatment. *Oncogene* **25**, 4633-4646.

Pelkmans, L., Fava, E., Grabner, H., Hannus, M., Habermann, B., Krausz, E. and Zerial, M. (2005). Genome-wide analysis of human kinases in clathrin- and caveolae/raft-mediated endocytosis. *Nature* **436**, 78-86.

Petit, A. M. V., Rak, J., Hung, M. C., Rockwell, P., Goldstein, N., Fendly, B. and Kerbel, R. S. (1997). Neutralizing antibodies against epidermal growth factor and ErbB-2/neu receptor tyrosine kinases down-regulate vascular endothelial growth factor production by tumor cells in vitro and in vivo - Angiogenic implications for signal transduction therapy of solid tumors. *American Journal of Pathology* **151**, 1523-1530.

Plotnikov, A. N., Schlessinger, J., Hubbard, S. R. and Mohammadi, M. (1999). Structural basis for FGF receptor dimerization and activation. *Cell* **98**, 641-650.

Prieto-Echague, V. and Miller, W. T. (2011). Regulation of ack-family nonreceptor tyrosine kinases. *Journal of signal transduction* **2011**, 1-9.

Prieto-Echaguee, V., Gucwa, A., Brown, D. A. and Miller, W. T. (2010). Regulation of Ack1 localization and activity by the amino-terminal SAM domain. *Bmc Biochemistry* **11**, 42-52.

Prieto-Echaguee, V., Gucwa, A., Craddock, B. P., Brown, D. A. and Miller, W. T. (2010). Cancer-associated Mutations Activate the Nonreceptor Tyrosine Kinase Ack1. *Journal of Biological Chemistry* **285**, 10605-10615.

Pugh, C. W. and Ratcliffe, P. J. (2003). The von Hippel-Lindau tumor suppressor, hypoxia-inducible factor-1 (HIF-1) degradation, and cancer pathogenesis. *Seminars in Cancer Biology* **13**, 83-89.

Puls, A., Schmidt, S., Grawe, F. and Stabel, S. (1997). Interaction of protein kinase C zeta with ZIP, a novel protein kinase c-binding protein. *Proceedings of the National Academy of Sciences of the United States of America* **94**, 6191-6196.

Radinsky, R., Risin, S., Fan, D., Dong, Z. Y., Bielenberg, D., Bucana, C. D. and Fidler, I. J. (1995). Level and function of epidermal growth-factor receptor predict the metastatic potential of human colon-carcinoma cells. *Clinical Cancer Research* **1**, 19-31.

Rajkumar, T. (2001). Growth factors and growth factor receptors in cancer. *Current Science* **81**, 535-541.

Rappoport, J. Z. and Simon, S. M. (2009). Endocytic trafficking of activated EGFR is AP-2 dependent and occurs through preformed clathrin spots. *Journal of Cell Science* **122**, 1301-1305.

Ravikumar, B., Futter, M., Jahreiss, L., Korolchuk, V. I., Lichtenberg, M., Luo, S., Massey, D. C. O., Menzies, F. M., Narayanan, U., Renna, M., et al. (2009). Mammalian macroautophagy at a glance. *Journal of Cell Science* **122**, 1707-1711.

Ravikumar, B., Imarisio, S., Sarkar, S., O'Kane, C. J. and Rubinsztein, D. C. (2008). Rab5 modulates aggregation and toxicity of mutant huntingtin through macroautophagy in cell and fly models of Huntington disease. *Journal of Cell Science* **121**, 1649-1660.

Ravikumar, B., Moreau, K., Jahreiss, L., Puri, C. and Rubinsztein, D. C. (2010). Plasma membrane contributes to the formation of pre-autophagosomal structures. *Nature Cell Biology* **12**, 747-757.

Rawlings, J. S., Rosler, K. M. and Harrison, D. A. (2004). The JAK/STAT signaling pathway. *Journal of Cell Science* **117**, 1281-1283.

Razi, M., Chan, E. Y. W. and Tooze, S. A. (2009). Early endosomes and endosomal coatomer are required for autophagy. *Journal of Cell Biology* **185**, 305-321.

Regan-Klapisz, E., Sorokina, I., Voortman, J., de Keizer, P., Roovers, R. C., Verheesen, P., Urbe, S., Fallon, L., Fon, E. A., Verkleij, A., et al. (2005). Ubiquilin recruits Eps15 into ubiquitin-rich cytoplasmic aggregates via a UIM-UBL interaction. *Journal of Cell Science* **118**, 4437-4450.

Reiss, N., Kanety, H. and Schlessinger, J. (1986). 5 enzymes of the glycolytic pathway serve as substrates for purified epidermal-growth-factor-receptor kinase. *Biochemical Journal* **239**, 691-697.

Ren, M. D., Xu, G. X., Zeng, J. B., De Lemos-Chiarandini, C., Adesnik, M. and Sabatini, D. D. (1998). Hydrolysis of GTP on rab11 is required for the direct delivery of transferrin from the pericentriolar recycling compartment to the cell surface but not from sorting endosomes. *Proceedings of the National Academy of Sciences of the United States of America* **95**, 6187-6192.

Reuter, C. W. M., Morgan, M. A. and Eckardt, A. (2007). Targeting EGF-receptor-signalling in squamous cell carcinomas of the head and neck. *British Journal of Cancer* **96**, 408-416.

Reuther, G. W., Lambert, Q. T., Booden, M. A., Wennerberg, K., Becknell, B., Marcucci, G., Sondek, J., Caligiuri, M. A. and Der, C. J. (2001). Leukemia-associated Rho guanine nucleotide exchange factor, a Dbl family protein found mutated in leukemia, causes transformation by activation of RhoA. *Journal of Biological Chemistry* **276**, 27145-27151.

Rhee, S. G. (2001). Regulation of phosphoinositide-specific phospholipase C. *Annual Review of Biochemistry* **70**, 281-312.

Rink, J., Ghigo, E., Kalaidzidis, Y. and Zerial, M. (2005). Rab conversion as a mechanism of progression from early to late endosomes. *Cell* **122**, 735-749.

Rodriguez, A., Duran, A., Selloum, M., Champy, M. F., Diez-Guerra, F. J., Flores, J. M., Serrano, M., Auwerx, J., Diaz-Meco, M. T. and Moscat, J. (2006). Mature-onset obesity and insulin resistance in mice deficient in the signaling adapter p62. *Cell Metabolism* **3**, 211-222.

Roepstorff, K., Grandal, M. V., Henriksen, L., Knudsen, S. L. J., Lerdrup, M., Grovdal, L., Willumsen, B. M. and van Deurs, B. (2009). Differential effects of EGFR ligands on endocytic sorting of the receptor. *Traffic* **10**, 1115-1127.

Roland, J. T., Kenworthy, A. K., Peranen, J., Caplan, S. and Goldenring, J. R. (2007). Myosin Vb interacts with Rab8a on a tubular network containing EHD1 and EHD3. *Molecular Biology of the Cell* **18**, 2828-2837.

Roskoski, R. (2004). Src protein-tyrosine kinase structure and regulation. *Biochemical and Biophysical Research Communications* **324**, 1155-1164.

Roth, T. F. and Porter, K. R. (1964). Yolk protein uptake in oocyte of mosquito Aedes aegyptil. *Journal of Cell Biology* **20**, 313-332.

Row, P. E., Liu, H., Hayes, S., Welchman, R., Charalabous, P., Hofmann, K., Clague, M. J., Sanderson, C. M. and Urbe, S. (2007). The MIT domain of UBPY constitutes a CHMP binding and endosomal localization signal required for efficient epidermal growth factor receptor degradation. *Journal of Biological Chemistry* **282**, 30929-30937.

Row, P. E., Prior, I. A., McCullough, J., Clague, M. J. and Urbe, S. (2006). The ubiquitin isopeptidase UBPY regulates endosomal ubiquitin dynamics and is essential for receptor down-regulation. *Journal of Biological Chemistry* **281**, 12618-12624.

Roxrud, I., Stenmark, H. and Malerod, L. (2010). ESCRT & Co. *Biology of the Cell* **102**, 293-318.

Rozakisadcock, M., McGlade, J., Mbamalu, G., Pelicci, G., Daly, R., Li, W., Batzer, A., Thomas, S., Brugge, J., Pelicci, P. G., et al. (1992). Association of the Shc and Grb2/Sem5 SH2-containing proteins is implicated in activation of the Ras pathway by tyrosine kinases. *Nature* **360**, 689-692.

Ryan, K., Calvo, O. and Manley, J. L. (2004). Evidence that polyadenylation factor CPSF-73 is the rnRNA 3 ' processing endonuclease. *Rna-a Publication of the Rna Society* **10**, 565-573.

Saeki, Y., Kudo, T., Sone, T., Kikuchi, Y., Yokosawa, H., Toh-e, A. and Tanaka, K. (2009). Lysine 63-linked polyubiquitin chain may serve as a targeting signal for the 26S proteasome. *Embo Journal* **28**, 359-371.

Sakaguchi, K., Okabayashi, Y., Kido, Y., Kimura, S., Matsumura, Y., Inushima, K. and Kasuga, M. (1998). Shc phosphotyrosine-binding domain dominantly interacts with epidermal growth factor receptors and mediates Ras activation in intact cells. *Molecular Endocrinology* **12**, 536-543.

Samaj, J., Baluska, F., Voigt, B., Schlicht, M., Volkmann, D. and Menzel, D. (2004). Endocytosis, actin cytoskeleton, and signaling. *Plant Physiology* **135**, 1150-1161.

Sanchez, P., De Carcer, G., Sandoval, I. V., Moscat, J. and Diaz-Meco, M. T. (1998). Localization of atypical protein kinase C isoforms into lysosome-targeted endosomes through interaction with p62. *Molecular and Cellular Biology* **18**, 3069-3080.

Sanz, L., Diaz-Meco, M. T., Nakano, H. and Moscat, J. (2000). The atypical PKC-interacting protein p62 channels NF-kappa B activation by the IL-1-TRAF6 pathway. *Embo Journal* **19**, 1576-1586.

Sanz, L., Sanchez, P., Lallena, M. J., Diaz-Meco, M. T. and Moscat, J. (1999). The interaction of p62 with RIP links the atypical PKCs to NF-kappa B activation. *Embo Journal* **18**, 3044-3053.

Schlessinger, J. (1988). Signal transduction by allosteric receptor oligomerization. *Trends in Biochemical Sciences* **13**, 443-447.

Schlessinger, J. (2000). Cell signaling by receptor tyrosine kinases. *Cell* **103**, 211-225.

Schneider, M. R. and Wolf, E. (2009). The epidermal growth factor receptor ligands at a glance. *Journal of Cellular Physiology* **218**, 460-466.

Schoeberl, B., Eichler-Jonsson, C., Gilles, E. D. and Muller, G. (2002). Computational modeling of the dynamics of the MAP kinase cascade activated by surface and internalized EGF receptors. *Nature Biotechnology* **20**, 370-375.

Sekito, T., Kawamata, T., Ichikawa, R., Suzuki, K. and Ohsumi, Y. (2009). Atg17 recruits Atg9 to organize the pre-autophagosomal structure. *Genes to Cells* **14**, 525-538.

Semerdjieva, S., Shortt, B., Maxwell, E., Singh, S., Fonarev, P., Hansen, J., Schiavo, G., Grant, B. D. and Smythe, E. (2008). Coordinated regulation of AP2 uncoating from clathrin-coated vesicles by rab5 and hRME-6. *Journal of Cell Biology* **183**, 499-511.

Semwogerere, D. and Weeks, E. R. (2005). Encyclopedia of biomaterials and biomedical engineering, Taylor & Francis.

Seshacharyulu, P., Ponnusamy, M. P., Haridas, D., Jain, M., Ganti, A. K. and Batra, S. K. (2012). Targeting the EGFR signaling pathway in cancer therapy. *Expert Opinion on Therapeutic Targets* **16**, 15-31.

Shaffer, J., Sun, G. Q. and Adams, J. A. (2001). Nucleotide release and associated conformational changes regulate function in the COOH-terminal Src kinase, Csk. *Biochemistry* **40**, 11149-11155.

Sharma, S. V., Bell, D. W., Settleman, J. and Haber, D. A. (2007). Epidermal growth factor receptor mutations in lung cancer. *Nature Reviews Cancer* **7**, 169-181.

Shen, F., Lin, Q., Gu, Y., Childress, C. and Yang, W. N. (2007). Activated Cdc42-associated kinase 1 is a component of EGF receptor signaling complex and regulates EGF receptor degradation. *Molecular Biology of the Cell* **18**, 732-742.

Shintani, T., Mizushima, N., Ogawa, Y., Matsuura, A., Noda, T. and Ohsumi, Y. (1999). Apg10p, a novel protein-conjugating enzyme essential for autophagy in yeast. *Embo Journal* **18**, 5234-5241.

Sibilia, M., Kroismayr, R., Lichtenberger, B. M., Natarajan, A., Hecking, M. and Holcmann, M. (2007). The epidermal growth factor receptor: from development to tumorigenesis. *Differentiation* **75**, 770-787.

Sigismund, S., Argenzio, E., Tosoni, D., Cavallaro, E., Polo, S. and Di Fiore, P. P. (2008). Clathrin-mediated internalization is essential for sustained EGFR signaling but dispensable for degradation. *Developmental Cell* **15**, 209-219.

Sigismund, S., Woelk, T., Puri, C., Maspero, E., Tacchetti, C., Transidico, P., Di Fiore, P. P. and Polo, S. (2005). Clathrin-independent endocytosis of ubiquitinated cargos. *Proceedings of the National Academy of Sciences of the United States of America* **102**, 2760-2765.

Simon, J. A. and Schreiber, S. L. (1995). Grb2 SH3 binding to peptides from Sos - evaluation of a general-model for SH3-ligand interactions. *Chemistry & Biology* **2**, 53-60.

Soldati, T. and Schliwa, M. (2006). Powering membrane traffic in endocytosis and recycling. *Nature Reviews Molecular Cell Biology* **7**, 897-908.

Soldati, T., Shapiro, A. D., Svejstrup, A. B. D. and Pfeffer, S. R. (1994). Membrane targeting of the small GTPase Rab9 is accompanied by nucleotide exchange. *Nature* **369**, 76-78.

Sorkin, A. and von Zastrow, M. (2009). Endocytosis and signalling: intertwining molecular networks. *Nature Reviews Molecular Cell Biology* **10**, 609-622.

Sorkin, A. D., Teslenko, L. V. and Nikolsky, N. N. (1988). The endocytosis of epidermal growth-factor in A431 cells - a pH of microenvironment and the dynamics of receptor complex dissociation. *Experimental Cell Research* **175**, 192-205.

Sou, Y., Waguri, S., Iwata, J., Ueno, T., Fujimura, T., Hara, T., Sawada, N., Yamada, A., Mizushima, N., Uchiyama, Y., et al. (2008). The Atg8 conjugation system is indispensable for proper development of autophagic isolation membranes in mice. *Molecular Biology of the Cell* **19**, 4762-4775.

Sousa, L. P., Lax, I., Shen, H. Y., Ferguson, S. M., De Camilli, P. and Schlessinger, J. (2012). Suppression of EGFR endocytosis by dynamin depletion reveals that EGFR signaling occurs primarily at the plasma membrane. *Proceedings of the National Academy of Sciences of the United States of America* **109**, 4419-4424.

Sousa, M. M. L., Steen, K. W., Hagen, L. and Slupphaug, G. (2011). Antibody cross-linking and target elution protocols used for immunoprecipitation significantly modulate signal-to noise ratio in downstream 2D-PAGE analysis. *Proteome Science* **9**, 45-52.

Staub, O. and Rotin, D. (2006). Role of ubiquitylation in cellular membrane transport. *Physiological Reviews* **86**, 669-707.

Stenmark, H. (2009). Rab GTPases as coordinators of vesicle traffic. *Nature Reviews Molecular Cell Biology* **10**, 513-525.

Stenmark, H., Parton, R. G., Steelemortimer, O., Lutcke, A., Gruenberg, J. and Zerial, M. (1994). Inhibition of Rab5 GTPase activity stimulated membrane-fusion in endocytosis. *Embo Journal* **13**, 1287-1296.

Stephan, J. S., Yeh, Y. Y., Ramachandran, V., Deminoff, S. J. and Herman, P. K. (2009). The Tor and PKA signaling pathways independently target the Atg1/Atg13 protein kinase complex to control autophagy. *Proceedings of the National Academy of Sciences of the United States of America* **106**, 17049-17054.

Stoddart, A., Jackson, A. P. and Brodsky, F. M. (2005). Plasticity of B cell receptor internalization upon conditional depletion of clathrin. *Molecular Biology of the Cell* **16**, 2339-2348.

Suzuki, K., Kirisako, T., Kamada, Y., Mizushima, N., Noda, T. and Ohsumi, Y. (2001). The pre-autophagosomal structure organized by concerted functions of APG genes is essential for autophagosome formation. *Embo Journal* **20**, 5971-5981.

Suzuki, K., Kubota, Y., Sekito, T. and Ohsumi, Y. (2007). Hierarchy of Atg proteins in pre-autophagosomal structure organization. *Genes to Cells* **12**, 209-218.

Takeshige, K., Baba, M., Tsuboi, S., Noda, T. and Ohsumi, Y. (1992). Autophagy in yeast demonstrated with proteinase-deficient mutants and conditions for its induction. *Journal of Cell Biology* **119**, 301-311.

Tamai, K., Tanaka, N., Nara, A., Yamamoto, A., Nakagawa, I., Yoshimori, T., Ueno, Y., Shimosegawa, T. and Sugamura, K. (2007). Role of Hrs in maturation of autophagosomes in mammalian cells. *Biochemical and Biophysical Research Communications* **360**, 721-727.

Tanida, I., Komatsu, M., Ueno, T. and Kominami, E. (2003). GATE-16 and GABARAP are authentic modifiers mediated by Apg7 and Apg3. *Biochemical and Biophysical Research Communications* **300**, 637-644.

Tanida, I., Mizushima, N., Kiyooka, M., Ohsumi, M., Ueno, T., Ohsumi, Y. and Kominami, E. (1999). Apg7p/Cvt2p: A novel protein-activating enzyme essential for autophagy. *Molecular Biology of the Cell* **10**, 1367-1379.

Taub, N., Teis, D., Ebner, H. L., Hess, M. W. and Huber, L. A. (2007). Late endosomal traffic of the epidermal growth factor receptor ensures spatial and temporal fidelity of mitogen-activated protein kinase signalling. *Molecular Biology of the Cell* **18**, 4698-4710.

Teng, L. S., Zheng, Y. and Wang, H. H. (2008). BRCA1/2 associated hereditary breast cancer. *Journal of Zhejiang University-Science B* **9**, 85-89.

Teo, M., Tan, L., Lim, L. and Manser, E. (2001). The tyrosine kinase ACK1 associates with clathrin-coated vesicles through a binding motif shared by arrestin and other adaptors. *Journal of Biological Chemistry* **276**, 18392-18398.

Thiel, K. W. and Carpenter, G. (2007). Epidermal growth factor receptor juxtamembrane region regulates allosteric tyrosine kinase activation. *Proceedings of the National Academy of Sciences of the United States of America* **104**, 19238-19243.

Thiery, J. P. and Sleeman, J. P. (2006). Complex networks orchestrate epithelial-mesenchymal transitions. *Nature Reviews Molecular Cell Biology* **7**, 131-142.

Threadgill, D. W., Dlugosz, A. A., Hansen, L. A., Tennenbaum, T., Lichti, U., Yee, D., Lamantia, C., Mourton, T., Herrup, K., Harris, R. C., et al. (1995). Targeted disruption of mouse EGF receptor-effect of genetic background on mutant phenotype. *Science* **269**, 230-234.

Tokunaga, F. and Iwai, K. (2012). LUBAC, a novel ubiquitin ligase for linear ubiquitination, is crucial for inflammation and immune responses. *Microbes and Infection* **14**, 563-572.

Tonks, N. K. (2006). Protein tyrosine phosphatases: from genes, to function, to disease. *Nature Reviews Molecular Cell Biology* **7**, 833-846.

Tooze, S. A. and Razi, M. (2009). The essential role of early endosomes in autophagy is revealed by loss of COPI function. *Autophagy* **5**, 874-875.

Trim, K. (2009). The role of vesicular trafficking in FGFR signalling. *Ph.D. Thesis.* University of Birmingham, United Kingdom.

Tsukada, M. and Ohsumi, Y. (1993). Isolation and characterization of autophagy-defective mutants of Saccharomyces cerevisiae. *Febs Letters* **333**, 169-174.

Tsutsumi, O., Kubota, Y. and Oka, T. (1987). Effect of sialoadenectomy, treatment with epidermal growth-factor (EGF) antiserum and replacement of EGF on the epidermis in mice. *Journal of Endocrinology* **113**, 193-197.

Turner, N. and Grose, R. (2010). Fibroblast growth factor signalling: from development to cancer. *Nature Reviews Cancer* **10**, 116-129.

Ubersax, J. A. and Ferrell, J. E. (2007). Mechanisms of specificity in protein phosphorylation. *Nature Reviews Molecular Cell Biology* **8**, 530-541.

Ullrich, O., Reinsch, S., Urbe, S., Zerial, M. and Parton, R. G. (1996). Rab11 regulates recycling through the pericentriolar recycling endosome. *Journal of Cell Biology* **135**, 913-924.

Ullrich, O., Stenmark, H., Alexandrov, K., Huber, L. A., Kaibuchi, K., Sasaki, T., Takai, Y. and Zerial, M. (1993). Rab GDP dissociation inhibitor as a general regulator for the membrance association of Rab proteins. *Journal of Biological Chemistry* **268**, 18143-18150.

UniProt. (2012). "Reorganizing the protein space at the Universal Protein Resource (UniProt)." Nucleic Acids Research, 40.

Urbe, S. (2005). Ubiquitin and endocytic protein sorting. *Essays in Biochemistry* **41**, 81-98.

Urbe, S., Mills, I. G., Stenmark, H., Kitamura, N. and Clague, M. J. (2000). Endosomal localization and receptor dynamics determine tyrosine phosphorylation of hepatocyte growth factor-regulated tyrosine kinase substrate. *Molecular and Cellular Biology* **20**, 7685-7692.

Urbe, S., Sachse, M., Row, P. E., Preisinger, C., Barr, F. A., Strous, G., Klumperman, J. and Clague, M. J. (2003). The UIM domain of Hrs couples receptor sorting to vesicle formation. *Journal of Cell Science* **116**, 4169-4179.

Vadlamudi, R. K., Joung, I., Strominger, J. L. and Shin, J. (1996). p62, a phosphotyrosine-independent ligand of the SH2 domain of p56(lck), belongs to a new class of ubiquitin-binding proteins. *Journal of Biological Chemistry* **271**, 20235-20237.

Vandersluijs, P., Hull, M., Webster, P., Male, P., Goud, B. and Mellman, I. (1992). The small GTP-binding protein Rab4 controls an early sorting event on the endocytic pathway. *Cell* **70**, 729-740.

Vandersluijs, P., Hull, M., Zahraoui, A., Tavitian, A., Goud, B. and Mellman, I. (1991). The small GTP-binding protein Rab4 is associated with early endosomes. *Proceedings of the National Academy of Sciences of the United States of America* **88**, 6313-6317.

Vaughan, C. K., Neckers, L. and Piper, P. W. (2010). Understanding of the Hsp90 molecular chaperone reaches new heights. *Nature Structural & Molecular Biology* **17**, 1400-1404.

Veale, D., Kerr, N., Gibson, G. J., Kelly, P. J. and Harris, A. L. (1993). The relationship of quantitative epidermal growth-factor receptor expression in nonsmall cell lung-cancer to long-term survival. *British Journal of Cancer* **68**, 162-165.

Vecchi, M., Polo, S., Poupon, V., van de Loo, J. W., Benmerah, A. and Di Fiore, P. P. (2001). Nucleocytoplasmic shuttling of endocytic proteins. *Journal of Cell Biology* **153**, 1511-1517.

Vecchione, A., Cooper, H. J., Trim, K. J., Akbarzadeh, S., Heath, J. K. and Wheldon, L. M. (2007). Protein partners in the life history of activated fibroblast growth factor receptors. *Proteomics* **7**, 4565-4578.

Vieira, A. V., Lamaze, C. and Schmid, S. L. (1996). Control of EGF receptor signaling by clathrin-mediated endocytosis. *Science* **274**, 2086-2089.

Vieira, O. V., Bucci, C., Harrison, R. E., Trimble, W. S., Lanzetti, L., Gruenberg, J., Schreiber, A. D., Stahl, P. D. and Grinstein, S. (2003). Modulation of Rab5 and Rab7 recruitment to phagosomes by phosphatidylinositol 3-kinase. *Molecular and Cellular Biology* **23**, 2501-2514.

von Zastrow, M. and Sorkin, A. (2007). Signaling on the endocytic pathway. *Current Opinion in Cell Biology* **19**, 436-445.

Waas, W. F., Rainey, M. A., Szafranska, A. E. and Dalby, K. N. (2003). Two rate-limiting steps in the kinetic mechanism of the serine/threonine specific protein kinase ERK2: A case of fast phosphorylation followed by fast product release. *Biochemistry* **42**, 12273-12286.

Wada, M., Nakanishi, H., Satoh, A., Hirano, H., Obaishi, H., Matsuura, Y. and Takai, Y. (1997). Isolation and characterization of a GDP/GTP exchange protein specific for the Rab3 subfamily Small G proteins. *Journal of Biological Chemistry* **272**, 3875-3878.

Walker, F., Orchard, S. G., Jorissen, R. N., Hall, N. E., Zhang, H. H., Hoyne, P. A., Adams, T. E., Johns, T. G., Ward, C., Garrett, T. P. J., et al. (2004). CR1/CR2 interactions modulate the functions of the cell surface epidermal growth factor receptor. *Journal of Biological Chemistry* **279**, 22387-22398.

Wang, Y., Pennock, S., Chen, X. M. and Wang, Z. X. (2002). Endosomal signaling of epidermal growth factor receptor stimulates signal transduction pathways leading to cell survival. *Molecular and Cellular Biology* **22**, 7279-7290.

Weidberg, H., Shvets, E., Shpilka, T., Shimron, F., Shinder, V. and Elazar, Z. (2010). LC3 and GATE-16/GABARAP subfamilies are both essential yet act differently in autophagosome biogenesis. *Embo Journal* **29**, 1792-1802.

Wells, A., Welsh, J. B., Lazar, C. S., Wiley, H. S., Gill, G. N. and Rosenfeld, M. G. (1990). Ligand-induced transformation by a noninternalizing epidermal growth-factor receptor. *Science* **247**, 962-964.

Whitehouse, C., Chambers, J., Howe, K., Cobourne, M., Sharpe, P. and Solomon, E. (2002). NBR1 interacts with fasciculation and elongation protein zeta-1 (FEZ1) and calcium and integrin binding protein (CIB) and shows developmentally restricted expression in the neural tube. *European Journal of Biochemistry* **269**, 538-545.

Wilde, A., Beattie, E. C., Lem, L., Riethof, D. A., Liu, S. H., Mobley, W. C., Soriano, P. and Brodsky, F. M. (1999). EGF receptor signaling stimulates SRC kinase phosphorylation of clathrin, influencing clathrin redistribution and EGF uptake. *Cell* **96**, 677-687.

Williams, R. L. and Urbe, S. (2007). The emerging shape of the ESCRT machinery. *Nature Reviews Molecular Cell Biology* **8**, 355-368.

Xie, W., Paterson, A. J., Chin, E., Nabell, L. M. and Kudlow, J. E. (1997). Targeted expression of a dominant negative epidermal growth factor receptor in the mammary gland of transgenic mice inhibits pubertal mammary duct development. *Molecular Endocrinology* **11**, 1766-1781.

Xu, Y. R., Tan, L. J., Grachtchouk, V., Voorhees, J. J. and Fisher, G. J. (2005). Receptor-type protein-tyrosine phosphatase-kappa regulates epidermal growth factor receptor function. *Journal of Biological Chemistry* **280**, 42694-42700.

Yamazaki, T., Zaal, K., Hailey, D., Presley, J., Lippincott-Schwartz, J. and Samelson, L. E. (2002). Role of Grb2 in EGF-stimulated EGFR internalization. *Journal of Cell Science* **115**, 1791-1802.

Yarom, N. and Jonker, D. J. (2011). The role of the epidermal growth factor receptor in the mechanism and treatment of colorectal cancer. *Discovery Medicine* **57**, 95-105.

Yeow-Fong, L., Lim, L. and Manser, E. (2005). SNX9 as an adaptor for linking synaptojanin-1 to the Cdc42 effector ACK1. *Febs Letters* **579**, 5040-5048.

Yokoyama, N. and Miller, W. T. (2003). Biochemical properties of the Cdc42-associated tyrosine kinase ACK1 - Substrate specificity, autophosphorylation, and interaction with Hck. *Journal of Biological Chemistry* **278**, 47713-47723.

Yoshimura, S., Gerondopoulos, A., Linford, A., Rigden, D. J. and Barr, F. A. (2010). Family-wide characterization of the DENN domain Rab GDP-GTP exchange factors. *Journal of Cell Biology* **191**, 367-381.

Zerial, M. and McBride, H. (2001). Rab proteins as membrane organizers. *Nature Reviews Molecular Cell Biology* **2**, 107-117.

Zhang, X., Pickin, K. A., Bose, R., Jura, N., Cole, P. A. and Kuriyan, J. (2007). Inhibition of the EGF receptor by binding of MIG6 to an activating kinase domain interface. *Nature* **450**, 741-744.

Zhang, X. W., Gureasko, J., Shen, K., Cole, P. A. and Kuriyan, J. (2006). An allosteric mechanism for activation of the kinase domain of epidermal growth factor receptor. *Cell* **125**, 1137-1149.

Zheng, Y. (2001). Dbl family guanine nucleotide exchange factors. *Trends in Biochemical Sciences* **26**, 724-732.

Zinchuk, V., Zinchuk, O. and Okada, T. (2007). Quantitative colocalization analysis of multicolor confocal immunofluorescence microscopy images: Pushing pixels to explore biological phenomena. *Acta Histochemica Et Cytochemica* **40**, 101-111.